Cylindrospermopsin transformation by manganese-oxidizing bacteria

vorgelegt von
M. Sc.
Erika Berenice Martínez Ruiz
ORCID: 0000-0003-2965-3884

an der Fakultät III – Prozesswissenschaften
der Technischen Universität Berlin
zur Erlangung des akademischen Grades

Doktor der Naturwissenschaften
– Dr. rer. nat. –

genehmigte Dissertation

Promotionsausschuss:

Vorsitzender: Prof. Dr. Ferdi L. Hellweger
Gutachter: Prof. Dr. Ulrich Szewzyk
Gutachterin: Prof. Dr. Silvia Pichardo Sánchez

Tag der wissenschaftlichen Aussprache: 03. März 2021

Berlin 2021

“A journey of a thousand miles begins with a single step”

Lao Tzu

“A scientist in her laboratory is not a mere technician: she is also a child confronting natural phenomena that impress her as though they were fairy tales”

Marie Curie

Abstract

Cylindrospermopsin is a highly persistent and toxic alkaloid toxin produced by cyanobacteria. Information regarding biological transformation of cylindrospermopsin is scarce, only a few cylindrospermopsin -removing microbial isolates and communities have been described, and so far, transformation products of biological processes have not been identified. Owing to the ability to remove a variety of pollutants, manganese-oxidizing bacteria have been proposed as a potential biological tool to remove diverse pollutants from water. In the present study, we investigated cylindrospermopsin transformation by different MOB isolated from natural and technical systems under diverse growth conditions. Tested manganese-oxidizing bacteria were *Pseudomonas* sp. strain OF001, *Ideonella* sp. strains A288 and A226, and *Rubrivivax* sp. strain A210. Cylindrospermopsin at an environmentally relevant concentration of 120 µg L^{-1} was removed in a range from 25 to 100% after 3 to 28 days of incubation when $MnCO_3$ was used as the Mn^{2+} source in the media with cylindrospermopsin removal rates between 0.38 and 37.01 µg L^{-1} day^{-1}. In the absence of Mn^{2+}, cylindrospermopsin removal by all the tested MOB was zero or lower than 20%. For the detection of cylindrospermopsin transformation products, the four strains were incubated with 7 mg L^{-1} of CYN for 4 to 34 days, depending on the growth rate of each strain. All tested manganese-oxidizing bacteria removed cylindrospermopsin to concentrations below the detection limit at rates ranging from 0.48 to 3.16 mg L^{-1} day^{-1}. *Pseudomonas* sp. OF001 was the fastest tested MOB removing 100% of cylindrospermopsin concentration within three days, while *Rubrivivax* sp. A210, and *Ideonella* sp. A288 and A226 removed 100% of cylindrospermopsin within 14 to 21 days. For all four manganese-oxidizing bacteria strains the same seven transformation products were detected and identified via mass spectrometric analysis (LC-MS/MS) and using an inclusion list of previously described transformation products of abiotic reactions, and further analysis of their fragmentation patterns. These results suggest that MOB follow a general mechanism for cylindrospermopsin transformation. The mixture of transformation products was tested for their hepatotoxicity using HepG2 and HepaRG cell lines. The transformation products exhibit negligible toxicity in both cell lines in comparison to pure cylindrospermopsin and controls without cylindrospermopsin. The genome of *Pseudomonas* sp. OF001, and *Rubrivivax* sp. A210 were analysed to identify *in silico* the enzymes responsible for the oxidation of Mn^{2+}, and to determine their metabolic potential. These strains were selected due to the removal efficiency of nearly 100% when environmentally relevant concentrations of cylindrospermopsin were used, and for the differences observed on the growth and removal requirements. For instance, strain OF001 required yeast extract as additional carbon source for the removal of cylindrospermopsin, but strain A210 transformed cylindrospermopsin in mineral media. Strain OF001 encodes

enzymes with high similarity to the Mn^{2+} oxidases in *P. putida* GB-1, while strain A210 encodes enzymes with high similarity to the Mn^{2+} oxidase in *Leptothrix discophora* SS-1. Both strains have the metabolic potential to grow over a wide range of O_2 concentrations, fix nitrogen, and reduce nitrate and sulfate in an assimilatory manner. In addition, the strain A210 encodes genes which may convey the ability to reduce nitrate in a dissimilatory manner, and fix carbon via the Calvin cycle. Moreover, strains OF001 and A210 have the metabolic potential to remove aromatic compounds via the catechol meta- and ortho-cleavage pathway, respectively. Considering the efficient removal of cylindrospermopsin by the tested strains, manganese-oxidizing bacteria might be used for water treatment to remove cylindrospermopsin and might contribute to the natural removal of cylindrospermopsin in freshwater systems.

Zusammenfassung

Cylindrospermopsin ist ein hoch persistentes Alkaloid-Toxin, das von Cyanobakterien produziert wird und besonders hepatotoxisch wirkt. Über den mikrobiellen Abbau von Cylindrospermopsin ist nur wenig bekannt und für die wenigen bekannten CYN-abbauende mikrobiellen Isolate und Gemeinschaften konnten bisher keine Transformationsprodukte identifiziert werden. Für Mangan-oxidierende Bakterien wurde gezeigt, dass sie eine Vielzahl von Schadstoffen mittels reaktiver Manganspezies entfernen können. Bisher war jedoch nicht bekannt, ob Mangan-oxidierende Bakterien auch Cylindrospermopsin über diesen Mechanismus entfernen können. In der vorliegenden Studie wurde der Einfluss verschiedener Mangan-oxidierende Bakterien Stämme auf Cylindrospermopsin untersucht. Die getestete Mangan-oxidierende Bakterien Stämme waren *Pseudomonas* sp. Stamm OF001, *Ideonella* sp. Stämme A288 und A226 sowie *Rubrivivax* sp. Stamm A210 und stammen aus technischen oder natürlichen Süßwasser Systemen. Die Mangan-oxidierende Bakterien Stämme wurden in Anwesenheit einer umweltrelevanten Cylindrospermopsin Konzentration von 120 µg L-1 in An- und Abwesenheit von Manganquellen inkubiert. Nach 3 bis 28 Tagen Inkubation wurden je nach getestetem Stamm 25 bis 100% Cylindrospermopsin durch MOB entfernt, mit Abbauraten zwischen 0.38 and 37.01 µg L^{-1} day^{-1}, wenn $MnCO_3$ als Mn^{2+}-Quelle in den Medien verwendet wurde. In Abwesenheit von Mn^{2+} wurde Cylindrospermopsin je nach Stamm zu weniger als 20% oder gar nicht entfernt. Zum Nachweis von Cylindrospermopsin-Transformationsprodukten wurden die vier Stämme mit 7 mg L-1 Cylindrospermopsin in Abhängigkeit der Wachstumsrate der Stämme für 4 bis 34 Tage inkubiert. Bei dieser höheren Cylindrospermopsin Konzentration entfernten alle getesteten Mangan-oxidierende Bakterien Cylindrospermopsin bis unterhalb der Nachweisgrenze von Cylindrospermopsin mit Raten zwischen 0,48 und 3,16 mg L^{-1} Tag^{-1} und gehören damit die höchsten Cylindrospermopsin Abbauraten dir für mikorbiellen Abbau beschrieben worden sind. *Pseudomonas* sp. OF001 zeigte dabei die höchsten Cylindrospermopsin Transformationsrate mit einer Transformation von 100% der ursprünglich eingesetzten Cylindrospermopsin-Konzentration innerhalb von drei Tagen. *Rubrivivax* sp. A210 sowie *Ideonella* sp. A288 und A226 transformierten 100% der ursprünglich eingesetzten Cylindrospermopsin-Konzentration innerhalb von 14 bis 21 Tagen. Für alle vier Mangan-oxidierende Bakterien -Stämme konnten die gleichen sieben Transformationsprodukte mittels massenspektrometrischer Analyse (LC-MS/MS), der Verwendung bereits beschriebener Transformationsprodukte abiotischer Reaktionen und der weiteren Analyse ihrer Fragmentierungsmuster nachgewiesen und identifiziert werden. Dieses Ergebnis legt nahe, dass Mangan-oxidierende Bakterien einem änlichen. Mechanismus für die Cylindrospermopsin-Transformation folgen. Um zu untersuchen ob von den Transformationsprodukten eine geringere hepatotoxische Wirkung ausgeht wurde die

Mischung der Transformationsprodukte mit HepG2- und HepaRG-Zelllinien getestet. Die Transformationsprodukte wiesen in beiden Zelllinien im Vergleich zu reinem Cylindrospermopsin und Kontrollen ohne Cylindrospermopsin eine vernachlässigbare Toxizität auf. Obwohl alle Mangan-oxidierende Bakterien Stämme die gleichen Transformationsprodukte bilden, zeigten sich jedoch in der Kultivierung entscheidenden Unterschieden zwischen den Stämmen. So konnte Stamm A210 im Gegensatz zu den anderen Stämmen Cylindrospermopsin auch in minimal Medium ohne zusätzliche organische Kohlenstoffquellen umsetzen. Um die metabolischen Grundlagen für diese Unterschiede zu verstehen und eine bessere Kenntnis der Enzyme, die für den Manganoxidationsmechanismus verantwortlich sind zu erhalten, wurden die Genome von *Pseudomonas* sp. OF001 und *Rubrivivax* sp. A210 wurde analysiert. Stamm OF001 kodiert Enzyme mit hoher Ähnlichkeit zu Mn^{2+}-Oxidasen aus *P. putida* GB-1, während der Stamm A210 Enzyme mit hoher Ähnlichkeit zur Mn^{2+}-Oxidase aus *Leptothrix discophora* SS-1 kodiert. Beide Stämme haben das metabolische Potenzial, über einen weiten Bereich von O_2-Konzentrationen zu wachsen, Stickstoff zu fixieren und Nitrat und Sulfat auf assimilatorische Weise zu reduzieren. Darüber hinaus kodiert der Stamm A210 Gene, die Stamm A210 erlauben könnten, Nitrat in einer dissimilatorischen Weise zu reduzieren und Kohlenstoff über den Calvin-Zyklus zu fixieren. Darüber hinaus haben die Stämme OF001 und A210 das metabolische Potenzial, aromatische Verbindungen über den Brenzcatechin meta- beziehungsweise ortho-Weg zu entfernen. In Anbetracht der effizienten Entfernung von Cylindrospermopsin durch die getesteten Stämme könnten Mangan-oxidierende Bakterien zur Wasserbehandlung zur Entfernung von Cylindrospermopsin eingesetzt werden und zur natürlichen Entfernung von Cylindrospermopsin in Süßwassersystemen beitragen. Die Ergebnisse dieser Arbeit weisen darauf hin, dass Mangan-oxidierende Bakterien zur biotechnologischen Entfernung von Cylindrospermopsin geeignet sein könnten und zudem eine wichtige Rolle in natürlichen Abbauprozessen von Cylindrospermopsin in Süßwassersystemen spielen könnten.

List of publications

Martínez-Ruiz, E.B., Cooper, M., Fastner, J., Szewzyk, U., 2020. Manganese-oxidizing bacteria isolated from natural and technical systems remove cylindrospermopsin. Chemosphere 238. https://doi.org/10.1016/j.chemosphere.2019.124625"

Martínez-Ruiz, E.B., Cooper, M., Al-Zeer, M.A., Kurreck, J., Adrian, L., Szewzyk, U., 2020. Manganese-oxidizing bacteria form multiple cylindrospermopsin transformation products with reduced human liver cell toxicity. Sci. Total Environ. 729, 138924. https://doi.org/10.1016/j.scitotenv.2020.138924

Martínez-Ruiz, E.B., Cooper, M., Barrero-Canosa, J., Bessarab, I., Haryono, M.A.S, Williams, R., Szewzyk, U., 2020. Comparative genome analysis reveals the metabolic diversity of *Pseudomonas* sp. OF001 and *Rubrivivax* sp. A210, able to transform CYN during manganese oxidation. Submitted to BMC genomics.

List of conferences

Manganese-oxidizing bacteria degrade cylindrospermopsin. Oral presentation at the Annual Conference of the Association for General and Applied Microbiology (VAAM), Mainz, Germany. May 17-20, 2019.

Biodegradation of cylindrospermopsin by manganese oxidizing bacteria. Oral presentation at the SETAC Europe 29th Annual Meeting, Helsinki, Finland, May 26-30, 2019.

Cylindrospermopsin transformation products formed by manganese-oxidizing bacteria show reduced toxicity in human cell line models. Oral presentation at the SETAC Europe 30th Annual Meeting, SETAC SciCon, May 3-7, 2020.

Biotransformation of cylindrospermopsin by manganese-oxidizing bacteria. Oral presentation at the conference *Natural Toxins: Environmental Fate and Safe Water Supply*, September 24 and 25, 2020.

Table of contents

List of figures

List of tables

Abbreviations

16S rDNA 16S ribosomal deoxyribonucleic acid
ANI average nucleotide identity
ANOVA One-way analysis of variance
BioOx Biogenic oxides
BioOx-S4 biogenic oxides produced in setup 4
BioOx-S7 biogenic oxides produced in setup 7
Calc calculated
CDS protein coding sequences
COG Cluster of Orthologous Groups
CRISPR Clustered Regularly Interspaced Short Palindromic Repeats
cyanoHABs Cyanobacteria harmful algal blooms
CYN Cylindrospermopsin
CYP cytochrome P450 enzymes
DAAD Deutscher Akademischer Austauschdienst
DDH DNA-DNA hybridization
DSMZ Deutsche Sammlung von Mikroorganismen und Zellkulturen
ENA European Nucleotide Archive
FBS Fetal bovince serum
GC Guanine-cytosine
GGDC Genome-to-genome distance calculator
GTDB Genome Taxonomy Database
HEPES 4-(2-hydroxyethyl)-1-piperazineethanesulfonic acid
HPLC High performance liquid chromatography
IC_{50} half maximal inhibitory concentration
KEGG Kyoto Encyclopedia of Genes and Genomes
Ibb I Leucoberbelin I
LC-MS/MS liquid chromatography combined with tandem mass spectrometry
Lept Leptothrix
LOD Limit of detection
LOQ limit of quantification
LSM2 modified Leptothrix strains medium
m/z mass-to-charge ratio
MaGE Magnifying Genomes
MCMC Markov Chain Monte Carlo
MICFAM Microscope gene families
misc_RNA miscellaneous RNA
MOB Manganese-oxidizing bacteria
MO-hpox haem peroxidases with Mn^{2+} oxidation activity
MO-mco manganese-oxidizing multicopper oxidases
MPC methyl-accepting chemotaxis proteins
NADH Nicotinamide adenine dinucleotide
NCBI National Center for Biotechnology Information
Non-MO-mco non-manganese oxidizing multicopper oxidase
NR neutral red
Obs observed
OD Optical density
ORF Open reading frame
PCBs poly- chlorobiphenyls
PCR polymerase chain reaction
PGDBs Pathway/Genome databases
Psu Pseudomonas
PVDF polyvinylidene difluoride
RNA Ribonucleic acid
RPMI Roswell Park Memorial Institute
rRNA ribosomal RNA
RT retention time
S Setup
SPR Subtree pruning and regrafting
TETRA tetra-nucleotide frequencies
tmRNA transfer-messenger RNA.
TP Transformation product
tRNA transfer RNA
TU Berlin Technische Universität Berlin
UHPLC Ultra high performance liquid chromatography
UV ultraviolet
XTT tetrazolium dye XTT
YE yeast extract

1 Introduction

1.1 Environmental factors influencing cyanobacterial blooms

Eutrophication is a natural evolutionary process of aquatic ecosystems related to the enrichment of water bodies with nutrients that leads to the production of organic material (Khan et al., 2014). The term was applied for the first time at the beginning of the 20th century to refer to the increasing concentration of phytoplankton in lakes (Thienemann 1918 and Naumann 1919 in Wurtsbaugh et al., 2019). Nowadays, eutrophication is considered one of the most important phenomena causing water quality impairment of all kinds of water bodies around the world, including freshwater and marine environments (Khan et al., 2014). Although eutrophication is considered a natural evolutionary process of aquatic ecosystems, anthropogenic activity is accelerating it (Ansari et al., 2011). When eutrophication of water bodies is a consequence of human activity, it is known as anthropogenic eutrophication or cultural eutrophication (Malone and Newton, 2020; Smith et al., 1999). In contrast to natural eutrophication, anthropogenic eutrophication occurs at a shorter time scale, accelerating the adverse environmental and health effects (Le Moal et al., 2019).

Different anthropogenic activities promote directly or indirectly cultural eutrophication including wastewater discharge into rivers, the increased use of fertilizers for agriculture, high energy demands, population expansion, construction of water diversion projects, and climate change (Glibert, 2017; Malone and Newton, 2020). Other activities might also significantly and regionally increase the load of nutrients in aquatic environments. For instance, animal waste from animal farming represents an important source of nutrient pollution. Aquaculture is another example of regional relevant nutrient load, due to the alteration of the natural cycling of nutrients (A. F. Bouwman et al., 2013; L. Bouwman et al., 2013; Peñuelas et al., 2012).

Since the 1970s, research has been conducted to understand the elements that trigger eutrophication (Le Moal et al., 2019). Nowadays, it is known that the main drivers of eutrophication are the increased load of nitrogen and phosphorus into the systems (Khan et al., 2014; Malone and Newton, 2020). However, the impact and response of the aquatic systems to the changes of nitrogen and phosphorus loads will also depend on other environmental factors such as temperature and light intensity (Bouraï et al., 2020; Dou et al., 2019; Yang et al., 2008).

The increase of nitrogen and phosphorus load into aquatic systems favours the proliferation of photosynthetic organisms, leading to structural and functional changes of all the communities in the ecosystems including phytoplankton, zooplankton, benthic organisms, and fish (Fig. 1.1). Environments previously dominated by benthic algae and macrophytes will

shift to a phytoplankton-dominated environment (Wurtsbaugh et al., 2019).The increase of phytoplankton biomass will reduce light penetration into the water column, and, therefore, light becomes a limiting factor. The increased amount of bacterial activity below the photosynthetic active zone leads to the depletion of oxygen and thus, to a state of anoxia (Glibert, 2017; Le Moal et al., 2019). All these changes will produce a loss of biodiversity (Azevedo et al., 2013) and a massive death of aquatic organisms (Le Moal et al., 2019; Paerl, 2017). Moreover, eutrophication can increase production of toxic or climate relevant gases like H_2S and CH_4 (Achá et al., 2018; Beaulieu et al., 2019).

One of the main consequences of the proliferation of phytoplankton biomass is the risk of the formation of harmful algal blooms by toxigenic cyanobacteria (Paerl, 2017).

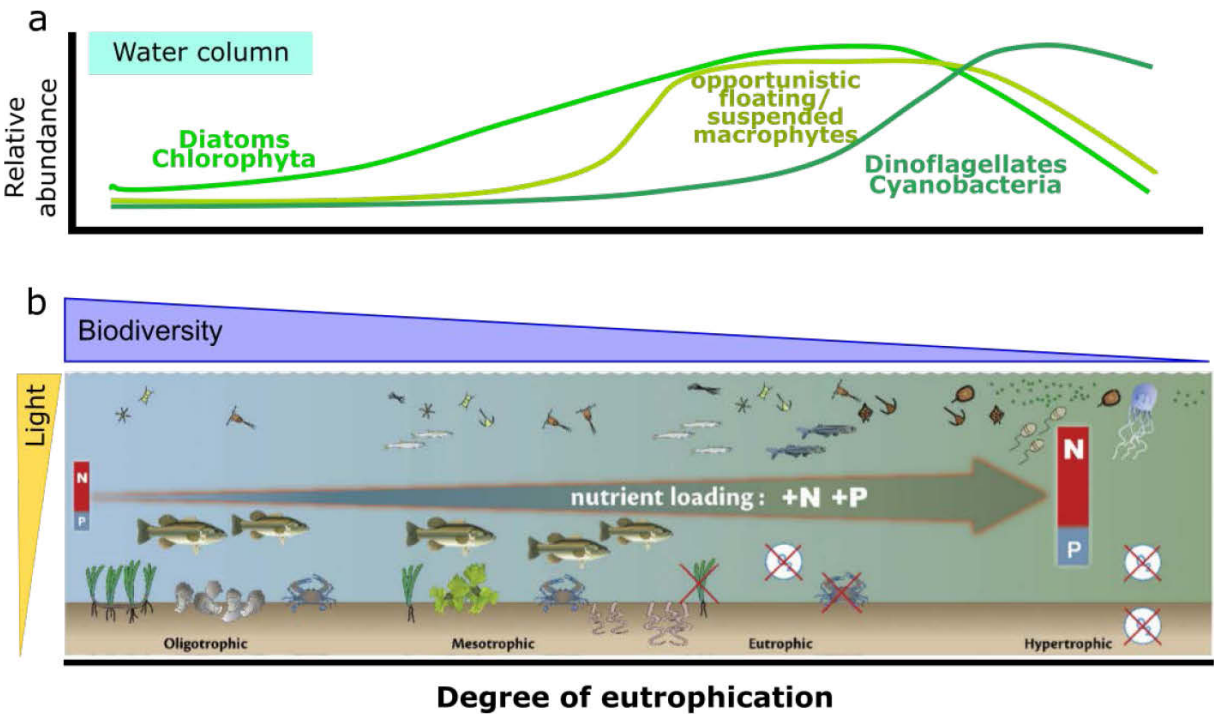

Fig. 1.1. Representation of expected changes on eutrophic systems. a) Succession of photosynthetic organisms expected in the water column, b) change in the aquatic system related to an increase of nitrogen and phosphorus load, including the loss of biodiversity and the presence of anoxic conditions. Modified from Glibert (2015) and Le Moal et al. (2019).

1.2 Cyanobacteria and cyanotoxins

Cyanobacteria are oxygenic photosynthetic prokaryotic organisms that inhabit diverse environments, including soil, seawater, freshwater, and even extreme environments such as hot springs, and polar regions (Flombaum et al., 2013; Whitton, 2012). Cyanobacteria are one of the oldest groups on Earth, and they were involved in the formation of the oxygenic atmosphere (Hamilton et al., 2016). Cyanobacteria are primary producers and key players in

the carbon and nitrogen cycles (Díez and Ininbergs, 2014). They are the origin of the chloroplast of eukaryotic algal and plant cells through an endosymbiotic event (Sharma et al., 2014) and contribute with around 20–30% to the primary productivity worldwide (Bullerjahn and Post, 2014; Lee et al., 2017).

As previously discussed, certain environmental factors and anthropogenic activities, promote cyanobacterial blooms in water systems (Liu et al., 2019; Richardson et al., 2019; Walls et al., 2018; Withers et al., 2014). When cyanobacterial blooms impact negatively the general state of the environment, the economy, and the health of humans and animals, they are called cyanobacteria harmful algal blooms (cyanoHABs) (Benayache et al., 2019; Watson et al., 2015). CyanoHABs occur in marine, and brackish environments, however, they are more common in freshwater systems (McGowan, 2016).

CyanoHABs affect water quality by changing its colour, producing unpleasant odour and affecting its taste (Wood, 2016). Nevertheless, one of the main problems associated to cyanoHABS is the ability of certain cyanobacterial species to produce secondary metabolites known as cyanotoxins, which are potentially toxic to humans, animals, and plants (Corbel et al., 2014; Merel et al., 2013; Wood, 2016; Zanchett and Oliveira-Filho, 2013). Human intoxication related to cyanotoxins has occurred all over the world with rare cases of death (Wood, 2016). Intoxication and death of animals associated to cyanotoxins have been also documented worldwide with more common fatal consequences than for humans. A diverse range of organisms has been affected including livestock (Negri et al., 1995), bees (May and McBarron, 1973), giraffes (Oberholster et al., 2006), sea otter (Miller et al., 2010), fish (Zanchett and Oliveira-Filho, 2013), birds (Papadimitriou et al., 2018), bats (Isidoro-Ayza et al., 2019), and dogs (Fastner et al., 2018). The most recent case of intoxication related to cyanobacteria and cyanotoxin production is the death of over 300 elephants in Botswana (Reuters Staff, 2020).

The main cyanotoxins exposure routes for humans are through the consumption of contaminated food, dietary supplementary, and water, and through recreational activities in contaminated water bodies (Giannuzzi et al., 2011; Lee et al., 2017; Mulvenna et al., 2012; Roy-Lachapelle et al., 2017; Svirčev et al., 2017).

Based on their target organs, cyanotoxins are classified as hepatotoxins, cytotoxins, neurotoxins and dermatotoxins (Merel et al., 2013). In table 1.1, a list of the main cyanotoxins, their mode of action, and the number of congeners is shown. The most commonly reported cyanotoxins over the world are microcystins, cylindrospermopsins, anatoxins, and saxitoxins (Svirčev et al., 2019).

Table 1.1. Main cyanotoxins and toxicological properties.

Toxin	Known analogs number	Main target organs	Mechanism of action
Microcystin	>250	Liver	Irreversible inhibition of protein phosphatases
Nodularin	10	Liver	Irreversible inhibition of protein phosphatases
Cylindrospermopsin	5	Liver and kidneys	Inhibition of protein synthesis
Anatoxin-a	8	Nervous system	Binding to nicotinic acetylcholinesterase
Anatoxin-a(s)	1	Nervous system	Inhibition of acetylcholinesterase
Saxitoxin	56	Nervous system	Binding to sodium channels
β-N-methylamino-L-alanine	1	Nervous system	Binding to glutamate receptors
Lyngbiatoxin	3	Skin	Activation of protein kinase C

Modified from Merel et al. (2013) and Svirčev et al. (2019).

1.3 Cylindrospermopsin (CYN)

Cylindrospermopsin is an alkaloid toxin with a cyclic sulfated guanidine moiety bound to a hydroxymethyluracil group (Fig. 1.1). To date, five analogues of CYN have been described: CYN, 7-epi-CYN, 7-deoxy-CYN (Banker et al., 2000; Norris et al., 1999; Ohtani et al., 1992), 7-deoxydesulfo-CYN and 7-deoxydesulfo-12-acetyl-CYN (Wimmer et al., 2014).

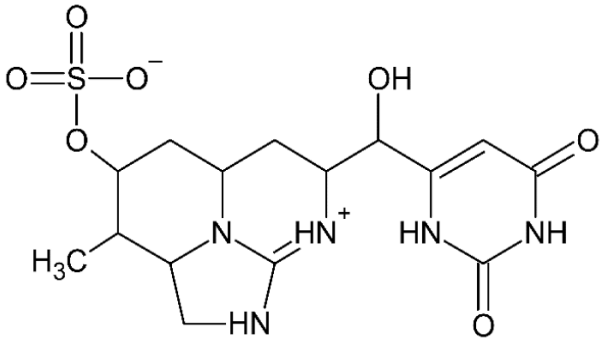

Fig. 1.2.Chemical structure of cylindrospermopsin

CYN is a zwitterion at neutral pH (Onstad et al., 2007) and hence highly water soluble (Griffiths and Saker, 2003). CYN is chemically stable under acidic and neutral pH, and between 4 and 100 °C (Adamski et al., 2016a; Chiswell et al., 1999). Moreover, photodegradation in natural environments is very limited and it mainly depends on UV-A (315–400 nm) radiation. Besides, photodegradation will be influenced by light penetration on the water column, and

thus, it is related to the turbidity and the suspended particles in water (Wörmer et al., 2010). Due to its physicochemical properties, CYN is a highly persistent compound in aquatic environments.

CYN is produced by several cyanobacterial strains including *Cylindrospermopsis raciborskii*, *Umezakia natans*, *Chrysosporum* sp., *Aphanizomenon* sp., *Microseira wollei*, *Anabaena* sp., and *Oscillatoria* sp. (Kokociński et al., 2017). CYN has been reported worldwide, and it is the second most reported cyanotoxin in Europe (Svirčev et al., 2019). Detected concentrations of CYN are usually below 10 μg L^{-1}. However, values up to 202 μg L^{-1} in natural environments have been reported (Rzymski and Poniedziałek, 2014). The highest CYN values in water systems measured are 589 and 800 μg L^{-1} in an aquaculture pond and in a farm dam, respectively (Saker and Eaglesham, 1999; Shaw et al., 2000).

CYN is mainly excreted by the cyanobacterial cells, and therefore 56–98% of CYN occurs extracellularly (Bormans et al., 2014; Preußel et al., 2009; Rücker et al., 2007), with the highest CYN concentration detected at the senescence of the cells (Chiswell et al., 1999; Davis et al., 2014).

The biological role of CYN has not been completely elucidated. The main hypothesis are i) that CYN works as an allelopathic compound to favour the production of alkaline phosphatase by other organisms to increase the amount of inorganic phosphate available for the CYN producer, and ii) that CYN works as grazing defence (Holland and Kinnear, 2013).

CYN is toxic to humans, and other organisms including, mammals, plants, fish, amphibians, molluscs, and crustaceans (de la Cruz et al., 2013; Kokociński et al., 2017). Bioaccumulation of CYN by some organisms like fish or plants also represent a potential risk for other organisms in higher trophic levels, including humans (Berry et al., 2012; Gutiérrez-Praena et al., 2013; Kinnear, 2010). Therefore, the presence of CYN represents a human health and an environmental problem. The first known human poisoning by CYN was the so-called Palm Island mystery disease in 1979. At that time, a hepatoenteritis outbreak was reported a few days after an algal bloom in the major water supply for the island, the Solomon dam, was treated with copper sulfate (Bourke et al., 1983; Byth, 1980; Griffiths and Saker, 2003). Years later, CYN produced by *Cylindrospermopsis raciborskii* was found as the most likely cause of the outbreak in Palm Island (Griffiths and Saker, 2003; Hawkins et al., 1985).

In humans and animals, the main target organs of CYN are the liver and the kidneys. Hepatic damage follows four consecutive phases, namely, protein synthesis inhibition, membrane proliferation, accumulation of fat droplets, and necrosis (Terao et al., 1994). Renal damage is related with the negative effects on the proximal and distal tubules (Falconer et al., 1999; Humpage and Falconer, 2003; Moraes and Magalhães, 2018; Terao et al., 1994).

Nevertheless, CYN affects also other organs including lungs, thymus, bone marrow, gastrointestinal tract, immune and nervous systems, and heart (Díez-Quijada et al., 2019; Falconer et al., 1999; Guzmán-Guillén et al., 2015; Humpage et al., 2000; Kubickova et al., 2019a, 2019b; Moraes and Magalhães, 2018; Oliveira et al., 2012; Seawright et al., 1999; Shaw et al., 2000; Terao et al., 1994).

The toxicity mechanism of CYN is mainly related to protein synthesis inhibition and oxidative stress. CYN inhibits protein synthesis by the detachment of ribosomes from the rough surfaced endoplasmic reticulum, leading to an accumulation of free ribosomes in the cytoplasm of the cells (Terao et al., 1994).

Oxidative stress is the imbalance of reactive oxygen species and the antioxidant response. It can be to the result of an increase in the reactive oxygen species or a decrease in the antioxidant cellular capacity (Sies, 1997). Oxidative stress affects the cellular macromolecules like proteins and lipids, which lead to an enzymatic inactivation, lipoperoxidation, DNA damage and finally to cell death (Pizzino et al., 2017; Winston and Di Giulio, 1991). CYN produces oxidative stress by different mechanisms including the inhibition of glutathione synthesis (Humpage et al., 2005; Runnegar et al., 2002), and the production of reactive oxygen species (Liebel et al., 2015; López-Alonso et al., 2013). Furthermore, CYN induces the upregulation of the genes encoding enzymes of the antioxidant response like catalase and thioredoxin reductase (Štraser et al., 2013).

The activation of CYN by cytochrome P450 is also considered relevant for its toxicity (Humpage et al., 2005; Pichardo et al., 2017). Administration of cytochrome P450 inhibitors like proadifen or ketoconazole reduced the toxicity of CYN on Swiss albino male mice, but it does not prevent protein synthesis inhibition (Froscio et al., 2003). A similar effect was observed when primary mouse hepatocytes were exposed to CYN. DNA damage was reduced with the administration of cytochrome P450 inhibitors (Humpage et al., 2005). Moreover, CYN induces the upregulation of different genes related to the expression of phase I and phase II enzymes involved in xenobiotics detoxification processes, evidencing a metabolic detoxification response (Štraser et al., 2013). However, phase I metabolites were not detected in HepaRG cells exposed to CYN, suggesting only a minor role of phase I metabolism in CYN toxicity (Kittler et al., 2016). Despite the lack of phase I metabolites detection in HepaRG cells, *in vivo* assays have evidenced the importance of CYN activation by cytochrome P450 in its toxicity mechanism (Norris et al., 2001).

1.3.1 Cylindrospermopsin transformation processes

Considering the threat that CYN represents to humans, animals, and the environment in general, it is important to develop safe and efficient CYN removal processes from water and to understand its fate in the environment for an improved risk assessment.

To date, different physicochemical reactions have been proposed for the efficient removal of CYN. Powdered activated carbon removed up to 20 μg L^{-1} of CYN (Ho et al., 2011). However, the use of activated carbon represents only a transfer of CYN to another material which will require further treatment to eliminate the adsorbed CYN. Other processes such as chlorination and ozonation transformed CYN at concentrations from 0.1 to 8.3 mg L^{-1} (León et al., 2019; Merel et al., 2010; Senogles-Derham et al., 2003; Yan et al., 2016). Photocatalysis, using TiO_2 and different wavelengths of light (Adamski et al., 2016b; Fotiou et al., 2015; León et al., 2019; G. Zhang et al., 2015), and advanced oxidation processes (He et al., 2014a, 2014b; Song et al., 2012), using hydroxyl and sulfate radical species, transformed efficiently CYN at concentrations up to 8.3 mg L^{-1}.

Several transformation products formed by the physicochemical transformation of CYN have been identified. Some transformation products are similar among different treatments, but the type of transformation products depends on the transformation method. Generally, it was observed that disregarding the transformation method used, the main CYN transformation reactions were oxidation, hydrogen abstraction, hydroxylation, and loss of the sulfate group. Besides, it was generally concluded that the most susceptible part of CYN to be transformed is the uracil moiety (Adamski et al., 2016b; Fotiou et al., 2015; He et al., 2014a, 2014b; León et al., 2019; Merel et al., 2010; Song et al., 2012; Yan et al., 2016; G. Zhang et al., 2015).

Among the mechanisms implemented to remove toxic compounds from water are biologically mediated processes. Biological degradation or biodegradation refers to the process of breaking down an organic compound into smaller or less complex compounds through the activity of microorganisms (Joutey et al., 2013). When biodegradation produces mineral components such as carbon dioxide and water is known as mineralization (Knapp and Bromley-Challoner, 2003). When the process involves the modification of the original compound to produce modified chemical structures, without reaching the production of mineral components, is known as biological transformation or biotransformation (Pal, 2017).

Biotransformation might represent an economical, eco-friendly and sustainable alternative to the removal of cyanotoxins by conventional methods from water (Ho et al., 2012). Biotransformation has the potential to produce fewer toxic transformation products, as previously observed for microcystin (Kumar et al., 2019). Moreover, biological removal is likely one of the most important natural attenuation mechanisms for CYN in water bodies (de la Cruz

et al., 2013; Dziga et al., 2016; Smith et al., 2008). However, the results in this regard are contrasting. CYN was not removed by microbial communities from freshwater bodies in Spain, regardless of whether they were previously exposed to CYN or not (Wormer et al., 2008). In contrast, CYN was removed by microbial communities that were previously exposed to CYN from a dam in Australia (Smith et al., 2008). Furthermore, microbial communities that had not been previously exposed to CYN from sand filter sediments and groundwater from an aquifer north of Berlin, Germany removed CYN under aerobic conditions. The same microbial communities removed CYN faster after they had a previous exposure to CYN (Klitzke et al., 2010; Klitzke and Fastner, 2012). These studies suggest that biological removal of CYN by microbial communities will be influenced by the previous contact of the communities with CYN, as well as the presence and composition of organic matter and the microbial community.

Information about specific organisms that remove CYN is limited in comparison, for instance, with microcystin, the most studied cyanotoxin worldwide (Ho et al., 2012; Kumar et al., 2019). So far, reported CYN degraders include only probiotic bacteria (Nybom et al., 2008), and two organisms isolated from freshwater bodies with previous reports of cyanoHABs, *Aeromonas* sp. R6 (Dziga et al., 2016) and *Bacillus* sp. AMRI-03 (Mohamed and Alamri, 2012). Despite the description of microbial communities and isolated organisms that remove CYN, it remains unknown if CYN is mineralized or if CYN is transformed. In case CYN transformation took place, it is unknown which transformation products are formed during biological removal processes (Dziga et al., 2016; Klitzke et al., 2010; Mohamed and Alamri, 2012; Nybom et al., 2008; Smith et al., 2008).

1.3.2 Toxicity assessment of CYN transformation products

Toxic effects produced by CYN have been extensively reported using *in vivo* and *in vitro* models (Berry et al., 2009; Chernoff et al., 2018; Gutiérrez-Praena et al., 2012; Humpage and Falconer, 2003; Pichardo et al., 2017; L. Wang et al., 2020). However, toxicity of CYN transformation products obtained after water treatment by several processes has been barely investigated.

Different cell lines have been used for *in vitro* toxicity assessment of CYN transformation products including human hepatoma cell lines HepG2 and C3A (Yan et al., 2016; G. Zhang et al., 2015), and human intestinal cell line Caco-2 (Merel et al., 2010). These cell lines were used as models for the evaluation of the toxicity on liver and human intestinal ephitelium.

In vivo toxicity assays of CYN transformation products have been only performed on P53 transgenic mice (Senogles-Derham et al., 2003). This mouse model has an alteration on

the P53 gene, which is responsible of the suppression of tumours (Lozano, 2010). P53 mice are a good model for the evaluation of mutagenic cancer inducing compounds (Tennant et al., 1996).

Transformation products formed after chlorination and ozonation were non-toxic for Caco-2 (Merel et al., 2010) and HepG2 cells (Yan et al., 2016). Nevertheless, 40% of male P53 transgenic mice exposed to the transformation products formed by chlorination showed liver fatty vacuolation (Senogles-Derham et al., 2003). No toxicity was reported when C3A cells were exposed to the transformation products formed after treatment of CYN with TiO_2 photocatalysis (G. Zhang et al., 2015). Noteworthy, the toxicity of CYN transformation products formed by biotransformation, and other photocatalytic or advanced oxidation processes was not always tested (Merel et al., 2010; Senogles-Derham et al., 2003; Yan et al., 2016; G. Zhang et al., 2015), and therefore, the information in this regard is scarce.

1.4 Manganese-oxidizing bacteria (MOB)

Manganese is the third most abundant transition metal in the Earth's crust (Yaroshevsky, 2006), and occurs in different oxidation states of which Mn^{2+}, Mn^{+3} and Mn^{4+} have biological significance (Geert Jan Brouwers et al., 2000). Manganese is soluble when Mn^{2+} occurs as a divalent cation together with chloride or sulfate, and is poorly soluble when it occurs together with carbonate or phosphate as Mn^{2+}, in complex with other ligands, and as oxides with an oxidation state of Mn^{3+} and Mn^{4+} (Tebo et al., 2004). Manganese oxides can be formed by abiotic and biotic processes. However, the oxidation of Mn^{2+} to Mn^{3+}/Mn^{4+} is largely accelerated by the activity of microorganisms such as bacteria and fungi (Tebo et al., 2005).

Iron is the most abundant transition metal in the Earth's crust (Yaroshevsky, 2006), and resembles manganese in several biochemical characteristics. For instance, manganese and iron are two ubiquitous abundant transition metals with a solubility-dependence on their redox state (Richardson and Nealson, 1989). Iron occurs in nature mainly as Fe^{2+} or Fe^{3+}, and the oxidation of Fe^{2+} forms insoluble oxides similar to those formed from Mn^{2+} oxidation. Manganese and iron are micronutrients, namely, at low concentrations both play a biological role as cofactor or as part of metalloenzymes and even the substitution of manganese in iron-containing enzymes has been even suggested (German et al., 2016), but at high concentrations they might be toxic for the cells (German et al., 2016; Kehl-Fie and Skaar, 2010).

Despite the multiple similarities between manganese and iron, one of the main differences between them is the stability of their reduced state. At circumneutral pH in aerobic

conditions Mn^{2+} is stable (Emerson, 2000; Ghiorse, 1984) and therefore in nature, its oxidation is mainly related to biological activity. In contrast, Fe^{2+} at circumneutral pH in aerobic conditions is highly susceptible to abiotic oxidation. However, under microaerophilic conditions or complexed by organic molecules, stability of Fe^{2+} increases and biological iron oxidation regains importance (Hedrich et al., 2011; Kappler et al., 2015; Maisch et al., 2019; Szewzyk et al., 2011).

Numerous bacterial groups are able to oxidize Mn^{2+} and Fe^{2+} (Corstjens et al., 1997, 1992; Schmidt, 2018; Schmidt et al., 2014). Through the oxidation of Mn^{2+} and Fe^{2+} these bacterial groups produce water-insoluble biogenic metal oxides and play therefore a pivotal role in the biogeochemical cycle of manganese, iron and other elements (Emerson, 2000; Tebo et al., 2005). In addition, manganese oxides often interact with other metals. For instance, the interaction of manganese oxides with iron forms ferromanganese oxides that are commonly found in the nature as ferromanganese crusts in various environments (Lee and Xu, 2016; Stein et al., 2001; Szewzyk et al., 2011; Vesper, 2012) including the deep sea and the ocean floor (Hein and Koschinsky, 2013), freshwater bodies (Strakhovenko et al., 2018), and soil (Timofeeva, 2008).

The growth of manganese- and iron-oxidizing bacteria, and the formation of ferromanganese oxides has furthermore been related to the clogging of water distributions pipes (Emerson, 2000; Szewzyk et al., 2011).Even though this group of organisms is often referred to as iron/manganese bacteria the term manganese oxidizing bacteria (MOB) will be used to refer to this group in the following due to the focus of the present thesis on the relevance of biological Mn^{2+} oxidation.

MOB reported to date belong to different phyla including Firmicutes, Proteobacteria, Actinobacteria, Bacteroidetes, and Cyanobacteria (Fig. 1.3) (Zhou and Fu, 2020). This broad phylogenetic affiliation is also associated with the highly metabolic variability among the MOB, (e.g. autotrophs, and heterotrophs). MOB are ubiquitous in nature, being reported in freshwater, marine and terrestrial ecosystems (Tebo et al., 2004; Zhou and Fu, 2020), but also in technical water systems (Cerrato et al., 2010; Marcus et al., 2017). In natural environments, MOB may coexist with different organisms including potentially toxigenic cyanobacteria (Santelli et al., 2014; Stein et al., 2001). Mechanisms of biological manganese oxidation are diverse and could be classified in two main groups: enzyme-mediated direct oxidation and non-enzyme mediated indirect oxidation (Hansel and Learman, 2015; Zhou and Fu, 2020).

To date, enzymes implicated in the enzyme-mediated direct Mn^{2+} oxidation by heterotrophic MOB are multicopper oxidases (MCOs) and haem peroxidases (Geszvain et al., 2012; Hansel and Learman, 2015; Zhou and Fu, 2020).

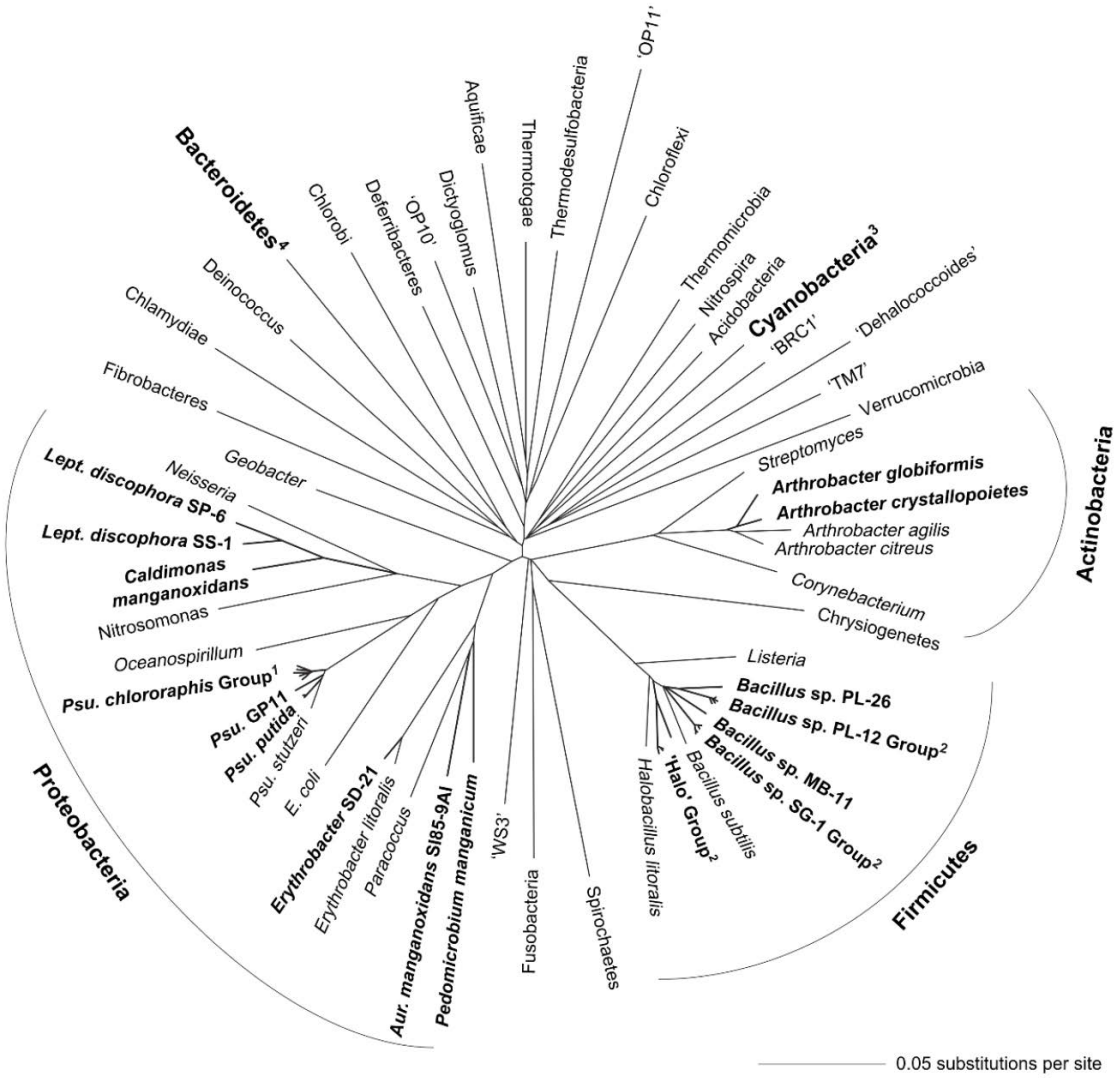

Fig. 1.3. Phylogenetic tree based on 16S rDNA sequences. Representative MOB are highlighted in bold. Superscript numbers represent that there is at least one reported organism belonging to that group, but not necessarily that all the family members are MOB. [1,2]Tebo et al. (2005), [3]Chaput et al. (2019), and [4]Akob et al., (2014) and Bohu et al. (2016) Lept.: *Leptothrix*; Psu.: *Pseudomonas*. Modified figure from Tebo et al. (2005, 2004).

MCOs are a family of enzymes that catalyzes an oxidation-reduction reaction (Soldatova et al., 2017; Spiro et al., 2008). MCOs have a broad substrate specificity and possess four characteristic copper-binding motifs (A-D) (Geszvain et al., 2012; Sakurai and Kataoka, 2007). In general, MCOs oxidize their substrates through the removal of one electron. However, in the case of MCO Mn^{2+} oxidation activity, the oxidation is catalysed via two sequential one-electron transfer steps that produce Mn^{3+} as intermediate. This two-electron transfer oxidation activity differentiates the Mn^{2+} oxidase MCOs from the non Mn^{2+} oxidases (Geszvain et al., 2012). However, not all multicopper oxidases mediate Mn^{2+} oxidation. So far, little is known about the structural determinants in multicopper oxidases related to Mn^{2+} oxidation activity (Zhou and Fu, 2020). Manganese-oxidizing multicopper oxidases have been

described in different organisms such as *Leptothrix discophora* SS-1 (Corstjens et al., 1997), *Pedomicrobium* sp. ACM 3067 (Ridge et al., 2007), *Bacillus* sp SG-1 (Gregory J Dick et al., 2008), and *Pseudomonas putida* GB-1 (Geszvain et al., 2013).

Animal haem peroxidases are enzymes with hemolysin-type calcium binding domains that catalyze the hydrogen peroxide-mediated oxidation of different substrates (Zámocký et al., 2015). Similarly as MCOs, not all haem peroxidases mediate Mn^{2+} oxidation. So far, the structural determinants in haem peroxidases related to Mn^{2+} oxidation activity are unknown (Zhou and Fu, 2020). Manganese-oxidizing haem peroxidases have been described in *Aurantimonas manganoxydans* SI85-9A1, *Erythrobacter* sp. strain SD-21 (Anderson et al., 2009), and *P. putida* GB-1 (Geszvain et al., 2016).

The non-enzymatic mediated indirect Mn^{2+} oxidation is carried out by the action of superoxide, an increase of pH by microbial metabolism, and anaerobic photo-driven processes (Zhou and Fu, 2020). In the superoxide-mediated manganese oxidation, the superoxide is produced extracellularly and then it interacts and oxidizes Mn^{2+}. This oxidation process was observed for *Roseobacter* sp. Azwk-3b (Learman et al., 2011). Manganese oxidation through an increase in pH can occur naturally. When some organisms alkalinize their media by the production of pH-active metabolites and Mn^{2+} is present, manganese oxidation might take place. Indirect oxidation of Mn^{2+} due to the increase in pH in culture media has been reported in the presence of the green algae *Chlorella* sp. (Richardson et al., 1988), *Stenotrophomonas* sp., and *Lysinibacillus* sp. (Barboza et al., 2015). Recently, manganese oxidation driven by light in strictly anaerobic conditions by anoxygenic photosynthetic microorganism was described. However, the mechanism has not been characterized yet (Daye et al., 2019).

The physiological role of manganese oxidation is still unknown. Nevertheless, several hypotheses have been formulated on the physiological role of manganese oxidation. For instance, it was proposed that Mn^{2+} oxidation could provide energy to support the growth of bacteria, but no conclusive results were shown (Kepkay and Nealson, 1987). However, a recent study demonstrated for the first time, the chemolitoautotrophy via Mn^{2+} oxidation of a bacterium affiliated to the phylum *Nitrospirae, Candidatus* Manganitrophus noduliformans. Mn^{2+} oxidation by *Candidatus* Manganitrophus noduliformans follows a similar mechanism as the lithotrophic iron oxidation and the respiratory metal reduction, involving the activity of *c*-type cytochromes and porin–cytochrome *c* protein complexes (Yu and Leadbetter, 2020). Other proposed functions of Mn^{2+} oxidation are the protection against toxicity of organic compounds, and reactive oxygen species (Banh et al., 2013; Zerfaß et al., 2019), breakdown of organic matter into utilizable substrates (Jones et al., 2018; Sunda and Kieber, 1994), and as a carbon reservoir (Estes et al., 2017). Nevertheless, the precise physiological role of

manganese oxidation in the diverse manganese-oxidizing bacterial groups remains unknown (Zhou and Fu, 2020).

Owing to the ability of MOB to oxidize Mn^{2+}, and in some cases Fe^{2+}, MOB have been used for the simultaneous removal of Mn^{2+} and Fe^{2+} from drinking water systems as a reliable and energy-efficient alternative to the chemical oxidation processes (Bruins, 2016; Katsoyiannis and Zouboulis, 2006; Marsidi et al., 2018; Mouchet, 1992; Pacini et al., 2005; Tobiason et al., 2016). Additionally, it has been shown that MOB removed different recalcitrant organic and inorganic pollutants from water such as diclofenac, benzotriazole, 17 α-ethinylestradiol, bisphenol A, As(III), and Sb(III) (Meerburg et al., 2012; Sochacki et al., 2018; Tran et al., 2018; H. Wang et al., 2019; Wang et al., 2017; Watanabe et al., 2013; Y. Zhang et al., 2015). The transformation of these recalcitrant compounds involves the indirect reaction of the pollutants with the reactive Mn^{3+}/Mn^{4+} species formed through the oxidation of Mn^{2+} by active MOB. Reactive Mn^{3+}/Mn^{4+} species interact with the pollutant and are concomitantly reduced to Mn^{2+} (Meerburg et al., 2012; Tran et al., 2018). Genomic analysis of the metabolic potential and the Mn^{2+} oxidation mechanism of isolated MOB might provide useful information to further understand the possible applicability of these organisms for biotechnological purposes. The genome analysis of some MOB have been performed to gain a better insight into the mechanism of manganese oxidation (Gregory J. Dick et al., 2008; X. Wang et al., 2020). However, so far, no reported pollutant-removing MOB strains have been analyzed on a genomic level to determine their metabolic potential.

Altogether, MOB might be promising candidates for future implementation for the removal of CYN from water. Moreover, considering the wide distribution of MOB in aquatic environments and their co-existence with potentially toxigenic cyanobacteria and their secondary metabolites, such as CYN, MOB might play an important role in the natural attenuation of CYN in natural aquatic environments.

1.5 Goal of this thesis

This thesis aims i) to investigate the CYN degradation by MOB, ii) to identify if MOB mineralized or transformed CYN, and if so, which transformation products were produced, and ii) to assess the cytotoxicity of the mixture of CYN transformation products against human hepatic cell lines compared to CYN, considering that the liver is the main target organ. For that purposes four MOB strains isolated from natural and technical systems under laboratory conditions were used. MOB used in the present study were *Pseudomonas* sp. OF001, *Ideonella* sp. A288 and A226, and *Rubrivivax* sp. A210. All tested MOB belong to the bacterial collection of the Laboratory of Environmental Microbiology, where the present thesis was

developed. In addition to the general introduction, this thesis consists of four chapters. A general description and particular objectives of each chapter are outlined below.

- In **chapter 2,** we aim to investigate the removal of CYN by MOB based on three main objectives. First, we focused on the influence of different factors on the removal of an environmentally relevant CYN concentration by MOB, including the presence and the absence of Mn^{2+} and/or Fe^{2+}, the type of Mn^{2+} source, and the absence of an additional carbon source. Second, we analysed the correlation between the amount of oxidized manganese and CYN removal. And third, we evaluated the contribution of active MOB in comparison with sterile biogenic oxides on the removal of CYN.
- In **chapter 3**, we aim to investigate the biological transformation of CYN by MOB based on two main objectives. First, we focused on the identification and comparison of transformation products formed by MOB to previously reported transformation products formed by different abiotic processes. And second, we evaluated the cytotoxicity of the mixture of transformation products against human hepatic cell lines, HepG2 and HepaRG cells, in comparison to CYN.
- In **chapter 4**, we aim to deepen our understanding of the metabolic potential of *Pseudomonas* sp. OF001 and *Rubrivivax* sp. A210 for their further applicability for pollutants removal. Besides, this information might help to better understand the role of MOB in natural environments. We established three main objectives, based on the analysis of their draft genomes. First, we focused on the *in silico* identification of enzymes potentially involved in manganese-oxidation. Second, we analysed the genome to identify relevant metabolic pathways including those related to energy harvesting and pollutants removal. And third, we studied the genome plasticity related to horizontal gene transfer mechanisms.
- In **chapter 5**, I aim to further investigate the influence of different growth factors on the biological transformation of CYN by MOB. The growth factors tested in this chapter were the presence of Fe^{2+} and the absence of an additional organic carbon source. I focussed on the identification and comparison of transformation products formed by one MOB strain using previously reported transformation products formed by different physicochemical reactions and comparing them to the products formed by biological transformation by MOB reported in chapter 2.
- In **chapter 6**, I discuss in a general context the main results presented in chapters 2 to 5 focusing on the relevance of MOB i) for biotechnological application for CYN removal, and ii) their role in the attenuation of CYN in natural environments. Moreover, I present the outlook of this research project to continue with this investigation.

2 Manganese-oxidizing bacteria isolated from natural and technical systems remove cylindrospermopsin

This chapter is the accepted version of the article published as

Martínez-Ruiz, E.B., Cooper, M., Fastner, J., Szewzyk, U., 2020. Manganese-oxidizing bacteria isolated from natural and technical systems remove cylindrospermopsin. Chemosphere 238. https://doi.org/10.1016/j.chemosphere.2019.124625

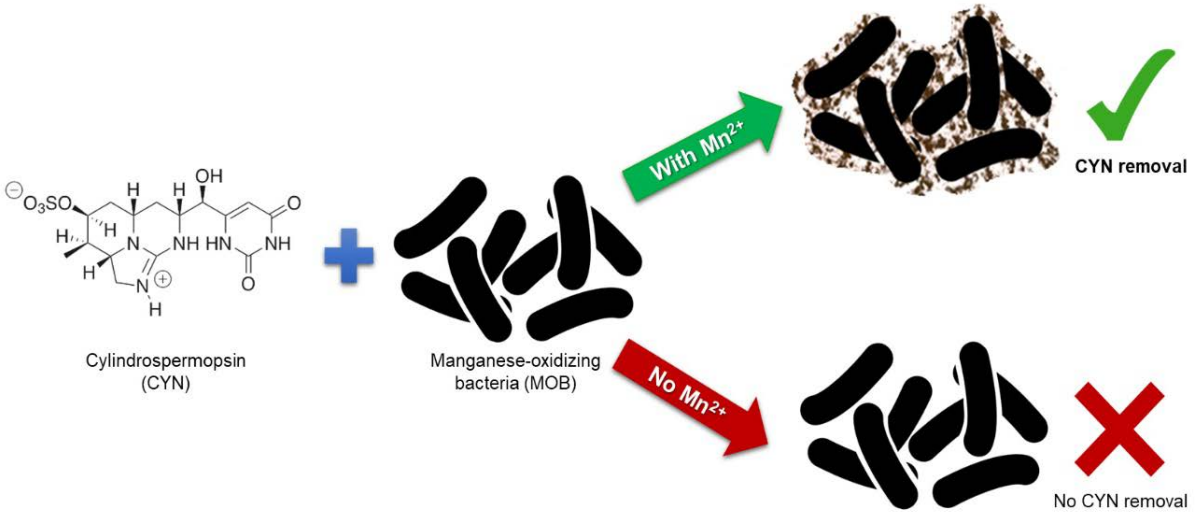

Abstract

The cyanotoxin cylindrospermopsin was discovered during a drinking water-related outbreak of human poisoning in 1979. Knowledge about the degradation of cylindrospermopsin in waterbodies is limited. So far, only few cylindrospermopsin-removing bacteria have been described. Manganese-oxidizing bacteria remove a variety of organic compounds. However, this has not been assessed for cyanotoxins yet. We investigated cylindrospermopsin removal by manganese-oxidizing bacteria, isolated from natural and technical systems. Cylindrospermopsin removal was evaluated under different conditions. We analysed the correlation between the amount of oxidized manganese and the cylindrospermopsin removal, as well as the removal of cylindrospermopsin by sterile biogenic oxides. Removal rates in the range of 0.4 - 37.0 mg L^{-1} day^{-1} were observed. When $MnCO_3$ was in the media *Pseudomonas* sp. OF001 removed ~100% of cylindrospermopsin in 3 days, *Comamonadaceae* bacterium A210 removed ~100% within 14 days, and *Ideonella* sp. A288 and A226 removed 65% and 80% within 28 days, respectively. In the absence of Mn^{2+}, strain A288 did not remove cylindrospermopsin, while the other strains removed 5-16%. The amount of manganese oxidized by the strains during the experiment did not correlate with the amount of cylindrospermopsin removed. However, the mere oxidation of Mn^{2+} was indispensable for cylindrospermopsin removal. Cylindrospermopsin removal ranging from 0 to 24% by sterile biogenic oxides was observed. Considering the efficient removal of cylindrospermopsin by the tested strains, manganese- oxidizing bacteria might play an important role in cylindrospermopsin removal in the environment. Besides, manganese-oxidizing bacteria could be promising candidates for biotechnological applications for cylindrospermopsin removal in water treatment plants.

Keywords: cyanotoxins, removal, manganese oxidation, biogenic oxides

2.1 Introduction

Cyanobacteria are prokaryotic organisms that can grow in different habitats such as seawater, freshwater, and soil; as well as in extreme environments like deserts, hot springs, and polar regions (Flombaum et al., 2013; Whitton and Pentecost, 2012). Some genera are considered toxigenic due to their ability to produce toxic chemical compounds known as cyanotoxins. They are responsible for the poisoning of humans, wild, and domestic animals (Wood, 2016). Cyanobacterial abundance increases as a consequence of eutrophication, raising the risk of intoxication due to the production of cyanotoxins (Merel et al., 2013).

Cylindrospermopsin (CYN) is an alkaloid cyanotoxin with a cyclic guanidine moiety bound to a hydroxymethyluracil group. It has various modes of action including hepatotoxicity, cytotoxicity, and neurotoxicity (Poniedziałek et al., 2012); and it is most likely the cause of the Palm Island mystery disease in 1979 (Griffiths and Saker, 2003).

CYN is produced by different cyanobacteria such as *Cylindrospermopsis raciborskii*, *Umezakia natans*, *Chrysosporum ovalisporum, Aphanizomenon* sp., and *Anabaena bergii* (Rzymski and Poniedziałek, 2014). It has been detected in America, Asia, Europe, Oceania, and even in Antarctica (Rzymski and Poniedziałek, 2014). In natural environments, the highest reported CYN concentrations are 120 μg L^{-1} in Queensland, Australia (Shaw et al., 1999), 126 μg L^{-1} in Italy (Messineo et al., 2009), and 202 μg L^{-1} in Florida, USA (Williams et al., 2006). A large fraction of CYN (56-98%) occurs extracellularly (Bormans et al., 2014; Rücker et al., 2007) with the highest concentration detected at the end of the cyanobacterial bloom (Chiswell et al., 1999).

CYN is chemically stable and highly persistent in aquatic environments (Wormer et al., 2008). Photodegradation of CYN is limited and dependent on the depth in the water column, showing lower degradation at greater depth (Wörmer et al., 2010). Removal of CYN by indigenous organisms was observed in sediments from Berlin, Germany (Klitzke et al., 2010) and in sludge from a drinking water treatment plant from Quebec, Canada (Maghsoudi et al., 2015). Removal of CYN was also reported in samples from a dam in Queensland, Australia (Smith et al., 2008). In contrast, no removal was observed using samples from freshwater bodies with and without previous exposure to CYN from Madrid, Spain (Wormer et al., 2008) and using samples from a lake without history of CYN from Missisquoi Bay, Canada (Maghsoudi et al., 2015).

In natural environments, such as freshwater systems, cyanobacteria may coexist with different organisms including manganese-oxidizing bacteria (MOB) (Santelli et al., 2014; Stein et al., 2001). MOB belong to different phylogenetic lineages with a broad physiological diversity including, for example autotrophic and heterotrophic organisms. MOB are widely distributed in

nature, and are also detected in drinking water systems (Tebo et al., 2005). MOB are able to oxidize Mn^{2+}, precipitating biogenic manganese oxides and thus playing an important role in the biogeochemical cycle of manganese and other elements (Tebo et al., 2004). The physiological role of Mn^{2+} oxidation is still unknown and is not essential for the survival of MOB (Spiro et al., 2008). Biogenic manganese oxides often interact with different metals. Ferromanganese (Fe and Mn) oxides are one of the most common in the nature. Biogenic manganese oxides are considered strong oxidants (Tebo et al., 2004), being able to oxidize a variety of organic and inorganic compounds (Hennebel et al., 2009). However, several *in vitro* studies showed that the active MOB, and not only the biogenic oxides, play an important role in the removal of organic pollutants (Meerburg et al., 2012; Sochacki et al., 2018; Tran et al., 2018). Thus, metabolic activity of MOB is considered to be essential for the removal of organic pollutants due to the formation of Mn^{3+} intermediates by biological Mn^{2+} oxidation (Meerburg et al., 2012; Tran et al., 2018).

MOB remove highly recalcitrant substances and may coexist in freshwater environments with cyanobacteria. To the best of our knowledge, the removal potential of CYN by MOB has not been investigated yet. Moreover, knowledge about isolated strains with the ability to remove CYN is still limited (Dziga et al., 2016; Mohamed and Alamri, 2012; Nybom et al., 2008). Therefore, in this study we evaluated CYN removal by different MOB strains isolated from natural and technical systems.

To investigate the removal of CYN by MOB, we focused especially on i) the influence of Mn^{2+} and/or Fe^{2+} and ii) the type of Mn^{2+} source on CYN removal. We also focused on iii) the correlation between the amount of oxidized manganese and CYN removal, iv) the role of active MOB on the removal of CYN compared to sterile biogenic oxides (BioOx), and v) the CYN removal in the absence of an additional carbon source. Selection of the parameters to be evaluated were chosen considering the isolation source, and the laboratory conditions under which these MOB have been cultivated.

2.2 Material and methods

2.2.1 Strain identification and culture conditions

Four aerobic neutrophilic MOB strains were obtained from the culture collection of the Laboratory of Environmental Microbiology from the Technical University of Berlin (TU Berlin), Germany. Based on preliminary tests and considering their isolation source, four MOB were selected: *Pseudomonas* sp. OF001, *Comamonadaceae* bacterium A210, *Ideonella* sp. A226, and *Ideonella* sp. A288. Strain OF001 was isolated from the effluent of an experimental fixed-bed biofilm bioreactor established for the removal of recalcitrant substances from wastewater

operated by the Laboratory of Environmental Process Engineering (TU Berlin). Strains A288, A210, and A226 were isolated from an iron manganese-depositing biofilm in a freshwater pond in the Lower Oder Valley National Park, Germany.

2.2.1.1 DNA extraction and PCR amplification

Cells from a pure 50 mL liquid culture from each strain were harvested by centrifugation at 15,000 x *g* for 3 min and washed three times with sterile Milli Q water under sterile conditions. DNA was extracted using the GeneMATRIX Soil DNA Purification Kit (EUR_X Gdańsk, Poland) following the manufacturer's instructions. The extracted genomic DNA was used as a template for the amplification of the 16S rDNA using the 63F forward and 1387R reverse primers previously reported by Marchesi et al. (1998) (PCR reaction mixture and cycling conditions shown in Appendix, Table A1 and A2). PCR products were purified (DNA Clean and Concentrator ® -5 kit, Zymo Research Europe GmbH, Freiburg, Germany) and Sanger sequenced in both directions (LGC Genomics, Berlin, Germany). Quality assessment was performed in Chromas v2.6.4. Obtained sequences were submitted to the NCBI Genbank (Accession numbers MK599476- MK599479).

We created a dataset of our sequences and closely related reference and non-reference sequences from the GenBank. They were aligned using MUSCLE (Edgar, 2004) in MEGA v7.0.25.

A phylogenetic tree was constructed with Bayesian inference (MrBayes v3.2.6 [Huelsenbeck and Ronquist, 2001; Ronquist and Huelsenbeck, 2003]) and Maximum Likelihood method (PhyML v3.1 [Guindon et al., 2010]). A bootstrap analysis was performed with 1000 replicates for the Maximum Likelihood tree, and also the MCMC for the Bayesian Inference with 1,000,000 generations was done. The trees were visualized using the software FigTree v1.4.4.

Consensus and summarization of both Maximum Likelihood and Bayesian Inference analysis tree was generated using DendroPy package v4.3.0 and SumTrees.py (Sukumaran and Holder, 2010), according to the default settings of a 50% majority-rule consensus tree.

2.2.1.2 Culture conditions

Bacteria were cultivated routinely in a medium developed for *Leptothrix* strains (Atlas, 2010), which was modified by our research group. This modified medium is referred to as LSM2 (medium content is shown in Appendix, Table A3). The pH of the medium was adjusted

to 7.2 before autoclaving. The medium was chosen because it was used for the isolation of MOB.

For the inoculum of the batch removal experiments, 300 µL of the culture in LSM2, were transferred to LSM2 without Fe^{2+} and Mn^{2+}. Cultures were cultivated twice in LSM2 without Fe^{2+} and Mn^{2+} previous to the removal assay, to ensure the absence of manganese and/or iron deposits in the inoculum. Flasks were incubated at room temperature (20.8 ± 2.2 °C) with shaking at 110 rpm.

For the production of BioOx, bacteria were grown in LSM2 without Fe^{2+} and Mn^{2+}, under the conditions above described. From the cultures in the exponential phase, 300 µL was transferred to media with $MnCO_3$ (setup 4 no Fe^{2+}) or $MnSO_4$ (setup 7 with $MnSO_4$) as the Mn^{2+} source (Table 2.1). Cultures were incubated for 2 days (*Pseudomonas* sp. OF001) or 14 days (other strains). Oxides produced in setup 7 are referred to as BioOx-S7 and oxides produced in the setup 4 are referred to as BioOx-S4.

Table 2.1. Media components of the setups used for the batch removal assays.

	Setup*						
	1 with buffer	2 no buffer	3 no Mn^{2+} no Fe^{2+}	4 no Fe^{2+}	5 no Mn^{2+}	6 no YE	7 with $MnSO_4$
NH_4Cl[a]	✓	✓	✓	✓	✓	✓	✓
$MnCO_3$ H_2O[a]	✓	✓	-	✓	-	✓	-
$MnSO_4$ H_2O[b]	-	-	-	-	-	-	✓
Yeast extract[a] (YE)	✓	✓	✓	✓	✓	-	✓
$Fe(NH_4)(SO_4)_2 \cdot 6$ H_2O[a]	✓	✓	-	-	✓	✓	✓
HEPES buffer[a]	✓	-	✓	✓	✓	✓	✓

*A short name for each setup was assigned according to the most representative characteristic of the composition of the medium. YE: yeast extract.
[a]: Concentration as it is described for LSM2 in table S3
[b]: 0.05 g L^{-1} as in the DSMZ Medium 803 (Atlas, 2010).
✓: added to the medium
-: not present in the medium

Subsequently, NaN_3 was added to the cultures to a final concentration of 30 mM to inactivate the cells. The cultures were incubated for an additional 24 h under the same conditions. BioOx from each flask were harvested by centrifugation at 15,000 x g for 3 min and washed three times with sterile Milli Q water under sterile conditions. Oxides derived from the four strains were transferred to independent sterile glass Petri dishes (60 x 17 mm). The remaining water was evaporated from the closed Petri dishes at 60 °C, followed by a dry heat

treatment at 120°C for 30 min. Oxidative activity of the BioOx was qualitatively confirmed using the redox indicator *N,N*-Dimethyl-*p*-phenylenediamine (data not shown). Inactivation of cells was evaluated qualitatively by streaking the culture onto solid LSM2 after the dry heat treatment. Inactivation of cells was considered succesful when no growth was detected after one month.

2.2.2 Batch removal assays

Pure CYN (>95% purity) was purchased from Enzo Life Science, Inc (New York, USA) and was resuspended with sterile Milli Q water to a final concentration of 500 mg L^{-1}.

Seven setups were used to evaluate the removal of CYN under different conditions. All the setups were prepared with 0.3 g L^{-1} NH_4Cl, 2 mL L^{-1} of trace elements solution and 2 mL L^{-1} of vitamin solution in Milli Q water as described in section 2.2.1. The pH of the medium was adjusted to 7.2 before autoclaving. All the other compounds were added according to the parameter to be analyzed (Table 2.1). Setups 1 and 2 were used to evaluate how pH variations in a buffered and in an unbuffered system affect the removal of CYN as pH has been considered a relevant parameter for the removal of CYN (Adamski et al., 2016a; Dziga et al., 2016; Mohamed and Alamri, 2012). It was investigated with setup 3 if CYN was removed by MOB in the simultaneous absence of Mn^{2+} and Fe^{2+}. In setup 4 and 5 it was evaluated whether the presence of only Fe^{2+} or only Mn^{2+} was essential for bacteria to remove CYN, respectively. Mn^{2+} oxidation is not essential for the survival of the MOB, and previous studies showed the importance of Mn^{2+} oxidation in the removal of recalcitrant substances (Meerburg et al., 2012; Sochacki et al., 2018; Tran et al., 2018). Mn often forms mixed oxides with iron and the strains used in this study were isolated using iron and manganese containing media. Tested strains were isolated and are routinely maintained in medium with yeast extract as the sole organic carbon source. It was determined with setup 6, whether MOB removed CYN when it was the sole organic carbon source available for growth. On a routine basis, the tested MOB are cultivated using $MnCO_3$ as the Mn^{2+} source, however the removal of other organic recalcitrant pollutants has been achieved using soluble Mn^{2+} sources like $MnSO_4$ or $MnCl_2$. For that reason, the influence of the type of Mn^{2+} source on CYN removal was evaluated in setup 7 by replacing $MnCO_3$ with $MnSO_4$. The concentration of total Mn^{2+} using $MnCO_3$ was 15 mM and using $MnSO_4$ was 0.3 mM. Different concentrations of $MnCO_3$ and $MnSO_4$ had to be applied because growth and Mn^{2+} oxidation of the strains was negatively affected when higher concentrations of $MnSO_4$ were used (data not shown). For that reason, the initial concentration of $MnSO_4$ in setup 7 was used as it is referred for the DSMZ medium 803 (Atlas, 2010). MOB in the media with either $MnCO_3$ or $MnSO_4$ formed BioOx, visually identifiable as brown dark

aggregates (Appendix, Fig. A1). BioOx were not observed in the absence of Mn^{2+} nor in the control (growth media without bacteria).

Bacteria were inoculated using 300 µL of the cultures described in *section 2.2.1.2* at exponential growth ($OD_{600\ nm}$) in sterile 100 mL Erlenmeyer flasks with 50 mL of medium. CYN was added to a mean final measured concentration of 118 µg L^{-1}. Bacteria were incubated in the dark under the conditions described in section 2.2.1.2. In order to evaluate the abiotic removal of CYN, flasks with medium and CYN but without bacteria were used as a control for each setup.

Three independent replicates were run per strain, as well as for the negative control.

The tested strains have different growth rates. In medium LSM2 without Mn^{2+} and Fe^{2+}, *Pseudomonas* sp. OF001 reached the exponential growth phase in less than 3 hours, *Ideonella* sp. A288 and A226 after 48 h, and strain A210 after 96 h. Based on the growth rates, samples were taken at specific intervals: daily during three days from the culture of *Pseudomonas* sp. OF001 and every 7^{th} day during 28 days from the cultures of the other three strains. The same scheme was followed for the negative controls. pH, and concentration of CYN and oxidized manganese in the media were quantified for the samples. At the end of each assay, the viability and purity of cells were evaluated qualitatively by inoculation onto solid LSM2 and incubation at room temperature (20.8 ± 2.2 °C). The same procedure was followed for the controls in order to discard any contamination.

We evaluated CYN concentration at the beginning and at the end of every experiment in all the setups of each strain. However, CYN concentration in mid time points was quantified at discrete time points according to the removal observed at the end of each experiment.

We quantified the evaporation of the media in the 28 days' assays (data not shown). The evaporation of media explains the apparent increase amount of 10-17% of CYN per mL observed in the controls (Fig. 2.1a-d).

2.2.3 CYN quantification

To determine CYN concentrations in controls and bacteria flasks, 1 mL samples were centrifuged at ~10,000 x g for 10 min at 4°C and filtered using 0.2 mm PVDF membranes in order to obtain supernatants free of bacteria and oxides. They were stored at -20°C until analysis. CYN concentrations were determined by liquid chromatography combined with tandem mass spectrometry (LC-MS/MS) using an Agilent 1290 series HPLC system (Agilent Technologies, Waldbronn, Germany) coupled to a API 5500 QTrap mass spectrometer (AB Sciex, Framingham, MA, USA) equipped with a turbo-ion spray interface (Appendix, Fig. A2) (Fastner et al., 2018).

The limit of quantification (LOQ) was 0.2 µg L^{-1}.

2.2.4 pH and oxidized manganese concentration

For pH measurements, 600 µL was taken from each replicate and pooled, to have a total of 1.8 mL per each setup from every strain and their respective controls. The sampling time followed the description in section 2.2.2.

The concentration of oxidized manganese was measured with the leucoberbelin blue I (lbb I) assay (Krumbein and Altmann, 1973), in setups in which Mn^{2+} was added (setups 1 with buffer, 2 no buffer, 4 no Fe^{2+}, 6 no YE, and 7 with $MnSO_4$). The leucobase is oxidized by either Mn^{3+} or Mn^{4+} to an intense blue reaction product. Therefore, the oxidized manganese in the present work represents both oxidized manganese forms. For the assay, 50 µL was taken from each flask and mixed with 250 µL of 0.04% lbb in 45 mM acetic acid. Samples were incubated for 20 min and centrifuged at 10,000 x g for 3 min. The absorbance at 630 nm was measured using $KMnO_4$ as standard.

2.2.5 CYN removal by BioOx

The removal of CYN by sterile BioOx formed in the absence of viable bacterial cells with either $MnCO_3$ or $MnSO_4$ as the Mn^{2+} source was evaluated.

BioOx were inoculated in separate flasks with 50 mL of media with the same composition as in the setups 4 (no Fe^{2+}) and 7 (with $MnSO_4$) with CYN at a final measured concentration of 123.5 µg L^{-1}. BioOx formed by *Pseudomonas* sp. OF001 were incubated for 7 days, while those produced by *Ideonella* sp. A288 and A226, and *Comamonadaceae* bacterium A210 for 28 days. The incubation times of the BioOx were chosen in order to compare the removal of CYN between BioOx without viable cells with the removal by active cells in a similar time. The concentration of CYN was quantified at the beginning and at the end of the assay.

2.2.6 Removal rate

The removal rate was calculated by dividing the difference of the initial CYN concentration and the lowest measured concentration, by the number of days in which the lowest CYN concentration was measured.

2.2.7 Statistical analysis

One-way analysis of variance (ANOVA) was performed to compare differences of total CYN removal, oxidized manganese concentrations, and CYN removal rates per day by the strains, followed by Dunnett's comparison test to evaluate statistical differences with the control, and by Tukey's pairwise comparison test for the multiple comparisons among setups, including control.

2.3 Results

CYN was removed by all strains under different cultivation conditions (Figures 2.1a–d.). However, different growth conditions influenced the efficiency of CYN removal. Overall, CYN removal rates between 0.38 and 37.01 µg L^{-1} day^{-1} were observed (Table 2.2).

2.3.1 Strain identification

To identify or confirm the identity of the bacterial strains, 16S rDNA sequences were evaluated. Based on the phylogenetic analysis with the 16S rDNA sequences (Appendix, Fig. A3), we determined that the isolate OF001 belongs to the genus *Pseudomonas*. The strain A226 is closely related to the *Ideonella* sp. strain A288, from which the whole genome has been sequenced (Braun et al., 2017). Based on the 16S rDNA and the phylogenetic analysis, no further classification to genus level was possible for strain A210. This organism is therefore referred to as a member of the *genera incertae sedis* of the *Comamonadaceae* family.

2.3.2 CYN removal in the presence of Mn^{2+} by MOB

To evaluate whether Mn^{2+} was required for the removal of CYN, we incubated MOB and CYN in media without a Mn^{2+} source or with $MnCO_3$ as the Mn^{2+} source. We observed that all tested MOB removed higher amount of CYN when $MnCO_3$ was added to the cultures than when no Mn^{2+} was provided (Table 2.2), demonstrating that the presence of Mn^{2+} improved CYN removal.

Pseudomonas sp. OF001 removed CYN at a higher rate and to a further extent than the other three tested strains (Fig. 2.1a). ~100% of CYN was removed by strain OF001 in all setups with $MnCO_3$ and yeast extract (setups 1 (with buffer), 2 (no buffer), and 4 (no Fe^{2+})) within 3 days, with a removal rate of about 36 µg L^{-1} day^{-1} (Table 2.2).

Table 2.2. Removal rates of the 4 MOB and % of CYN remaining in the different setups. Removal rates of the 4 MOB and % of CYN remaining in the different setups. Average values (n = 3). Removal time was calculated at the indicated time. *Indicates significant difference (P < 0.01) respect to control at the time given (Dunnett's test). Different letters indicate significant difference (P < 0.05) in accordance to Tukey's pairwise comparisons among the 4 strains. -: not evaluated

Setup	Strain	% CYN remaining	Time (d)	Removal rate (µg L^{-1} day^{-1})
S1 with buffer	*Pseudomonas* sp. OF001	< 1^{a*}	3	36.1^{a}
	Comamonadaceae bacterium A210	< 1^{a*}	14	8.6^{b}
	Ideonella sp. A226	44^{b*}	28	2.4^{c}
	Ideonella sp. A288	63^{b*}	28	1.6^{c}
S2 no buffer	*Pseudomonas* sp. OF001	1^{a*}	3	35.5^{a}
	Comamonadaceae bacterium A210	24^{b*}	28	3.1^{b}
	Ideonella sp. A226	43^{c*}	28	2.4^{b}
	Ideonella sp. A288	74^{d*}	28	1.1^{c}
S3 no Mn^{2+} no Fe^{2+}	*Pseudomonas* sp. OF001	107^{a}	3	0.0^{a}
	Comamonadaceae bacterium A210	90^{b*}	28	0.4^{b}
	Ideonella sp. A226	90^{b*}	28	0.4^{b}
	Ideonella sp. A288	114^{a}	28	0.0^{a}
S4 no Fe^{2+}	*Pseudomonas* sp. OF001	4^{a*}	3	37.0^{a}
	Comamonadaceae bacterium A210	< 1^{a*}	28	4.4^{b}
	Ideonella sp. A226	20^{b*}	28	3.4^{b}
	Ideonella sp. A288	35^{b*}	28	3.0^{b}
S5 no Mn^{2+}	*Pseudomonas* sp. OF001	95^{a}	3	0.0^{a}
	Comamonadaceae bacterium A210	84^{a*}	28	0.7^{b}
	Ideonella sp. A226	88^{a*}	28	0.5^{b}
	Ideonella sp. A288	112^{b}	28	0.0^{a}
S6 no YE	*Pseudomonas* sp. OF001	-	-	-
	Comamonadaceae bacterium A210	23^{a*}	28	3.3^{a}
	Ideonella sp. A226	91^{b*}	28	0.4^{b}
	Ideonella sp. A288	91^{b*}	28	0.4^{b}
7 with $MnSO_4$	*Pseudomonas* sp. OF001	78^{a*}	3	8.4^{a}
	Comamonadaceae bacterium A210	77^{a*}	28	1.0^{b}
	Ideonella sp. A226	82^{a*}	28	0.8^{bc}
	Ideonella sp. A288	103^{b}	28	0.0^{c}

Ideonella sp. A288 removed a higher amount of CYN in all setups with $MnCO_3$ and yeast extract than in the absence of both compounds. Strain A288 removed 65% of CYN with a removal rate of 3.0 µg L^{-1} day^{-1} in setup 4 (no Fe^{2+}) (Table 2.2). In setup 1 (with buffer) and in setup 2 (no buffer) strain A288 removed around one third (37%) and one fourth (26%) of the original CYN concentration within 28 days, respectively (Fig. 2.1b).

Comamonadaceae bacterium A210 showed higher CYN removal in all setups with $MnCO_3$ than in all other tested conditions. Strain A210 removed around 100% of CYN in 14 days in setup 1 (with buffer) and in 28 days in setup 4 (no Fe^{2+}) with removal rates of 8.6 and

4.4 µg L^{-1} day^{-1}, respectively (Table 2.2). Strain A210 removed 76% of the initial CYN concentration in setup 2 (no buffer) (Fig. 2.1c).

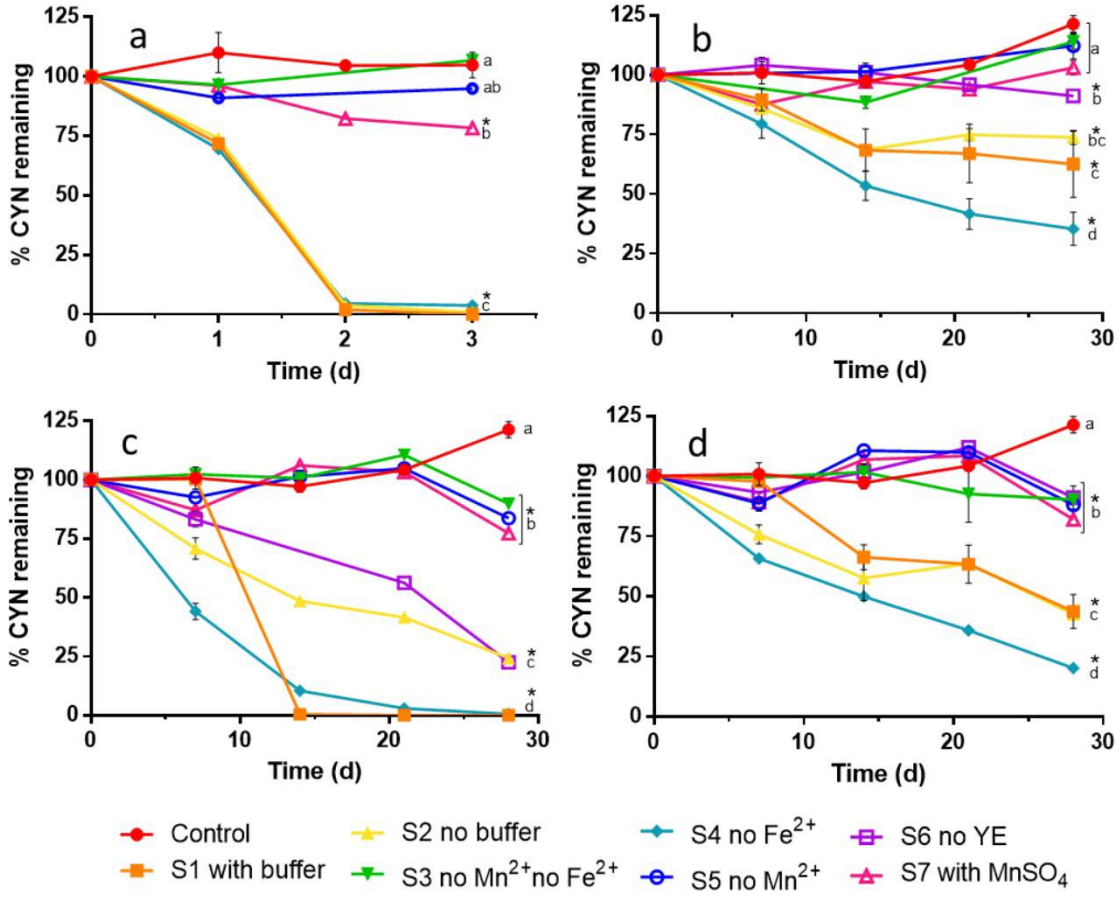

Fig. 2.1. CYN removal curves. a) *Pseudomonas* sp. OF001, b) *Ideonella* sp. A288, c) *Comamonadaceae* bacterium A210 and d) *Ideonella* sp. A226. Initial CYN concentration: 118 µg L^{-1}. Mean values ± standard error bars (n = 3). *Indicates significant differences respect to control (P < 0.05). S: setup; YE: yeast extract; % CYN remaining: concentration of CYN quantified in the medium with respect the initial concentration. Control group represents the mean of all the control flasks ± standard error (n = 18 for strain OF001 and n = 21 for the other strains). CYN concentration below the LOQ was taken as 0.1 µg L^{-1}.

Ideonella sp. A226 showed the highest removal in all setups with $MnCO_3$ and yeast extract. Strain A226 removed 80% of CYN in setup 4 (no Fe^{2+}) within 28 days, with a removal rate of 3.4 µg L^{-1} day^{-1} (Table 2.2). In setup 1 (with buffer) and 2 (no buffer), strain A226 removed around 56% of the initial CYN concentration in 28 days (Fig. 2.1d).

Pseudomonas sp. OF001 and *Ideonella* sp. A288 did not remove CYN in the absence of Mn^{2+} (Fig. 2.1a-d). *Comamonadaceae* strain A210 and *Ideonella* sp. A226 removed 10-16% of CYN when only Fe^{2+} instead of Mn^{2+} (setup 5), or neither Fe^{2+} nor Mn^{2+} (setup 3) was added to the media (Fig. 2.1a-d).

2.3.2.1 Influence of the Mn^{2+} source on CYN removal

To determine the influence of the Mn^{2+} source on the CYN removal by the tested strains, MOB were incubated using $MnSO_4$ (setup 7) instead of $MnCO_3$ as the Mn^{2+}. When $MnSO_4$ was added, all tested organisms removed CYN with lower removal rates than when $MnCO_3$ was added to the cultures (Table 2.2).

Pseudomonas sp. OF001 removed 22% of the initial CYN concentration, while *Comamonadaceae* bacterium A210 removed 23% (Fig. 2.1a and c). *Ideonella* sp. A226 removed 18% of CYN within 28 days (Fig. 2.1d). *Ideonella* sp. A288 did not remove CYN when $MnSO_4$ was used as the Mn^{2+} source indication that the type of Mn^{2+} source influenced CYN removal.

2.3.2.2 CYN removal in the presence of an additional carbon source

MOB were incubated without yeast extract (setup 6) to evaluate CYN removal in the absence of an additional organic carbon source.

Pseudomonas sp. OF001 did not grow without yeast extract, therefore the removal of CYN under this condition (setup 6) was not evaluated. *Ideonella* sp. A288 and A226 removed 9% of CYN within 28 days when no additional organic carbon source was added (Fig. 2.1b and d).

Comamonadaceae bacterium A210 removed 77% of the initial CYN concentration without yeast extract in the growth medium within 28 days. Strain A210 was the only organism among the tested bacteria that removed a comparable amount of CYN with and without yeast extract, suggesting strain A210 uses CYN as an alternative organic carbon source (Fig. 2.1c).

2.3.2.3 Influence of Fe^{2+} on CYN removal

To evaluate whether the Fe^{2+} influences CYN removal, Fe^{2+} was added to the growth media where $MnCO_3$ and yeast extract was present.

Addition of Fe^{2+} increased the rates of CYN removal of strain A210 2-fold (from 4.4 to 8.6 μg L^{-1} day^{-1}) (Table 2.2). In contrast, strain A288 and A226 removed lower amounts of CYN in the presence of Fe^{2+}. CYN removal by strain OF001 was similar (<1%) in presence or absence of Fe^{2+} (Table 2.2)

2.3.2.4 pH influence on CYN removal

To evaluate the influence of pH variations on CYN removal, MOB were inoculated in a buffered (setup 1) and unbuffered (setup 2) system. Whereas the pH in the buffered medium was between 7.1 and 7.6, during cultivation of MOB with CYN, pH was between 7.0 and 8.3 in the unbuffered medium (Appendix, Fig. A4 and A5).

We observed similar CYN removal in the buffered and the unbuffered system for strains OF001, A288, and A226 (Fig. 2.1a, b, and d). In contrast, strain A210 showed better CYN removal rate in the buffered system (pH 7.2-7.4) than in the unbuffered one (pH 7.2-8.1), which indicates that CYN removal by strain A210 is pH sensitive (Fig. 2.1c).

2.3.3 Influence of the amount of oxidized manganese formed during cultivation on CYN removal

We quantified the amount of oxidized manganese in the medium with Ibb I to evaluate if a higher amount of oxidized manganese correlated with a higher CYN removal. No clear correlation between CYN removal and the amount of oxidized manganese was observed.

Pseudomonas sp. OF001 produced a higher concentration of oxidized manganese when $MnCO_3$ instead of $MnSO_4$ was present in the media (Fig. 2.2a). The highest amount of CYN was removed in setups with the highest amount of oxidized manganese.

Comparing the concentration of oxidized manganese by *Ideonella* sp. A288 among the different setups, the strain oxidized the highest amount of Mn^{2+} in setup 1 (with buffer) and 4 (no Fe^{2+}), and formed significantly less oxidized manganese in setups 2 (no buffer), 6 (no YE), and 7 (with $MnSO_4$). Removal of CYN in setup 4 was the highest, however in setup 1 and 2 the removal was similar in spite of the different amount of oxidized manganese (Fig. 2.2b).

Higher concentrations of oxidized manganese formed by *Comamonadaceae* bacterium A210 (Fig. 2.2c) were observed in setups 1 (with buffer), 4 (no Fe^{2+}), and 6 (no YE), than in setups 2 (no buffer) and 7 (with $MnSO_4$). However, the removal of CYN in setup 2 was similar to the removal in setup 6, even though the amount of oxidized manganese differed substantially (Fig. 2.2c).

The oxidation of Mn^{2+} by *Ideonella* sp. A226 was similar in all setups, even though we observed a significantly higher CYN removal in setups 1, 2, and 4 than in other setups (Fig. 2.2d).

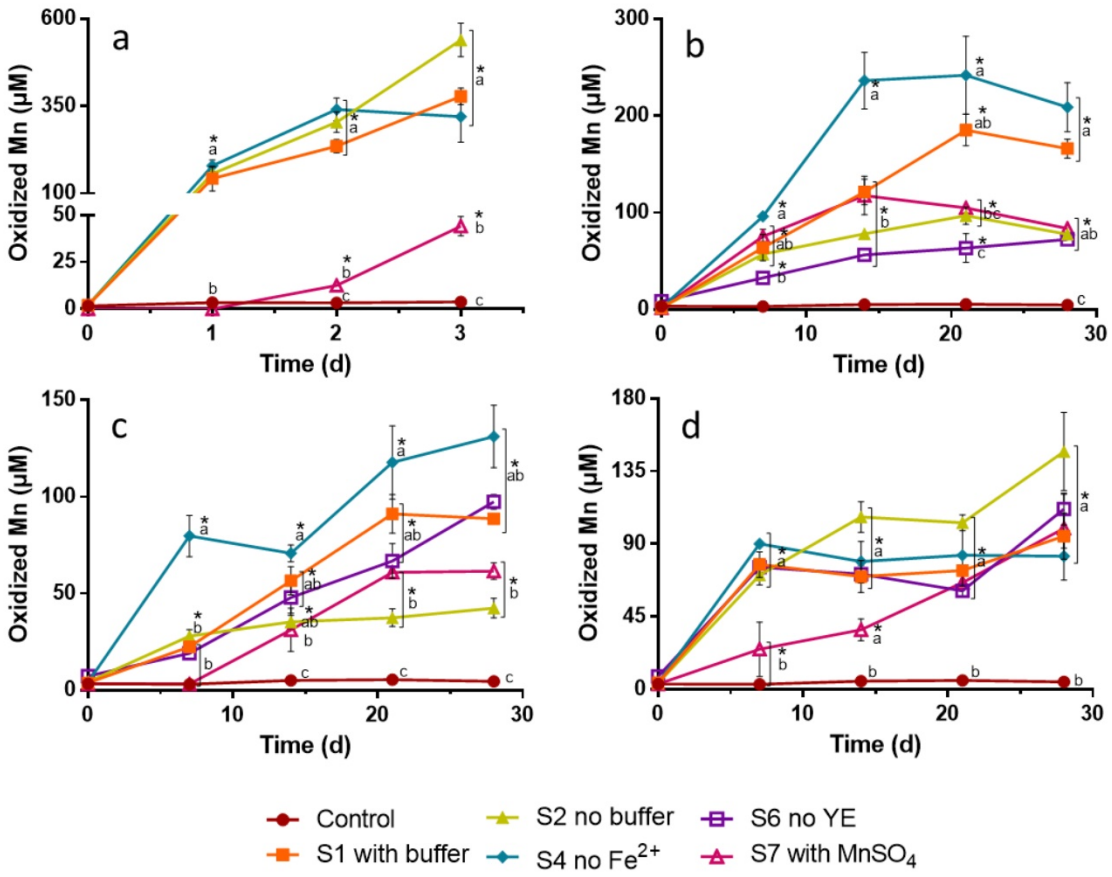

Fig. 2.2. Concentration of MnOx produced during batch removal assays. a) *Pseudomonas* sp. OF001, b) *Ideonella* sp. A288, c) *Comamonadaceae* bacterium A210 and d) *Ideonella* sp. A226. Mean values ± standard error bars (n = 3). *Indicates significant differences respect to control (P < 0.05). Different letters indicate significant differences (P < 0.05) for each sampling time, after Tukey's pairwise comparisons. S: setup; YE: yeast extract. Control group represents the mean of all the control flasks ± standard error (n = 12 for strain OF001 and n = 15 for the other strains).

2.3.4 CYN removal by BioOx

To determine if the BioOx, produced by the tested strains, removed CYN in the absence of viable cells, CYN was incubated with sterile BioOx. The BioOx produced from $MnCO_3$ (BioOx-S4, no Fe^{2+}) or $MnSO_4$ (BioOx-S7, with $MnSO_4$) were used to compare reactivity of BioOx towards CYN from different manganese sources.

The BioOx-S4 produced by strain OF001 from $MnCO_3$ removed 24% of CYN, while BioOx-S7 formed from $MnSO_4$ did not remove CYN. The removal of CYN by viable *Pseudomonas* sp. OF001 in the presence of $MnCO_3$ was 4-fold higher (~100%) than the removal by the sterile BioOx-S4 (24%) (Fig. 2.3a and b).

The BioOx-S4 and the BioOx-S7 produced by the strains A288, A210, and A226 removed 0 to 4% of CYN, whereas viable bacteria in the media with $MnCO_3$ (26 to ~100%) or $MnSO_4$ (18 to 23%) removed in a higher amount of CYN (Fig. 2.3a and b). These results indicate that viable MOB are required for removing CYN.

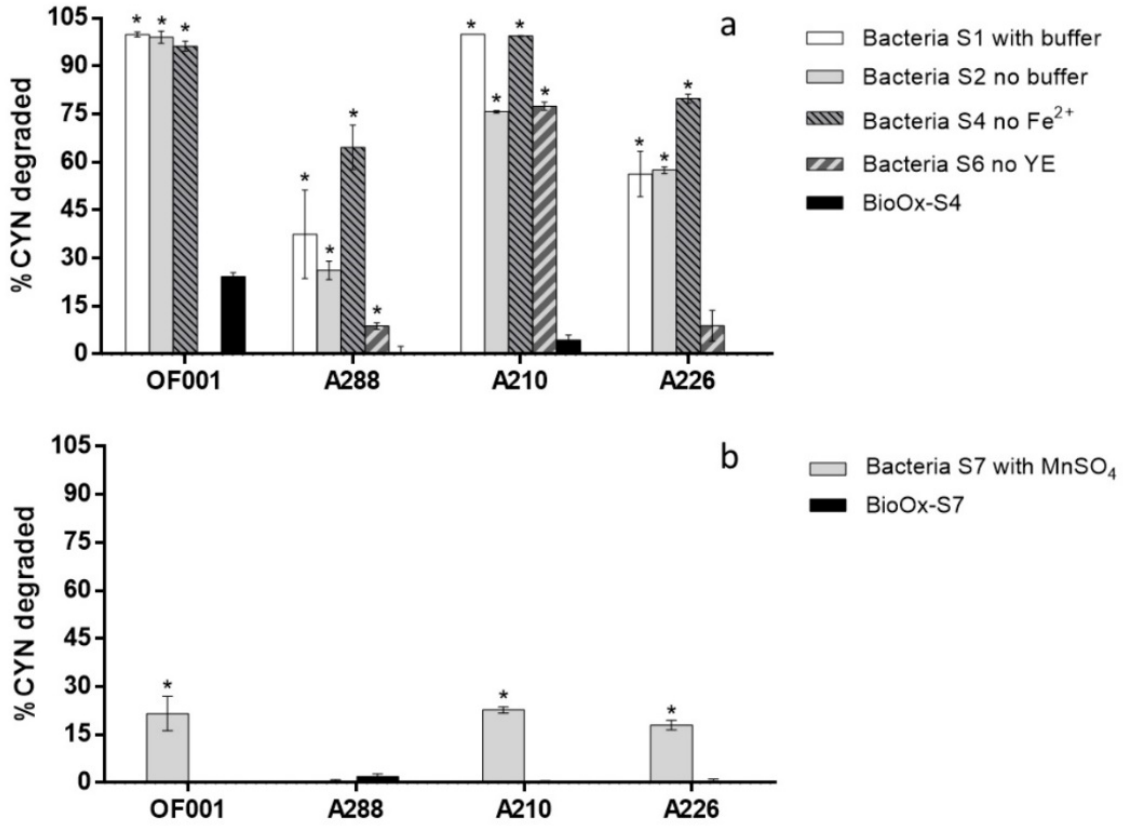

Fig. 2.3. Comparison of the CYN removal by viable bacteria and BioOx. a) Bacteria vs. BioOx-S4 and b) Bacteria vs. BioOx-S7. Mean values ± standard error bars (n = 3). *Indicates significant differences respect to BioOx (P < 0.05). S: setup.

2.4 Discussion

Information about bacterial removal of CYN is scarce, and only a few strains with this ability have been isolated and described (Dziga et al., 2016; Mohamed and Alamri, 2012). To the best of our knowledge, the role of MOB in the removal of CYN has not been studied so far. MOB occur frequently in freshwater systems (Johnson et al., 2012; Palermo and Dittrich, 2016; Santelli et al., 2014; Sommers et al., 2002; Stein et al., 2001; Sternbeck, 1995; Zakharova et al., 2012) and could therefore impact the fate of CYN in the environment. We observed removal of CYN at environmentally relevant concentrations by manganese-oxidizing bacteria isolated from natural and technical systems. In addition, we found that MOB removed CYN at different rates and to a different extent under diverse cultivation conditions. These results suggest that not all MOB are equally suitable for the potential application in technical systems for CYN removal.

For instance, the most efficient removal of CYN in the present work was achieved by *Pseudomonas* sp. strain OF001 followed by *Comamonadaceae* bacterium A210, the latter removing the total amount of initial CYN after a longer incubation time than strain OF001. In

addition, *Comamonadaceae* bacterium A210 showed a high removal of CYN in the absence of yeast extract in contrast to the other tested MOB strains. *Ideonella* sp. A288 and A226 also removed CYN, but with lower efficiency and at lower rates than the former strains. The ability to oxidize manganese is widespread among different bacterial phylogenetic lineages (Tebo et al., 2005). Considering that we observed CYN removal for all tested MOB, regardless of their isolation source, we expect that also other MOB catalyse the removal of CYN.

All organisms in this study can grow in the absence of Mn^{2+}, as it has been described for MOB (Spiro et al., 2008). However, the CYN removal activity depended on the presence of Mn^{2+} evidenced by low to no (0□16%) removal of CYN in the absence of this element. Also, the successful removal of other organic xenobiotics as 17α-ethynylestradiol (Tran et al., 2018), and diclofenac (Meerburg et al., 2012) was accomplished or substantially improved when Mn^{2+} was added to the growth media. To our surprise, the removal of CYN changed when $MnSO_4$ instead of $MnCO_3$ was used as the Mn^{2+} source. When $MnCO_3$ was added instead of $MnSO_4$, all the MOB tested in this study showed the highest CYN removal rates and removal efficiencies. This is in contrast with previous studies using MOB for the removal of different organic compounds (Meerburg et al., 2012; Sochacki et al., 2018; Tran et al., 2018), in which soluble sources of Mn^{2+}, including $MnSO_4$ or $MnCl_2$ in similar concentrations as in the present work, removed all tested substance successfully. The initial concentration of Mn^{2+} added as $MnSO_4$ was lower (0.3 mM) than the concentration added as $MnCO_3$ (15 mM). However, between 67 to 85% of Mn^{2+} (based on the stoichiometry of Mn added as $MnSO_4$) remained in the medium at the end of the assay (Fig. 2.2a-d), showing that Mn^{2+} was not a limiting factor for the bacteria. Thus, increasing the amount of Mn^{2+} as $MnSO_4$ should not modify the CYN removal. In addition, so far no studies evaluate the removal of organic compounds in the presence of insoluble $MnCO_3$. Nonetheless, $MnCO_3$ has been used previously as the Mn^{2+} source for the cultivation and isolation of MOB (Schmidt et al., 2014). Based on our results, we propose that CYN removal by the tested strains is not affected by the initial amount of Mn^{2+} or the amount of manganese oxides formed in the media, but by the type of Mn^{2+} source. The reasons why the tested bacteria remove CYN better when they oxidize $MnCO_3$ instead of $MnSO_4$ still remains to be elucidated.

Pseudomonas sp. OF001 (~37 μg L^{-1} day^{-1}) showed higher CYN removal rates than *Bacillus* sp. AMRI-03 (15 μg L^{-1} day^{-1}) when it was cultivated with a similar initial CYN concentration (100 μg L^{-1}) and at a similar pH of 7-8 (Mohamed and Alamri, 2012). All MOB tested in this study showed a similar or even higher rate of CYN removal than the bacterial consortium tested by Smith et al. (2008), with a removal rate of 0.3 to 24 μg L^{-1} day^{-1} at initial CYN concentrations of 3-76 μg L^{-1}. In contrast, the removal rates of all the MOB in this study were lower than the removal rates of *Aeromonas* sp. R6, ranging between 280 to 700 μg L^{-1}

day^{-1} with initial CYN concentrations of 1-20 mg L^{-1} (Dziga et al., 2016). CYN removal is influenced by the initial concentration of CYN (Mohamed and Alamri, 2012; Smith et al., 2008). The environmentally relevant concentration that we used in our experiments (118 µg L^{-1}) could contribute to the lower CYN removal rates observed compared to CYN removal rates observed with *Aeromonas* sp. R6 (Dziga et al., 2016).

We evaluated the influenced of pH on CYN removal in buffered and unbuffered media because for other CYN removers the influence of pH on CYN removal was reported. Highest CYN removal was reported in culture media with pH ranging from 6.5 to 8 for *Aeromonas* sp. R6 (Dziga et al., 2016) and from 7 to 8 for *Bacillus* sp. AMRI-03 (Mohamed and Alamri, 2012). In accordance, we observed high CYN removal by all the tested MOB in pH between 7.0 and 8.3. Nevertheless, the removal of CYN by *Comamonadaceae* bacterium A210 was lower at higher pH. Possibly, the enzymes of strain A210 involved in manganese oxidation work optimally at pH closer to 7.

CYN removal in the absence of an additional organic carbon source was studied for strains A288, A210, and A226. Strain OF001 did not grow in the absence of yeast extract and CYN, thus CYN removal under this condition was not evaluated. Low CYN removal activity in the absence of yeast extract by strains A288 and A226 suggests that the two *Ideonella* strains were not able to use CYN as a carbon source; CYN removal by *Ideonella* was observed only when another organic carbon source was present. In contrast, *Comamonadaceae* bacterium A210 removed 77% of CYN in yeast extract-free media. Even though we cannot exclude that strain A210 may fix CO_2 or use carbonates as a carbon source for growth, strain A210 could use CYN as an alternative carbon and/or nitrogen source, based on the high removal rates observed. The use of CYN as an additional carbon and nitrogen source, when the easiest carbon source is depleted, was proposed for *Bacillus* sp. AMRI-03 (Mohamed and Alamri, 2012) and *Aeromonas* sp. R6 (Dziga et al., 2016).

The influence of Fe^{2+} onto CYN removal was evaluated because three of the tested MOB were isolated from an iron-manganese biofilm and many MOB are also able to precipitate iron (Schmidt et al., 2014). Besides, manganese oxides commonly contain other elements like iron (Vesper, 2012). El Gheriany et al. (2009) demonstrated that iron might influence the production of the manganese-oxidizing enzymes of *Leptothrix discophora*-SS, which could explain the differences observed for CYN removal with and without Fe^{2+}.

Manganese oxides are known for their ability to oxidize various organic compounds (Tebo et al., 2004). In our study, BioOx in the absence of active bacteria showed low or no (0-24%) CYN removal. In accordance, several reports demonstrated that the removal of many organic compounds was significantly lower or even absent when only sterile BioOx were present, showing the important role of viable MOB in the removal of compounds such as

benzotriazole (Sochacki et al., 2018), 17α-ethynylestradiol (Tran et al., 2018), and diclofenac (Meerburg et al., 2012). On the other hand, other studies showed that BioOx removed 17α-ethynylestradiol in the absence of viable cells (Sabirova et al., 2008). The differences observed might be related to the structure of the BioOx formed by the tested strains.

The precise mechanism of the removal of CYN by the tested MOB strains at a molecular level was not investigated yet. In the present study, it was found that viable MOB cells and $MnCO_3$ as manganese source were required for the efficient removal of CYN. However, we hypothesize that the removal of CYN by MOB follows a similar mechanism as described for *Pseudomonas putida* for the removal of other organic compounds (Meerburg et al., 2012; Tran et al., 2018). Briefly, the removal pathway starts with the enzymatic oxidation of Mn^{2+} in the medium. The oxidation releases as a final product insoluble BioOx containing Mn^{4+}, with Mn^{3+} as an intermediate. The highly reactive intermediate Mn^{3+} would either complete the oxidation to Mn^{4+} or oxidize other chemical compounds. When BioOx (Mn^{4+}) are produced, they may continue with the oxidation of other compounds and Mn^{2+} is again available for enzymatic re-oxidation by the viable bacteria (Meerburg et al., 2012; Tran et al., 2018). In this process, the presence of viable bacteria as well as Mn^{2+}, are necessary for the continuous re-oxidation of Mn^{2+} to allow efficient removal of the organic substance, which is in accordance with the results of our study. Nevertheless, the four tested strains showed different CYN removal efficiencies and rates, and removed CYN under different conditions such as the absence or presence of an additional carbon source. Therefore, our findings suggest that more complex processes contribute to the removal of CYN, and not only the mere oxidation of Mn^{2+}.

The mechanism for CYN removal by MOB remains unknown. However, biological processes related to the presence of viable bacteria (e.g. co-metabolism) are required for substantial CYN removal. Adsorption on the cellular structure based on ionic charges, seems unlikely. CYN sorption by the biomass was not observed in any of the control setups and at the tested pH, cylindrospermopsin remains as a zwitterion (Adamski et al., 2016a), decreasing the possibility of adsorption.

The description of new organisms which can remove CYN contributes to a better understanding of the fate of cyanotoxins in the environment. It also allows a deeper insight into the role of MOB in the removal of recalcitrant organic substances and thus, further elucidates their potential as candidates for the treatment of water to remove organic pollutants, including CYN.

2.5 Conclusions

We considered five points as the most valuable conclusions from this work:

1. MOB removed CYN at environmentally relevant concentrations in presence of $MnCO_3$.

2. The participation of viable bacteria actively oxidizing Mn^{2+} was the key factor for efficient CYN removal.

3. The mere active oxidation of Mn^{2+} is important, independent of the final concentration of BioOx in the medium.

4. An additional carbon source available in the media is necessary for the removal of CYN by *Pseudomonas* sp. OF001, and *Ideonella* sp. A288 and A226.

5. MOB might be promising candidates for future implementations in water treatments for the removal of CYN.

2.6 Acknowledgments

Erika B. Martinez-Ruiz is a DAAD (Deutscher Akademischer Austauschdienst) scholarship holder. We would like to thank Marcella Nega for the helpful discussions.

3 Manganese-oxidizing bacteria form multiple cylindrospermopsin transformation products with reduced human liver cell toxicity

This chapter is the accepted version of the article published as

Martínez-Ruiz, E.B., Cooper, M., Al-Zeer, M.A., Kurreck, J., Adrian, L., Szewzyk, U., 2020. Manganese-oxidizing bacteria form multiple cylindrospermopsin transformation products with reduced human liver cell toxicity Sci. Total Environ. 729, 138924. https://doi.org/10.1016/j.scitotenv.2020.138924

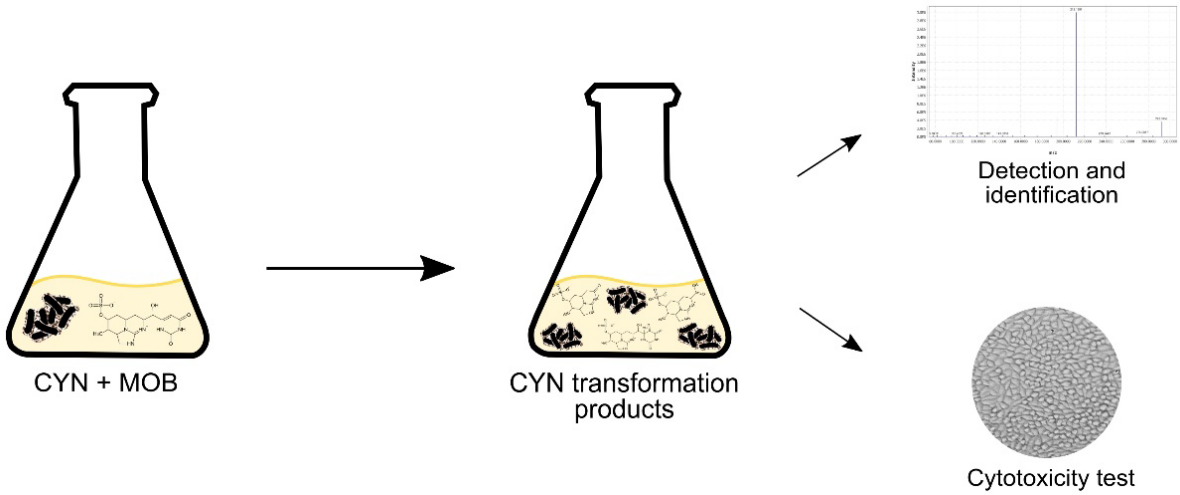

Abstract

Cylindrospermopsin (CYN) is a toxic alkaloid highly persistent in aquatic environments. Biological removal of CYN was described previously. However, no transformation products formed by biological processes could be identified so far. Here, we describe that various manganese-oxidizing bacteria (MOB) transform CYN completely at an initial mean concentration of 7 mg L^{-1} (17 µM) within 3 to 34 days. Regardless of the strain, and transformation rate, transformation of CYN by MOB led to the same seven transformation products identified by mass spectrometry, which suggests that the removal of CYN by MOB follows a similar mechanism. Oxidation was the main transformation process, and the uracil moiety was the most susceptible part of the CYN molecule. In vitro cytotoxicity tests with the transformation products of CYN formed by one of the tested strains against the two human liver cell lines HepG2 and HepaRG, revealed that the transformation products were substantially less toxic than pure CYN for both cell lines. The results suggest that incubation with MOB might be an option for water treatment to remove CYN and may allow more detailed studies on the fate of CYN in the environment.

Keywords: CYN, cyanotoxins, HepG2, HepaRG, biogenic oxides, mass spectrometry, degradation

3.1 Introduction

Environmental factors such as warming, extreme natural events, and eutrophication increase non-harmful and harmful cyanobacterial blooms, and consequently increase the risk of intoxication related to the production of cyanotoxins (Liu et al., 2019; Merel et al., 2013; Richardson et al., 2019; Walls et al., 2018). Cyanotoxins are secondary metabolites, produced by various cyanobacterial genera, and are toxic to humans, animals, and plants (Corbel et al., 2014; Wood, 2016).

Cylindrospermopsin (CYN) is an alkaloid cyanotoxin, composed of a cyclic sulfated guanidine moiety bound to a hydroxymethyluracil group. CYN-producing cyanobacteria, such as *Cylindrospermopsis raciborskii*, *Umezakia natans*, *Chrysosporum ovalisporum, Aphanizomenon* spp., and *Anabaena* spp. occur in aquatic environments worldwide (Rzymski and Poniedziałek, 2014). CYN is a zwitterion at neutral pH (Onstad et al., 2007) and therefore highly water-soluble (Griffiths and Saker, 2003). Most of the CYN is excreted by the cyanobacterial cells, so that 56–98% of the CYN can be found extracellularly with the highest concentration detected at the stationary phase (Bormans et al., 2014). CYN is stable under acidic and neutral pH and between 4 and 100 °C (Adamski et al., 2016a; Chiswell et al., 1999). Natural photodegradation of CYN is limited (Wörmer et al., 2010). All these characteristics make it highly persistent in aquatic environments. Therefore, research on specific processes aiming at removing and transforming CYN has been conducted.

Different physicochemical treatments, such as advanced oxidation (He et al., 2014b), chlorination (Merel et al., 2010), UV irradiation (Adamski et al., 2016b), and ozonation (Yan et al., 2016) can efficiently remove CYN. Identified transformation products involved typically reactions of oxidation, hydrogen abstraction, hydroxylation, and loss of the sulfate group. Generally, the uracil moiety of the CYN molecule is the most susceptible functional group to modifications, including the cleavage of the whole uracil group (Adamski et al., 2016b, 2016a; Fotiou et al., 2015; He et al., 2014a; Merel et al., 2013; Song et al., 2012; Yan et al., 2016; G. Zhang et al., 2015). In the case of CYN treated by chlorination, a chlorine compound known as 5-chloro-cylindropermopsin is formed by the substitution of a hydrogen atom at C7 by a chlorine atom (Merel et al., 2010). Transformation products from some of these abiotic processes are less toxic than pure CYN (Merel et al., 2010; Yan et al., 2016; G. Zhang et al., 2015).

Biological transformation could represent an economical alternative to the removal of cyanotoxins, with the potential to produce fewer toxic transformation products, as previously shown for microcystin (Kumar et al., 2019). In addition, biotransformation may be an important natural process to remove CYN from water bodies (Dziga et al., 2016; Smith et al., 2008). Nevertheless, in this regard, results are ambiguous. For example, microbial communities from

freshwater bodies from Spain, with and without previous exposure to CYN, did not degrade 100 µg L^{-1} of CYN after 40 days (Wormer et al., 2008). However, microbial communities from a dam in Australia, previously exposed to CYN, removed up to 76 µg L^{-1} of CYN (Smith et al., 2008). Moreover, bacterial communities of freshwater sediments from sand filters and groundwater removed CYN, showing that CYN removal can also take place in sediments (Klitzke et al., 2010).

A few isolated organisms have been described with the ability to remove CYN in a range of 0.010 to 1.5 mg L^{-1}. Such organisms include probiotic bacteria (Nybom et al., 2008), *Bacillus* sp. (Mohamed and Alamri, 2012) and *Aeromonas* sp. (Dziga et al., 2016) isolated from a freshwater body, either with or without previous exposure to CYN, as well as different strains of manganese-oxidizing bacteria (MOB) isolated from a freshwater body and a bioreactor (Martínez-Ruiz et al., 2020b). Although the removal of CYN by bacterial communities (Klitzke et al., 2010; Smith et al., 2008) and isolated strains (Dziga et al., 2016; Martínez-Ruiz et al., 2020b; Mohamed and Alamri, 2012) has been reported, there is no information about the formation of transformation products or the mineralization of CYN by bacteria.

MOB are a phylogenetically diverse group of organisms with a broad physiological diversity (e.g. autotrophs and mixotrophs), able to oxidize Mn^{2+} to Mn^{3+} and Mn^{4+} (Tebo et al., 2005). MOB transform different organic and inorganic pollutants as a side reaction only when Mn^{2+} is oxidized in batch assays and bioreactor scale (Meerburg et al., 2012; Sochacki et al., 2018; Tran et al., 2018; Zhang et al., 2015). As a result of the manganese oxidation, MOB precipitate biogenic manganese oxides that are strong natural oxidants (Hennebel et al., 2009; Tebo et al., 2004) and play thus an important role in the biogeochemical cycle of manganese and other elements (Tebo et al., 2004). Biogenic manganese oxides often interact with different metals like Fe, forming ferromanganese oxides, which are common in the nature (Lee and Xu, 2016; Stein et al., 2001; Vesper, 2012). Manganese oxidation is not essential for the survival of MOB, and its physiological role is still poorly understood (Spiro et al., 2008). MOB are present in drinking water systems (Cerrato et al., 2010) and are widely distributed in the nature (Tebo et al., 2004). For instance, in freshwater systems of the Lower Oder Valley National Park, MOB may coexist with potentially toxigenic cyanobacteria such as *Anabaena* spp. (Scheer, 2010). MOB transform CYN in presence of Mn^{2+} (Martínez-Ruiz et al., 2020b), but it was unknown if transformation products are formed and whether these transformation products exhibit lower toxicity than CYN.

Humans may be exposed to CYN and its transformation products through the consumption of contaminated food (Guzmán-Guillén et al., 2017; Prieto et al., 2017) and water (Bourke et al., 1983; Byth, 1980). Recreational activities in contaminated water bodies represent other potential sources of exposure (Poniedziałek et al., 2012). CYN possesses

diverse modes of actions including hepatotoxicity, cytotoxicity, and neurotoxicity. The liver is considered the main target organ of CYN (Poniedziałek et al., 2012), and therefore, its toxicity has been studied using human hepatic cells as *in vitro* models (Gutiérrez-Praena et al., 2019; Huguet et al., 2019; Kittler et al., 2016).

The most widely used human hepatoma cell line used in toxicological research is the hepatocellular carcinoma cell line HepG2 (Donato et al., 2015). HepG2 cells are easy-to-handle and highly proliferative cells that express various hepatic functions. Nevertheless, the expression of some cytochrome P450 enzymes (CYP) from phase I and phase II enzymes of the pollutants metabolism, and membrane transporters are reduced or not present in HepG2 cells (Donato et al., 2015; Guillouzo and Guguen-Guillouzo, 2018). In contrast, HepaRG, a human bipotent progenitor cell line, express the majority of phase I and II enzymes of the pollutants metabolism, as well as membrane transporters, mainly in their differentiated state (Guillouzo et al., 2007). The differentiated state of HepaRG cells represents the physiology of human hepatocytes better than HepG2 cells (Gerets et al., 2012; Guillouzo and Guguen-Guillouzo, 2018), so they may be more sensitive for human liver cytotoxicity testing (Guillouzo et al., 2007; Yokoyama et al., 2018).

In our previous study, we reported the ability of MOB to transform the environmentally relevant concentrations of 118 µg L^{-1} CYN under different growth conditions (Martínez-Ruiz et al., 2020b). We found that CYN is removed only when metabolically active MOB grow in the presence of Mn^{2+}. The best removal rates were observed when $MnCO_3$ was used as the Mn^{2+} source, and yeast extract was added (Martínez-Ruiz et al., 2020b). However, it remained unknown if transformation products are formed and if these transformation products are toxic.

Based on the previous information about CYN removal and MOB, we hypothesized that i) MOB transform CYN by a common mechanism regardless of their phylogeny and isolation origin, and ii) transformation products produced by MOB are less toxic than pure CYN. Therefore, we investigated i) the biological transformation of CYN by MOB at a sixty-fold higher concentration than previously reported, focusing on the identification and comparison of the transformation products formed by various MOB, and ii) the cytotoxicity of the mixture of CYN transformation products against human HepG2 and HepaRG cells compared to CYN.

3.2 Material and methods

3.2.1 Strains and culturing conditions

Pseudomonas sp. OF001, *Comamonadaceae* bacterium A210, *Ideonella* sp. A226, and *Ideonella* sp. A288 were obtained from the culture collection of the Laboratory of Environmental Microbiology from the TU Berlin, Germany (Martínez-Ruiz et al., 2020b). Strain

OF001 (GenBank accession number MK599476) was isolated from the effluent of an experimental fixed-bed biofilm bioreactor established for the removal of recalcitrant substances from wastewater operated by the Laboratory of Environmental Process Engineering (TU Berlin). Strains A288, A210, and A226 (GenBank accession numbers MK599477, MK599478, and MK599479, respectively) were isolated from an iron manganese-depositing biofilm in a freshwater pond in the Lower Oder Valley National Park, Germany. Bacteria were routinely cultivated in a medium developed for *Leptothrix* strains (Atlas, 2010), known as LSM2. In the present study, a modified LSM2 was used, to which $Fe(NH_4)_2(SO_4)_2 \cdot 6H_2O$ was not added. This modified medium is referred to as modified LSM2. The detailed composition of the medium is listed in Table S3.1 (Appendix). The pH of the medium was adjusted to 7.2 with 1 M NaOH before autoclaving. For the inoculum of the batch transformation assay, 300 µL of the culture in modified LSM2, were transferred to modified LSM2 without $MnCO_3$. This was necessary to allow for the assessment of the bacterial growth phase because the biogenic oxides and $MnCO_3$ interfere with OD measurements. Cultures were cultivated twice in modified LSM2 without $MnCO_3$ previous to the transformation assay, to ensure the absence of manganese oxides in the inoculum. Flasks were incubated at room temperature (20.8 ± 2.2 °C) with shaking at 110 rpm for 18 h (*Pseudomonas* sp. OF001), 2 days (*Ideonella* sp. A288), 3 days (*Ideonella* sp. A226), and 5 days (strain A210).

3.2.2 CYN transformation assays

CYN (>95% purity) was purchased from Enzo Life Science, Inc (New York, USA). CYN was resuspended in sterile Milli Q water to a final concentration of 500 mg L^{-1}. All MOB tested in this study remove CYN at the highest rates when $MnCO_3$ and yeast extract are present in the medium (Martínez-Ruiz et al., 2020b). Therefore, all cultures contained 1 g L^{-1} $MnCO_3$ and 0.5 g L^{-1} yeast extract (Carl Roth, Karlsruhe, Germany). Bacteria were inoculated into 3 mL modified LSM2 in sterile glass tubes (12 x 100 mm), using 30 µL of manganese-free precultures at exponential growth (OD_{600} nm). CYN was added to a final mean concentration of 7 mg L^{-1}. This concentration is approximately 60-times higher than the commonly detected CYN concentration in the environment (Messineo et al., 2009; Shaw et al., 1999). However, a high concentration of CYN was selected to increase the probability to detect CYN transformation products. Bacteria were incubated on a shaker at 110 rpm at room temperature (21 ± 2 °C) in the dark for 4 days (*Pseudomonas* sp. OF001), 21 days (*Ideonella* sp. A288 and strain A210), and 27 days (*Ideonella* sp. A226).

Samples were taken at discrete time points based on preliminary assays and the reported removal patterns/rates of CYN by each strain (Martínez-Ruiz et al., 2020b).

At the end of each assay, viability and purity of cells were evaluated qualitatively by

inoculating the strains onto solid modified LSM2 and incubation at room temperature (20.8 ± 2.2 °C). The same procedure was followed for the controls in order to discard any contamination.

As a control for the abiotic transformation of CYN, modified LSM2 with CYN, but without bacteria was evaluated. Modified LSM2 with bacteria, but without CYN was used as a control to test for bacterial metabolites. Two independent replicates were run per strain and per control.

3.2.3 Analysis of CYN and its transformation products

For chemical analyses 400 µL culture liquid were sampled, centrifuged at ~10,000 x g for 10 min at 4 °C and filtered using 0.22 µm PVDF membranes to remove bacteria and manganese oxides. Samples were stored at -20°C until analysis.

The detection of transformation products was carried out using an Orbitrap Fusion Tribrid Mass Spectrometer (Thermo Fisher Scientific, Bremen, Germany) coupled to a UHPLC. Chromatographic separation was performed using a Hypersil GOLD C18 column (150 x 2.1 mm, 3 µm, Thermo Scientific) in a UHPLC Dionex UltiMate 3000 RS (Thermo Fisher Scientific, Bremen, Germany). Separation conditions were used as previously reported with slight modifications (Fastner et al., 2018). Briefly, the mobile phase consisted of water (A) and methanol (B) both with 0.1% formic acid. A linear gradient was applied from 1% to 25% B within 5 min at a flow rate of 0.2 mL min^{-1}, and back to 1% B for 7 min. The effluent was monitored and CYN was quantified with a UV detector set at 262 nm. The injection volume was 5 µL and the oven temperature 25 °C. For the Orbitrap, heated electrospray ionization source parameters were: spray voltage of 3.5 kV and ion transfer tube temperature at 325 °C. Sheath, auxiliary, and sweep gas flow rate were 35, 10, and 0 (arbitrary units), respectively. Data acquisition was performed in full-scan mode.

Using an inclusion list with the *m/z* values and charge state, we conducted a target screening of the MS^1 traces for the expected *m/z* values of transformation products previously reported for transformation of CYN by physicochemical procedures (Adamski et al., 2016b, 2016a; Fotiou et al., 2015; Guzmán-Guillén et al., 2017; He et al., 2014b, 2014a; León et al., 2019; Merel et al., 2010; Song et al., 2012; Yan et al., 2016). The *m/z* value of potential CYN transformation products was searched scanning from 100 to 500 *m/z* under positive ion mode as previously reported (Fotiou et al., 2015; Guzmán-Guillén et al., 2017; He et al., 2014b, 2014a; Prieto et al., 2017; Song et al., 2012). If the instrument detects a mass spectral peak fulfilling the criteria specified in the inclusion list, an MS^2 spectrum is obtained for the associated precursor ion. Orbitrap resolution was 120000 for MS^1 and 60000 for MS^2.

The limit of quantification (LOQ) of CYN was 0.05 mg L^{-1}. The limit of detection (LOD) of CYN was 0.001 mg L^{-1}.

3.2.4 Transformation products identification

Potential transformation products in microbial cultures were further evaluated by manually checking: i) the absence of the corresponding *m/z* signals in control samples a) sterile modified LSM2 with CYN and b) modified LSM2 without CYN but with bacterial growth), ii) peak intensities along the incubation time, and iii) MS^2 fragmentation patterns. Fragmentation patterns were compared with published data (Adamski et al., 2016a, 2016b; Fotiou et al., 2015; Guzmán-Guillén et al., 2017; He et al., 2014a, 2014b; Yan et al., 2016). Transformation products without published MS^2 fragments were tentatively identified based on the precise MS^1 mass, and the distribution of the isotope abundance. Error limits of 10 ppm of the *m/z* and the MS^2 fragments of the potential transformation products were allowed.

3.2.5 Preparation of CYN transformation products for cytotoxicity assessment

Pseudomonas sp. OF001 was inoculated using 30 µL of the cultures in sterile glass tubes (12 x 100 mm) with 3 mL of modified LSM2 and incubated as described above. CYN was added to the cultures to final concentrations of 4 or 12 mg L^{-1}. Sterile or inoculated controls were set up without CYN. Samples of 400 µL volume were taken at day 0, 4 and 7, centrifuged at 10,000 x g for 10 min at 4°C and filtered through 0.2 µm PVDF membranes to obtain supernatants free of bacteria and oxides. Samples were then stored at -20°C until analysis. Samples at time 0 contained pure CYN, and samples of day 4 and 7 contained the mixture of transformation products of CYN. Two independent CYN transformation assays each with three replicates per CYN concentration, including the controls, were run. The cultivation supernatants were diluted 1:4 in the new medium to obtain a final CYN concentration of 1 or 3 mg L^{-1}.

3.2.6 Cell cultures

Human hepatoma HepG2 cells were cultured in RPMI medium (Biowest, France) supplemented with 10% fetal bovine serum (FBS, c.c.pro GmbH, Oberdorla, Germany). Human bipotent progenitor cells HepaRG cells purchased from Biopredic (Saint Grégoire, France) were cultured as described previously (Hiller et al., 2018). Briefly, HepaRG cells were grown in Williams E medium (PAN Biotech, Aidenbach, Germany) supplemented with 10% FBS, 2 mM L-glutamine (Biowest, Nuaillé, France), 5 µg mL^{-1} recombinant human insulin (PAN

Biotech), 50 µM hydrocortisone hemisuccinate (Sigma, Steinheim, Germany), and 1% penicillin/streptomycin (Biowest). After 14 days of incubation, differentiation of HepaRG cells was induced by adding 1.7% of DMSO (Sigma). Cells were incubated for additional 14 days before their application in cytotoxicity assays. Both cell line cultures were incubated at 37 °C and 5% CO_2 in a humidified atmosphere.

3.2.7 Cytotoxicity assessment

HepG2 and HepaRG cells were seeded onto clear sterile 96-well cell culture microplates with flat bottom (Greiner Bio-One, Frickenhausen, Germany) and incubated for 24 h at 37 °C and 5% CO_2 to obtain a final cell number of 4 x 10^5 and 1 x 10^5 cells per well for cytotoxicity assessment, respectively. After 24 h of incubation, the RPMI or Williams E culture medium was replaced with a mixture of three parts of fresh RPMI or Williams E medium and one part of filtered supernatant of the *Pseudomonas* sp. OF001 culture with CYN or the mixture of transformation products obtained as described above. As positive controls for cell viability HepG2 or HepRG cells were grown in RPMI or Williams E medium with either i) supernatant of the *Pseudomonas* sp. OF001 culture in modified LSM2 without CYN or transformation products or ii) supernatant of sterile modified LSM2 medium. As blank RPMI or Williams E medium without hepatic cells with i) supernatant of the *Pseudomonas* sp. OF001 culture in modified LSM2 medium without CYN or transformation products or ii) supernatant of sterile modified LSM2 medium, were used. Cells were exposed to the test substances for 24 h, and at the end of the assay, viability and proliferation was determined and compared to controls. Viability of cells was evaluated using the tetrazolium dye XTT (XTT) and neutral red (NR) assays with the kits “In Cytotox-XTT” and “In Cytotox-NR” (Xenometrix, Allschwil, Switzerland) following the manufacturer’s instruction. XTT and NR. Absorbance was measured at 450 and 540 nm, respectively, with a reference wavelength at 690 nm using an Ao microplate reader (Azure Biosystems, California, USA).

Two independent transformation assays with three replicates of each supernatant of *Pseudomonas* sp. OF001 with CYN (1 and 3 mg L^{-1} of CYN as initial concentration) or the mixture of transformation products (from day 4 and 7) were tested with HepG2 cells (n = 6). For HepaRG cells assays, we chose randomly three samples of supernatant of *Pseudomonas* sp. OF001 with CYN of each of the tested initial CYN concentrations (1 and 3 mg L^{-1} of CYN), from the two independent transformation assays. In this setup, we assured that at least one sample per each independent transformation assay was included. Also, for the mixture of transformation products (from day 4 and 7) three samples were chosen randomly, including at least one sample per each independent transformation assay (n = 3).

3.2.8 Removal rate

The removal rate was calculated by dividing the difference of the initial CYN concentration and the concentration measured on the last day where the CYN concentration was above the LOQ, by the number of days in which this CYN concentration was measured.

3.2.9 Data analysis and statistical analysis

Transformation products were analyzed with the MZmine v2.38 software (Pluskal et al., 2010). Chemical structures were drawn with ChemDraw (PerkinElmers Informatics). The dplyr R package on RStudio version 3.4.2 was used for statistical analysis (Wickham et al., 2019). Figures were made with the ggplot (Wickham, 2016) and gridExtra (Auguie, 2017) R package. One-way analysis of variance (ANOVA) followed by Tukey's pairwise comparison test for the multiple comparisons among CYN and transformation products at different times were performed.

3.3 Results and discussion

3.3.1 CYN removal

In a previous study we showed the removal of CYN by MOB, at environmentally relevant concentrations (Martínez-Ruiz et al., 2020b). In this study we aimed at the identification of CYN transformation products and therefore used a high concentration of 7 mg L^{-1} of CYN. We observed that all four tested strains removed CYN to concentrations below the detection limit, and at higher rates than described in our previous study (Fig. 3.1) (Martínez-Ruiz et al., 2020b). These results are in agreement with previous studies showing a strong influence of the initial CYN concentration onto the rate of its removal (Dziga et al., 2016; Mohamed and Alamri, 2012; Smith et al., 2008). In these studies the presence of specific genes and enzymes involved in CYN degradation was proposed, similarly as reported for microcystin (Dziga et al., 2013). Higher removal rates at higher CYN concentrations could thereby be explained by an enhanced induction of genes related to CYN removal (Dziga et al., 2016; Mohamed and Alamri, 2012; Smith et al., 2008). However, the mechanism for the removal of pollutants by MOB is proposed to be based on the unspecific reaction of reactive Mn species with the pollutant (Meerburg et al., 2012; Tran et al., 2018). Therefore, other parameters may influence CYN removal rates which will be further discussed in the section *3.3.2 Identification of CYN and its transformation products*.

The fastest CYN removal was observed for *Pseudomonas* sp. OF001, removing CYN within three days. *Ideonella* sp. A288, and *Comamonadaceae* bacterium A210, removed CYN

in 14 days, whereas *Ideonella* sp. A226 removed CYN in 27 days (Fig. 1). In our previous study with environmentally relevant CYN concentrations, strain OF001 showed the highest CYN removal rate followed by strain A210, while strain A226 and A288 removed only 80% and 65% of CYN after 28 days, respectively.

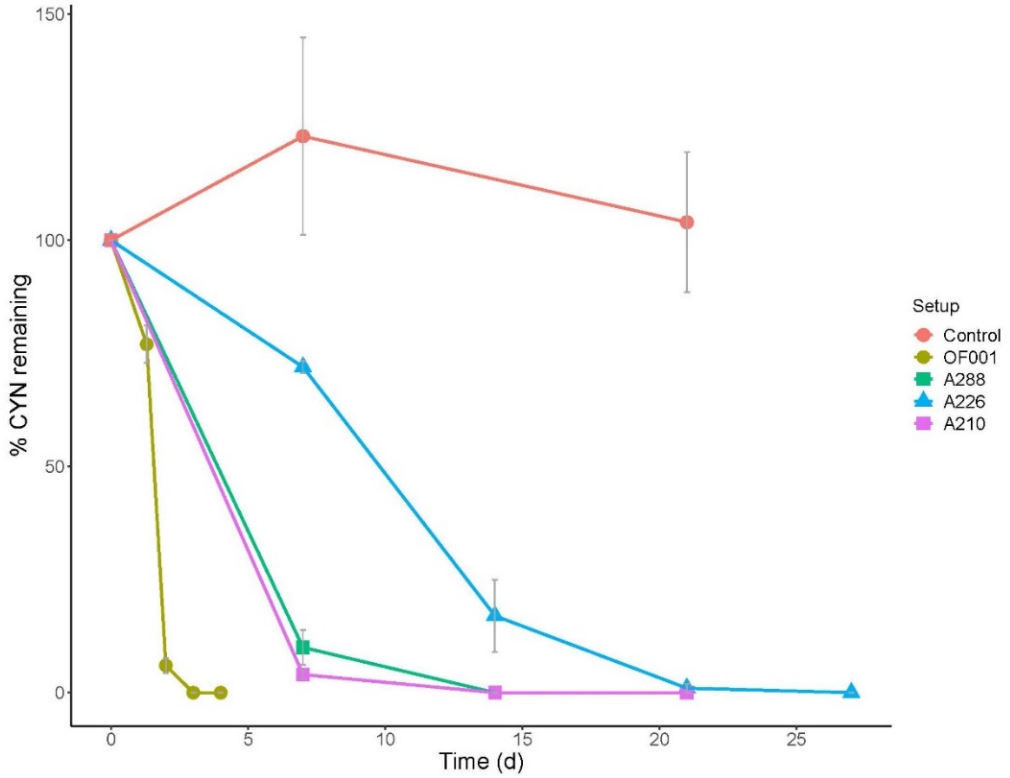

Fig. 3.1. CYN transformation over time by four different MOB. Control: CYN in the medium without MOB. The four MOB were *Pseudomonas* sp. OF001, *Ideonella* sp. strains A288 and A226, and *Comamonadaceae* bacterium A210. They were all grown in LSM2 medium with an initial CYN concentration of 7 mg L^{-1}. CYN concentration below the LOQ was taken as 0.025 mg L^{-1}. Two independent replicates were run per strain and per control (n = 2), error bars represent standard deviation and are provided to show the variation of the samples at each point.

CYN at 7 mg L^{-1} is 60-times higher than the concentration used in our previous study, however not all the removal rates of the tested MOB followed the same 60x increase rate. All tested MOB showed higher CYN removal rates when 7 mg L^{-1} of CYN was added as initial concentration, instead of 0.118 mg L^{-1} of CYN (Martínez-Ruiz et al., 2020). At 7 mg L^{-1}, CYN removal rates ranged from 0.48 to 3.16 mg L^{-1} day^{-1} compared to rates at 0.118 mg L^{-1} of CYN from 0.003 to 0.037 mg L^{-1} day^{-1}. In addition, at 7 mg L^{-1} all tested MOB showed higher CYN removal rates than *Aeromonas* sp. R6 and *Bacillus* sp. AMRI-03, the strains with the highest reported CYN removal rates so far. *Aeromonas* sp. R6 removed 0.070 to 0.280 µg L^{-1} day^{-1} when 1 to 20 mg L^{-1} of CYN were added as initial CYN concentration (Dziga et al., 2016), while *Bacillus* sp. AMRI-03 removed 0.050 µg L^{-1} day^{-1} when an initial amount of 0.5 mg L^{-1} of CYN was added (Mohamed and Alamri, 2012).

3.3.2 Identification of CYN and its transformation products

In our liquid chromatography / mass spectrometric analysis CYN eluted at a retention time (RT) of 8.09 min with a *m/z* value of 416.1234. Fragmentation of the isolated peak generated five fragments (Appendix, Fig. A6a) which correspond to the loss of SO_3 (*m/z* 336.1662), the loss of SO_3 and H_2O (*m/z* 318.1558), the loss of the hydroxymethyl uracil moiety (*m/z* 274.0853), the loss of the hydroxymethyl uracil moiety and SO_3 (*m/z* 194.1285), and the loss of the hydroxymethyl uracil moiety and SO_3 and H_2O (*m/z* 176.1180) (Guzmán-Guillén et al., 2012).

With the approach followed in the present study, the same seven CYN transformation products were detected for each MOB. Calculated chemical formulae, RTs, observed *m/z* values for singly charged ions ($[M+H]^+$ ions), calculated formulae, calculated *m/z* values and calculated mass errors are shown in Table 3.1. For all calculations of the precursor masses, the mass error is below 0.5 ppm, corresponding to 0.0002 Da for the largest error. Evolution over time of the transformation products indicates non-linear transformation (Fig. 3.2). Relative abundances in the present study are based on peak intensity and do not necessary reflect the concentration of the products. We could not obtain neat standards of the proposed transformation products to calibrate the quantification. The evolution of transformation products generated by all the tested MOB transforming CYN in modified LSM2 followed a general trend in the relative abundances throughout the assay (Fig. 3.2).

Our results show that the uracil moiety is the most susceptible group of CYN for modification, which is in agreement with transformation processes described in previous reports using abiotic reactions (Adamski et al., 2016b, 2016a; Fotiou et al., 2015; He et al., 2014b; Yan et al., 2016). TP_{448} was the transformation product with the highest molecular weight and the only detected product in which the ring of the uracil moiety was still present. Previously reported fragmentation pattern of TP_{448} reported a fragment with an *m/z* of either 274 (He et al., 2014b) or 350 (Fotiou et al., 2015). These fragments could not be identified in our study. Instead, one fragment with a *m/z* of 430.1025 potentially related to the loss of H_2O was detected (Appendix, Fig. A6b). However, the presence of three isotopes of TP_{448}, provided more evidence for the tentative identification of this product (Appendix, Fig. A6b). The detection of TP_{448} suggests hydroxylation of CYN possibly at the double bond between C5 and C6 in the methyluracil group (Fig. 3.3). The highest relative abundance of TP_{448} was detected at the early stage of incubation for all MOB (2 days for strain OF001, and 7 days for the other three strains), and diminished at the last stage. TP_{448} was also identified after treatment of CYN with advanced oxidation processes (He et al., 2014b; Song et al., 2012), and photocatalysis (Fotiou et al., 2015; G. Zhang et al., 2015).

Table 3.1. Transformation products of CYN formed by MOB.

						Fragmentation ions			
	RT (min)	m/z obs.	Putative chemical formula	m/z calc.	Mass error (ppm)	m/z obs.	Fragment formula	m/z calc.	Mass error (ppm)
CYN	8.09	416.1234	$C_{15}H_{21}N_5O_7S$	416.1234	0	336.1662	$C_{15}H_{21}N_5O_4$	336.1666	-1.2
						318.1558	$C_{15}H_{19}N_5O_3$	318.1561	-0.9
						274.0853	$C_{10}H_{15}N_3O_4S$	274.0856	-1.1
						194.1285	$C_{10}H_{15}N_3O$	194.1288	-1.6
						176.1180	$C_{10}H_{13}N_3$	176.1182	-1.1
TP_{290}	3.64	290.0804	$C_{10}H_{15}N_3O_5S$	290.0805	-0.3	210.1232	$C_{10}H_{15}N_3O_2$	210.1237	-2.4
						192.1129	$C_{10}H_{13}N_3O$	192.1131	-1
TP_{292a}	5.76	292.0961	$C_{10}H_{17}N_3O_5S$	292.0962	-0.3	212.1389	$C_{10}H_{17}N_3O_2$	212.1394	-2.4
						194.1284	$C_{10}H_{15}N_3O$	194.1288	-2.1
						176.1179	$C_{10}H_{13}N_3$	176.1182	-1.7
TP_{292b}	8.41	292.0961	$C_{10}H_{17}N_3O_5S$	292.0962	-0.3	212.1388	$C_{10}H_{17}N_3O_2$	212.1394	-2.8
						194.1284	$C_{10}H_{15}N_3O$	194.1288	-2.1
						176.1181	$C_{10}H_{13}N_3$	176.1182	-0.6
TP_{308}	6.13	308.091	$C_{10}H_{17}N_3O_6S$	308.0911	-0.3	228.1339	$C_{10}H_{17}N_3O_3$	228.1343	-1.8
						210.1231	$C_{10}H_{15}N_3O_2$	210.1237	-2.9
TP_{320}	8.84	320.0909	$C_{11}H_{17}N_3O_6S$	320.0911	-0.6	240.1337	$C_{11}H_{17}N_3O_3$	240.1343	-2.5
						222.1233	$C_{11}H_{15}N_3O_2$	222.1237	-1.8
TP_{347}	9.59	347.1019	$C_{12}H_{18}N_4O_6S$	347.1020	-0.3	267.1450	$C_{12}H_{18}N_4O_3$	267.1451	-0.4
TP_{448}	3.88	448.1135	$C_{15}H_{21}N_5O_9S$	448.1133	0.5	430.1027	$C_{15}H_{19}N_5O_8S$	430.1027	0

TP represent the transformation product with the *m/z* indicated as subscript number. *m/z* values for singly charged ions ($[M+H]^+$ ions). *m/z* observed is the average value of CYN or transformation product in all the samples. obs.: observed; calc.: calculated.

All other transformation products detected in this study contained four or less nitrogen atoms within their structure, suggesting the loss or the opening of the uracil ring structure (Fig. 3.3). The MS^2 fragmentation spectra of TP_{347} showed two fragments with *m/z* of 267.1453, and 199.1436 (Appendix, Fig. A6c). Fotiou et al. (2015) reported TP_{347} as a transformation product upon photocatalytic treatment of CYN, but no fragmentation pattern was described. Nevertheless, the fragmentation pattern that we described for TP_{347} in the present study is in good agreement with the chemical structure previously proposed for TP_{347} by Fotiou et al (2015). TP_{347} is produced most likely by further oxidation of TP_{448} leading to the uracil ring-fragmentation. TP_{347} was the product formed with the lowest relative abundance in modified LSM2 setups with strain OF001, A288 and A226. We could not detect TP_{347} when CYN was transformed by strain A210 under standard modified LSM2 cultivation conditions. However, TP_{347} was formed by all the other MOB strains. Therefore, we cannot exclude the possibility that strain A210 also formed TP_{347} in modified LSM2 under standard conditions in quantities below detection limit at the selected sampling times.

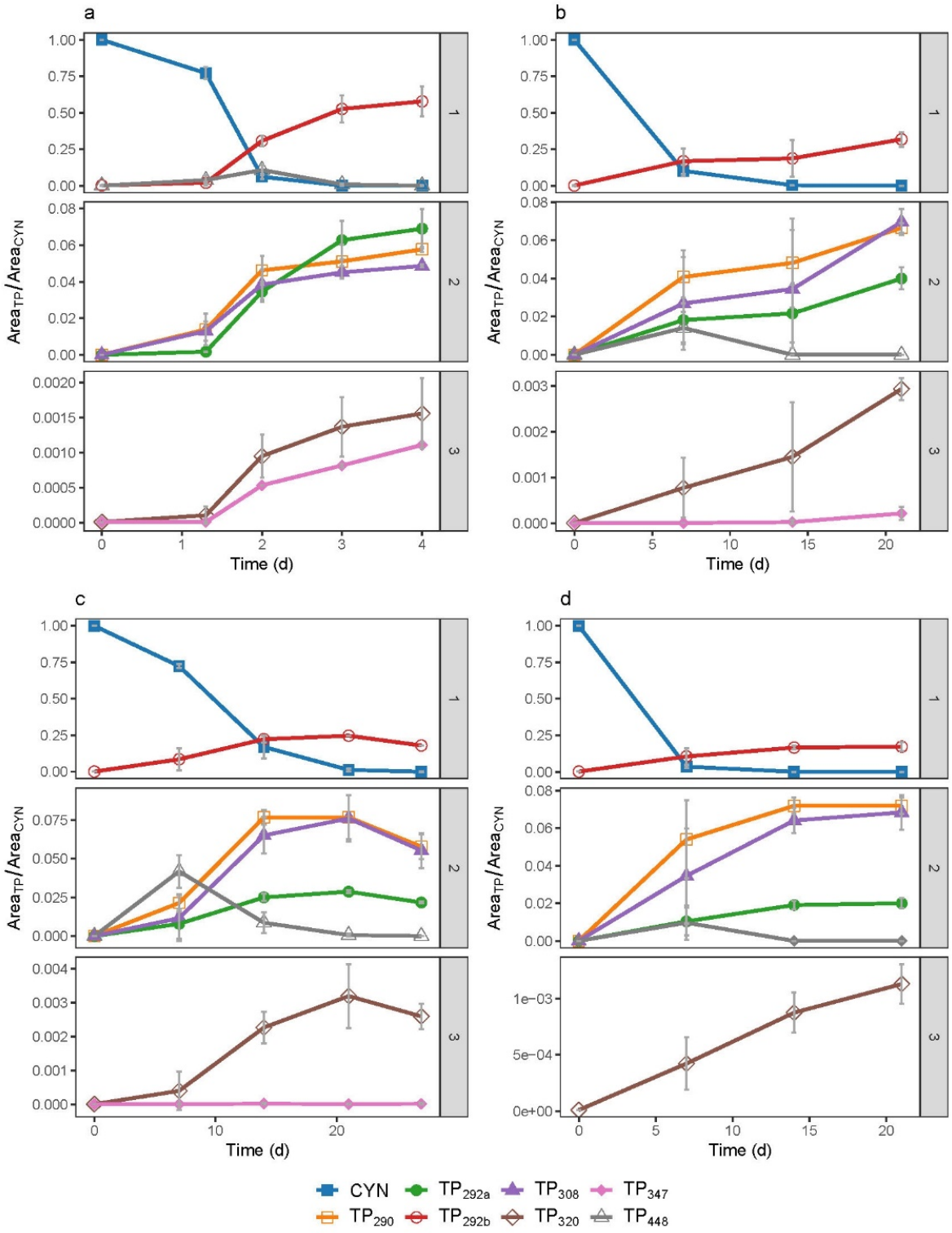

Fig. 3.2. Generation of transformation products shown in Figure 3.3 over the incubation time of MOB. a) *Pseudomonas* sp. OF001, b) *Ideonella* sp. A288, c) *Ideonella* sp. A226, d) *Comamonadaceae* bacterium A210. Initial CYN concentration: 7 mg L^{-1}. $Area_{TP}$: transformation products' peak area, and $Area_{CYN}$: CYN' peak area of the initial amount of CYN from LC-MS results. The three vertically combined graphs have different y-axis scales and show compounds according to their $Area_{TP}$ / $Area_{CYN}$ values. Note for the different scales also on the x-axis. Two independent replicates were run per strain and per control (n = 2), error bars represent standard deviation and are provided to show the variation of the samples at each point.

According to the proposed transformation pathway shown in Figure 3.3, TP_{320} is formed due to the hydroxylation process of TP_{347} and the reminiscent fragment of the uracil group is removed. The MS^2 spectra of TP_{320} revealed two fragments with *m/z* of 240.1338 and 222.1233, respectively (Appendix, Fig. A6d). The former corresponds to the loss of SO_3, while the latter corresponds to the loss of SO_3 and H_2O. MS^2 fragments are in agreement with those already reported for TP_{320} in a study using ozonation to transform CYN (Yan et al., 2016). TP_{320} was the second least abundant identified product. However, its relative abundance increased throughout the assay for all tested MOB (Fig. 3.2). TP_{320} has been generated also from photocatalysis (Fotiou et al., 2015) and advanced oxidation processes (He et al., 2014b, 2014a; Song et al., 2012).

The hydroxylation of TP_{320}, with a loss of CO, formed $TP_{308.}$ Two fragments of TP_{308} with *m/z* values of 228.1339 and 210.1232 were detected in the MS^2 spectra (Appendix, Fig. A6e). The chemical structure of a compound with the same *m/z* value as TP_{308}, detected by ozonation of CYN, was proposed by Yan et al. (2016) However, they did not report the fragmentation pattern, and consequently we could not assign TP_{308} unequivocally to the one that Yan et al. proposed (2016). Therefore, we propose a chemical structure based on the *m/z* value and the fragmentation pattern. Further studies should be conducted to better characterize and confirm the chemical structure of TP_{308}. Over the transformation assay time, TP_{308} increases until reaching a plateau after 2 and 7 days when strains OF001, and A210 were transforming CYN, respectively. In the case of strain A226, TP_{308} reached the highest relative abundance after 21 days, and decreased afterwards (Fig. 3.2). TP_{308} increased faster within 7 days of CYN transformation by strain A288, and continued increasing until reaching the highest relative abundance at day 21.

Compound TP_{292} was detected at two different RT (~5.76 and ~8.41), thus named as TP_{292a} and TP_{292b}. For both types of TP_{292} three fragments with *m/z* of 212.1388, 194.1284, and 176.1180 were identified in the MS^2 spectra, indicating the loss of SO_3 and the loss of one or two H_2O molecules (Appendix, Fig. A6f). Observed fragmentation patterns coincide with previous reports, and allow a tentative identification of the product (Adamski et al., 2016a, 2016b; Guzmán-Guillén et al., 2017; Prieto et al., 2017; Yan et al., 2016). TP_{292} may be formed by the hydroxylation of TP_{320} and the simultaneous removal of the carboxyl group, or by the oxidation of TP_{308}. The different retention times together with the same *m/z* value, and same fragmentation patterns of TP_{292a} and TP_{292b} suggests the detection of diastereoisomers as described previously for CYN transformation products obtained by different cooking techniques (Guzmán-Guillén et al., 2017; Prieto et al., 2017) and ozonation (Yan et al., 2016). Interestingly, alkaline (Adamski et al., 2016a), photocatalytic (Adamski et al., 2016b), and advanced oxidation (He et al., 2014b) treatment of CYN led to the formation of TP_{292} but not the formation of diastereoisomers. In all the assays of the four MOB strains, TP_{292b} was formed

in a higher relative abundance than TP_{292a}. TP_{292b} was the transformation product detected with the highest relative abundance of all the identified products (Fig. 3.2).

Further dehydration/oxidation of TP_{308} or TP_{292a-b} might yield the ketone TP_{290}. The two MS^2 fragments of TP_{290} with *m/z* values of 210.1238 and 192.1129 correspond to the sequential loss of SO_3 and H_2O (Appendix, Fig. A6g), and coincide with those already reported after treatment of CYN by photocatalysis (Adamski et al., 2016b) or cooking (Guzmán-Guillén et al., 2017; Prieto et al., 2017). Even though TP_{290} was also identified after advanced oxidation (He et al., 2014b) and ozonation (Yan et al., 2016) of CYN, no MS^2 fragments were described. TP_{290} showed an increasing relative abundance at the beginning of the assay reaching a plateau and staying constant until the last day of sampling in the case of strain A288, and A210. For strain A226, TP_{290} reached the highest relative abundance on day 14 and decreased from then on. In contrast, with strain OF001 TP_{290}, showed a rapid increase in the first 48 h, continuing at a slower rate during the rest of the assay (Fig. 3.2).

With the approach followed in the present study, we were able to detect the same seven transformation products formed by the four tested MOB, however, we cannot rule out the possibility that more were produced. Based on molecular masses of the transformation products, relative abundances, and previously reported reaction pathways, we propose a transformation scheme shown in Figure 3.3. A molecule not detected in the present work, was included based on previous reports to complement the proposed pathway. Further studies will have to be carried out to evaluate the presence of CYN biotransformation products in the environment.

The tentative identification of the same seven transformation products formed among all the tested MOB and that all transformation products were produced mainly by oxidation reactions support the hypothesis that CYN is transformed by a similar mechanism as proposed by Meerburg et al.(2012) and Tran et al. (2018), suggesting that MOB transform pollutants indirectly by the oxidation of Mn^{2+}. Active MOB produced reactive Mn^{3+}/Mn^{4+} species through the oxidation of Mn^{2+}, and these reactive species Mn^{3+}/Mn^{4+} are reduced to Mn^{2+} by the concomitant oxidation of the pollutant. Thus, CYN might be transformed by MOB via the unspecific interaction with reactive Mn species, even though the existence of an enzyme-substrate interaction cannot be completely excluded. Instead, other factors might influence CYN removal rates and the catalysed transformation reaction by MOB such as the different Mn oxidation rates or differences in structure and composition of the biogenic oxides of each MOB (Martínez-Ruiz et al., 2020b).

To date, five CYN derivatives produced by cyanobacteria have been described. All of them preserve the uracil moiety (Sadler, 2015). Therefore, transformation of CYN derivatives by MOB by the unspecific action of the reactive Mn species might be possible, even though

the type and amount of transformation products formed, may differ from the ones observed in the present study.

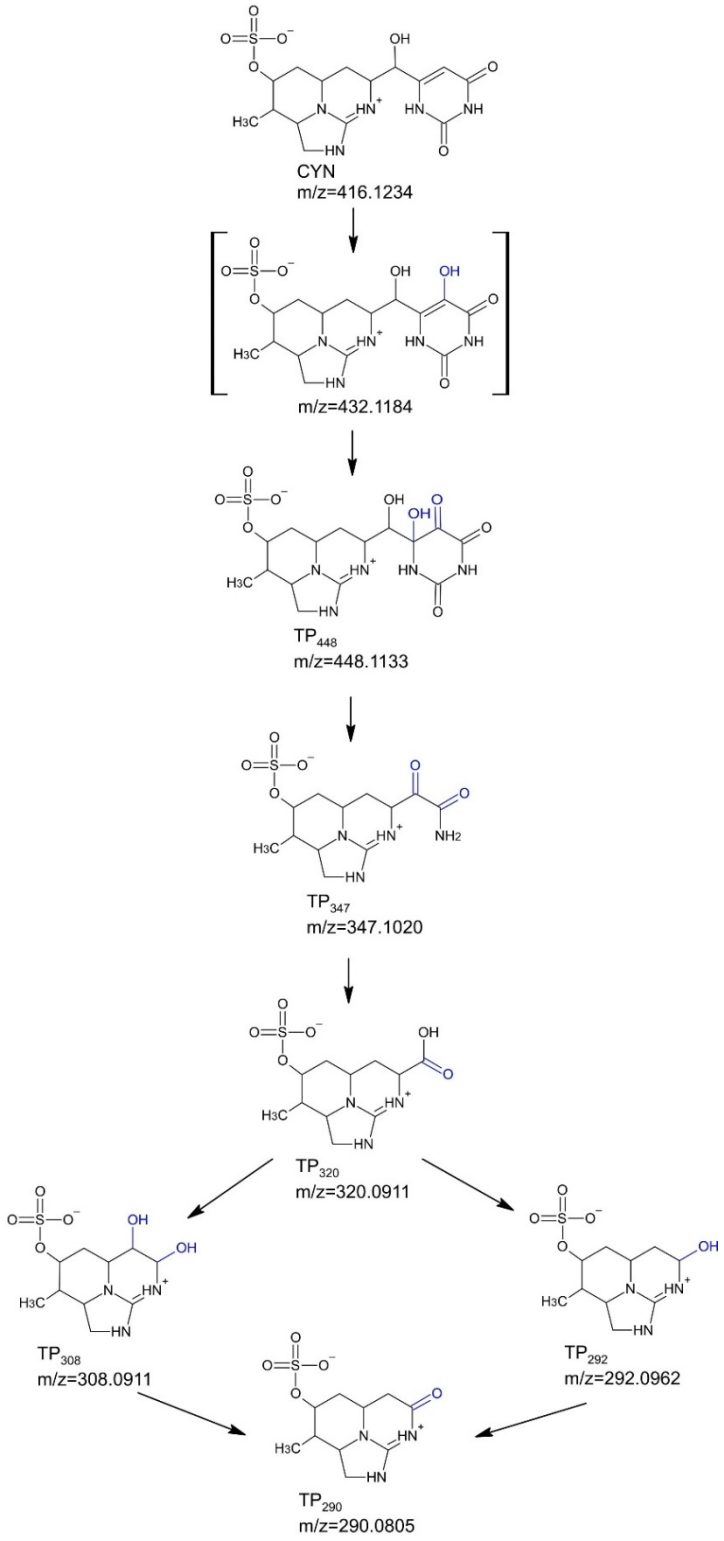

Fig. 3.3. Degradation products and proposed reaction pathways of CYN degradation by MOB. The compound in parentheses was not observed in the present study but has previously been reported (Fotiou et al., 2015; He et al., 2014b; Song et al., 2012; Yan et al., 2016). TP_{292a} and TP_{292b} are included in the scheme as TP_{292}.

3.3.3 Evaluation of cytotoxicity of CYN and its transformation products on human hepatic cells

We used the human hepatic cell lines HepG2 and HepaRG to evaluate the toxicity of CYN and the mixture of CYN transformation products generated by *Pseudomonas* sp. OF001, knowing that the liver is the main target organ of CYN (Poniedziałek et al., 2012).

For cytotoxicity evaluation, we selected the fastest CYN degrader, *Pseudomonas* sp. OF001, to produce the mixture of seven transformation products. The transformation product mixtures generated by *Pseudomonas* sp. OF001 after 4 and 7 days of growth with 4 and 12 mg L^{-1} of initial CYN concentration were collected. Several studies have reported dose-response curves and IC_{50} values of CYN for both human hepatic cell lines (Gutiérrez-Praena et al., 2019; Kittler et al., 2016; Neumann et al., 2007; Štraser et al., 2011). Taking into account that the objective of the present study was to compare the effect of pure CYN with the mixture of transformation products, the two CYN concentrations were selected to be in a range of concentrations in which toxic effects produced by CYN have been reported (Gutiérrez-Praena et al., 2019; Neumann et al., 2007; Štraser et al., 2011). Dose-response curves for the tentatively identified transformation products could not be established, because standards are not available.

The mixture of transformation products produced from both initial CYN concentrations at the two sampling points (day 4 and 7) showed much less toxicity in HepG2 cell lines than 1 and 3 mg L^{-1} of pure CYN (Fig. 3.4a-b). Indeed, cells exposed to the transformation products mixture had a cell viability of 93 to 97% and 105 to 110% with respect to the control without significant differences in the XTT and NR assay, respectively. This is in accordance with the reduced cytotoxicity of the transformation products formed by ozonation comparing with CYN on HepG2 cells (Yan et al., 2016). Moreover, our results are also in accordance with cytotoxicity studies with CYN transformation products formed by photocatalysis on the human hepatocellular carcinoma cell line C3A (G. Zhang et al., 2015). The transformation products mixture produced by photocatalysis (G. Zhang et al., 2015) and ozonation (Yan et al., 2016) strongly differed in composition to the mixture identified in this study, however both contained several products that we have also detected, such as TP_{290} and TP_{448}. Similarly, transformation products formed by chlorination of CYN showed reduced cytotoxicity compared to CYN using the human intestinal cell line Caco-2 (Merel et al., 2010), even though the three transformation products detected were different from those identified in this study. Interestingly, transformation products detected in all the mixtures previously tested to evaluate their toxicity, contained modifications at the uracil moiety as the transformation products detected in the present study. These results support the observation that the modification of the uracil moiety is crucial for toxicity reduction of CYN (Banker et al., 2001). Thus, the detection of

transformation products with different modifications at the uracil moiety, from simple hydroxylation to complete cleavage of the uracil group, might explain the reduction of toxicity of the mixture obtained in the present study.

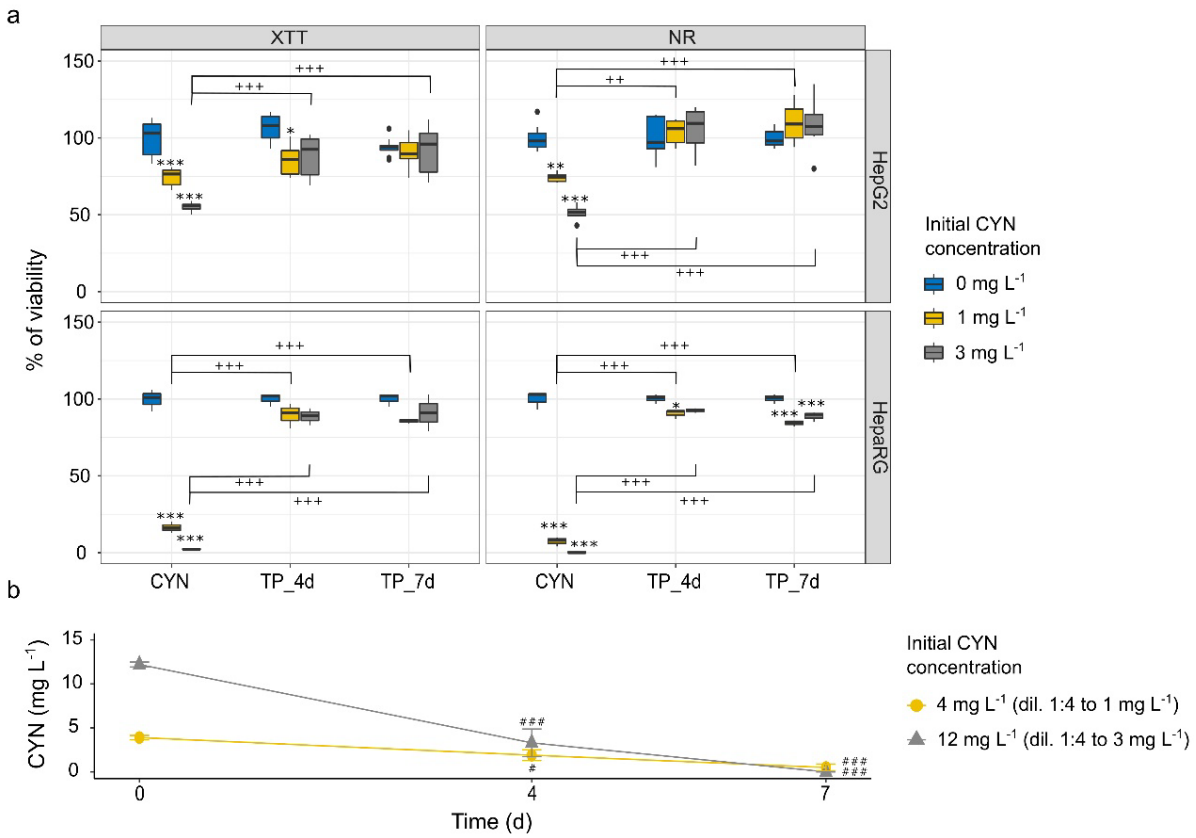

Fig. 3.4. Cytotoxicity of CYN and the mixture of transformation products. a) Viability of HepG2 and HepaRG cells exposed for 24 h to pure CYN and the mixture of transformation products. CYN: sample at time 0 of CYN incubated with *Pseudomonas* sp. OF001; TP_4d: mixture of transformation products after 4 days of incubation of CYN with *Pseudomonas* sp. OF001; TP_7d: mixture of transformation products after 7 days of incubation of CYN with *Pseudomonas* sp. OF001. b) CYN concentration in the supernatant tested for cytotoxicity. The samples were diluted 1:4 for the cytotoxicity test. Mean values ± standard error bars (HepG2 cells n = 6, HepaRG cells n = 3). * in *a* indicates significant differences with respect the control (blue box) of each group of samples (CYN, TP_4d, TP_7d); * $P < 0.05$, ** $P < 0.01$; *** $P < 0.001$. $^{+}$ in *a* indicate significant differences of TP_4d and TP_7d with respect CYN; $^{+}$ $P < 0.05$, $^{++}$ $P < 0.01$; $^{+++}$ $P < 0.001$. $^{\#}$ in *b* indicates significant differences of CYN concentration at day 4 and 7 with respect time 0; $^{\#}$ $P < 0.05$, $^{\#\#}$ $P < 0.01$; $^{\#\#\#}$ $P < 0.001$.

Viability of HepG2 cells decreased after 24 h of exposure to both CYN concentrations (1 and 3 mg L^{-1}). HepG2 cells exposed to 1 mg L^{-1} of CYN had a viability of 75% with respect to the control in XTT and NR assays (Fig. 3.4a-b). Cells exposed to 3 mg L^{-1} of CYN showed 59% (XTT), and 51% (NR) viability with respect to the control (Fig. 3.4a-b). In accordance, Yan et al.(Yan et al., 2016) reported viability of ~80% and ~60% of HepG2 cells with the MTT assay when they were exposed for 24 h to 1.2 (3 µM) and 4.2 mg L^{-1} (10 µM) of CYN, respectively.

Similarly, when Gutiérrez-Praena et al. exposed HepG2 cells to 1 and 3 mg L^{-1} of CYN, MTS assay evidenced 90 and 70% viable HepG2 cells, respectively (Gutiérrez-Praena et al., 2019).

HepG2 cell lines are a common model for cytotoxicity assessment of hepatotoxic compounds, like CYN (Froscio et al., 2009; Gutiérrez-Praena et al., 2019; Liebel et al., 2016; Pichardo et al., 2017; Štraser et al., 2013; Yan et al., 2016). However, HepaRG cells reflect the physiology of human hepatocytes much better than HepG2 cells (Gerets et al., 2012; Guillouzo and Guguen-Guillouzo, 2018). Therefore, we decided to confirm the reduction of toxicity of CYN and the mixture of transformation products, using differentiated HepaRG cells.

As observed for HepG2 cells, CYN had a cytotoxic effect on HepaRG cells as well; however, the toxicity was much more pronounced in the case of HepaRG cells (Fig. 3.4a-b). Viability of HepaRG cells exposed to CYN at 1 mg L^{-1} dropped to only 15% (XTT) and 8% (NR), respectively, with respect to the control. Cell viability of CYN at 3 mg L^{-1} was below 2% as evidenced by XTT and NR assays. Similarly, complete inhibition of HepaRG cells exposed for 24 h to 5.2 mg L^{-1} (12.5 µM) of CYN was quantified with the NR assay by Huguet et al.(2019). However, in the same study, when HepaRG cells were exposed to 1.2 mg L^{-1} (3 µM) of CYN, viability was 60% after 24 h. The IC_{50} values of CYN in HepaRG cells, evaluated with XTT, and NR tests reported by Kittler et al. were ~1.2 mg L^{-1} (3 and 2.7 µM) (2016) We did not evaluate the IC_{50} in the present study, but the values reported by Kittler et al. suggest a lower toxicity of CYN onto HepaRG cells than the toxicity that we observed. Experimental conditions such as passage number of the cells, and the solvent of CYN solution could explain the differences in the cytotoxic effects of CYN in HepaRG cells.

An interesting finding is the pronounced higher cytotoxicity of CYN on HepaRG than on HepG2 cells. One reason might be that CYN influences the expression of genes that are notably higher expressed in differentiated HepaRG cells than in HepG2 cells, such as CYP isoforms genes (e.g. *CYP2C8*, *CYP1A1*, *CY2A13*), genes related to phase II enzymes (e.g. UGT2B4-UDP glucuronosyltransferase, GSTA2-glutathione *S*-transferase alpha 2), and genes related to cell cycle (e.g. PCNA-proliferating, cell nuclear antigen, CDK1-cyclin-dependent kinase 1) (Huguet et al., 2019; Štraser et al., 2013). This could explain the observed differences and suggests that HepaRG cells are a more sensitive and suitable model than HepG2 cells to evaluate toxicity of hepatotoxins, such as CYN, and their transformation products.

In contrast to CYN, the mixture of transformation products formed by *Pseudomonas* sp. OF001 from both initial CYN concentrations (4 and 12 mg L^{-1}, diluted 1:4 for cytotoxicity assessment) after 4 and 7 days of incubation, showed no toxicity to HepaRG cells, with a viability of 85–91% with no significant difference with respect to the control in the XTT assay (Fig. 3.4a-b). The NR assay evidenced a reduced cytotoxicity of the transformation products mixture with a viability of 84–91% in the NR assay (Fig. 3.4a-b).

To the best of our knowledge, HepaRG cells have not yet been used to study the toxicity of CYN transformation products despite the fact that they reflect the biological function of hepatocytes better than HepG2 cells. HepaRG are well-known to express genes that metabolize pollutants at higher levels and are therefore better suited to carry out toxicity studies. While we observed strong toxicity of CYN on HepaRG – an effect that was much more pronounced than with HepG2 cells –, we did not measure substantial toxicity of the transformation products. We cannot exclude the possibility that additional transformation products which were below the detection limit of our analyses were formed by *Pseudomonas* sp. OF001. However, our experiments show that the mixtures of transformation products exert negligible cytotoxicity, either on HepG2 or on HepaRG cells.

3.4 Conclusions

In respect of our initial hypothesis and the stated objectives we have two major conclusions: First, we detected and tentatively identified seven CYN transformation products formed by all tested MOB. Transformation products formed due to biological activity have so far never been described. We also observed that CYN was transformed at higher rates when higher CYN concentrations were used compared to our previous study. The detection of the same transformation products among the tested MOB, despite the different CYN removal rates, origin of the strains, and phylogenetic lineages, suggests a general mechanism for CYN transformation by MOB. Even though the precise mechanism of CYN transformation is unknown, the identification of transformation products will help to further understand the process. Second, we showed that the toxicity of the mixture of transformation products on hepatic human cell lines was substantially reduced compared to CYN. The reduction of hepatotoxicity by MOB could be exploited by implementation of MOB treatment for the removal of CYN from water. Three of the four tested MOB were isolated from a freshwater pond in the Lower Oder Valley National Park, where potentially toxigenic cyanobacteria have been observed. Therefore, MOB might interact with cyanotoxins in natural environments. Thus, the identification of biologically produced CYN transformation products may contribute to a better understanding of the fate of CYN in the environment and the role of MOB in the removal of pollutants.

3.5 Acknowledgments

We thank Bernd Krostitz-Schroeer and Benjamin Scheer for excellent technical support and Jan Birkigt for helpful discussions. We thank Calvin Hon for English proofreading. Erika B. Martinez-Ruiz was supported by a research scholarship from the DAAD (Deutscher

Akademischer Austauschdienst). The project was partially funded by the Deutsche Forschungsgemeinschaft (DFG SZ 44/12-2). The authors declare no competing financial interest.

4 Genome analysis of *Pseudomonas* sp. OF001 and *Rubrivivax* sp. A210 suggests multicopper oxidases catalyze manganese oxidation required for cylindrospermopsin transformation

Martínez-Ruiz, E.B., Cooper, M., Barrero-Canosa, J., Bessarab, I., Haryono, M.A.S, Williams, R., Szewzyk, U., 2020. Submitted to BMC genomics

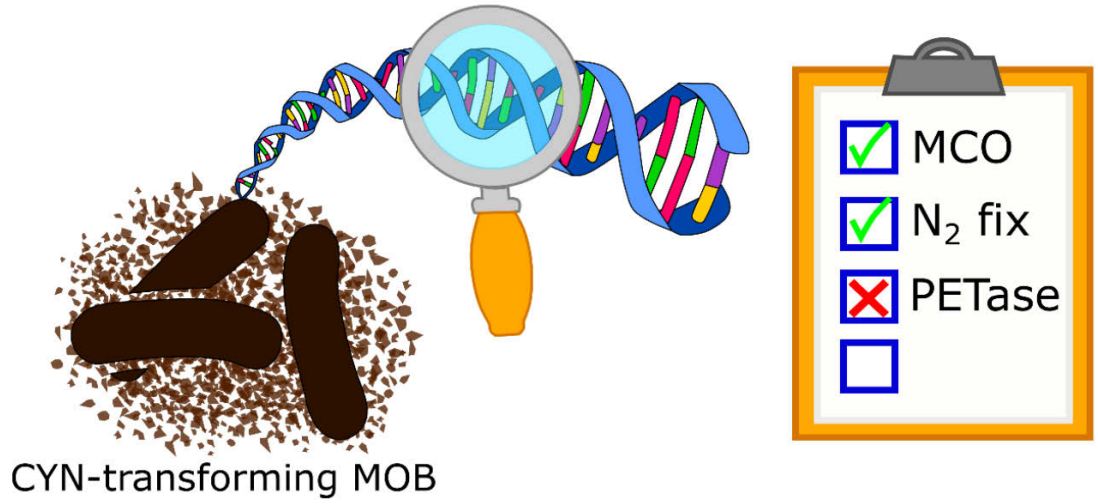

Abstract

Background

Cylindrospermopsin is a highly persistent cyanobacterial secondary metabolite toxic to humans and other living organisms. Strain OF001 and A210 are manganese oxidizing bacteria (MOB) able to transform cylindrospermopsin during the oxidation of Mn^{2+}. So far, the enzymes involved in manganese oxidation in strain OF001 and A210 are unknown. Therefore, we analyze the genomes of two cylindrospermopsin-transforming MOB, *Pseudomonas* sp. OF001 and *Rubrivivax* sp. A210, to identify enzymes that could catalyze the oxidation of Mn^{2+}. We also investigated specific metabolic features related to pollutant degradation and explored the metabolic potential of these two MOB with respect to the role they may play in biotechnological applications and/or in the environment.

Results

Strain OF001 encodes two multicopper oxidases and one haem peroxidase potentially involved in Mn^{2+} oxidation, with a high similarity to manganese-oxidizing enzymes described for *Pseudomonas putida* GB-1 (80%, 83% and 42% respectively). Strain A210 encodes one multicopper oxidase potentially involved in Mn^{2+} oxidation, with a high similarity (59%) to the manganese-oxidizing multicopper oxidase in *Leptothrix discophora* SS-1. Strain OF001 and A210 have genes that might confer them the ability to remove aromatic compounds via the catechol meta- and ortho-cleavage pathway, respectively. Based on the genomic content, both strains may grow over a wide range of O_2 concentrations, including microaerophilic conditions, fix nitrogen, and reduce nitrate and sulfate in an assimilatory fashion. Moreover, the strain A210 encodes genes which may convey the ability to reduce nitrate in a dissimilatory manner, and fix carbon via the Calvin cycle. Both MOB encode CRISPR-Cas systems, several predicted genomic islands, and phage proteins, which likely contribute to their genome plasticity.

Conclusions

The genomes of *Pseudomonas* sp. OF001 and *Rubrivivax* sp. A210 encode sequences with high similarity to already described MCOs which may catalyze manganese oxidation required for cylindrospermopsin transformation. Furthermore, the analysis of the general metabolism of two MOB strains may contribute to a better understanding of the niches of cylindrospermopsin-removing MOB in natural habitats and their implementation in biotechnological applications to treat water.

Keywords

Metabolic potential, manganese-oxidizing bacteria, biotransformation, cyanotoxins

4.1 Background

Cylindrospermopsin (CYN) is a secondary metabolite produced by several cyanobacteria, toxic for humans and other living organisms (Poniedziałek et al., 2012). The two bacterial strains OF001 and A210 transform the cyanotoxin CYN during the oxidation of Mn^{2+} (Martínez-Ruiz et al., 2020b, 2020a). Strain OF001 belongs to the gammaproteobacteria and was isolated from the effluent of an experimental fixed-bed biofilm reactor established for the removal of recalcitrant substances from wastewater. Strain A210 belongs to the betaproteobacteria and was isolated from an iron manganese-depositing biofilm in a freshwater pond in the Lower Oder Valley National Park, Germany.

The removal of CYN by both strains required the active oxidation of $MnCO_3$ whereas no or low CYN removal was observed with $MnSO_4$ or in setups without manganese. Sterile biogenic oxides formed by the strains did not show any influence on CYN removal, highlighting the importance of the active manganese oxidation. Both strains are able to remove 100% of CYN at the highest rates reported for biological CYN removal so far (Martínez-Ruiz et al., 2020b, 2020a). Furthermore, analysis of CYN transformation products revealed that the same seven transformation products were formed by both strains corroborating the important role of manganese oxidation. However, strain OF001 and A210 showed important differences. *Pseudomonas* sp. strain OF001 degraded CYN within 3 days. Whereas strain A210 degraded CYN within 14 to 28 days when cultivated under the same conditions. Moreover, strain OF001 required yeast extract as additional carbon source for the removal of CYN. In contrast, strain A210 was able to transform CYN in mineral media (Martínez-Ruiz et al., 2020b).

So far, little is known about biological CYN removal (Dziga et al., 2016; Martínez-Ruiz et al., 2020b, 2020a; Mohamed and Alamri, 2012; Nybom et al., 2008). Even though several bacterial strains have been reported to remove CYN, to date, no enzymes or defined metabolic pathway for the transformation of CYN have been identified (Kormas and Lymperopoulou, 2013; Kumar et al., 2019). Moreover, for biological CYN removal, no transformation products have been identified except for CYN transformed by MOB (Martínez-Ruiz et al., 2020a).

MOB are present in terrestrial (W. Yang et al., 2013), marine and freshwater environments (Hansel and Learman, 2015; Schmidt et al., 2014; Szewzyk et al., 2011; Tebo et al., 2005), but they also occur in drinking water systems and reactors aiming at the removal of manganese and other pollutants (Cerrato et al., 2010; Szewzyk et al., 2011; Tobiason et al., 2016; Y. Zhang et al., 2015). MOB belong to diverse phylogenetic lineages with a broad physiological diversity (e.g. autotrophs and mixotrophs) (Tebo et al., 2005, 2004; Zhou and Fu, 2020). Through the oxidation of Mn^{2+}, MOB form water-insoluble biogenic manganese oxides, which are one of the strongest natural oxidants (Hennebel et al., 2009; Tebo et al., 2004). Biogenic manganese oxides often interact with other compounds and thus play an important

role in the biogeochemical cycle of manganese and other elements (Lee and Xu, 2016; Stein et al., 2001; Tebo et al., 2004; Zhou and Fu, 2020).

The physiological role of manganese oxidation is not fully understood. Manganese oxidation was proposed to provide energy to support the growth of bacteria. However, no conclusive results were shown (Kepkay and Nealson, 1987). Other proposed functions are the protection against the toxicity of organic compounds, and reactive oxygen species (Banh et al., 2013; Zerfaß et al., 2019), the breakdown of organic matter into utilizable substrates (Jones et al., 2018; Sunda and Kieber, 1994), and the use as a carbon reservoir (Estes et al., 2017). Nevertheless, the precise physiological role of manganese oxidation remains unknown (Zhou and Fu, 2020). Different manganese oxidation mechanisms have been described including non-enzymatic pathways based on a pH increase, the oxidation through superoxide production, or an anaerobically photo-driven reaction; and enzymatic reactions generally associated to the activity of multicopper oxidases (MCO) and haem peroxidases (Geszvain et al., 2012; Hansel and Learman, 2015; Zhou and Fu, 2020).

Besides CYN, MOB transform different organic and inorganic pollutants including, diclofenac, benzotriazole, 17 α-ethinylestradiol, bisphenol A, As(III), and Sb(III) (Martínez-Ruiz et al., 2020a, 2020b; Meerburg et al., 2012; Sochacki et al., 2018; Tran et al., 2018; H. Wang et al., 2019; Wang et al., 2017; Watanabe et al., 2013). The mechanism of pollutant transformation was proposed to be based on an unspecific oxidation by reactive manganese Mn^{3+}/Mn^{4+} species that are formed through the oxidation of Mn^{2+} (Meerburg et al., 2012). For CYN transformation, a similar mechanism was assumed based on the requirement of active Mn^{2+} oxidation for efficient CYN removal and the formation of the same transformation products among all tested MOB, including strain OF001 and A210 (Martínez-Ruiz et al., 2020a). Thus, it is suggested that MOB act as suppliers of biogenic oxides that indirect oxidize the pollutants. However, the intrinsic capacity of MOB to remove organic compounds has not been deeply investigated (Zhou and Fu, 2020).

The whole genome sequences of some MOB have been analysed previously to gain a better insight into the mechanism of manganese oxidation (Gregory J. Dick et al., 2008; X. Wang et al., 2020). However, so far, no reported pollutant-removing MOB strains were analyzed on a genomic level. Besides, for strain OF001 and A210, information about the metabolic potential, including also about genes potentially involved in manganese oxidation, was missing. The genomic analysis of strain OF001 and strain A210 might allow to identify enzymes potentially involved in the oxidation of manganese based on the comparison with manganese oxidizing enzymes reported to date. Furthermore, metabolic differences between the two MOB strains became evident during cultivation experiments in presence of CYN (Martínez-Ruiz et al., 2020b), and further dissimilarities could be assumed. Such metabolic

differences could be relevant for the application of the strains for the removal of pollutants from water in technical systems including but not limited to wastewater or drinking water treatment plants, and for the understanding of the niche they may occupy in natural environments.

Therefore, in this study, we analysed the draft genomes of the MOB strains OF001 and A210, both of which are able to transform CYN during oxidation of $MnCO_3$. We aim to provide further insight into i) manganese oxidation mechanism, ii) other metabolic pathways relevant for pollutant removal, iii) energy harvesting processes such as respiration, iv) their metabolic potential in comparison with their closest described phylogenetic relatives, and v) genome plasticity related to horizontal gene transfer mechanisms.

4.2 Results and discussion

4.2.1 General genome features

Genome quality estimation determined with CheckM showed that both genomes are of high quality (>90% completeness and <5% contamination). Genomes of strains OF001 and A210 have a completeness of 99.59 and 99.38%, respectively, with a contamination level of 2.12 and 0.35%.

The genome sequence of strain OF001 contains 4,476,686 bp in 65 contigs with a N50 contig length of 147,742 bp, and a GC content of 68.01%. The genome of strain OF001 encodes 4845 genes of which 4720 are protein coding sequences (CDS). Furthermore, one 16S, one 23S, and six 5S rRNA genes were identified in the genome of OF001, as well as, sixty-seven tRNA genes that enable recognition of codons for all 20 amino acids.

The genome sequence of strain A210 contains 5,371,534 bp in 72 contigs with a N50 contig length of 327,374 bp, and a GC content of 69.54%. The genome of strain A210 encodes 5184 genes from which 5112 are CDS. In addition, one 5S-23S-16S rRNA operon, and 52 tRNA genes were identified in the genome of strain A210. Genome quality estimation and general genomic features are summarized in Table 4.1.

Genome Taxonomy Database tool kit (GTDB-tk) was used to classify the bacterial genomes. GTDB-tk analysis classified strain OF001 as a member of the *Pseudomonas*_K group. According to the GTDB (May, 2020) *P. oryzae*, *P. sagittaria*, *P. linyingensis*, and *P. guangdongensis* belong to the *Pseudomonas*_K group. The genus status of the strain OF001 in the *Pseudomonas*_ K group was supported by the genetic relatedness determined by whole-genome analysis and 16S rRNA phylogeny (Fig. A7).

Table 4.1 Genomic features of strains OF001 and A210.

	OF001	A210
N50	147,742	327,374
Number of contigs	65	72
CheckM completeness	99.59%	99.38%
CheckM contamination	2.12%	0.35%
Complete genome size (bp)	4,476,686	5,371,534
Undetermined bases	6,400	7,100
% GC	68.01	69.54
% Protein coding density	90.64	93.09
Pseudogene	6	2
CDS	4720	5112
Genes assigned to:		
COG	3436 (72.70%)	3798 (74.27%)
KEGG	2490 (52.7%)	2632 (51.5%)
Hypothetical proteins / unknown function	1327 (28.08%)	1492 (29.17%)
Fragment CDS	6	2
tRNA	67	52
rRNA	8	3
misc_RNA	43	14
tmRNA	1	1

CDS: coding sequences, COG: Cluster of Orthologous Groups; KEGG: Kyoto Encyclopedia of Genes and Genomes; tRNA: transfer RNA; rRNA, ribosomal RNA; misc_RNA: miscellaneous RNA; tmRNA: transfer-messenger RNA.

To determine the species affiliation of *Pseudomonas* sp. OF001 average nucleotide identity (ANI), and tetra-nucleotide frequencies (TETRA) analysis were done. The analysis revealed highest similarity between strain OF001 and *P. oryzae* KCTC 32247 with an ANI based on BLAST (ANIb) value of 89.06%, an ANI based on MUMmer (ANIm) value of 90.98%, and a TETRA value of 0.998 (Fig. 4.1a). Organisms with an ANI value above 95%, and a TETRA value above 0.99 are suggested to delineate the same species level (Goris et al., 2007; Richter et al., 2016; Richter and Rosselló-Móra, 2009). TETRA values should be in agreement with ANI values to support the species assignation (Richter and Rosselló-Móra, 2009). TETRA values of strain OF001 and the organisms of the *Pseudomonas*_K group were higher than 0.99, but ANI values were below the species limit. Together, the data suggest strain OF001 is a potential new species of the *Pseudomonas*_K group.

GTDB-tk analysis classified strain A210 as a member of the *Rubrivivax* genus. According to the GTDB database this genus belongs to the order Burkholderiales and has so far only three described species: *R. benzoatilyticus*, *R. gelatinosus, and R. albus* (Nagashima et al., 2012; Ramana et al., 2006; Sheu et al., 2020).

Based on the phylogenetic analysis using the whole 16S rRNA gene sequence (Fig. A8a), strain A210 could not be classified at genus level. Organisms with high similarity to the

16S rRNA gene sequence of strain A210 were mainly bacteria of the *genera incertae sedis* from the *Comamonadaceae* family (*Aquabacterium, Ideonella, Leptothrix, Roseateles, Rubrivivax, Sphaerotilus*) (Fig. A8a). However, phylogenomic analysis of strain A210 done with TYGS platform affiliated A210 with organisms of the genus *Rubrivivax* (Fig. A8b), supporting the results obtained with the GTDB-tk.

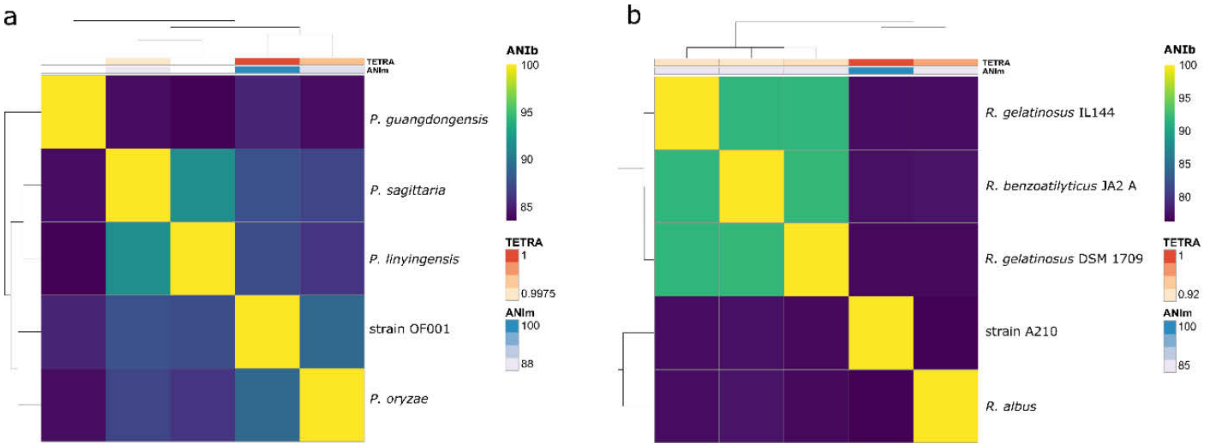

Fig. 4.1. Heatmap representing the degree of similarity of the MOB genomes. a) *Pseudomonas* sp. OF001, and b) *Rubrivivax* sp. A210. Heatmaps was derived from the average nucleotide identity (ANI) matrix based on BLAST (ANIb) Dendrogram directly reflects the degree of identity between genomes. ANIm: ANI based on MUMmer; TETRA: correlation indexes of the tetra-nucleotide frequencies; DDH d_4: DDH calculated with the formula d_4, which is the non-logarithmic version of formula d_5 (used for the Appendix, Fig. S4.1 and S4.2). Formula d_4 is highly recommended when using draft genomes to assure confident results (Meier-Kolthoff et al., 2013).

ANI, and TETRA analysis were done with the genome of A210 to analyze species affiliation. The analysis showed the highest similarity of *Rubrivivax* sp. A210 with *R. benzoatilyticus* JA2 with an ANIb value of 76.69%, an ANIm value of 84.45%, and a TETRA value of 0.913 (Fig. 4.1b). Thus suggesting, strain A210 is a potential new species of the genus *Rubrivivax*.

4.2.2 Pan and core genome

The pan-genome of the *Pseudomonas*_K group genomes comprised 20,296 genes belonging to 6,805 MICFAM (Microscope Families)(Miele et al., 2011; Vallenet et al., 2017). The core-genome comprised 11,985 genes that correspond to 1,957 MICFAM, and the variable-genome contained 8,311 corresponding to 4,848 MICFAM. The *Pseudomonas* sp. OF001 genome contains 1,091 strain-specific genes from 1,052 MICFAM that correspond to 24.08% strain-specific coding sequences. With this, strain OF001 contains the highest number of CDS from the *Pseudomonas*_K group genomes analyzed (Fig. A9a). Among the strain-

specific genes in OF001, we found genes related to mercury resistance, transport, and foreign DNA (see also section *3.5 Elements potentially acquired by horizontal gene transfer*).

Pan- and core-genome size evolutions were estimated with the four available genomes of the *Pseudomonas*_K group and the genome of strain OF001. The curve of the pan-genome of strain OF001 and *Pseudomonas*_K group did not reach the plateau, suggesting that the pan-genome of *Pseudomonas*_K group is open and the sequences of other genomes from this group might increase the gene pool of novel genes (Fig. A10a). The plateau of the core-genome is reached with the five genomes selected and is composed of approximately 2,000 MICFAM (Fig. A10b).

The pan-genome of *Rubrivivax* genomes comprised 23,140 genes belonging to 9,974 MICFAM. The core-genome comprises 10,154 genes that correspond to 1,629 MICFAM, and the variable-genome contains 12,986 genes corresponding to 8,345 MICFAM. The *Rubrivivax* sp. A210 genome contains 2,123 strain-specific genes from 2,035 MICFAM that correspond to 42.98% strain-specific coding sequences (Fig. A9b). Among the strain-specific genes in A210, we found genes related to transport like ABC transporters, and cytochromes (see also section 3*.4.3 Aerobic respiration*).

Pan- and core-genome size evolutions were estimated according to the genomes selected for the A210 analysis (Fig. A10c-d). The core-genome plateau is apparently reached with the analyzed genomes and is composed of approximately 1,600 MICFAM.

4.2.3 Genes potentially involved in manganese oxidation

In *Pseudomonas* sp. OF001, we detected three different homologues of manganese-oxidizing multicopper oxidases (MO-mco's) (OF001_u20185, OF001_u60094, and OF001_u90046). Gene name, accession number, locus tag in the evaluated genomes, E-value, and percent similarity of amino acid alignments are shown in Table A4. All three MO-mco's homologues of strain OF001 belong to the homologous cupredoxin superfamily (IPR008972), according to the InterPro-based analysis. The amino acid sequences encoded by OF001_u20185 and OF001_u60094 exhibit the four characteristic motifs found in multicopper oxidases, in the same order and in a similar position as observed in McoA and MnxG from *P. putida* GB-1 (Fig. 4.2a, b). In addition, MO-mco's homologues OF001_u20185 and OF001_u60094, showed the highest similarity to the Mn^{2+} oxidases *mnxG (80%)* and *mcoA (83%)* from *P. putida* GB-1 (Geszvain et al., 2013), whereas OF001_u90046 showed the highest similarity to *moxA* (51%) from *Pedomicrobium* sp. ACM 3067 (Ridge et al., 2007). All three MO-mco's contain non-cytoplasmic domains covering almost the whole protein, and

a transmembrane domain or a transmembrane helix. The presence of non-cytoplasmic and transmembrane domains suggests that these enzymes are loosely bound to the outer membrane, which is in agreement with the localization of MO-mco's in other MOB (Corstjens et al., 1997; Gregory J Dick et al., 2008; Geszvain et al., 2013).

OF001_u60094 in *Pseudomonas* sp. OF001 is located in a predicted operon similar to *mnxG* in *P. putida* GB-1 (Geszvain and Tebo, 2010). The operon is composed out of five additional genes with high similarity to those located in the *mnxG* operon of *P. putida* GB-1, (63–76% according to blastp analysis, Fig. 4.2c). Expression of the MO-mco's in *P. putida* GB-1 is regulated by a two-component pathway, *mnxS1*/*mnxS2*/*mnxR* (Geszvain and Tebo, 2010). In the genome of strain OF001, we found putative homologues to the *mnxS2* histidine kinase, and to the *mnxR* regulator, arranged in a similar operon structure as in *P. putida* GB-1 (Fig. 4.2d) (Geszvain and Tebo, 2010). Our results suggest that the regulation of the MO-mco's of strain OF001 follows a similar regulation to the one observed in *P. putida* GB-1.

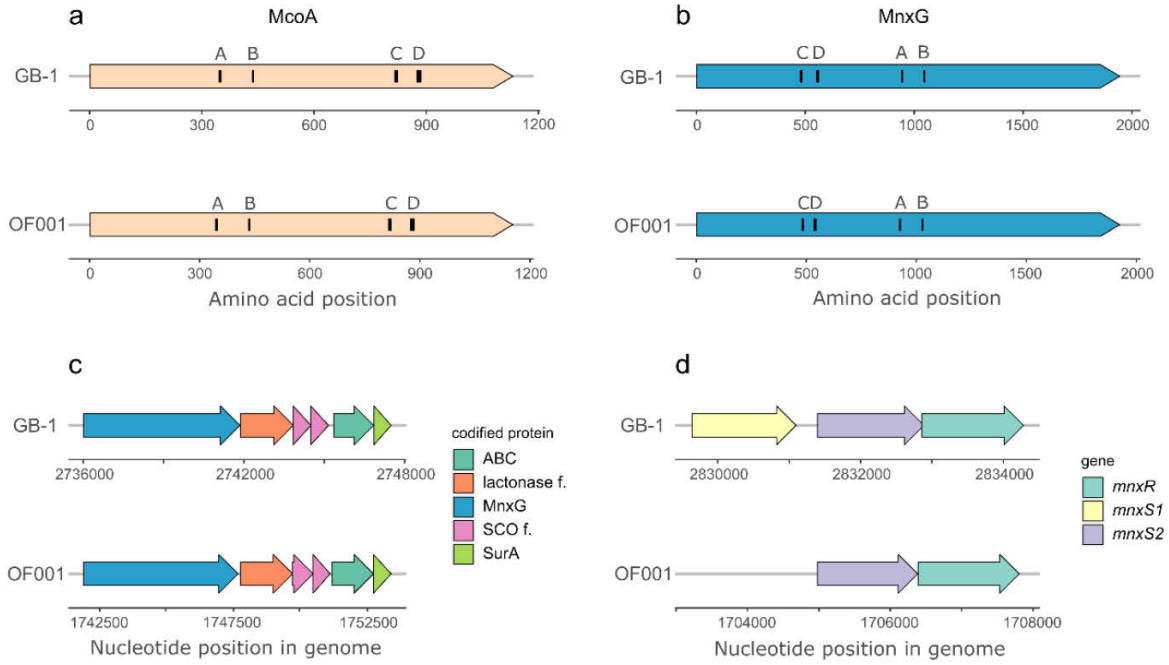

Fig. 4.2. Genetic organization of regulatory system and MO-mco's in *P. putida* GB-1 and *Pseudomonas* sp. OF001. a) McoA protein of strain GB-1, and the putative homolog found in strain OF001, b) MnxG protein of strain GB-1, and the putative homolog found in strain OF001, c) predicted operon organization in which *mnxG* (MO-mco) is found in strain GB-1, and putative homologues found in a predicted operon in strain OF001, and d) regulatory system for Mn^{2+} oxidation of strain GB-1, and putative homologues found in strain OF001. Capital letters (A-D) in a), and b) represent the multicopper oxidases motifs (Spiro et al., 2008). *mnxR*: response regulator; *mnxS1* and *mnxS2*: sensor histidine kinases; ABC: ABC transporter; lactonase f.: beta-propeller fold lactonase family protein; *mnxG*: MO-mco, SCO f. SCO family protein; SurA: SurA N-terminal domain-containing protein, McoA: MO-mco, MnxG: MO-mco.

Furthermore, two homologues of manganese-oxidizing haem peroxidases (MO-hpox's) (OF001_u100035, and OF001_u220048) were identified in strain OF001. The putative MO-hpox homologue OF001_u100035 showed the highest similarity with the Mn^{2+} oxidase *mopA* of *P. putida* GB-1 (42%). Together with the MO-hpox of *A. manganoxydans* SI85-9A1, they belong to the haem peroxidase superfamily (IPR010255). The MO-hpox homologue OF001_ u220048, showed highest similarity to *mopA* of *Erythrobacter* sp. SD-21 and neither of the two belong to the haem peroxidase superfamily. No cytoplasmic or non-cytoplasmic domains could be identified for the putative MO-hpox's homologues of strain OF001. Therefore, we evaluated the probable subcellular localization with LocTree (Goldberg et al., 2014). Both putative MO-hpox's of OF001 are likely secreted to the media, similar as previously described for several MO-hpox's of other MOB (Anderson et al., 2009; Corstjens et al., 1997; Gregory J Dick et al., 2008; Geszvain et al., 2016, 2013; Ridge et al., 2007).

In the genome of *Rubrivivax* sp. A210, five MO-mco's homologues were identified (RA210_u420004, RA210_u30250, RA210_u110082, RA210_u10102, and RA210_u100111) (Table A4). Two MO-hpox's homologues (RA210_u10091, and RA210_u140033) were identified, but were discarded for further analysis due to very low coverage of the query sequences (Table A4).

All MO-mco's homologues of strain A210 belong to the homologous cupredoxin superfamily (IPR008972), according to the InterPro-based analysis. They contain non-cytoplasmic domains which cover almost the whole protein, and possess either a transmembrane domain or a transmembrane helix, except for RA210_ u420004. This suggests that these enzymes are loosely bound to the outer membranes, similar as previously reported for other MO-mco's (Corstjens et al., 1997; Gregory J Dick et al., 2008; Geszvain et al., 2013). RA210_u30250 shows highest similarity (59%) to the *mofA* gene of *L. discophora* SS-1 (Corstjens et al., 1997). In addition, the amino acid sequence of RA210_u30250 encodes the four characteristic motifs found in multicopper oxidases in the same order and in a similar position than those found in MofA from *L. discophora* SS-1 (Fig. 4.3a). In addition, it is located in a predicted operon similar to *mofA* in *L. discophora* SS-1 (Fig. 4.3b). The *mof* operon in *L. discophora* SS-1 is composed out of *mofA*, *mofB* and *mofC* (G. J. Brouwers et al., 2000). The putative *mof* operon in strain A210 encodes five genes, including the putative *mofA* homologue, and two genes with high similarity to *mofB* (68%) and *mofC* (60%), together with a putative metallochaperon, and an exported protein of unknown function (RA210_u30246 – RA210_u30250).

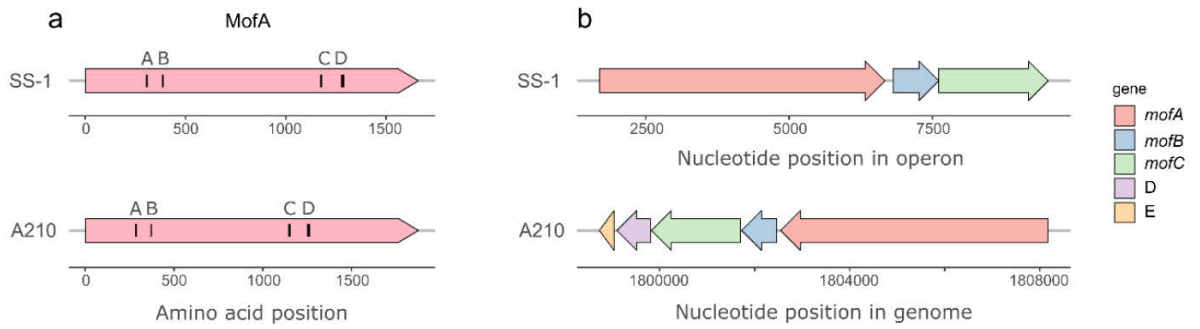

Fig. 4.3. Genetic organization of the MO-mco in *L. discophora* SS-1 and *Rubrivivax* sp. A210. a) MofA protein of strain SS-1, and the putative homolog found in strain A210, and b) predicted operon organization in which *mofA* (MO-mco) is found in strain SS-1, and the putative homologues found in a predicted operon in strain A210. Capital letters (A-D) in a) represent the multicopper oxidases motifs (Spiro et al., 2008). *mofA*: MO-mco; *mofB*: macrophage infectivity potentiator (mip); *mofC*: Cytochrome c domain-containing protein. Note that in a) the operon in strain SS-1 is represented based on the total length of the operon because the genome has not been sequence. Capital letters in b) are the other two proteins predicted within the operon of strain A210, D: copper metallochaperone, and E: protein of unknown function.

In spite of the low homology between MO-mco's from different organisms, we attempted to gain further evidence for the Mn^{2+} oxidation activity of the suggested multicopper oxidases by using a phylogenetic approach. For this purpose, a phylogenetic tree was constructed with sequences of MO-mco and non-MO-mco retrieved form the NCBI database excluding the newly identified putative MO-mco homologues (Table A5), to discard the possibility that the new sequences were the main factor driving the topology of the tree (Fig. A11). Subsequently, the putative MO-mco homologues of the strains OF001 and A210 were added. Phylogenetic analysis revealed one cluster of all MO-mco sequences and one cluster of non-MO-mco (Fig. 4.4). The only identified outlier was *moxA* from *Pedomicrobium* sp. ACM 3067, a reported MO-mco, affiliated with the non-MO-mco. Possibly, this is due to an uncertain assignation as suggested previously by Anderson et al. (2009). In contrast to OF001_u20185, OF001_u60094, and RA210_u30250, the proteins encoded by OF001_u90046, and RA210_u100111 did not cluster with the MO-mco (Fig. 4.4). This result suggests that the two annotated multicopper oxidases OF0011_u90046 and RA210_u100111 in *Pseudomonas* sp. OF001 and *Rubrivivax* sp. A210, respectively, do not possess the Mn^{2+} oxidation activity. Collectively, the data suggest that the best candidates for Mn^{2+} oxidation are MO-mco OF001_u20185, OF001_u60094, and MO-hpox OF001_u100035 in strain OF001 and MO-mco RA210_u30250 in strain A210.

Our results indicate that both MOB strains, OF001 and A210, oxidize manganese through enzyme-mediated mechanisms. In spite of the evidences found based on the genomic analysis, further experiments are required to determine which enzymes are involved in the oxidation of Mn^{2+} in *Pseudomonas* sp. OF001 and *Rubrivivax* sp. A210.

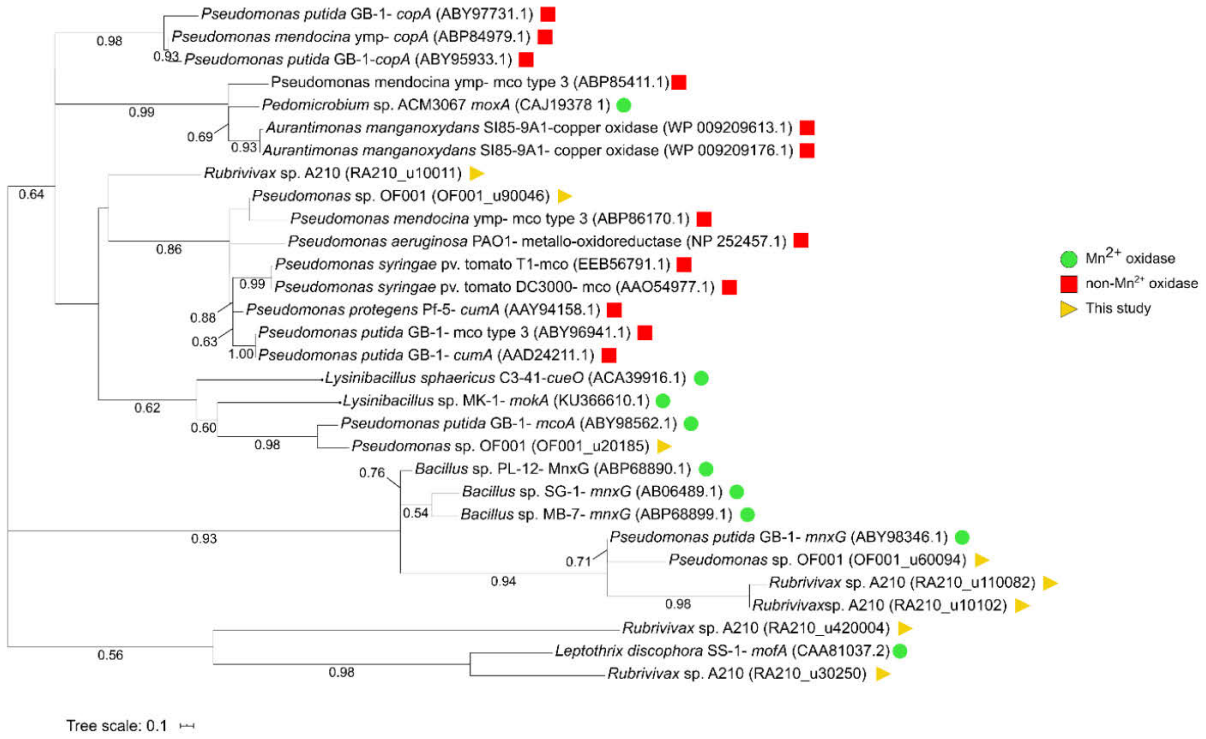

Fig. 4.4. Maximum Likelihood phylogenetic tree based on multicopper oxidases sequences with and without reported Mn^{2+} oxidation activity. Numbers in the branches represent bootstrap value. Scale bar represent sequence divergence.

4.2.4 General metabolism

4.2.4.1 Organic carbon metabolism

Pseudomonas sp. OF001 and *Rubrivivax* sp. A210 possess all genes necessary for commonly found central carbohydrate metabolism in aerobic organism including glycolysis (Embden-Meyerhof-Parnas), gluconeogenesis, tricarboxylic acid cycle (Krebs cycle), and the non-oxidative branch of the pentose phosphate pathway, to support basic growth. In both MOB, genes involved in the oxidative branch of the pentose phosphate pathway were incomplete which is in accordance with its absence in many aerobic and thermophilic organisms (Stincone et al., 2015).

4.2.4.2 CO_2 fixation

Pseudomonas sp. OF001 possesses several genes encoding enzymes related to CO_2 fixation via the Calvin cycle, however the key enzyme D-ribulose-1,5-bisphosphate carboxylase/oxygenase (RuBisCO) is missing. This is in accordance with our previous study which demonstrated the growth of strain OF001 only in presence of an organic carbon source (Martínez-Ruiz et al., 2020b).

In contrast, *Rubrivivax* sp. A210 has the complete repertoire of genes required for CO_2 fixation via the Calvin cycle, including the RuBisCO, which is supported by previous studies of our group showing that A210 was able to grow in mineral media (Martínez-Ruiz et al., 2020b). The *cbb* operon in strain A210 has all genes predicted to be encoded together with the RuBisCO small (cbxSP) and large (cbbL) subunits (*gpx*, *cbbYP, prkB, fbp, cbxXC*). The presence of genes coding for enzymes of the Calvin cycle in strain A210 is in accordance with their detection in the three described species of the *Rubrivivax* genus *R. albus* (Sheu et al., 2020)*, R. gelatinosus* (Nagashima et al., 2012) and *R. benzoatilyticus* (Ramana et al., 2006).

4.2.4.3 Aerobic respiration

All genes for oxidative phosphorylation and aerobic respiration were present in *Pseudomonas* sp. OF001. Among them, twenty genes annotated as cytochromes, including 14 *c*-type, 5 *b*-type, and 1 *d*-type cytochromes were found. Also, several predicted terminal oxidases are present including cytochrome *bd*-type quinol oxidase, cytochrome *c* oxidases, and cbb_3-type cytochrome *c* oxidases.

cbb_3-type cytochrome *c* oxidases in the genome of strain OF001 are predicted to be organized in two operons, one operon containing *cbbP* and *cbbQON* genes, similar as reported for other bacteria (Ekici et al., 2012; Koch et al., 1998; Kulajta et al., 2006; Preisig et al., 1996), and one operon containing a copy of *cbbPO* and a gene of unknown function. Next to the *cbbPQON* operon, a predicted operon with three (*ccoSIG*) genes encoding the enzymes responsible of the assembly of cbb_3-type cytochrome *c* oxidases was observed (Durand et al., 2018). The *ccoH* assembly factor for the cbb_3-type cytochrome oxidase is missing in strain OF001, suggesting that it follows a *ccoH*-independent assembly mechanism, similar as described for *H. pylori*, and *R. gelatinosus* (Durand et al. 2018).

Likewise, all genes for oxidative phosphorylation and aerobic respiration were found in *Rubrivivax* sp. A210. Thirty-nine genes were annotated as cytochromes, including thirty *c*-type, and nine *b*-type cytochromes. Predicted terminal oxidases are present, including cytochrome *c* oxidases and cbb_3-type cytochrome *c* oxidases. *cbb*3-type cytochrome *c* oxidases and the enzymes responsible of their assembly in the genome of strain A210 are predicted to be organized in a single operon *ccoISNOQPG*. Similar as for OF001, the *ccoH* assembly factor for the cbb_3-type cytochrome oxidase is missing in strain A210, which suggest that it also follows a *ccoH*-independent assembly mechanism likewise to strain OF001.

The presence of diverse cytochrome oxidases, with high O_2 affinity, rather than only cytochrome *c* oxidases, indicate the potential of strain OF001 and A210 to grow under a wide

range of O_2 concentrations.

4.2.4.4 Nitrogen metabolism

Pseudomonas sp. OF001 possesses genes predicted to participate in ammonium uptake, including specific transporters like *amtB* and genes involved in the regulation of the process such as *glnA*, *glnL*, and *glnK* (Atkinson and Ninfa, 1999; Blauwkamp and Ninfa, 2002; Gosztolai et al., 2017; Magasanik, 1982; Pahel et al., 1982; Schreier and Sonenshein, 1986). The genes are predicted to be arranged within different operons, with *glnA* as a single regulated gene, located immediately downstream from the operon encoding *glnG* and *glnL*.

In addition, the genome of *Pseudomonas* sp. OF001 encodes the genes *nifDKH*, implicated in nitrogen fixation. Nitrogenase genes in strain OF001 are not predicted to form an operon, but cluster together in the genome. The detection of the *nifDKH* genes is in accordance with their detection in the genomes of the two taxonomically closest organisms to OF001, *P. linyingensis* (He et al., 2012) and *P. sagittaria* (Lin et al., 2013).

Furthermore, strain OF001 encodes genes related with assimilatory nitrate reduction, including nitrate transport, the ammonium-forming nitrite reductase small subunit *nasD*, and the nitrate reductase *nasA* (Kawasaki et al., 1997; Mohan and Cole, 2007; Ramos et al., 1993; Yukioka et al., 2017). Strain OF001 also possesses two nitrite reductases, one in a predicted operon together with the nitrate reductase *nasA*, and the other as an independent regulated gene. Genes involved in dissimilatory nitrate reduction were missing. This is in agreement with the absence of genes involved in dissimilatory nitrate reduction in the closest related *Pseudomonas*_K group.

Similar to strain OF001, the genome of *Rubrivivax* sp. A210 encodes genes predicted to participate in ammonium uptake in five predicted operons, including specific transporters like *amtB* and genes involved in the regulation of the process such as *glnA*, *glnL,* and *glnK* (Atkinson and Ninfa, 1999; Blauwkamp and Ninfa, 2002; Gosztolai et al., 2017; Magasanik, 1982; Pahel et al., 1982; Schreier and Sonenshein, 1986). However, in contrast to strain OF001, the *glnB* gene is encoded in the genome of strain A210. GlnB is a PII signal transcription protein, homologue to GlnK (Arcondéguy et al., 2001). Both are key for the metabolic regulation of ammonium uptake. The presence of the *glnK* and *glnB* genes in *Rubrivivax* sp. A210 suggests that ammonium uptake in strain A210 follows a similar regulation as described for *Escherichia coli*. (Gosztolai et al., 2017; Yurgel et al., 2010). GlnB found in Proteobacteria is commonly associated with glutamine synthetase genes (Sant'Anna et al., 2009), and likewise, the *glnB* gene of strain A210 is located in an operon structure next to the

glutamine synthetase *nadE*.

The genes *nifDKH*, implicated in nitrogen fixation, are encoded in the genome of *Rubrivivax* sp. A210 similarly as observed for all three known *Rubrivivax* species (Nagashima et al., 2012; Ramana et al., 2006; Sheu et al., 2020). The *nifDKH* genes are located in a predicted operon structure together with a putative ferredoxin and a conserved protein of unknown function. Ferredoxin may mediate nitrogenase activity when ammonium is available for uptake (Egener et al., 2001; Martin et al., 1989; Poudel et al., 2018; Yakunin et al., 1993).

Moreover, strain A210 encodes genes related with assimilatory nitrate reduction, including nitrate transport, the ammonium-forming nitrite reductase small subunit *nirB*, and the nitrate reductase *nasA* (Kawasaki et al., 1997; Mohan and Cole, 2007; Ramos et al., 1993; Yukioka et al., 2017).

In contrast to strain OF001, in the genome of strain A210 genes related with dissimilatory nitrate reduction were detected, including nitrate reductase *narGHI*, and nitrite reductase *nirBD.* Noteworthy, in the three described species of the *Rubrivivax* genus (Nagashima et al., 2012; Ramana et al., 2006; Sheu et al., 2020)*,* genes coding for enzymes related to dissimilatory nitrate reduction were not detected.The enzymes related with the dissimilatory and assimilatory nitrate reduction are organized in two predicted operons.

The genomic data indicate that both MOB strains have the ability to assimilate ammonium. In addition, it seems likely that OF001 can use nitrate in an assimilatory but not dissimilatory pathway. In contrary, the genomic data suggest that *Rubrivivax* sp. A210 has not only the genomic potential to assimilate nitrate, but also to perform anaerobic respiration using nitrate as final electron acceptor. This characteristic may confer a higher flexibility to strain A210, compared to OF001, to adapt to changing conditions in technical and natural environments.

4.2.4.5 Sulfur metabolism

Pseudomonas sp. OF001 harbours all genes required for assimilatory sulfate reduction, which are organised in several predicted operons, and some as single regulated genes. Strain OF001 also possesses different sulfate transporters including ABC type UWA (Sirko et al., 1995), the proton: sulfate symporter or putative sulfate : bicarbonate antiporter SulP (Loughlin et al., 2002; Van De Kamp et al., 1999), and the high affinity sulfate transporter CysZ, essential for sulfate uptake at low concentrations (Parra et al., 1983; Rückert et al., 2005). No genes required for dissimilatory sulfate reduction were detected in the genome of strain OF001.

Rubrivivax sp. A210 harbors several genes required for assimilatory sulfate reduction, organised in three predicted operons. However, A210 lacks the adenylyl sulfate kinase *cysC*, responsible of the transformation of adenosine 5'-phosphosulfate (APS) to 3'-phosphoadenosine-5'-phosphosulfate (PAPS), which is an essential step in the assimilatory sulfate reduction (Kushkevych et al., 2020). Nevertheless, other organisms like *P. aeruginosa*, *Sinorhizobium meliloti*, and *Burkholderia cenocepacia* lacking *cysC*, reduce APS via the phosphoadenosine phosphosulfate reductase *cysH* to sulphite (Abola et al., 1999; Bick et al., 2000; Iwanicka-Nowicka et al., 2007). Strain A210 also possesses different sulfate transporters like ABC type UWA (Sirko et al., 1995). Similar to strain OF001 and other *Rubrivivax* species, not all genes involved in dissimilatory sulfate reduction were identified in strain A210.

4.2.4.6 Cell motility and biofilm formation

Proteins for motility, including genes related to chemotaxis, and flagellar proteins were present in the genome of *Pseudomonas* sp. OF001. Genes encoding flagellar proteins in strain OF001 belong to the *flg*, and *fli* family, which are part of the core set of flagellar genes (Liu and Ochman, 2007). Among the genes related to the central signal transduction pathway for chemotaxis, we found *cheAWYBR* genes, and the transmembrane chemoreceptors, methyl-accepting chemotaxis proteins (MCPs) in the genome of strain OF001. This is in agreement with the description of the closest relatives of strain OF001, *P. oryzae*, *P. sagittaria*, *P. guangdongensis*, and *P. linyingensis*, as motile bacteria (He et al., 2012; Lin et al., 2013; G. Yang et al., 2013; Yu et al., 2013). Sixty-four genes associated with biofilm formation were found in the genome of *Pseudomonas* sp. OF001, including *siaD*, *bifA*, and *fleQ*.

In the genome of *Rubrivivax* sp. A210 genes required for motility were present, including genes related to chemotaxis, and genes encoding flagellar proteins. Similar as in strain OF001, in strain A210 found genes encoding flagellar proteins belong to the *flg*, and *fli* family. Strain A210 possesses *cheAWYBR* genes, and the transmembrane chemoreceptors MCPs, which are related to the central signal transduction pathway for chemotaxis. The taxonomically closest bacteria to strain A210, *R. gelatinosus,* and *R. benzoatilyticus*, are also motile bacteria (Nagashima et al., 2012; Ramana et al., 2006). However, despite the presence of motility-related genes in *R. albus*, the absence of motility was experimentally evidenced (Sheu et al., 2020). Therefore, further experiments are required to verify motility of strain A210. One hundred twenty one genes associated with biofilm formation were found in the genome of *Rubrivivax* sp. A210, including *sadC*, *pilI*, and *pslH*.

As discussed above, both strains contain genes that encode proteins involve in biofilm formation, which is in agreement with the isolation of both MOB from biofilms. Moreover, both

strains form biofilm in pure culture.

4.2.4.7 Organic compound degradation

Genes for the aerobic degradation of aromatic compounds via the catechol meta-cleavage pathway, and for the specific degradation of benzoate, phenol, and benzene, including phenol/toluene 2-monooxygenases (NADH), benzoate/toluate 1,2-dioxygenases, and catechol 2,3-dioxygenases, were detected in *Pseudomonas* sp. OF001. In addition, strain OF001 may have the potential to transform other compounds like 2-, 3- and 4-fluorobenzoate, toluene, steroids, citalopram, trinitrotoluene, p-methylbenzoate, trans-cinnamate, phenylpropanoate, and 4-hydroxyphenylacetate. This is in accordance with the ability of several *Pseudomonas* spp. to transform diverse organic pollutants such as benzoate, toluene, phenol, and poly- chlorobiphenyls (PCBs) (Nogales et al., 2017).

Because strain OF001 is able to degrade the cyanotoxin CYN we were also interested in the potential of the strains to degrade other cyanobacterial toxins. However, specific enzymes for the degradation of cyanotoxins are described only for microcystin, the most studied cyanotoxin (Kormas and Lymperopoulou, 2013; Kumar et al., 2019). No genes involved in microcystin degradation were found in the genome of OF001. Although biodegradation of CYN is considered one of the main natural attenuation processes (de la Cruz et al., 2013), no specific genes involved in their transformation are known yet (Martínez-Ruiz et al., 2020a).

Rubrivivax sp. A210 harbors genes involved in the aerobic degradation of aromatic compounds via the catechol ortho-cleavage pathway, and for the specific degradation of benzoate, and 3- and 4-fluorobenzoate, including benzoate/toluate 1,2-dioxygenases, muconate cycloisomerase, and catechol 1,2-dioxygenase. Similarly, the closely-related strain *R. bezoatilyticus* JA2 catabolizes different aromatic compounds including benzoate (Ramana et al., 2006). Strain A210 also has the potential to transform other compounds such as 4-methylcatechol, acrylonitrile, 2-fluorobenzoate, and trinitrotoluene.

Because strain A210 is able to degrade CYN similarly as strain OF001, we searched the genome for genes related to cyanotoxin transformation. We could not find genes associated with the transformation of microcystin.

4.2.5 Elements potentially acquired by horizontal gene transfer

4.2.5.1 Genomic islands

Genomic islands are genomic regions potentially obtained by horizontal gene transfer that can drive strain differentiation and support adaptation. Analysis of *Pseudomonas* sp. OF001 genome with IslandViewer 4 led to the identification of at least 12 genomic islands with size ranges from 4.2 to 70.5 Kb (Fig. A12a). Genomic islands in strain OF001 include genes associated with transposases, phage proteins, CRISPR systems, 147 proteins of unknown function, toxin-antitoxin systems, metal-related proteins, and mercury resistance. Metal resistance genes are related with environmental pollution, and specifically, mercury resistance genes are the genes most frequently associated with genomic islands (Reva and Bezuidt, 2012)

Analysis of *Rubrivivax* sp. A210 genome with IslandViewer 4 led to the identification of at least 8 genomic islands with size ranges from 3.8 to 99.5 Kb (Fig. A12b). Genomic islands in strain A210 included genes associated with transposases, phage proteins, 136 proteins of unknown function, toxin-antitoxin systems, transporters, and nitrate reduction. Genes related to nitrogen metabolism associated to genomic island have been previously reported (Loux et al., 2015; Zhu et al., 2018).

4.2.5.2 Prophages

Using, PHASTER (PHAge Search Tool Enhanced Release), we detected four incomplete and three intact prophage regions (Score ≥ 100) in *Pseudomonas* sp. OF001 genome (Table A6 and Fig. A13a). The three intact prophages were named OF001 region 2, OF001 region 5, and OF001 region 7 based on the genome location retrieved by PHASTER. A summary of the distribution and genetic features of these prophages is shown in Figure A13b. All prophages in OF001 exhibited structural proteins, including major capsid, fiber, and tail proteins.

Based on the proteomic tree generated with the VIPTree server, all complete prophages in OF001 belong to the order Caudovirales (Fig. A14). OF001 region 2 and OF001 region 5 were classified in the family Siphoviridae, while OF001 region 7 was classified in the family Myoviridae. Interestingly, OF001 region 2 and OF001 region 7 display putative site-specific integrases and excisionases, indicating site-specific recombination (Grindley et al., 2006). Multiple prophages have already been observed in other members of the genus *Pseudomonas* (de Sousa, 2020; Dziewit and Radlinska, 2016; Martínez-García et al., 2014; Paulsen et al., 2005).

Within A210 genome, two incomplete prophages of 28.8 and 9.9 kb were detected (Table A6 and Fig. S13c). No complete prophage was identified.

4.2.6 CRISPR-Cas systems

Using the CRISPRCas finder tool, we identified one complete class 1 CRISPR-Cas system, with a level of confidence of 4 (levels from 1 to 4, representing level 4 the most confident identification (Couvin et al., 2018)) in the genome of OF001 (Table A7 and A8). The seven *cas* genes are downstream of the repeat/spacer region. The repeats and spacers were compared with the CRISPRCas database (Pourcel et al., 2020) and were highly similar to sequences found in other bacteria including some Pseudomonads like *P. stutzeri*, *P. aeruginosa*, and *Pseudomonas* sp. phDV1 (Table A9 and A10). From the taxonomically closest organisms to strain OF001, only *P. guandongensis* has one confirmed class 1 CRISPR-Cas system.

In the genome of A210, one complete class 1 CRISPR-Cas system, with a level of confidence of 4, and one CRISPR region without *cas* genes associated, with a level of confidence of 2 were identified (Table A7 and A8). The three *cas* genes associated to the complete CRISPR-Cas loci are downstream of the repeat/spacer region. The repeats and spacers of the CRISPR region with a level of confidence 4 were compared with the CRISPRCas database (Pourcel et al., 2020) and, for the majority of them, no matching were found (Table A11 and A12). For the three spacers and two repeats, only results with a similarity around 50% were found. The organisms were these repeats and spacers were found are *Verrucomicrobium spinosum, Raphidiopsis curvata, Pectobacterium carotovorum* and *Opitutaceae bacterium*. The taxonomically closest organisms to strain A210, *R. gelatinosus* and *R. benzoatilyticus*, have two CRISPRs without associated *cas* genes, and 4 incomplete and 2 complete CRISPR-Cas systems, respectively.

Class 1 CRISPR-Cas systems, as the one found in both MOB, are the most abundant class in Beta and Gammaproteobacteria, and in general in archaea and bacteria (Makarova et al., 2020).

The presence of CRISPR-Cas systems in strain OF001 and A210 might represent protection from phage infections, but could represent a disadvantage if useful genes for competitive adaptation cannot be acquired via external DNA (Bhaya et al., 2011).

Together the presence of genomic islands, including phage material and CRISPR-Cas systems in *Pseudomonas* sp. OF001 and *Rubrivivax* sp. A210 suggest that both MOB have

undergone diverse genetic changes related to different horizontal gene transfer mechanisms which likely contribute to their genome plasticity.

4.2.7 Implications of the metabolic potential of strains OF001 and A210

In this study, we aimed at a better understanding of the metabolic capacities of the two CYN removing MOB which could potentially contribute to the biotechnological use of MOB for the removal of pollutants from water. In agreement with the genomes of other MOB with so far uncharacterized degradation ability (Gregory J. Dick et al., 2008; X. Wang et al., 2020), the content of the genomes of strain OF001 and strain A210 suggests a potential metabolic versatility and thus, a broader application potential.

The genomic potential of MOB strains OF001 and A210 for the degradation of different organic compounds via specific enzymatic pathways might complement the unspecific transformation pathways of substances like diclofenac (Nega, 2020) and CYN (Martínez-Ruiz et al., 2020b, 2020a), via manganese oxidation. Our results suggest that strain OF001 and A210 might be able to remove different organic pollutants by a coupled mechanism involving specific enzymatic activity and unspecific oxidation by the reactive manganese species, as has been observed for the removal of phenolic compounds, which are common wastewater pollutants (G. Wang et al., 2019). Moreover, it seems likely that the MOB described in this study transform other organic compounds like carbofuran, ciprofloxacin, and 17α-ethinylestradiol, similar to other MOB (Liu et al., 2017; Tran et al., 2018; Tu et al., 2014).

Both analyzed MOB, strain OF001 and A210, transform CYN indirectly through the oxidation of Mn^{2+} (Martínez-Ruiz et al., 2020a), and according to the results of this study most likely mediated by the activity of multicopper oxidases and heme peroxidases. The unspecific transformation of CYN by MOB does not require an adaptation phase or a pre-conditioned towards the toxin as it is known for many enzymatically catalyzed processes. Therefore, the use of MOB to remove the only periodically occurring CYN molecule, might represent an advantage in comparison to other biological removal processes that require a pre-conditioning with the toxin to remove it. Moreover, the unspecific oxidation of organic pollutants via reactive manganese species might allow for the removal of other cyanotoxins, however further studies are required.

The different metabolic pathways encoded in the genome of strain OF001 and strain A210 also suggest different fields of application aiming at the removal of pollutants. For instance, the ability of strain A210 to thrive and degrade CYN in the absence of an organic carbon source suggests that it is more suitable for an application in settings, in which readily

degradable organic carbon sources are depleted, such as reactors for the removal of pollutants from secondary wastewater. Also, due to the metabolic potential of strain A210, it may adapt within the reactor or the biofilm to varying oxygen concentrations or even the depletion of oxygen by a shift to nitrate respiration (Wu et al., 2015). Moreover, both strains are able to form biofilms which may allow them to establish and be retained on fixed bed reactors.

Pseudomonas sp. OF001 showed the highest CYN removal efficiency and the fastest growth from all tested MOB (Martínez-Ruiz et al., 2020b). Furthermore, it was isolated from a fixed-bed reactor system, however, the genome of strain OF001 encodes less diverse metabolic pathways to adapt to changing environments. Together, this data suggests that studies investigating degradation potential of MOB should consider the phylogenetic and metabolic diversity of MOB to identify the most suitable organisms that fulfil the requirements of the removal system.

The metabolic diversity of strains OF001 and A210 also suggests an important role of MOB in the removal of CYN in different habitats. For instance, strain A210 was isolated from a freshwater lake in the National Park Lower Oder Valley in Germany. This strain has the metabolic potential to dissimilatory reduced nitrate, which is an important mechanism to control nitrogen loading in aquatic environments (Burgin et al., 2015; Li et al., 2020; S. Wang et al., 2020). Dissimilatory nitrate reduction to ammonium has been related to the promotion of eutrophic conditions in water systems, due to the release of ammonium that could be used preferentially by cyanobacteria, and therefore favouring cyanobacterial blooms (Li et al., 2020). MOB strains with the ability to denitrify and degrade CYN may be therefore tightly interconnected with the production and removal of the cyanotoxin. Furthermore, the metabolic versatility of MOB may allow them to inhabit sediments and water columns. Therefore, MOB might contribute to the removal of CYN produced by benthic organisms in sediments, but also might transform CYN produced by planktonic cyanobacteria in the water column. However, further studies on the occurrence and distribution of MOB in CYN contaminated environments are required.

4.3 Conclusions

In summary, this study provides an insight into the molecular basis of Mn^{2+} oxidation, and into the metabolic potential of two CYN-transforming MOB strains. We identified sequences in *Pseudomonas* sp. OF001 and *Rubrivivax* sp. A210 that show high similarity to already described MCOs which may catalyze manganese oxidation required for CYN transformation. Furthermore, considering the mechanism proposed for the removal of other pollutants by MOB the multicopper oxidases found in both strains and the haem peroxidase

identified in strain OF001 might covey the ability to both strains to transform also other pollutants susceptible to reactive Mn species. Both MOB share the potential to grow over a wide range of O_2 concentrations, to fix nitrogen, and reduce nitrate and sulfate via the assimilatory pathway. Both strains encode pathways that might enable them to remove different aromatic compounds such as benzoate, benzene, and phenol. However, while strain A210 harbors the genomic potential to fix CO_2 and to reduce nitrate as final respiratory electron acceptor, strain OF001 requires additional organic carbon sources and lacks the ability for dissimilatory nitrate reduction. The analysis of the general metabolism of two MOB strains able to remove organic pollutants such as CYN and DCF might help to implement MOB in biotechnological applications and contributes to a better understanding of the natural niches of CYN-removing MOB in natural habitats.

4.4 Materials and methods

4.4.1 Strains, culturing conditions and genomic DNA extraction

Pseudomonas sp. OF001 and *Rubrivivax* sp. A210 were obtained from the culture collection of the Laboratory of Environmental Microbiology from the TU Berlin, Germany (Martínez-Ruiz et al., 2020b). Bacteria were routinely cultivated in a medium that was originaly developed for *Leptothrix* strains (Atlas, 2010), which was modified by our research group and is known as LSM2.

Cells from a pure, fresh 50 mL liquid culture from each strain were harvested by centrifugation at 15,000 x *g* for 3 min and washed three times with sterile Milli Q water under sterile conditions. Total genomic DNA was extracted using the GeneMATRIX Soil DNA Purification Kit (EUR_X Gdańsk, Poland) following the manufacturer's instructions. Quality and quantity of the extracted DNA was determined using QubitTM fluorometric quantitation and NanoDrop 2000 (both Thermo Fisher Scientific, Bremen, Germany).

4.4.2 Genome sequencing, assembly and annotation

The genome of both MOB strains was sequenced on an Illumina MiSeq platform with a read length of 301 bp (paired end). The genome of each isolate was assembled using SPAdes 3.10.1 and draft genomes obtained using manual binning procedures based on coverage-GC plots performed in R 3.6.1 (Fig A15). Genome quality estimation based on completeness and contamination was determined with CheckM (Parks et al., 2015). Genome annotation was performed with the interface Magnifying Genomes (MaGE) of the MicroScope web-based service from GenoScope (Vallenet et al., 2013). Protein coding genes were

classified based on the annotation into Cluster of Orthologous Groups (COG) functional categories (Tatusov, 2000) with the automatic classification COG tool at Microscope platform. Function and pathway analysis were performed using BlastKOALA web tool of KEGG (Kyoto Encyclopedia of Genes and Genomes) database according to the KEGG groups of orthologs (Kanehisa et al., 2016), and using MicroCyc tool of the MicroScope web-based service from GenoScope (Vallenet et al., 2013) which is a collection of microbial Pathway/Genome databases (PGDBs). PGDBs within MicroScope are generated by comparing the genome annotations to the metabolic reference database MetaCyc (Caspi et al., 2018). In the present work, metabolic potential will refer to the possibility of the strains to follow a specific metabolic pathway based only on their genome information, without being so far experimentally corroborated.

The data for this study have been deposited in the European Nucleotide Archive (ENA) at EMBL-EBI under project number PRJEB40009 with accession numbers GCA_904426495 and GCA_904426505 for strain OF001 and A210, respectively (https://www.ebi.ac.uk/ena/browser/view/PRJEB40009).

4.4.3 Genomes comparison

First classification of the genomes was determined according to the Genome Taxonomy Database (GTDB) using the GTDB-tool kit (GTDB-tk) v.1.1.0 integrated in the MicroScope web-based service (Chaumeil et al., 2019; Parks et al., 2018; Vallenet et al., 2017). GTDB-tk provides a taxonomic classification of bacterial and archaeal genomes based on the combination of the GTDB reference tree, the relative evolutionary divergence and the ANI value against reference genomes (Chaumeil et al., 2019). GTDB proposed a bacterial taxonomy based on the phylogeny inferred from the concatenation of 120 ubiquitous single-copy proteins that normalizes taxonomic ranks by using the relative evolutionary divergence (Parks et al., 2018). Therefore, it is considered that the analysis performed by GTDB-tk has an advantage over other phylogenies currently in use (Parks et al., 2018).

Genomes sequences were uploaded to the Type strain genome server (TYGS), a free bioinformatics platform (https://tygs.dsmz.de) for a whole genome-based taxonomic analysis (Meier-Kolthoff and Göker, 2019). TYGS platform runs automatically all the analysis. Briefly, TYGS performed first a determination of closely related type strain genomes, comparing the query genome against all available genomes in the TYGS database with the MASH algorithm (Ondov et al., 2016) and selecting ten type strains. Then, additionally ten close related type strains were determined based on the 16S rRNA sequence extracted from the query genome using RNAmmer (Lagesen et al., 2007). 16S rRNA sequences were compared with BLAST

(Camacho et al., 2009) against the TYGS database. The best 50 matching types were used to calculate precise distances using the Genome BLAST distance phylogeny approach (GBDP) (Meier-Kolthoff et al., 2013). The distances calculated by GBDP were then used to determine the ten closest type strain genomes for each query. Afterwards, GBDP conducted all pairwise comparisons among the set of genomes selected in the previous steps, and inferred accurate intergenomic distances under the algorithm “trimming” and distance formula d_5 (Meier-Kolthoff et al., 2013). One hundred distance replicates were calculated each. *In silico* DNA-DNA hybridization (DDH) analysis were calculated using the recommended settings of the Genome-to-genome distance calculator (GGDC) 2.1 (Meier-Kolthoff et al., 2013). The resulting intergenomic distances were used to infer a balanced minimum evolution tree with branch support via FASTME 2.1.4 including subtree pruning and regrafting (SPR) postprocessing (Lefort et al., 2015). Branch support was inferred from 100 pseudo-bootstrap replicates each.

JSpeciesWS (Richter et al., 2016) was used to calculate the average nucleotide identity (ANI) values (Richter et al., 2016) based on BLAST (ANIb) (Camacho et al., 2009; Goris et al., 2007) and MUMmer (ANIm) (Kurtz et al., 2004), and to calculate the correlation indexes of the tetra-nucleotide frequencies (TETRA) (Teeling et al., 2004).

For the ANI and TETRA analysis, the genome of strain OF001 was compared to the Pseudomonads belonging to the *Pseudomonas*_K group: *P. oryzae* (GCA_900104805.1), *P. sagittaria* (GCA_900109175.1), *P. guangdongensis* (GCA_900105885.1), and *P. liyingensis* (GCA_900115715.1).

For the ANI and TETRA analysis, the genome of strain A210 was compared to the genomes of the three species of the genus *Rubrivivax*: *R. benzoatilyticus* JA2 (GCA_000420125.1), *R. gelatinosus* IL144 (GCA_000284255.1), *R. gelatinosus* DSM 1709 (GCA_00430905.1), and *R. albus* ICH-03 (GCA_004016515.1).

4.4.4 Core- and pan-genome

Determination of the core- and pan-genome analysis was performed with the Pan/Core-genome tool from the MicroScope web-based service (Vallenet et al., 2013). The analysis is based on the computation of Microscope gene families (MICFAM) using a single linkage clustering algorithm of homologous genes sharing an amino-acid alignment coverage and identity above the defined threshold (Miele et al., 2011). This analysis considered i) any MICFAM associated with at least one gene from every genome used for the comparison as a part of the core-genome, ii) any MICFAM associated with at least 2 compared genomes as a part of the variable- genome, and iii) the sum of the core-genome and variable-genome as the

pan-genome (Vallenet et al., 2017). Parameter of 50/80 was selected (50% amino-acid identity, 80% amino-acid alignment coverage). All bacterial genomes used for the comparison with the genomes of strain OF001 or strain A210 that were not available in the MicroScope database were also annotated with MaGe from GenoScope (Vallenet et al., 2013).

For the pan- and core-genome analysis, the same strains as for the ANI and TETRA analysis, were used.

4.4.5 Manganese-oxidation genes

We used the blastp function on the Microscope web server (Camacho et al., 2009; Vallenet et al., 2020) to identify potential Mn^{2+} oxidases in *Pseudomonas* sp. OF001 and *Rubrivivax* sp. A210, using experimentally verified Mn^{2+} oxidases of other manganese-oxidizing bacteria. Nine sequences of multicopper oxidases and three sequences of haem peroxidases related with the oxidation of Mn^{2+} in other MOB were used for the search (Table A4). Multicopper oxidases and haem peroxidases with Mn^{2+} oxidation activity will be referred as MO-mco and MO-hpox, respectively. We considered as homologue any protein with an E-value lower than 10^{-10}.

Mn^{2+} oxidases and putative homologues found in OF001 and A210 were functionally analyzed with the InterPro web server (Mitchell et al., 2019). InterPro web server classifies proteins into families, and predicts functional domains and important sites of the proteins, integrating protein signatures from 13 different databases. We predicted the sub-cellular localization with LocTree3 (Goldberg et al., 2014) of those putative homologues without a predicted cytoplasmic or non-cytoplasmic domain according to the InterPro analysis.

To determine a possible phylogenetic relationship between manganese-oxidizing multicopper oxidases (MO-mco) and non-manganese oxidizing multicopper oxidases (non-MO-mco), we created a dataset sequences of multicopper oxidases with experimental evidence of Mn^{2+} oxidation (Corstjens et al., 1997; Francis and Tebo, 2002; Geszvain et al., 2016, 2013; Ridge et al., 2007; Tang et al., 2019) and multicopper oxidases with experimental evidence of non-Mn^{2+} oxidation activity (Anderson et al., 2009; Geszvain et al., 2013) and included our sequences. They were aligned using MUSCLE (Edgar, 2004) in MEGA v7.0.25. A phylogenetic tree was constructed with Maximum Likelihood method in MEGA v7.025. A bootstrap analysis was performed with 1000 replicates for the Maximum Likelihood tree.

4.4.6 Operon prediction

Operon prediction was done using the FGENESB program (Solovyev and Salamov, 2011). FGENESB gene prediction algorithm is based on Markov chain models of coding regions, start of translation, and termination sites. Predicted genes are then used for the operon models using distances between ORFs frequencies of neighboring genes in known bacterial genomes, and positions of predicted promoters and terminators (Solovyev and Salamov, 2011).

4.4.7 Elements potentially acquired by horizontal gene transfer

4.4.7.1 Genomic islands

Genomic islands were predicted with the IslandPath-DIMOB (Hsiao et al., 2003) and SIGI-HMM (Waack et al., 2006) method included in the IslandViewer 4 tool using the default settings (Bertelli et al., 2017). Among the prediction methods included in IslandViewer 4 tool, SIGI-HMM has the highest precision and overall accuracy (Langille et al., 2008).

4.4.7.2 Prophages

Putative phages from *Pseudomonas* sp. OF001 and *Rubrivivax* sp. A210 were predicted with PHASTER (PHAge Search Tool Enhanced Release) web server (Arndt et al., 2016). PHASTER classifies genome regions with a score below 70 as incomplete, between 70 to 90 as questionable, and greater than 90 as complete prophages (Arndt et al., 2016).

The resulting complete prophage genomes were annotated with multiPhATE v.1.0 (multiple-genome Phage Annotation Toolkit and Evaluator) (Ecale Zhou et al., 2019) using Phanotate to predict ORFs (Mcnair et al., 2019). PhAnToMe (Phage Annotation Tools and Methods), pVOGs (Grazziotin et al., 2017), and SwissProt (Bairoch and Apweiler, 2000) databases were used for the identification of the homologs of the input genomes and its predicted gene and peptide sequences. Additionally, highly divergent structural proteins were detected with iVireons (Seguritan et al., 2012) and confirmed with VIRALPro (Galiez et al., 2016).

To classify the complete prophages, a whole proteomic tree based on genome-wide similarities was computed by tBLASTx, using the VIPTree web server v.1.9 (Nishimura et al., 2017).

4.4.8 CRISPR-Cas systems

The presence of Clustered Regularly Interspaced Short Palindromic Repeats (CRISPR) and their associated genes (*cas*) was evaluated with CRISPRCasFinder (Couvin et al., 2018). CRISPRCasFinder include a rating system which classifies the detected CRISPRs to differentiate between CRISPR-like elements and true CRISPRs. Evidence levels from 1 to 4 are assigned, with 1 representing the lowest evidence classification and 4 the most confident identification (Couvin et al., 2018).

Spacers and repeat regions detected in both genomes were searched with BLAST (blastn) against the CRISPRCasdb to identify their presence in other organisms. CRISPRCasdb contains CRISPR arrays and *cas* genes from complete genome sequences (Pourcel et al., 2020).

4.4.9 Data graphics

Figures were made with the R packages ggplot2 (Wickham, 2016), gridExtra (Auguie, 2017), pheatmap (Kolde, 2015), VennDiagram (Chen and Boutros, 2011), and gggenes (Wilkins, 2019), using Viridis (Garnier, 2018) and RcolorBrewer (Neuwirth, 2014) packages for colouring in RStudio version 1.0.153 (R Core Team, 2020, 2016). Genomic maps of prophages were generated using the Snapgene® software (GSL Biotech). Trees generated with the TYGS tool and the multicopper oxidase tree were visualized and annotated with the online server iTOL (Letunic and Bork, 2019).

Acknowledgments

Erika B. Martinez-Ruiz was supported by a research scholarship from the DAAD (Deutscher Akademischer Austauschdienst). Contributions of Mindia A. S. Haryono, Irina Bessarab, and Rohan B. H. Williams are funded by the Singapore National Research Foundation and Ministry of Education under the Research Centre of Excellence Programme. The authors declare no competing financial interest. The LABGeM (CEA/Genoscope & CNRS UMR8030), the France Génomique and French Bioinformatics Institute national infrastructures (funded as part of Investissement d'Avenir program managed by Agence Nationale pour la Recherche, contracts ANR-10-INBS-09 and ANR-11-INBS-0013) are acknowledged for support within the MicroScope annotation platform.

5 Influence of growth conditions of MOB on CYN removal rate and the formation of transformation products.

5.1 Introduction

Cylindrospermopsin (CYN) is an alkaloid cyanotoxin with a cyclic sulfated guanidine moiety bound to a hydroxymethyluracil group. *Cylindrospermopsis raciborskii* was the first identified CYN producer (Ohtani et al., 1992), but lately, various other cyanobacteria genera have been identified as CYN producers worldwide, including *Cylindrospermopsis raciborskii*, *Umezakia natans*, *Chrysosporum ovalisporum, Aphanizomenon* spp., and *Anabaena* spp. (Rzymski and Poniedziałek, 2014). CYN is stable in a wide range of temperatures and is highly water-soluble (Adamski et al., 2016a; Griffiths and Saker, 2003; Onstad et al., 2007). CYN is highly persistent in aquatic environments, hence, it is important to research specific processes aiming at removing and transforming CYN.

Different abiotic processes, including advanced oxidation (He et al., 2014b), chlorination (Merel et al., 2010), UV irradiation (Adamski et al., 2016b), and ozonation (Yan et al., 2016) have been used to efficiently remove CYN. The products of these abiotic reactions have been identified and, in some cases, a reduction of toxicity in comparison with pure CYN was evidenced.

Biotransformation might be an economical and sustainable alternative to the abiotic processes to remove CYN in technical systems. Moreover, biotransformation is considered one of the main natural CYN attenuation processes (de la Cruz et al., 2013). To date, only a few isolated CYN degraders have been described including probiotic bacteria (Nybom et al., 2008), *Bacillus* sp. AMRI-03 (Mohamed and Alamri, 2012) and *Aeromonas* sp. R6 (Dziga et al., 2016) isolated from freshwater bodies with previous reports of cyanoHABs or in eutrophic conditions, as well as different strains of manganese-oxidizing bacteria (MOB) isolated from natural and technical systems (Martínez-Ruiz et al., 2020b). Despite the reported removal ability of the above mentioned isolated strains, detection and identification of transformation products was carried out only for the transformation by MOB (Martínez-Ruiz et al., 2020a).

MOB are a group of organisms able to oxidize Mn^{2+} to Mn^{3+} and Mn^{4+}, producing water-insoluble aggregates as a result of the reaction (Tebo et al., 2005). These aggregates, also known as biogenic manganese oxides, are one of the strongest oxidants in the nature (Hennebel et al., 2009; Tebo et al., 2004). As an indirect reaction of Mn^{2+} oxidation, MOB transform different organic and inorganic pollutants (Meerburg et al., 2012; Sochacki et al., 2018; Tran et al., 2018; Zhang et al., 2015). Biogenic manganese oxides often interact with

other elements like Fe, forming ferromanganese oxides. Indeed, ferromanganese oxides are one of the most common forms of biogenic oxides in the environment (Geszvain et al., 2012; Lee and Xu, 2016; Stein et al., 2001; Vesper, 2012). MOB are present in drinking water systems (Cerrato et al., 2010) and are widely distributed in the nature (Tebo et al., 2004), where they may coexist with potentially toxigenic cyanobacteria (Scheer, 2010).

In **chapter 2**, I reported the ability of MOB to remove CYN at the environmentally relevant concentration of 118 µg L^{-1} CYN under different growth conditions. The best removal rates were observed when $MnCO_3$ was used as the Mn^{2+} source, and yeast extract was added as the carbon source. Among all the tested MOB, only strain A210 showed a high removal of CYN in a yeast extract-free medium (Martínez-Ruiz et al., 2020b). Moreover, strain A210 was the only MOB able to remove CYN at a higher rate in the presence of Fe^{2+} than in the absence of this element. In **chapter 3**, I evidenced the ability of MOB to transform CYN into the same seven transformation products at the highest transformation rates ever reported for biological CYN transformation. MOB transform CYN in the presence of Mn^{2+} into a mixture of products that exhibit lower toxicity than CYN (Martínez-Ruiz et al., 2020a). However, the growth media used for the transformation assays had yeast extract and had not additional Fe^{2+}. Thus, it remains unknown if the same transformation products are formed by strain A210 in the presence of Fe^{2+} and with and without an additional organic carbon source.

Therefore, I investigated the biological transformation of CYN by strain A210 at a sixty-fold higher concentration than the previously reported (Martínez-Ruiz et al., 2020b) in the presence of Fe^{2+} with and without yeast extract.

5.2 Materials and methods

5.2.1 Strains and culturing conditions

Rubrivivax sp. A210 was obtained from the culture collection of the Laboratory of Environmental Microbiology from the TU Berlin, Germany (Martínez-Ruiz et al., 2020b). Strain A210 (GenBank accession number MK599478) was isolated from an iron manganese-depositing biofilm in a freshwater pond in the Lower Oder Valley National Park, Germany. It was routinely grown in LSM2 medium (Table A3). The pH of the medium was adjusted to 7.2 with 1 M NaOH before autoclaving. Strain A210 was cultivated consecutively twice in LSM2 without Mn^{2+} and Fe^{2+} to avoid the presence of iron-manganese deposits in the inoculum of the transformation assays. Flasks were incubated at room temperature (21 ± 2 °C), at 110 rpm.

5.2.2 CYN transformation assays

CYN (>95% purity) was purchased from Enzo Life Science, Inc (New York, USA). CYN was resuspended in sterile Milli Q water to a final concentration of 500 mg L^{-1}. Bacteria were inoculated into 3 mL LSM2 media in sterile glass tubes (12 x 100 mm), using 30 µL of manganese-free precultures at exponential growth (OD_{600} nm). Cultures contained 1 g L^{-1} $MnCO_3$. Per each glass tube, 3 µL of Fe^{2+} stock solution ($Fe(NH_4)_2(SO_4)_2 \cdot 6H_2O$) was added. CYN was added to a final mean concentration of 7 mg L^{-1}. This concentration is approximately 60-times higher than the commonly detected CYN concentration in the environment (Messineo et al., 2009; Shaw et al., 1999). However, a high concentration of CYN was used to increase the probability to detect CYN transformation products. In addition, the same concentration of CYN allows me to compare the relative abundances of the products with those reported in **chapter 3** (Martínez-Ruiz et al., 2020a), in case of the detection of similar transformation products. Bacteria were incubated on a shaker at 110 rpm at room temperature (21 ± 2 °C) in the dark.

As a control for the abiotic transformation of CYN, culture media LSM2 i) with Fe^{2+} and yeast extract, and ii) with Fe^{2+} and without yeast extract, with CYN, but without bacteria were evaluated. Media LSM2 i) with Fe^{2+} and yeast extract, and ii) with Fe^{2+} and without yeast extract with bacteria, but without CYN were used as a control to test for bacterial metabolites. Two independent replicates were run per strain and per control.

Samples were taken at discrete time points based on preliminary assays and the reported removal patterns/rates of CYN by strain A210 (Martínez-Ruiz et al., 2020b).

Viability and purity of cells were qualitatively evaluated at the end of each assay by inoculating the strains onto solid modified LSM2 and incubation at room temperature (20.8 ± 2.2 °C). To discard any contamination, the same procedure was followed for the controls in order

5.2.3 Analysis of CYN and its transformation products.

Samples were taken and processed as previously described (Martínez-Ruiz et al., 2020a). The detection of transformation products was carried out using an Orbitrap Fusion Tribrid Mass Spectrometer (Thermo Fisher Scientific, Bremen, Germany) coupled to a UHPLC. Chromatographic separation was performed using a Hypersil GOLD C18 column (150 x 2.1 mm, 3 µm, Thermo Scientific) in a UHPLC Dionex UltiMate 3000 RS (Thermo Fisher Scientific, Bremen, Germany). Separation conditions were used as previously reported (Martínez-Ruiz et al., 2020a). Briefly, the mobile phase consisted of water (A) and methanol (B) both with 0.1%

formic acid. A linear gradient was applied from 1% to 25% B within 5 min at a flow rate of 0.2 mL min^{-1}, and back to 1% B for 7 min. The effluent was monitored and CYN was quantified with a UV detector set at 262 nm. The injection volume was 5 µL and the oven temperature 25 °C. For the Orbitrap, heated electrospray ionization source parameters were: spray voltage of 3.5 kV and ion transfer tube temperature at 325 °C. Sheath, auxiliary, and sweep gas flow rate were 35, 10, and 0 (arbitrary units), respectively. Data acquisition was performed in full-scan mode.

A target screening of the MS^1 traces for the expected *m/z* values of transformation products previously reported for transformation of CYN by abiotic procedures was conducted (Adamski et al., 2016b, 2016a; Fotiou et al., 2015; Guzmán-Guillén et al., 2017; He et al., 2014b, 2014a; León et al., 2019; Merel et al., 2010; Song et al., 2012; Yan et al., 2016), using an inclusion list with the *m/z* values and charge state. The *m/z* value of potential CYN transformation products was searched scanning from 100 to 500 *m/z* under positive ion mode as previously reported (Fotiou et al., 2015; Guzmán-Guillén et al., 2017; He et al., 2014b, 2014a; Martínez-Ruiz et al., 2020a; Prieto et al., 2017; Song et al., 2012). If the instrument detect a mass spectral peak fulfilling the criteria specified in the inclusion list, an MS^2 spectrum is obtained for the associated precursor ion. Orbitrap resolution was 120000 for MS^1 and 60000 for MS^2. The limit of quantification (LOQ) of CYN was 0.05 mg L^{-1}.

5.2.4 Transformation products identification.

Potential transformation products in cultures of strain A210 were further evaluated by manually checking the same parameters as Martínez-Ruiz et al. (2020a) Fragmentation patterns were compared with published data (Adamski et al., 2016a, 2016b; Fotiou et al., 2015; Guzmán-Guillén et al., 2017; He et al., 2014a, 2014b; Martínez-Ruiz et al., 2020a; Yan et al., 2016), including fragmentation patterns of products formed by MOB in **chapter 3**. Transformation products without published MS^2 fragments were tentatively identified based on the precise MS^1 mass, and the distribution of the isotope abundance. Error limits of 10 ppm of the *m/z* and the MS^2 fragments of the potential transformation products were allowed.

5.2.5 Removal rate

The removal rate was calculated by dividing the difference of the initial CYN concentration and the concentration measured on the last day where the CYN concentration was above the LOQ, by the number of days in which this CYN concentration was measured.

5.2.6 Data analysis and statistical analysis.

Transformation products were analyzed with the MZmine v2.38 software (Pluskal et al., 2010). The dplyr R package on RStudio version 3.4.2 was used for statistical analysis (Wickham et al., 2019). Figures were made with the ggplot (Wickham, 2016) and gridExtra (Auguie, 2017) R package. One-way analysis of variance (ANOVA) followed by Tukey's pairwise comparison test for the multiple comparisons among CYN and transformation products at different times were performed.

5.3 Results and Discussion

It was previously shown that strain A210 can remove CYN in the absence of yeast extract in contrast to the other three investigated strains in previous chapters. In addition, strain A210 removed CYN at a higher rate when Fe^{2+} was added to the media than in a Fe^{2+}- free medium in comparison to the other MOB strains (Martínez-Ruiz et al., 2020b). Therefore, I analysed CYN transformation products formed by strain A210 in the presence of Fe^{2+} with and without yeast extract in the growth medium. In both conditions, the same seven transformation products as those formed by strain OF001, A288, A210 and A226 (Martínez-Ruiz et al., 2020a) were detected, based on observed retention time *m/z* values, formation along the incubation time and fragmentation patterns.

In good agreement with the previous study (Martínez-Ruiz et al., 2020b), strain A210 removed about 100% of CYN in the presence of Fe^{2+} (Fig. 5.1). However, CYN removal under this condition was slightly slower than the removal in the absence of Fe^{2+} observed in **chapter 3** (Fig. 3.1). Removal rate in presence of Fe^{2+} and yeast extract at day 7 was 0.90 mg L^{-1} day^{-1}, which is lower than the removal rate of 1.10 mg L^{-1} day^{-1} observed for strain A210 in medium without Fe^{2+} and with yeast extract at day 7 (Martínez-Ruiz et al., 2020a).

The slowest CYN removal was observed when strain A210 transformed CYN in the growth medium with Fe^{2+} and without yeast extract (Fig. 5.2). Under these conditions, strain A210 removed about 100% of CYN within 34 days at a removal rate of 0.25 mg L^{-1} day^{-1}. This removal rate is 70-fold higher than the previously reported CYN removal rate of strain A210 in the same growth conditions, but with a lower initial CYN concentration (Martínez-Ruiz et al., 2020b). In contrast to my previous study using environmentally relevant concentrations of CYN, strain A210 cultivated in medium with Fe^{2+} but without yeast extract removed around 80% of the total CYN (Martínez-Ruiz et al., 2020b). Thus, the influence of the initial CYN concentration on the removal rate of MOB was again confirmed.

When Fe^{2+} was added to the growth medium of strain A210, relative abundances of TP_{448}, TP_{320}, TP_{292a-b}, and TP_{290} were two- to three-fold higher (Fig. 5.2) than when Fe^{2+} was absent (Fig. 3.2). Differences might be related to the influence of Fe^{2+} on manganese-oxidizing enzymes as reported for *Leptothrix discophora* SS-1 (El Gheriany et al., 2009). Thus, it is likely that Fe^{2+} impacts on the production of reactive Mn species by strain A210, leading to different oxidation rates of CYN and the transformation products.

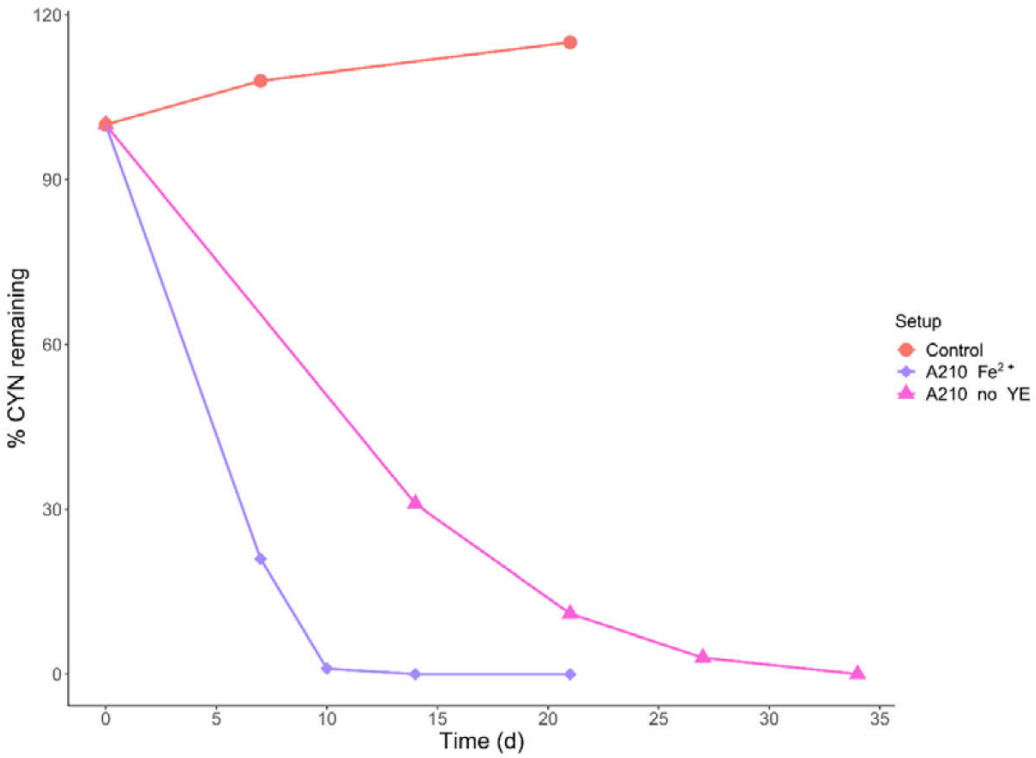

Fig. 5.1. CYN transformation over time by *Rubrivivax* sp. A210. Control: CYN in the medium without MOB. Strain A210 was grown in LSM2 medium i) with yeast extract and Fe^{2+} and ii) without yeast extract but with Fe^{2+}, with an initial CYN concentration of 7 mg L^{-1}. YE: yeast extract.

In contrast to the other strains tested in the present thesis, strain A210 was the only strain able to remove CYN in the absence of yeast extract (Martínez-Ruiz et al., 2020b). Therefore, based on results of **chapter 2**, it was hypothesized that strain A210 use CYN as a carbon source, when no other organic carbon sources are available, as was previously reported for other CYN-degraders (Dziga et al., 2016; Martínez-Ruiz et al., 2020c; Mohamed and Alamri, 2012). If this hypothesis would have been proven, I would observe a lower accumulation of transformation products or no products would be detected. However, based on the present results, this hypothesis was rejected.

Disregarding growth conditions, strain A210 cultivated in yeast extract-free medium showed two- to eight-fold accumulation of TP_{292a} and TP_{292b}, being the highest abundance of

these products in comparison with all the tested MOB in **chapter 3** (Fig. 3.2). The other transformation products were detected with a similar abundance as in the transformation assays performed with other MOB strains (Fig. 3.2). Currently, it is not possible to give an explanation for this phenomenon. Nevertheless, results suggest that strain A210, in the absence of yeast extract, may use CO_2 or CO_3 as carbon source instead of using CYN or its transformation products. However, further studies would be required to confirm this speculation.

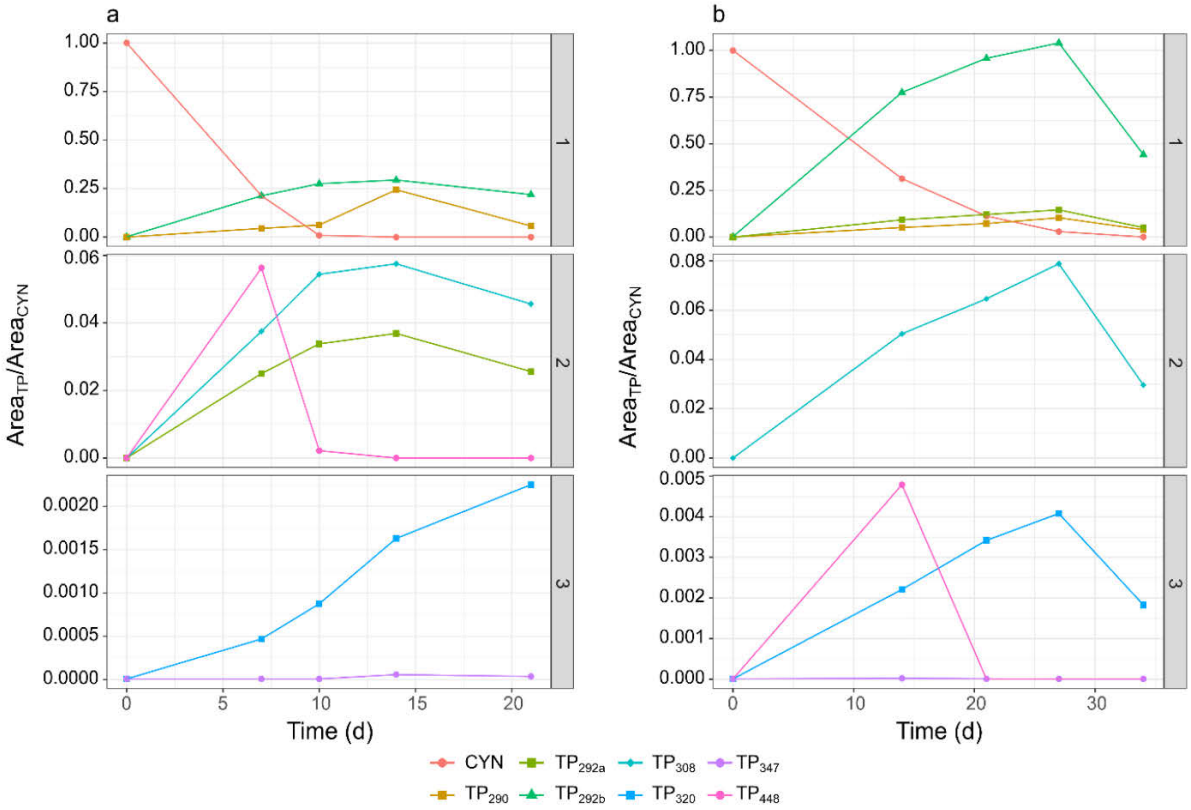

Fig. 5.2. Generation of transformation products shown in Fig. 5.1 over the incubation time of strain A210. *Rubrivivax* sp. A210 a) with yeast extract and Fe^{2+}, b) without yeast extract but with Fe^{2+}. The initial CYN concentration was 7 mg L^{-1}. $Area_{TP}$: transformation products' peak area, and $Area_{CYN}$: CYN' peak area of the initial amount of CYN from LC-MS results. The three vertically combined graphs have different y-axis scales and show compounds according to their $Area_{TP}/Area_{CYN}$ values.

5.4 Conclusion

In summary, strain A210 formed the same seven CYN transformation products as other MOB. In presence of Fe^{2+}, with and without an additional carbon source, strain A210 transformed CYN into the same seven transformation products than those detected in the presence of yeast extract and the absence of Fe^{2+} shown in **chapter 3.** Detection of the same transformation products formed by strain A210, despite the different CYN removal rates, and

growth conditions, provide further evidence supporting that a general mechanism for CYN transformation is followed by MOB. Even though the precise mechanism of CYN transformation is unknown, the identification of transformation products will help to further understand the process.

6 Discussion, conclusions and outlook

6.1 Discussion and conclusions

The aim of this thesis was to evaluate the transformation of CYN by MOB, including the description and the evaluation of the toxicity of the transformation products. In addition, a genomic analysis of the two MOB with the fastest CYN transformation rates was carried out. The genomic analysis was focused on the identification of the most likely mechanism for manganese-oxidation and the description of their metabolic potential.

The knowledge generated in the present thesis contributes to a better understanding of the biotechnological applicability of MOB to remove CYN from water, and to further understand the likely role of MOB in the natural attenuation of CYN in waterbodies

6.1.1 MOB as promising candidates for CYN removal

Despite the potential of MOB to remove different organic pollutants, their CYN removal ability was never tested. As it was discussed in **chapter 2**, the four tested MOB, *Pseudomonas* sp. OF001, *Ideonella* sp. A288 and A226, and *Rubrivivax* sp. A210, removed CYN at environmentally relevant concentrations to a different extent, depending on the cultivation conditions. Highest removal rates were observed when $MnCO_3$ was used as the Mn^{2+} source.

Results evidenced that the key factor for the efficient removal of CYN was the participation of viable bacteria actively oxidizing Mn^{2+}, regardless of the final concentration of manganese oxides in the medium. It could be demonstrated that each strain has different growth requirements for the removal of CYN. For instance, *Pseudomonas* sp. OF001 removed CYN at the highest rates only when an additional carbon source was added to the media, while *Rubrivivax* sp. A210 removed CYN at a high extent even when grown in a mineral media.

Results of **chapter 2** were the first report showing that MOB are involved in the removal of CYN and suggest that CYN removal by MOB follows a similar mechanism as the one proposed for the removal of other organic pollutants by MOB (Meerburg et al., 2012; Tran et al., 2018). This mechanism involves the indirect oxidation of the pollutant by the Mn^{3+}/Mn^{4+} produced as a result of the Mn^{2+} oxidation.

Previous studies report that biological CYN removal by isolated organisms and bacterial communities need an adaptation phase (lag phase) (Dziga et al., 2016; Klitzke et al., 2010; Smith et al., 2008). Based on pre-conditioning experiments, it was suggested that previous exposure to CYN shortened the lag phase (Klitzke et al., 2010). However, the

necessity of an adaptation phase for CYN removal could limit the use of those organisms for water treatment, considering that CYN may occur periodically and not as a constant pollutant (Wiedner et al., 2008). In this regard, fast growing MOB like *Pseudomonas* sp. OF001 might have an advantage over previously reported CYN-degraders. MOB likely transform CYN by the concomitant oxidation of Mn^{2+}, and therefore would not need a previous exposure to CYN to activate any specific metabolic pathway for its removal.

The removal of CYN by MOB was evidenced in **chapter 2**, however, it was not clear whether transformation products were formed by MOB and whether they exhibited a similar or lower toxicity than CYN or not. This was investigated in **chapter 3**. To increase the probability to detect transformation products, the concentration of CYN was increased by 60-times compared to the concentration of CYN used in **chapter 2**. At this high CYN concentration, all tested MOB transformed CYN at the highest rates ever reported for microbial CYN removal considering isolated CYN degraders and CYN-degrading communities (Dziga et al., 2016; Mohamed and Alamri, 2012; Smith et al., 2008).

All tested MOB transform CYN at different removal rates. However, there is no clear explanation for the variation of transformation rates among MOB strains. I consider three possible factors influencing CYN transformation rates, namely, growth rate, Mn^{2+} oxidation rate and type of biogenic manganese oxides. Firstly, it was shown in **chapter 2** that the amount of oxidized manganese was not always related to the amount of CYN removal. However, I quantified the amount of oxidized manganese suspended in the media and not the manganese oxidation rate per organism. The mechanism proposed for the removal of CYN and other pollutants involves an oxidation-reoxidation process of manganese mediated by viable cells with the concomitant oxidation of the pollutant (Meerburg et al., 2012; Tran et al., 2018). Therefore, it is expected that higher Mn^{2+} oxidation rates represent higher CYN transformation rates.

Secondly, oxidation rates could also be influenced by the bacterial growth rate. Due to the formation of biogenic oxides, the precise quantification of bacteria growth with common methods as the optical density is not feasible. However, evaluation of the bacteria growth rate in Mn^{2+}-free media evidenced that *Pseudomonas* sp. OF001 has the fastest growth among all the tested MOB. As shown in **chapter 2**, strain OF001 was also the fastest CYN-degrader. Thus, high removal rates might be related to a fast growth.

Finally, the type of biogenic manganese oxide might also affect CYN transformation rates. Oxidation products differ from strain to strain (Zhou and Fu, 2020), and their structure is influenced by various external factors, including the initial concentration of Mn^{2+}, pH, ionic strength, oxidation mechanism, and the presence of other metals (Emerson, 2000).

Considering that all tested MOB belong to different phylogenetic lineages and are metabolically distinct, I expect that biogenic manganese oxides of various types and reactivity are formed by each tested MOB.

The approach followed in the present thesis allowed for the detection and the tentative identification of seven CYN transformation products formed by all the tested MOB, disregarding CYN transformation rates, isolation source, growth conditions, and phylogenetic lineages of the MOB, as described in **chapter 3** and **chapter 5**. This supports the hypothesis presented in **chapter 2** that MOB transform CYN by a general mechanism based on the unspecific oxidation of the compounds by the reactive manganese species formed due to the oxidation of Mn^{2+}.

The mixture of transformation products tentatively identified in **chapter 3** was substantially less toxic than pure CYN. CYN is considered a cytotoxic toxin due to the wide range of organs that might affect, which includes not only the liver, but also kidneys, lungs, gastrointestinal tract, and nervous system (Falconer et al., 1999; Guzmán-Guillén et al., 2015; Kubickova et al., 2019a; Terao et al., 1994). Even though, I evaluated only the hepatotoxicity of the mixture of CYN transformation products, the modifications on the uracil moiety observed in the transformation products detected in **chapter 3** suggest a reduction of the general toxicity of CYN against all the organs (Banker et al., 2001). Thus, the reduction of CYN hepatotoxicity by MOB supports their implementation for the removal of CYN from water, with a high likelihood that no toxic products will be formed.

Results in **chapter 2** demonstrated that each MOB strain has different growth requirements influencing the removal of CYN. Results in **chapter 3** suggest that a general mechanism for CYN was followed by all the MOB here tested. However, it was unclear if changes in growth conditions could influence the transformation of CYN, leading to the formation of different products or mineralization. In **chapter 5**, I addressed this question. It was evidenced that *Rubrivivax* sp. A210 cultivated in a mineral media transformed CYN into the same seven transformation products than MOB cultivated in media with an additional organic carbon source. Thus, supporting the hypothesis of a general mechanism for CYN transformation followed by MOB. Moreover, the production of the same seven transformation products by strain A210 that exhibit lower cytotoxicity as shown in **chapter 3**, supports the implementation of strain A210 also for the treatment of low organic content water. For instance, for reactors aiming at the removal of pollutants from secondary wastewater.

Results on **chapter 3** were the first description of transformation products of CYN formed due to biological activities. Although the precise mechanism of CYN removal was not identified, the identification of the transformation products provides useful information to further

understand the process. MOB transform CYN through an unspecific mechanism associated with the oxidation of Mn^{2+} and the reactivity of Mn^{3+}/Mn^{4+} species. However, the involvement of other mechanisms into the CYN transformation by MOB cannot be ruled out. It remains unknown to which extent reactive manganese species are responsible for CYN oxidation and which other processes are involved in further CYN transformation. For instance, G. Wang et al. (2019), described a coupled mechanism for the transformation of phenolic compounds, which involves an initial transformation of the compound by the activity of specific enzymes, and a further transformation by the reactive manganese species.

It is also important to highlight that the unspecific CYN transformation mechanism of MOB is not the only bacterial CYN transformation mechanism. Previously described CYN-degraders were not classified as MOB and the production of biogenic oxides was not mentioned (Dziga et al., 2016; Mohamed and Alamri, 2012; Nybom et al., 2008). CYN removal by non-MOB strains suggests that different transformation reactions are catalysed by other bacteria. Unknown mechanisms might be related to specific enzymes that use CYN as substrate, similarly as the specific enzymes that transform microcystin, the most commonly detected cyanotoxin worldwide (Bourne et al., 2001).

Pseudomonas sp. OF001 and *Rubrivivax* sp. A210 were the only organisms among the tested MOB to transform 100% CYN at environmentally relevant concentrations at very different culture conditions, and therefore, they were selected for a genomic analysis on **chapter 4** to understand their metabolic potential for biotechnological interests and to provide further information related to molecular basis of the Mn^{2+} oxidation mechanism.

The genomic analysis presented in **chapter 4** evidenced that the genome of strain OF001 encodes enzymes with a high similarity to those Mn^{2+} oxidases of *Pseudomonas putida* GB-1 (Geszvain et al., 2016, 2013). The genomic analysis also evidenced that the genome of strain A210 encodes enzymes with high similarity to those Mn^{2+} oxidases in *Leptothrix discophora* SS-1 (Corstjens et al., 1997). These results suggest that both MOB strains oxidize manganese through enzyme-mediated mechanisms. Additionally, *Pseudomonas* sp. OF001 and *Rubrivivax* sp. A210 oxidize Mn^{2+} without an increase of pH in the media, as observed in **chapter 2.** These results dismiss the change in pH as the Mn^{2+} oxidation mechanism in both organisms and reinforce the hypothesis of an enzyme-mediated Mn^{2+} oxidation.

Furthermore, both strains encode enzymes for the specific transformation of organic pollutants such as benzoate, and other aromatic compounds via the catechol meta- and ortho-cleavage. Strain OF001 and A210 remove CYN (**chapter 2, 3** and **5**) most likely, by the unspecific activity of the reactive manganese species. Therefore, the potential to remove

pollutants by specific and unspecific mechanisms increases the value of the tested MOB for biotechnological applications aiming at the removal of various organic pollutants from water.

Pseudomonas sp. OF001 and *Rubrivivax* sp. A210 do not possess the genes encoding for microcystinases, the responsible enzymes for the transformation of microcystin (Bourne et al., 2001). However, a recent report evidenced the removal of low concentrations of a common water pollutant (2-hydroxy-4- methoxybenzophenone-5-sulfonic acid) and microcystin when the MOB *Pseudomonas* sp. QJX-1 was incorporated into the system (Jian et al., 2019). Both compounds were removed by strain QJX-1 most likely following the same unspecific mechanism proposed for the removal of other pollutants, including CYN (Martínez-Ruiz et al., 2020a; Meerburg et al., 2012; Tran et al., 2018). Thus, MOB, including strains OF001 and A210, might be able to transform microcystin by the concomitant oxidation of Mn^{2+} rather than by the specific activity of microcystinases. Considering that the cyanotoxins nodularins have a similar chemical structure as microcystins (Pearson et al., 2010), a transformation by MOB seems likely.

Strain OF001 and A210 had different growth requirements that were further corroborated by the metabolic potential encoded at the genomic level, as described in **chapter 4**. The information related to the metabolic diversity of strains OF001 and A210 will allow a deeper understanding of the metabolic capacities of the two CYN removing MOB which could potentially be implemented for the removal of pollutants including manganese and iron ions.

MOB are used in drinking water treatment to remove Mn^{2+} (Katsoyiannis and Zouboulis, 2004; Mouchet, 1992; Pacini et al., 2005; Tobiason et al., 2016), which is consider toxic at high concentrations (O'Neal and Zheng, 2015). The Environmental Protection Agency of the United States established as a maximum tolerable level 0.05 mg L^{-1} of manganese in drinking water (U.S. EPA, revised November 2020), while the World Health organization set 0.4 mg L^{-1} of manganese as a guide value (World Health Organization, 2011). Manganese is released to waterbodies as a natural process, but anthropogenic activities like discharge of industrial and domestic wastewater, waste from livestock, mining, and the use of pesticides contribute to their presence (Marsidi et al., 2018). The same anthropogenic activities are the source of iron in water. Similarly as manganese, iron is an essential element, which at high concentrations produces toxic effects (Kehl-Fie and Skaar, 2010). The Environmental Protection Agency of the United States established as a maximum tolerable level 0.3 mg L^{-1} of iron in drinking water (U.S. EPA, revised November 2020). Considering that various MOB strains are able to oxidize simultaneously manganese and iron (Corstjens et al., 1997, 1992; Schmidt, 2018; Schmidt et al., 2014), the simultaneous biological removal of both elements has been widely implemented for water treatment (Marsidi et al., 2018; Mouchet, 1992).

Our results, together with previous reports of the removal of different organic pollutants by MOB, suggest that the Mn^{2+} oxidation of MOB might be exploited together with the removal of CYN and other organic and inorganic pollutants like iron. Accordingly, MOB might accomplish the removal of Mn^{2+} with the concomitant removal of CYN and other pollutants. For instance, Bai et al. (2016) observed higher removal rates of Mn^{2+}, Fe^{2+}, As^{3+}, and Sb^{3+} in quartz-sand columns after the MOB *Pseudomonas* sp. QJX-1 was inoculated, compared to those columns without the inoculation of the manganese-oxidizing strain. Furthermore, Zhang et al. (2015) evidenced high removal of diclofenac and sulfamethoxazole in lab-scale aerated biofilters inoculated with MOB, in which manganese was also completely removed from water.

6.1.2 Probable participation of MOB in natural attenuation of CYN

Biological removal of CYN is considered one of the main natural attenuation processes (de la Cruz et al., 2013; Dziga et al., 2016; Smith et al., 2008). In freshwater systems, MOB could co-exist with toxigenic cyanobacteria (Santelli et al., 2014; Stein et al., 2001). Indeed, three of the four MOB used in the present study were isolated from a freshwater pond in the Lower Oder Valley National Park, where potentially toxigenic cyanobacteria have been observed (Scheer, 2010). However, the lack of knowledge regarding the potential of MOB to remove CYN did not allow previous correlation of MOB and natural CYN attenuation.

As reported in **chapter 2** and **3**, MOB isolated from natural environments efficiently remove CYN, suggesting a role of MOB in the removal of CYN from freshwater bodies. MOB are found in sediments but also in the water column (Keim et al., 2015), where they might interact and remove CYN that is produced either by planktonic cyanobacteria (Poniedziałek et al., 2012) but also by benthic organisms (Bormans et al., 2014; Gaget et al., 2017; Poirier-Larabie et al., 2020).

As discussed in **chapter 2**, the presence of Fe^{2+} influences CYN removal by MOB at a lower extent than Mn^{2+} oxidation. When Fe^{2+} was added to the media, both *Ideonella* strains had lower CYN removal rates than in a Fe^{2+}-free media. Moreover, as it was observed in **chapter 5,** the presence of Fe^{2+} also reduced CYN removal rates of *Rubrivivax* sp. A210. Nevertheless, in presence or absence of Fe^{2+} in the media, the same less toxic transformation products were formed. Mn^{2+} and Fe^{2+} are two elements commonly found together in the environment, being Fe^{2+} more abundant than Mn^{2+} (Emerson, 2000; Schmidt, 2018). Results suggest that the common presence of Fe^{2+} in the nature might affect the removal rates of CYN by MOB at strain-specific level. However, even in presence of Fe^{2+}, the transformation of CYN to less toxic products by MOB in freshwater bodies might take place.

The transformation products described in **chapter 3** and **chapter 5** provide useful information to understand the fate of CYN in the environment. Considering that oxidation of manganese is a widespread ability among different bacterial groups (Tebo et al., 2005), and that all the tested MOB in the present work transform CYN to the same transformation products, it is expected that other MOB that also occur naturally in aquatic environments might transform CYN as well. Furthermore, the transformation of CYN by MOB cultivated in mineral media reported in **chapter 5** suggests a role of MOB in CYN transformation also in water bodies with low organic carbon load.

The results in **chapter 4**, evidenced the metabolic potential of strains OF001 and A210 to grow over a wide range of O_2 concentrations, including microaerophilic conditions, fix nitrogen, reduce nitrate and sulfate in an assimilatory way. Moreover, strain A210 encodes to enzymes related to dissimilatory nitrate reduction, and carbon fixation via Calvin cycle. Therefore, it might be expected that MOB with the ability to remove CYN inhabit different niches in the environment including the water column and the oxic-anoxic layer of the sediments, thus playing a pivotal role in the natural attenuation of CYN in water systems. Moreover, the potential carbon fixation by strain A210 suggests that some MOB might also play a role in the carbon cycle in waterbodies through the dark carbon fixation (Santoro et al., 2013). This process is expected mainly at the oxic-anoxic interfaces like the upper layer of the sediments (García-Cantizano et al., 2005), which MOB inhabit.

Aquatic environments are commonly affected by run-off from farmlands, and domestic and industrial discharges. These anthropogenic sources promote cultural eutrophication of waterbodies and increase pollutant concentrations (Glibert, 2017; Schulz, 2001). In such environments, a complex mixture of toxic compounds can be expected, which can include pesticides, metals, microplastics, and cyanotoxins (Metcalf and Codd, 2020). The environmental impact and the health significance of the co-occurrence of cyanotoxins and other pollutants has not been deeply studied. In this regard, the potential of MOB to remove several organic and inorganic pollutants by the combined activity of specific and unspecific mechanisms as discussed from **chapter 2** to **5**, suggest an important role of MOB in the removal of cyanotoxins and various classes of pollutants in natural systems deeply affected by anthropogenic pollution.

6.2 Outlook

The information generated in the present study contributes with useful information regarding the previously unknown CYN removal ability of MOB, including transformation rates,

biological transformation products, and the negligible toxicity of the mixture of transformation products in comparison with pure CYN. Furthermore, it supplies valuable information related to the metabolic potential of two CYN-transforming MOB to promote their application for biotechnological purposes and the molecular basis of the enzymes involved in Mn oxidation. Altogether, it deepens our understanding of the role of MOB in the removal of CYN and other organic pollutants, and allows a better understanding of the fate of CYN in aquatic environments.

I consider that further studies should focus in three main points: CYN removal for biotechnological applications, general metabolism and manganese oxidation mechanism of MOB, and the influence of MOB and manganese oxidation into the fate of CYN in aquatic environments.

Knowing that the four tested MOB remove CYN, it would be of great importance to evaluate the removal efficiency under different conditions like lower Mn^{2+} concentration, other Mn^{2+} sources like $MnCl_2$, or lower organic matter load, to try to simulate the characteristics of drinking water or groundwater. Furthermore, the removal efficiency of CYN variants with reported toxicity like 7-epi-CYN, and 7-deoxy-CYN (Adamski et al., 2014; Neumann et al., 2007), and CYN variants with suspected toxicity as 7-deoxydesulfo-CYN and 7-deoxydesulfo-12-acetyl-CYN (Wimmer et al., 2014) should be investigated.

Moreover, the removal of CYN by two or more different MOB could be evaluated. For instance, the mixture of *Pseudomonas* sp. OF001 and *Rubrivivax* sp. A210 might increase the removal rates at lower or none organic matter load. Perhaps, while strain A210 might provide the easily degradable carbon sources that strain OF001 requires to grow, both organisms together would remove CYN at high rates without the initial addition of a carbon source.

The evaluation of the biofilm formation capacity of the CYN-transforming strains, as well as their efficiency to remove CYN while immobilized in a column would be of great importance to determine whether they could be used as an inoculum applicable to remove CYN for water treatment. In addition, tested MOB in the present study could be inoculated in specific reactors in order to evaluate their adaptation to the columns, how the indigenous community of bacteria is altered, and, if in those conditions, CYN transformation is still carried out.

Even though the four tested organisms oxidized Mn^{2+}, the enzymes related to this process are not fully characterized. Therefore, the enzymes that were *in silico* identified to be most likely involved in Mn^{2+} oxidation should be further analysed to either corroborate their Mn^{2+} oxidase activity or to discard them and search for other alternatives.

Related with the Mn^{2+} oxidation process, it would be of great importance to characterize biogenic oxides produced by the tested MOB with regard to the structure, Mn^{3+}/Mn^{4+} composition, and Mn:Fe ratio. This information may provide an answer for the differences in transformation rates that we observed, but also for the general characterization of the tested MOB.

Additionally, it might be relevant to experimentally validate *in vitro* the physiological traits encoded in the genome of *Pseudomonas* sp. OF001 and *Rubrivivax* sp. A210. This information will be helpful for the general characterization of the MOB. Moreover, it should be evaluated if the tested MOB remove other cyanotoxins and organic compounds, either by a specific enzymatic pathway or by the unspecific mechanism related to Mn^{2+} oxidation.

The description of transformation products formed by MOB might help to investigate the fate of CYN in water bodies. To this end, it could be analysed the presence of the identified transformation products in aquatic environments, where CYN and MOB are found, to evaluate *in situ* the contribution of MOB into the removal of CYN in natural environments.

7 References

Abola, A.P., Willits, M.G., Wang, R.C., Long, S.R., 1999. Reduction of adenosine-5'-phosphosulfate instead of 3'-phosphoadenosine- 5'-phosphosulfate in cysteine biosynthesis by *Rhizobium meliloti* and other members of the family *Rhizobiaceae*. J. Bacteriol. 181, 5280–5287. https://doi.org/10.1128/jb.181.17.5280-5287.1999

Achá, D., Guédron, S., Amouroux, D., Point, D., Lazzaro, X., Fernandez, P.E., Sarret, G., 2018. Algal bloom exacerbates hydrogen sulfide and methylmercury contamination in the emblematic high-altitude Lake Titicaca. Geosciences 8. https://doi.org/10.3390/geosciences8120438

Adamski, M., Chrapusta, E., Bober, B., Kamiński, A., Białczyk, J., 2014. Cylindrospermopsin: cyanobacterial secondary metabolite. Biological aspects and potential risk for human health and life. Oceanol. Hydrobiol. Stud. 43, 442–449. https://doi.org/10.2478/s13545-014-0148-5

Adamski, M., Zmudzki, P., Chrapusta, E., Bober, B., Kaminski, A., Zabaglo, K., Latkowska, E., Bialczyk, J., 2016a. Effect of pH and temperature on the stability of cylindrospermopsin. Characterization of decomposition products. Algal Res. 15, 129–134. https://doi.org/10.1016/j.algal.2016.02.020

Adamski, M., Zmudzki, P., Chrapusta, E., Kaminski, A., Bober, B., Zabaglo, K., Bialczyk, J., 2016b. Characterization of cylindrospermopsin decomposition products formed under irradiation conditions. Algal Res. 18, 1–6. https://doi.org/10.1016/j.algal.2016.05.027

Akob, D.M., Bohu, T., Beyer, A., Schäffner, F., Händel, M., Johnson, C.A., Merten, D., Büchel, G., Totsche, K.U., Küsel, K., 2014. Identification of Mn(II)-oxidizing bacteria from a low-pH contaminated former uranium mine. Appl. Environ. Microbiol. 80, 5086–5097. https://doi.org/10.1128/AEM.01296-14

Anderson, C.R., Johnson, H.A., Caputo, N., Davis, R.E., Torpey, J.W., Tebo, B.M., 2009. Mn(II) oxidation is catalyzed by heme peroxidases in *Aurantimonas manganoxydans* strain SI85-9A1 and *Erythrobacter* sp. strain SD-21. Appl. Environ. Microbiol. 75, 4130–4138. https://doi.org/10.1128/AEM.02890-08

Ansari, A.A., Gill, Sarvajeet Singh, Khan, F.A., 2011. Eutrophication: Threat to aquatic ecosystems, in: Ansari, A.A., Gill, S. S., Lanza, G.R., Rast, W. (Eds.), Eutrophication: Causes, Consequences and Control. Springer Netherlands, Netherlands, pp. 1–394. https://doi.org/https://doi.org/10.1007/978-90-481-9625-8_7

Arcondéguy, T., Jack, R., Merrick, M., 2001. PII signal transduction proteins, pivotal players in microbial nitrogen control. Microbiol. Mol. Biol. Rev. 65, 80–105. https://doi.org/10.1128/MMBR.65.1.80

Arndt, D., Grant, J.R., Marcu, A., Sajed, T., Pon, A., Liang, Y., Wishart, D.S., 2016. PHASTER: a better, faster version of the PHAST phage search tool. Nucleic Acids Res. 44, W16–

W21. https://doi.org/10.1093/nar/gkw387

Atkinson, M.R., Ninfa, A.J., 1999. Characterization of the GlnK protein of *Escherichia coli*. Mol. Microbiol. 32, 301–313. https://doi.org/10.1046/j.1365-2958.1999.01349.x

Atlas, R., 2010. Handbook of Microbiological Media, Fourth Edition, Fourth edi. ed. Taylor & Francis Group, LLC, Washington, D. C. https://doi.org/10.1201/EBK1439804063

Auguie, B., 2017. gridExtra: Miscellaneous functions for "Grid" graphics. R Packag. version 2.3. https://doi.org/https://CRAN.R-project.org/package=gridExtra

Azevedo, L.B., van Zelm, R., Elshout, P.M.F., Hendriks, A.J., Leuven, R.S.E.W., Struijs, J., de Zwart, D., Huijbregts, M.A.J., 2013. Species richness-phosphorus relationships for lakes and streams worldwide. Glob. Ecol. Biogeogr. 22, 1304–1314. https://doi.org/10.1111/geb.12080

Bai, Y., Chang, Y., Liang, J., Chen, C., Qu, J., 2016. Treatment of groundwater containing Mn(II), Fe(II), As(III) and Sb(III) by bioaugmented quartz-sand filters. Water Res. 106, 126–134. https://doi.org/10.1016/j.watres.2016.09.040

Bairoch, A., Apweiler, R., 2000. The SWISS-PROT protein sequence database and its supplement TrEMBL in 2000. Nucleic Acids Res. 28, 45–48. https://doi.org/10.1093/nar/28.1.45

Banh, A., Chavez, V., Doi, J., Nguyen, A., Hernandez, S., Ha, V., Jimenez, P., Espinoza, F., Johnson, H.A., 2013. Manganese (Mn) oxidation increases intracellular Mn in *Pseudomonas putida* GB-1. PLoS One 8, e77835. https://doi.org/10.1371/journal.pone.0077835

Banker, R., Carmeli, S., Werman, M., Teltsch, B., Porat, R., Sukenik, A., 2001. Uracil moiety is required for toxicity of the cyanobacterial hepatotoxin cylindrospermopsin. J. Toxicol. Environ. Heal. Part A Curr. issues 62, 281–288. https://doi.org/http://dx.doi.org/10.1080/009841001459432

Banker, R., Teltsch, B., Sukenik, A., Carmeli, S., 2000. 7-epicylindrospermopsin, a toxic minor metabolite of the cyanobacterium *Aphanizomenon ovalisporum* from Lake Kinneret, Israel. J. Nat. Prod. 63, 387–389. https://doi.org/10.1021/np990498m

Barboza, N.R., Amorim, S.S., Santos, P.A., Reis, F.D., Cordeiro, M.M., Guerra-Sá, R., Leão, V.A., 2015. Indirect manganese removal by *Stenotrophomonas* sp. and *Lysinibacillus* sp. isolated from Brazilian mine water. Biomed Res. Int. 2015. https://doi.org/10.1155/2015/925972

Beaulieu, J.J., DelSontro, T., Downing, J.A., 2019. Eutrophication will increase methane emissions from lakes and impoundments during the 21st century. Nat. Commun. 10, 3–7. https://doi.org/10.1038/s41467-019-09100-5

Benayache, N.-Y., Nguyen-Quang, T., Hushchyna, K., McLellan, K., Afri-Mehennaoui, F.-Z., Bouaïcha, N., 2019. An overview of cyanobacteria harmful algal bloom (CyanoHAB)

issues in freshwater ecosystems, in: Gokce, D. (Ed.), Limnology - Some New Aspects of Inland Water Ecology. IntechOpem, pp. 13–37. https://doi.org/10.5772/intechopen.84155

Berry, J.P., Gibbs, P.D.L., Schmale, M.C., Saker, M.L., 2009. Toxicity of cylindrospermopsin, and other apparent metabolites from *Cylindrospermopsis raciborskii* and *Aphanizomenon ovalisporum*, to the zebrafish (*Danio rerio*) embryo. Toxicon 53, 289–299. https://doi.org/1doi:10.1016/j.toxicon.2008.11.016

Berry, J.P., Jaja-Chimedza, A., Dávalos-Lind, L., Lind, O., 2012. Apparent bioaccumulation of cylindrospermopsin and paralytic shellfish toxins by finfish in lake catemaco (Veracruz, Mexico). Food Addit. Contam. - Part A Chem. Anal. Control. Expo. Risk Assess. 29, 314–321. https://doi.org/10.1080/19440049.2011.597785

Bertelli, C., Laird, M.R., Williams, K.P., Lau, B.Y., Hoad, G., Winsor, G.L., Brinkman, F.S.L., 2017. IslandViewer 4: Expanded prediction of genomic islands for larger-scale datasets. Nucleic Acids Res. 45, W30–W35. https://doi.org/10.1093/nar/gkx343

Bhaya, D., Davison, M., Barrangou, R., 2011. CRISPR-Cas Systems in Bacteria and Archaea: Versatile Small RNAs for Adaptive Defense and Regulation. Annu. Rev. Genet. 45, 273–297. https://doi.org/10.1146/annurev-genet-110410-132430

Bick, J.A., Dennis, J.J., Zylstra, G.J., Nowack, J., Leustek, T., 2000. Identification of a new class of 5'-adenylylsulfate (APS) reductases from sulfate-assimilating bacteria. J. Bacteriol. 182, 135–142. https://doi.org/10.1128/JB.182.1.135-142.2000

Blauwkamp, T.A., Ninfa, A.J., 2002. Physiological role of the GlnK signal transduction protein of *Escherichia coli*: survival of nitrogen starvation. Mol. Microbiol. 46, 203–214. https://doi.org/10.1046/j.1365-2958.2002.03153.x

Bohu, T., Akob, D.M., Abratis, M., Lazar, C.S., 2016. Biological low-pH Mn(II) oxidation in a manganese deposit. Appl. Environ. Microbiol. 82, 3009–3021. https://doi.org/10.1128/AEM.03844-15.Editor

Bormans, M., Lengronne, M., Brient, L., Duval, C., 2014. Cylindrospermopsin accumulation and release by the benthic cyanobacterium *Oscillatoria* sp. PCC 6506 under different light conditions and growth phases. Bull. Environ. Contam. Toxicol. 92, 243–247. https://doi.org/10.1007/s00128-013-1144-y

Bouraï, L., Logez, M., Laplace-Treyture, C., Argillier, C., 2020. How do eutrophication and temperature interact to shape the community structures of phytoplankton and fish in Lakes? Water (Switzerland) 12. https://doi.org/10.3390/w12030779

Bourke, A.T.C., Hawes, R.B., Neilson, A., Stallman, N.D., 1983. An outbreak of hepato-enteritis (the Palm Island mystery disease) possibly caused by algal intoxication. Toxicon 21, 45–48. https://doi.org/10.1016/0041-0101(83)90151-4

Bourne, D.G., Riddles, P., Jones, G.J., Smith, W., Blakeley, R.L., 2001. Characterisation of a gene cluster involved in bacterial degradation of the cyanobacterial toxin microcystin LR.

Environ. Toxicol. 16, 523–534. https://doi.org/10.1002/tox.10013

Bouwman, A.F., Beusen, A.H.W., Overbeek, C.C., Bureau, D.P., Pawlowski, M., Glibert, P.M., 2013. Hindcasts and future projections of global inland and coastal nitrogen and phosphorus loads due to finfish aquaculture. Rev. Fish. Sci. 21, 112–156. https://doi.org/10.1080/10641262.2013.790340

Bouwman, L., Beusen, A., Glibert, P.M., Overbeek, C., Pawlowski, M., Herrera, J., Mulsow, S., Yu, R., Zhou, M., 2013. Mariculture: Significant and expanding cause of coastal nutrient enrichment. Environ. Res. Lett. 8. https://doi.org/10.1088/1748-9326/8/4/044026

Brouwers, G. J., Corstjens, P.L.A.M., De Vrind, J.P.M., Verkamman, A., De Kuyper, M., De Vrind-De Jong, E.W., 2000. Stimulation of Mn^{2+} oxidation in *Leptothrix discophora* SS-1 by Cu^{2+} and sequence analysis of the region flanking the gene encoding putative multicopper oxidase MofA. Geomicrobiol. J. 17, 25–33. https://doi.org/10.1080/014904500270468

Brouwers, Geert Jan, Vijgenboom, E., Corstjens, P.L.A.M., de Vrind-de Jong, E.W., 2000. Bacterial Mn^{2+} oxidizing systems and multicopper oxidases: An overview of mechnisms and functions. Geomicrobiol. J. 17, 1–24. https://doi.org/https://doi.org/10.1080/014904500270459

Bruins, J., 2016. Manganese removal from groundwater- Role of biological and physico-chemical autocatalytic processes.

Bullerjahn, G.S., Post, A.F., 2014. Physiology and molecular biology of aquatic cyanobacteria. Front. Microbiol. 5, 1–2. https://doi.org/10.3389/fmicb.2014.00359

Burgin, A.J., Hamilton, S.K., Gardner, W.S., McCarthy, M.J., 2015. Nitrate reduction, denitrification, and dissimilatory nitrate reduction to ammonium in wetland sediments 519–537. https://doi.org/10.2136/sssabookser10.c28

Byth, S., 1980. Palm Island mystery disease. Med. J. Aust. 2, 40–42. https://doi.org/10.5694/j.1326-5377.1986.tb113890.x

Camacho, C., Coulouris, G., Avagyan, V., Ma, N., Papadopoulos, J., Bealer, K., Madden, T.L., 2009. BLAST+: Architecture and applications. BMC Bioinformatics 10, 1–9. https://doi.org/10.1186/1471-2105-10-421

Caspi, R., Billington, R., Fulcher, C.A., Keseler, I.M., Kothari, A., Krummenacker, M., Latendresse, M., Midford, P.E., Ong, Q., Ong, W.K., Paley, S., Subhraveti, P., Karp, P.D., 2018. The MetaCyc database of metabolic pathways and enzymes. Nucleic Acids Res. 46, D633–D639. https://doi.org/10.1093/nar/gkx935

Cerrato, J.M., Falkinham, J.O., Dietrich, A.M., Knocke, W.R., McKinney, C.W., Pruden, A., 2010. Manganese-oxidizing and -reducing microorganisms isolated from biofilms in chlorinated drinking water systems. Water Res. 44, 3935–3945. https://doi.org/10.1016/j.watres.2010.04.037

Chaput, D.L., Fowler, A.J., Seo, O., Duhn, K., Hansel, C.M., Santelli, C.M., 2019. Mn oxide formation by phototrophs: Spatial and temporal patterns, with evidence of an enzymatic superoxide-mediated pathway. Sci. Rep. 9, 1–14. https://doi.org/10.1038/s41598-019-54403-8

Chaumeil, P.-A., Mussig, A.J., Hugenholtz, P., Parks, D.H., 2019. GTDB-Tk: a toolkit to classify genomes with the Genome Taxonomy Database. Bioinformatics 36, 1925–1927. https://doi.org/10.1093/bioinformatics/btz848

Chen, H., Boutros, P.C., 2011. VennDiagram: a package for the generation of highly-customizable Venn and Euler diagrams in R. BMC Bioinformatics 12. https://doi.org/https://doi.org/10.1186/1471-2105-12-35

Chernoff, N., Hill, D.J., Chorus, I., Diggs, D.L., Huang, H., King, D., Lang, J.R., Le, T.T., Schmid, J.E., Travlos, G.S., Whitley, E.M., Wilson, R.E., Wood, C.R., 2018. Cylindrospermopsin toxicity in mice following a 90-d oral exposure. J. Toxicol. Environ. Heal. - Part A Curr. Issues 81, 549–566. https://doi.org/10.1080/15287394.2018.1460787

Chiswell, R.K., Shaw, G.R., Eaglesham, G., Smith, M.J., Norris, R.L., Seawright, A.A., Moore, M.R., 1999. Stability of cylindrospermopsin, the toxin from the cyanobacterium, *Cylindrospermopsis raciborskii*: Effect of pH, temperature, and sunlight on decomposition. Environ. Toxicol. 14, 155–161. https://doi.org/doi.org/10.1002/(SICI)1522-7278(199902)14:1<155::AID-TOX20>3.0.CO;2-Z

Corbel, S., Mougin, C., Bouaïcha, N., 2014. Cyanobacterial toxins: Modes of actions, fate in aquatic and soil ecosystems, phytotoxicity and bioaccumulation in agricultural crops. Chemosphere 96, 1–15. https://doi.org/10.1016/j.chemosphere.2013.07.056

Corstjens, P.L.A.M., De Vrind, J.P.M., Westbroek, P., De Vrind-De Jong, E.W., 1992. Enzymatic iron oxidation by *Leptothrix discophora*: Identification of an iron-oxidizing protein. Appl. Environ. Microbiol. 58, 450–454. https://doi.org/10.1128/aem.58.2.450-454.1992

Corstjens, P.L.A.M., Devrind, J.P.M., Goosen, T., de Vrind-de Jong, E.W., 1997. Identification and molecular analysis of the *Leptothrix discophora* SS-1 *mofA* gene, a gene putatively encoding a manganese-oxidizing protein with copper domains. Geomicrobiol. J. 14, 91–108. https://doi.org/10.1080/01490459709378037

Couvin, D., Bernheim, A., Toffano-Nioche, C., Touchon, M., Michalik, J., Néron, B., Rocha, E.P.C., Vergnaud, G., Gautheret, D., Pourcel, C., 2018. CRISPRCasFinder, an update of CRISRFinder, includes a portable version, enhanced performance and integrates search for Cas proteins. Nucleic Acids Res. 46, W246–W251. https://doi.org/10.1093/nar/gky425

Davis, T.W., Orr, P.T., Boyer, G.L., Burford, M.A., 2014. Investigating the production and release of cylindrospermopsin and deoxy-cylindrospermopsin by *Cylindrospermopsis raciborskii* over a natural growth cycle. Harmful Algae 31, 18–25.

https://doi.org/10.1016/j.hal.2013.09.007

Daye, M., Klepac-Ceraj, V., Pajusalu, M., Rowland, S., Farrell-Sherman, A., Beukes, N., Tamura, N., Fournier, G., Bosak, T., 2019. Light-driven anaerobic microbial oxidation of manganese. Nature 576, 311–314. https://doi.org/10.1038/s41586-019-1804-0

de la Cruz, A.A., Hiskia, A., Kaloudis, T., Chernoff, N., Hill, D., Antoniou, M.G., He, X., Loftin, K., O'Shea, K., Zhao, C., Pelaez, M., Han, C., Lynch, T.J., Dionysiou, D.D., 2013. A review on cylindrospermopsin: the global occurrence, detection, toxicity and degradation of a potent cyanotoxin. Environ. Sci. Process. Impacts 15, 1979. https://doi.org/10.1039/c3em00353a

de Sousa, L.P., 2020. Mobile genetic elements in *Pseudomonas stutzeri*. Curr. Microbiol. 77, 179–184. https://doi.org/10.1007/s00284-019-01812-7

Dick, Gregory J., Podell, S., Johnson, H.A., Rivera-Espinoza, Y., Bernier-Latmani, R., McCarthy, J.K., Torpey, J.W., Clement, B.G., Gaasterland, T., Tebo, B.M., 2008. Genomic insights into Mn(II) oxidation by the marine alphaproteobacterium *Aurantimonas* sp. strain SI85-9A1. Appl. Environ. Microbiol. 74, 2646–2658. https://doi.org/10.1128/AEM.01656-07

Dick, Gregory J, Torpey, J.W., Beveridge, T.J., Tebo, B.M., 2008. Direct identification of a bacterial manganese(II) oxidase, the multicopper oxidase MnxG, from spores of several different marine *Bacillus* species. Appl. Environ. Microbiol. 74, 1527–1534. https://doi.org/10.1128/AEM.01240-07

Díez-Quijada, L., Llana-Ruiz-Cabello, M., Cătunescu, G.M., Puerto, M., Moyano, R., Jos, A., Cameán, A.M., 2019. *In vivo* genotoxicity evaluation of cylindrospermopsin in rats using a combined micronucleus and comet assay. Food Chem. Toxicol. 132, 110664. https://doi.org/10.1016/j.fct.2019.110664

Díez, B., Ininbergs, K., 2014. Ecological importance of cyanobacteria, in: Sharma, N.K., Rai, A.K., Stal, L.J. (Eds.), Cyanobacteria: An Economic Perspective. John Wiley & Sons, Ltd., pp. 43–63. https://doi.org/10.1002/9781118402238.ch3

Donato, M.T., Tolosa, L., Gómez-Lechón, M.J., 2015. Culture and functional characterization of human hepatoma HepG2 cells, in: Vinken, M., Rogiers, V. (Eds.), Protocols in in Vitro Hepatocyte Research. Methods in Molecular Biology. Humana Press, New York, NY, New York, pp. 77–93. https://doi.org/10.1007/978-1-4939-2074-7

Dou, M., Ma, X., Zhang, Yan, Zhang, Yongyong, Shi, Y., 2019. Modeling the interaction of light and nutrients as factors driving lake eutrophication. Ecol. Modell. 400, 41–52. https://doi.org/10.1016/j.ecolmodel.2019.03.015

Durand, A., Bourbon, M.L., Steunou, A.S., Khalfaoui-Hassani, B., Legrand, C., Legrand, A., Astier, C., Ouchane, S., 2018. Biogenesis of the bacterial cbb_3 cytochrome *c* oxidase: Active subcomplexes support a sequential assembly model. J. Biol. Chem. 293, 808–818.

https://doi.org/10.1074/jbc.M117.805184

Dziewit, L., Radlinska, M., 2016. Two inducible prophages of an antarctic *Pseudomonas* sp. ANT_H14 use the same capsid for packaging their genomes - Characterization of a novel phage helper-satellite system. PLoS One 11, 1–27. https://doi.org/10.1371/journal.pone.0158889

Dziga, D., Kokocinski, M., Maksylewicz, A., Czaja-Prokop, U., Barylski, J., 2016. Cylindrospermopsin biodegradation abilities of *Aeromonas* sp. isolated from Rusałka Lake. Toxins (Basel). 8, 55. https://doi.org/10.3390/toxins8030055

Dziga, D., Wasylewski, M., Wladyka, B., Nybom, S., Meriluoto, J., 2013. Microbial degradation of microcystins. Chem. Res. Toxicol. 26, 841–852. https://doi.org/10.1021/tx4000045

Ecale Zhou, C.L., Malfatti, S., Kimbrel, J., Philipson, C., McNair, K., Hamilton, T., Edwards, R., Souza, B., Hancock, J., 2019. multiPhATE: Bioinformatics pipeline for functional annotation of phage isolates. Bioinformatics 35, 4402–4404. https://doi.org/10.1093/bioinformatics/btz258

Edgar, R.C., 2004. MUSCLE: Multiple sequence alignment with high accuracy and high throughput. Nucleic Acids Res. 32, 1792–1797. https://doi.org/10.1093/nar/gkh340

Egener, T., Martin, D.E., Sarkar, A., Reinhold-Hurek, B., 2001. Role of a ferredoxin gene cotranscribed with the *nifHDK* operon in N_2 fixation and nitrogenase “switch-off” of *Azoarcus* sp. strain BH72. J. Bacteriol. 183, 3752–3760. https://doi.org/10.1128/JB.183.12.3752-3760.2001

Ekici, S., Pawlik, G., Lohmeyer, E., Koch, H.G., Daldal, F., 2012. Biogenesis of cbb_3-type cytochrome *c* oxidase in *Rhodobacter capsulatus*. Biochim. Biophys. Acta 1817, 898–910. https://doi.org/10.1038/jid.2014.371

El Gheriany, I.A., Bocioaga, D., Hay, A.G., Ghiorse, W.C., Shuler, M.L., Lion, L.W., 2009. Iron requirement for Mn(II) oxidation by *Leptothrix discophora* SS-1. Appl. Environ. Microbiol. 75, 1229–1235. https://doi.org/10.1128/AEM.02291-08

Emerson, D., 2000. Microbial oxidation of Fe(II) and Mn(II) at circumneutral pH, in: Lovley, D.R. (Ed.), Environmental Microbe - Metal Interactions. ASM Press, Washington, D. C., pp. 31–52.

Estes, E.R., Andeer, P.F., Nordlund, D., Wankel, S.D., Hansel, C.M., 2017. Biogenic manganese oxides as reservoirs of organic carbon and proteins in terrestrial and marine environments. Geobiology 15, 158–172. https://doi.org/10.1111/gbi.12195

Falconer, I.R., Hardy, S.J., Humpage, A.R., Froscio, S.M., Tozer, G.J., Hawkins, P.R., 1999. Hepatic and renal toxicity of the blue-green alga (cyanobacterium) *Cylindrospermopsis raciborskii* in male Swiss Albino mice. Environ. Toxicol. 14, 143–150. https://doi.org/10.1002/(SICI)1522-7278(199902)14:1<143::AID-TOX18>3.0.CO;2-H

Farris, J.S., 1972. Estimating phylogenetic trees from distance matrices. Am. Nat. 106, 645–

668.

Fastner, J., Beulker, C., Geiser, B., Hoffmann, A., Kröger, R., Teske, K., Hoppe, J., Mundhenk, L., Neurath, H., Sagebiel, D., Chorus, I., 2018. Fatal neurotoxicosis in dogs associated with tychoplanktic, anatoxin-a producing *Tychonema* sp. in mesotrophic Lake Tegel, Berlin. Toxins (Basel). 10, 60. https://doi.org/10.3390/toxins10020060

Flombaum, P., Gallegos, J.L., Gordillo, R.A., Rincón, J., Zabala, L.L., Jiao, N., Karl, D.M., Li, W.K.W., Lomas, M.W., Veneziano, D., Vera, C.S., Vrugt, J., Martiny, A.C., 2013. Present and future global distributions of the marine cyanobacteria *Prochlrococcus* and *Synechococcus*. PNAS 110, 9824–9829. https://doi.org/10.1073/pnas.1307701110/-/DCSupplemental.www.pnas.org/cgi/doi/10.1073/pnas.1307701110

Fotiou, T., Triantis, T., Kaloudis, T., Hiskia, A., 2015. Photocatalytic degradation of cylindrospermopsin under UV-A, solar and visible light using TiO_2. Mineralization and intermediate products. Chemosphere 119, S89–S94. https://doi.org/10.1016/j.chemosphere.2014.04.045

Francis, C.A., Tebo, B.M., 2002. Enzymatic manganese(II) oxidation by metabolically dormant spores of diverse *Bacillus* species. Appl. Environ. Microbiol. 68, 874–880. https://doi.org/10.1128/AEM.68.2.874-880.2002

Froscio, S.M., Fanok, S., Humpage, A.R., 2009. Cytotoxicity screening for the cyanobacterial toxin cylindrospermopsin. J. Toxicol. Environ. Heal. - Part A Curr. Issues 72, 345–349. https://doi.org/10.1080/15287390802529906

Froscio, S.M., Humpage, A.R., Burcham, P.C., Falconer, I.R., 2003. Cylindrospermopsin-induced protein synthesis inhibition and its dissociation from acute toxicity in mouse hepatocytes. Environ. Toxicol. 18, 243–251. https://doi.org/10.1002/tox.10121

Gaget, V., Humpage, A.R., Huang, Q., Monis, P., Brookes, J.D., 2017. Benthic cyanobacteria: A source of cylindrospermopsin and microcystin in Australian drinking water reservoirs. Water Res. 124, 454–464. https://doi.org/10.1016/j.watres.2017.07.073

Galiez, C., Magnan, C.N., Coste, F., Baldi, P., 2016. VIRALpro: A tool to identify viral capsid and tail sequences. Bioinformatics 32, 1405–1407. https://doi.org/10.1093/bioinformatics/btv727

García-Cantizano, J., Casamayor, E.O., Gasol, J.M., Guerrero, R., Pedrós-Alió, C., 2005. Partitioning of CO_2 incorporation among planktonic microbial guilds and estimation of in situ specific growth rates. Microb. Ecol. 50, 230–241. https://doi.org/10.1007/s00248-004-0144-9

Garnier, S., 2018. viridis: Default color maps from “matplotlib”. R Packag. version 0.5.1.

Gerets, H.H.J., Tilmant, K., Gerin, B., Chanteux, H., Depelchin, B.O., Dhalluin, S., Atienzar, F.A., 2012. Characterization of primary human hepatocytes, HepG2 cells, and HepaRG cells at the mRNA level and CYP activity in response to inducers and their predictivity for

the detection of human hepatotoxins. Cell Biol. Toxicol. 28, 69–87. https://doi.org/10.1007/s10565-011-9208-4

German, N., Lüthje, F., Hao, X., Rønn, R., Rensing, C., 2016. Microbial virulence and interactions with metals, in: Progress in Molecular Biology and Translational Science. Elsevier Inc., pp. 27–49. https://doi.org/10.1016/bs.pmbts.2016.05.010

Geszvain, K., Butterfield, C., Davis, R.E., Madison, A.S., Lee, S.-W., Parker, D.L., Soldatova, A., Spiro, T.G., Luther, G.W., Tebo, B.M., 2012. The molecular biogeochemistry of manganese(II) oxidation. Biochem. Soc. Trans. 40, 1244–1248. https://doi.org/10.1042/BST20120229

Geszvain, K., McCarthy, J.K., Tebo, B.M., 2013. Elimination of manganese(II,III) oxidation in *Pseudomonas putida* GB-1 by a double knockout of two putative multicopper oxidase genes. Appl. Environ. Microbiol. 79, 357–366. https://doi.org/10.1128/AEM.01850-12

Geszvain, K., Smesrud, L., Tebo, B.M., 2016. Identification of a third Mn(II) oxidase enzyme in *Pseudomonas putida* GB-1. Appl. Environ. Microbiol. 82, 3774–3782. https://doi.org/10.1128/AEM.00046-16

Geszvain, K., Tebo, B.M., 2010. Identification of a two-component regulatory pathway essential for Mn(II) oxidation in *Pseudomonas putida* GB-1. Appl. Environ. Microbiol. 76, 1224–1231. https://doi.org/10.1128/AEM.02473-09

Ghiorse, W.C., 1984. Biology of iron- and manganese-depositing bacteria. Annu. Rev. Microbiol. 38, 515–550.

Giannuzzi, L., Sedan, D., Echenique, R., Andrinolo, D., 2011. An acute case of intoxication with cyanobacteria and cyanotoxins in recreational water in Salto Grande Dam, Argentina. Mar. Drugs 9, 2164–2175. https://doi.org/10.3390/md9112164

Glibert, P.M., 2017. Eutrophication, harmful algae and biodiversity — Challenging paradigms in a world of complex nutrient changes. Mar. Pollut. Bull. 124, 591–606. https://doi.org/10.1016/j.marpolbul.2017.04.027

Glibert, P.M., 2015. More than propagule pressure: Successful invading algae have physiological adaptations suitable to anthropogenically changing nutrient environments. Aquat. Ecosyst. Heal. Manag. 18, 334–341. https://doi.org/10.1080/14634988.2015.1027137

Goldberg, T., Hecht, M., Hamp, T., Karl, T., Yachdav, G., Ahmed, N., Altermann, U., Angerer, P., Ansorge, S., Balasz, K., Bernhofer, M., Betz, A., Cizmadija, L., Do, K.T., Gerke, J., Greil, R., Joerdens, V., Hastreiter, M., Hembach, K., Herzog, M., Kalemanov, M., Kluge, M., Meier, A., Nasir, H., Neumaier, U., Prade, V., Reeb, J., Sorokoumov, A., Troshani, I., Vorberg, S., Waldraff, S., Zierer, J., Nielsen, H., Rost, B., 2014. LocTree3 prediction of localization. Nucleic Acids Res. 42, 350–355. https://doi.org/10.1093/nar/gku396

Goris, J., Konstantinidis, K.T., Klappenbach, J.A., Coenye, T., Vandamme, P., Tiedje, J.M.,

2007. DNA-DNA hybridization values and their relationship to whole-genome sequence similarities. Int. J. Syst. Evol. Microbiol. 57, 81–91. https://doi.org/10.1099/ijs.0.64483-0

Gosztolai, A., Schumacher, J., Behrends, V., Bundy, J.G., Heydenreich, F., Bennett, M.H., Buck, M., Barahona, M., 2017. GlnK facilitates the dynamic regulation of bacterial nitrogen assimilation. Biophys. J. 112, 2219–2230. https://doi.org/10.1016/j.bpj.2017.04.012

Grazziotin, A.L., Koonin, E. V., Kristensen, D.M., 2017. Prokaryotic Virus Orthologous Groups (pVOGs): A resource for comparative genomics and protein family annotation. Nucleic Acids Res. 45, D491–D498. https://doi.org/10.1093/nar/gkw975

Griffiths, D.J., Saker, M.L., 2003. The Palm Island mystery disease 20 years on: A review of research on the cyanotoxin cylindrospermopsin. Environ. Toxicol. 18, 78–93. https://doi.org/10.1002/tox.10103

Grindley, N.D.F., Whiteson, K.L., Rice, P.A., 2006. Mechanisms of site-specific recombination. Annu. Rev. Biochem. 75, 567–605. https://doi.org/10.1146/annurev.biochem.73.011303.073908

Guillouzo, A., Corlu, A., Aninat, C., Glaise, D., Morel, F., Guguen-Guillouzo, C., 2007. The human hepatoma HepaRG cells: A highly differentiated model for studies of liver metabolism and toxicity of xenobiotics. Chem. Biol. Interact. 168, 66–73. https://doi.org/10.1016/j.cbi.2006.12.003

Guillouzo, A., Guguen-Guillouzo, C., 2018. HepaRG cells as a model for hepatotoxicity studies, in: Rasmussen, T.P. (Ed.), Stem Cells in Birth Defects Research and Developmental Toxicology. John Wiley & Sons, Inc., pp. 309–339. https://doi.org/10.1002/9781119283249.ch12

Guindon, S., Dufayard, J.F., Lefort, V., Anisimova, M., Hordijk, W., Gascuel, O., 2010. New algorithms and methods to estimate maximum-likelihood phylogenies: Assessing the performance of PhyML 3.0. Syst. Biol. 59, 307–321. https://doi.org/10.1093/sysbio/syq010

Gutiérrez-Praena, D., Guzmán-Guillén, R., Pichardo, S., Moreno, F.J., Vasconcelos, V., Jos, Á., Cameán, A.M., 2019. Cytotoxic and morphological effects of microcystin-LR, cylindrospermopsin, and their combinations on the human hepatic cell line HepG2. Environ. Toxicol. 34, 240–251. https://doi.org/10.1002/tox.22679

Gutiérrez-Praena, D., Jos, Á., Pichardo, S., Moreno, I.M., Cameán, A.M., 2013. Presence and bioaccumulation of microcystins and cylindrospermopsin in food and the effectiveness of some cooking techniques at decreasing their concentrations: A review. Food Chem. Toxicol. 53, 139–152. https://doi.org/10.1016/j.fct.2012.10.062

Gutiérrez-Praena, D., Jos, Á., Pichardo, S., Moyano, R., Blanco, A., Monterde, J.G., Cameán, A.M., 2012. Time-dependent histopathological changes induced in Tilapia (*Oreochromis niloticus*) after acute exposure to pure cylindrospermopsin by oral and intraperitoneal

route. Ecotoxicol. Environ. Saf. 76, 102–113. https://doi.org/10.1016/j.ecoenv.2011.10.008

Guzmán-Guillén, R., Maisanaba, S., Prieto Ortega, A.I., Valderrama-Fernández, R., Jos, Á., Cameán, A.M., 2017. Changes on cylindrospermopsin concentration and characterization of decomposition products in fish muscle (*Oreochromis niloticus*) by boiling and steaming. Food Control 77, 210–220. https://doi.org/10.1016/j.foodcont.2017.02.035

Guzmán-Guillén, R., Manzano, I.L., Moreno, I.M., Ortega, A.I.P., Moyano, R., Blanco, A., Cameán, A.M., 2015. Cylindrospermopsin induces neurotoxicity in tilapia fish (*Oreochromis niloticus*) exposed to *Aphanizomenon ovalisporum*. Aquat. Toxicol. 161, 17–24. https://doi.org/10.1016/j.aquatox.2015.01.024

Guzmán-Guillén, R., Prieto, A.I., González, A.G., Soria-Díaz, M.E., Cameán, A.M., 2012. Cylindrospermopsin determination in water by LC-MS/MS: Optimization and validation of the method and application to real samples. Environ. Toxicol. Chem. 31, 2233–2238. https://doi.org/10.1002/etc.1954

Hamilton, T.L., Bryant, D.A., Macalady, J.L., 2016. The role of biology in planetary evolution: Cyanobacterial primary production in low-oxygen Proterozoic oceans. Environ. Microbiol. 18, 325–340. https://doi.org/10.1111/1462-2920.13118

Hansel, C.M., Learman, D.R., 2015. Geomicrobiology of manganese, in: Ehrlich, H., Newman, D., Kappler, A. (Eds.), Ehrlich's Geomicrobiology. CRC Press, Boca Raton, FL, pp. 403–433. https://doi.org/10.1201/b19121

Hawkins, P.R., Runnegar, M.T.C., Jackson, A.R.B., Falconer, I.R., 1985. Severe hepatotoxicity caused by the tropical cyanobacterium (blue-green alga) *Cylindrospermopsis reciborskii* (Woloszynska) Seenaya and Subba Raju isolated from a domestic wtare supplyy reservoir. Appl. Environ. Microbiol. 50, 1292–1295.

He, W.H., Wang, Y.N., Du, X., Zhou, Y., Jia, B., Bian, J., Liu, S.J., Chen, G.C., 2012. *Pseudomonas linyingensis* sp. nov.: A novel bacterium isolated from wheat soil subjected to long-term herbicides application. Curr. Microbiol. 65, 595–600. https://doi.org/10.1007/s00284-012-0187-3

He, X., de la Cruz, A.A., O'Shea, K.E., Dionysiou, D.D., 2014a. Kinetics and mechanisms of cylindrospermopsin destruction by sulfate radical-based advanced oxidation processes. Water Res. 63, 168–178. https://doi.org/10.1016/j.watres.2014.06.004

He, X., Zhang, G., De La Cruz, A.A., O'Shea, K.E., Dionysiou, D.D., 2014b. Degradation mechanism of cyanobacterial toxin cylindrospermopsin by hydroxyl radicals in homogeneous UV/H_2O_2 process. Environ. Sci. Technol. 48, 4495–4504. https://doi.org/10.1021/es403732s

Hedrich, S., Schlömann, M., Barrie Johnson, D., 2011. The iron-oxidizing proteobacteria. Microbiology 157, 1551–1564. https://doi.org/10.1099/mic.0.045344-0

Hein, J.R., Koschinsky, A., 2013. Deep-ocean ferromanganese crusts and nodules, in: Holland, H.D., Turekian, K.K. (Eds.), Treatise on Geochemistry. Published by Elsevier Inc., pp. 273–291. https://doi.org/10.1016/B978-0-08-095975-7.01111-6

Hennebel, T., De Gusseme, B., Boon, N., Verstraete, W., 2009. Biogenic metals in advanced water treatment. Trends Biotechnol. 27, 90–98. https://doi.org/10.1016/j.tibtech.2008.11.002

Hiller, T., Berg, J., Elomaa, L., Röhrs, V., Ullah, I., Schaar, K., Dietrich, A.C., Al-Zeer, M.A., Kurtz, A., Hocke, A.C., Hippenstiel, S., Fechner, H., Weinhart, M., Kurreck, J., 2018. Generation of a 3D liver model comprising human extracellular matrix in an alginate/gelatin-based bioink by extrusion bioprinting for infection and transduction studies. Int. J. Mol. Sci. 19, 1–17. https://doi.org/10.3390/ijms19103129

Ho, L., Lambling, P., Bustamante, H., Duker, P., Newcombe, G., 2011. Application of powdered activated carbon for the adsorption of cylindrospermopsin and microcystin toxins from drinking water supplies. Water Res. 45, 2954–2964. https://doi.org/10.1016/j.watres.2011.03.014

Ho, L., Sawade, E., Newcombe, G., 2012. Biological treatment options for cyanobacteria metabolite removal - A review. Water Res. 46, 1536–1548. https://doi.org/10.1016/j.watres.2011.11.018

Holland, A., Kinnear, S., 2013. Interpreting the possible ecological role(s) of cyanotoxins: Compounds for competitive advantage and/or physiological aide? Mar. Drugs 11, 2239–2258. https://doi.org/10.3390/md11072239

Hsiao, W., Wan, I., Jones, S.J., Brinkman, F.S.L., 2003. IslandPath: Aiding detection of genomic islands in prokaryotes. Bioinformatics 19, 418–420. https://doi.org/10.1093/bioinformatics/btg004

Huelsenbeck, J.P., Ronquist, F., 2001. MrBAYES: Bayesian inference for phylogeny. Bioinformatics 17, 754–755. https://doi.org/10.1093/bioinformatics/17.8.754

Huguet, A., Lanceleur, R., Quenault, H., Le Hégarat, L., Fessard, V., 2019. Identification of key pathways involved in the toxic response of the cyanobacterial toxin cylindrospermopsin in human hepatic HepaRG cells. Toxicol. Vitr. 58, 69–77. https://doi.org/10.1016/j.tiv.2019.03.023

Humpage, A.R., Falconer, I.R., 2003. Oral toxicity of the cyanobacterial toxin cylindrospermopsin in male Swiss albino mice: Determination of no observed adverse effect level for deriving a drinking water guideline value. Environ. Toxicol. 18, 94–103. https://doi.org/10.1002/tox.10104

Humpage, A.R., Fenech, M., Thomas, P., Falconer, I.R., 2000. Micronucleus induction and chromosome loss in transformed human white cells indicate clastogenic and aneugenic action of the cyanobacterial toxin, cylindrospermopsin. Mutat. Res. - Genet. Toxicol.

Environ. Mutagen. 472, 155–161. https://doi.org/10.1016/S1383-5718(00)00144-3

Humpage, A.R., Fontaine, F., Froscio, S., Burcham, P., Falconer, I.R., 2005. Cylindrospermopsin genotoxicity and cytotoxicity: Role of cytochrome P-450 and oxidative stress. J. Toxicol. Environ. Heal. - Part A 68, 739–753. https://doi.org/10.1080/15287390590925465

Isidoro-Ayza, M., Jones, L., Dusek, R.J., Lorch, J.M., Landsberg, J.H., Wilson, P., Graham, S., 2019. Mortality of little brown bats (*Myotis lucifugus carissima*) naturally exposed to microcystin-LR. J. Wildl. Dis. 55, 266–269. https://doi.org/10.7589/2018-02-047

Iwanicka-Nowicka, R., Zielak, A., Cook, A.M., Thomas, M.S., Hryniewicz, M.M., 2007. Regulation of sulfur assimilation pathways in *Burkholderia cenocepacia*: Identification of transcription factors CysB and SsuR and their role in control of target genes. J. Bacteriol. 189, 1675–1688. https://doi.org/10.1128/JB.00592-06

Jian, Z., Bai, Y., Chang, Y., Liang, J., Qu, J., 2019. Removal of micropollutants and cyanobacteria from drinking water using KMnO4 pre-oxidation coupled with bioaugmentation. Chemosphere 215, 1–7. https://doi.org/10.1016/j.chemosphere.2018.10.013

Johnson, K.W., Carmichael, M.J., McDonald, W., Rose, N., Pitchford, J., Windelspecht, M., Karatan, E., Bräuer, S.L., 2012. Increased abundance of *Gallionella* spp., *Leptothrix* spp. and total bacteria in response to enhanced Mn and Fe concentrations in a disturbed southern appalachian high elevation wetland. Geomicrobiol. J. 29, 124–138. https://doi.org/10.1080/01490451.2011.558557

Jones, M.E., Nico, P.S., Ying, S., Regier, T., Thieme, J., Keiluweit, M., 2018. Manganese-driven carbon oxidation at oxic-anoxic interfaces. Environ. Sci. Technol. 52, 12349–12357. https://doi.org/10.1021/acs.est.8b03791

Joutey, N.T., Bahafid, W., Sayel, H., El Ghachtouli, N., 2013. Biodegradation: Involved microorganisms and genetically engineered microorganisms, in: Chamy, R., Rosenkranz, F. (Eds.), Biodegradation- Life of Science. InTech, Rijeka, Croatia, pp. 289–320. https://doi.org/dx.doi.org/10.5772/56194

Kanehisa, M., Sato, Y., Morishima, K., 2016. BlastKOALA and GhostKOALA: KEGG tools for functional characterization of genome and metagenome sequences. J. Mol. Biol. 428, 726–731. https://doi.org/10.1016/j.jmb.2015.11.006

Kappler, A., Emerson, D., Gralnick, J.A., Roden, E.E., Muehe, E.M., 2015. Geomicrobiology of iron. Ehrlich's Geomicrobiol. Sixth Ed. 343–400. https://doi.org/10.1201/b19121

Katsoyiannis, I.A., Zouboulis, A.I., 2006. Use of iron- and manganese-oxidizing bacteria for the combined removal of iron, manganese and arsenic from contaminated groundwater. Water Qual. Res. J. Canada 41, 117–129. https://doi.org/10.2166/wqrj.2006.014

Katsoyiannis, I.A., Zouboulis, A.I., 2004. Biological treatment of Mn(II) and Fe(II) containing

groundwater: Kinetic considerations and product characterization. Water Res. 38, 1922–1932. https://doi.org/10.1016/j.watres.2004.01.014

Kawasaki, S., Arai, H., Kodama, T., Igarashi, Y., 1997. Gene cluster for dissimilatory nitrite reductase (*nir*) from *Pseudomonas aeruginosa*: Sequencing and identification of a locus for heme d_1 biosynthesis. J. Bacteriol. 179, 235–242. https://doi.org/10.1128/jb.179.1.235-242.1997

Kehl-Fie, T.E., Skaar, E.P., 2010. Nutritional immunity beyond iron: a role for manganese and zinc. Curr. Opin. Chem. Biol. 14, 218–224. https://doi.org/10.1016/j.cbpa.2009.11.008

Keim, C.N., Nalini, H.A., de Lena, J.C., 2015. Manganese oxide biominerals from freshwater environments in Quadrilatero Ferrifero, Minas Gerais, Brazil. Geomicrobiol. J. 32, 549–559. https://doi.org/10.1080/01490451.2014.978513

Kepkay, P.E., Nealson, K.H., 1987. Growth of a manganese oxidizing *Pseudomonas* sp. in continuous culture. Arch. Microbiol. 148, 63–67. https://doi.org/10.1007/BF00429649

Khan, F.A., Naushin, F., Rehman, F., Masoodi, A., Irfan, M., Hashmi, F., Ansari, Abid A., 2014. Eutrophication: Global Scenario and Local Threat to Dynamics of Aquatic Ecosystems, in: Ansari, A. A., Gill, S.S. (Eds.), Eutrophication: Causes, Consequences and Control: Volume 2. Springer Science+Business Media, Dordrecht, pp. 17–27. https://doi.org/10.1007/978-94-007-7814-6

Kinnear, S., 2010. Cylindrospermopsin: A decade of progress on bioaccumulation research. Mar. Drugs 8, 542–564. https://doi.org/10.3390/md8030542

Kittler, K., Hurtaud-Pessel, D., Maul, R., Kolrep, F., Fessard, V., 2016. In vitro metabolism of the cyanotoxin cylindrospermopsin in HepaRG cells and liver tissue fractions. Toxicon 110, 47–50. https://doi.org/10.1016/j.toxicon.2015.11.007

Klitzke, S., Apelt, S., Weiler, C., Fastner, J., Chorus, I., 2010. Retention and degradation of the cyanobacterial toxin cylindrospermopsin in sediments - The role of sediment preconditioning and DOM composition. Toxicon 55, 999–1007. https://doi.org/10.1016/j.toxicon.2009.06.036

Klitzke, S., Fastner, J., 2012. Cylindrospermopsin degradation in sediments - The role of temperature, redox conditions, and dissolved organic carbon. Water Res. 46, 1549–1555. https://doi.org/10.1016/j.watres.2011.12.014

Knapp, J.S., Bromley-Challoner, K., 2003. Recalcitrant organic compounds, in: Mara, D., Horan, N. (Eds.), The Handbook of Water and Watewater Microbiology. pp. 559–595. https://doi.org/https://doi.org/10.1016/B978-012470100-7/50035-2

Koch, H.G., Hwang, O., Daldal, F., 1998. Isolation and characterization of *Rhodobacter capsulatus* mutants affected in cytochrome cbb_3 oxidase activity. J. Bacteriol. 180, 969–978. https://doi.org/10.1128/jb.180.4.969-978.1998

Kokociński, M., Cameán, A.M., Carmeli, S., Guzmán-Guillén, R., Jos, Á., Mankiewicz-Boczek,

J., Metcalf, J.S., Moreno, I.M., Prieto, A.I., Sukenik, A., 2017. Cylindrospermopsin and congeners, in: Meriluoto, J., Spoof, L., Codd, G.A. (Eds.), Handbook of Cyanobacterial Monitoring and Cyanotoxin Analysis. John Wiley & Sons, Ltd., pp. 127–137. https://doi.org/10.4081/aiol.2017.7221

Kolde, R., 2015. pheatmap: Pretty heatmaps. R Packag. version 1.0.8.

Kormas, K.A., Lymperopoulou, D.S., 2013. Cyanobacterial toxin degrading bacteria: Who are they? Biomed Res. Int. 2013. https://doi.org/10.1155/2013/463894

Krumbein, W.E., Altmann, H.J., 1973. A new method for the detection and enumeration of manganese oxidizing and reducing microorganisms. Helgoländer Wissenschaftliche Meeresuntersuchungen 25, 347–356. https://doi.org/10.1007/BF01611203

Kubickova, B., Babica, P., Hilscherová, K., Šindlerová, L., 2019a. Effects of cyanobacterial toxins on the human gastrointestinal tract and the mucosal innate immune system. Environ. Sci. Eur. 31. https://doi.org/10.1186/s12302-019-0212-2

Kubickova, B., Laboha, P., Hildebrandt, J.P., Hilscherová, K., Babica, P., 2019b. Effects of cylindrospermopsin on cultured immortalized human airway epithelial cells. Chemosphere 220, 620–628. https://doi.org/10.1016/j.chemosphere.2018.12.157

Kulajta, C., Thumfart, J.O., Haid, S., Daldal, F., Koch, H.G., 2006. Multi-step assembly pathway of the *cbb*$_3$-type cytochrome *c* oxidase complex. J. Mol. Biol. 355, 989–1004. https://doi.org/10.1016/j.jmb.2005.11.039

Kumar, P., Hegde, K., Brar, S.K., Cledon, M., Kermanshahi-pour, A., 2019. Potential of biological approaches for cyanotoxin removal from drinking water: A review. Ecotoxicol. Environ. Saf. 172, 488–503. https://doi.org/10.1016/j.ecoenv.2019.01.066

Kurtz, S., Phillippy, A., Delcher, A.L., Smoot, M., Shumway, M., Antonescu, C., Salzberg, S.L., 2004. Versatile and open software for comparing large genomes. Genome Biol. 5. https://doi.org/10.1186/gb-2004-5-2-r12

Kushkevych, I., Cejnar, J., Treml, J., Dordević, D., Kollar, P., Vítězová, M., 2020. Recent advances in metabolic pathways of sulfate reduction in intestinal bacteria. Cells 9. https://doi.org/10.3390/cells9030698

Lagesen, K., Hallin, P., Rødland, E.A., Stærfeldt, H.H., Rognes, T., Ussery, D.W., 2007. RNAmmer: Consistent and rapid annotation of ribosomal RNA genes. Nucleic Acids Res. 35, 3100–3108. https://doi.org/10.1093/nar/gkm160

Langille, M.G.I., Hsiao, W.W.L., Brinkman, F.S.L., 2008. Evaluation of genomic island predictors using a comparative genomics approach. BMC Bioinformatics 9, 1–10. https://doi.org/10.1186/1471-2105-9-329

Le Moal, M., Gascuel-Odoux, C., Ménesguen, A., Souchon, Y., Étrillard, C., Levain, A., Moatar, F., Pannard, A., Souchu, P., Lefebvre, A., Pinay, G., 2019. Eutrophication: A new wine in an old bottle? Sci. Total Environ. 651, 1–11.

https://doi.org/10.1016/j.scitotenv.2018.09.139

Learman, D.R., Voelker, B.M., Vazquez-Rodriguez, A.I., Hansel, C.M., 2011. Formation of manganese oxides by bacterially generated superoxide. Nat. Geosci. 4, 95–98. https://doi.org/10.1038/ngeo1055

Lee, J., Lee, S., Jiang, X., 2017. Cyanobacterial toxins in freshwater and food: important sources of exposure to humans. Annu. Rev. Food Sci. Technol. 8, 281–304. https://doi.org/10.1146/annurev-food-030216-030116

Lee, S., Xu, H., 2016. XRD and TEM studies on nanophase manganese oxides in freshwater ferromanganese nodules from Green Bay, Lake Michigan. Clays Clay Miner. 64, 523–536. https://doi.org/10.1346/CCMN.2016.064032

Lefort, V., Desper, R., Gascuel, O., 2015. FastME 2.0: A comprehensive, accurate, and fast distance-based phylogeny inference program. Mol. Biol. Evol. 32, 2798–2800. https://doi.org/10.1093/molbev/msv150

León, C., Boix, C., Beltrán, E., Peñuela, G., López, F., Sancho, J. V., Hernández, F., 2019. Study of cyanotoxin degradation and evaluation of their transformation products in surface waters by LC-QTOF MS. Chemosphere 229, 538–548. https://doi.org/10.1016/j.chemosphere.2019.04.219

Letunic, I., Bork, P., 2019. Interactive Tree of Life (iTOL) v4: Recent updates and new developments. Nucleic Acids Res. 47, 256–259. https://doi.org/10.1093/nar/gkz239

Li, X., Song, C., Zhou, Z., Xiao, J., Wang, S., Yang, L., Cao, X., Zhou, Y., 2020. Comparison of community and function of dissimilatory nitrate reduction to ammonium (DNRA) bacteria in Chinese Shallow Lakes with different eutrophication degrees. Water (Switzerland) 12, 1–15. https://doi.org/10.3390/w12010174

Liebel, S., de Oliveira Ribeiro, C.A., de Magalhães, V.F., da Silva, R. de C., Rossi, S.C., Randi, M.A.F., Filipak Neto, F., 2015. Low concentrations of cylindrospermopsin induce increases of reactive oxygen species levels, metabolism and proliferation in human hepatoma cells (HepG2). Toxicol. Vitr. 29, 479–488. https://doi.org/10.1016/j.tiv.2014.12.022

Liebel, S., Regina Grötzner, S., Dietrich Moura Costa, Daniele Antônio Ferreira Randi, M., Alberto de Oliveira Ribeiro, C., Filipak Neto, F., 2016. Cylindrospermopsin effects on protein profile of HepG2 cells. Toxicol. Mech. Methods 26, 554–563. https://doi.org/10.1080/15376516.2016.1216209

Lin, S.Y., Hameed, A., Liu, Y.C., Hsu, Y.H., Lai, W.A., Chen, W.M., Shen, F.T., Young, C.C., 2013. *Pseudomonas sagittaria* sp. nov., a siderophore-producing bacterium isolated from oil-contaminated soil. Int. J. Syst. Evol. Microbiol. 63, 2410–2417. https://doi.org/10.1099/ijs.0.045567-0

Liu, M., Ma, J., Kang, L., Wei, Y., He, Q., Hu, X., Li, H., 2019. Strong turbulence benefits toxic

and colonial cyanobacteria in water: A potential way of climate change impact on the expansion of Harmful Algal Blooms. Sci. Total Environ. 670, 613–622. https://doi.org/10.1016/j.scitotenv.2019.03.253

Liu, R., Ochman, H., 2007. Stepwise formation of the bacterial flagellar system. Proc. Natl. Acad. Sci. U. S. A. 104, 7116–7121. https://doi.org/10.1073/pnas.0700266104

Liu, Z., Wang, Jia, Qian, S., Wang, G., Wang, Jinling, Liao, S., 2017. Carbofuran degradation by biogenic manganese oxides. Bull. Environ. Contam. Toxicol. 98, 420–425. https://doi.org/10.1007/s00128-016-1940-2

López-Alonso, H., Rubiolo, J.A., Vega, F., Vieytes, M.R., Botana, L.M., 2013. Protein synthesis inhibition and oxidative stress induced by cylindrospermopsin elicit apoptosis in primary rat hepatocytes. Chem. Res. Toxicol. 26, 203–212. https://doi.org/10.1021/tx3003438

Loughlin, P., Shelden, M.C., Tierney, M.L., Howitt, S.M., 2002. Structure and function of a model member of the SulP transporter family. Cell Biochem. Biophys. 36, 183–190. https://doi.org/10.1385/CBB:36:2-3:183

Loux, V., Mariadassou, M., Almeida, S., Chiapello, H., Hammani, A., Buratti, J., Gendrault, A., Barbe, V., Aury, J.M., Deutsch, S.M., Parayre, S., Madec, M.N., Chuat, V., Jan, G., Peterlongo, P., Azevedo, V., Le Loir, Y., Falentin, H., 2015. Mutations and genomic islands can explain the strain dependency of sugar utilization in 21 strains of *Propionibacterium freudenreichii*. BMC Genomics 16, 1–19. https://doi.org/10.1186/s12864-015-1467-7

Lozano, G., 2010. Mouse models of p53 functions. Cold Spring Harb. Perspect. Biol. 2, 1–12. https://doi.org/10.1101/cshperspect.a001115

Magasanik, B., 1982. Genetic control of nitrogen assimilation in bacteria. Annu. Rev. Genet. 16, 135–168.

Maghsoudi, E., Fortin, N., Greer, C., Duy, S.V., Fayad, P., Sauvé, S., Prévost, M., Dorner, S., 2015. Biodegradation of multiple microcystins and cylindrospermopsin in clarifier sludge and a drinking water source: Effects of particulate attached bacteria and phycocyanin. Ecotoxicol. Environ. Saf. 120, 409–417. https://doi.org/10.1016/j.ecoenv.2015.06.001

Maisch, M., Lueder, U., Laufer, K., Scholze, C., Kappler, A., Schmidt, C., 2019. Contribution of microaerophilic iron(II)-oxidizers to iron(III) mineral formation. Environ. Sci. Technol. 53, 8197–8204. https://doi.org/10.1021/acs.est.9b01531

Makarova, K.S., Wolf, Y.I., Iranzo, J., Shmakov, S.A., Alkhnbashi, O.S., Brouns, S.J.J., Charpentier, E., Cheng, D., Haft, D.H., Horvath, P., Moineau, S., Mojica, F.J.M., Scott, D., Shah, S.A., Siksnys, V., Terns, M.P., Venclovas, Č., White, M.F., Yakunin, A.F., Yan, W., Zhang, F., Garrett, R.A., Backofen, R., van der Oost, J., Barrangou, R., Koonin, E. V., 2020. Evolutionary classification of CRISPR–Cas systems: a burst of class 2 and derived variants. Nat. Rev. Microbiol. 18, 67–83. https://doi.org/10.1038/s41579-019-0299-x

Malone, T.C., Newton, A., 2020. The globalization of cultural eutrophication in the coastal ocean: causes and consequences. Front. Mar. Sci. 7, 1–30. https://doi.org/10.3389/fmars.2020.00670

Marchesi, J.R., Sato, T., Weightman, A.J., Martin, T.A., Fry, J.C., Hiom, S.J., Wade, W.G., 1998. Design and evaluation of useful bacterium-specific PCR primers that amplify genes coding for bacterial 16S rRNA. Appl. Environ. Microbiol. 64, 795–799.

Marcus, D.N., Pinto, A., Anantharaman, K., Ruberg, S.A., Kramer, E.L., Raskin, L., Dick, G.J., 2017. Diverse manganese(II)-oxidizing bacteria are prevalent in drinking water systems Daniel. Environ. Microbiol. Rep. 9, 120–128. https://doi.org/https://doi.org/10.1111/1758-2229.12508

Marsidi, N., Abu Hasan, H., Sheikh Abdullah, S.R., 2018. A review of biological aerated filters for iron and manganese ions removal in water treatment. J. Water Process Eng. 23, 1–12. https://doi.org/10.1016/j.jwpe.2018.01.010

Martin, A.E., Burgess, B.K., Iismaa, S.E., Smartt, C.T., Jacobson, M.R., Dean, D.R., 1989. Construction and characterization of an *Azotobacter vinelandii* strain with mutations in the genes encoding flavodoxin and ferredoxin I. J. Bacteriol. 171, 3162–3167. https://doi.org/10.1128/jb.171.6.3162-3167.1989

Martínez-García, E., Jatsenko, T., Kivisaar, M., de Lorenzo, V., 2014. Freeing *Pseudomonas putida* KT2440 of its proviral load strengthens endurance to environmental stresses. Environ. Microbiol. 17. https://doi.org/10.1111/1462-2920.12492

Martínez-Ruiz, E.B., Cooper, M., Al-Zeer, M.A., Kurreck, J., Adrian, L., Szewzyk, U., 2020a. Manganese-oxidizing bacteria form multiple cylindrospermopsin transformation products with reduced human liver cell toxicity. Sci. Total Environ. 729, 138924. https://doi.org/10.1016/j.scitotenv.2020.138924

Martínez-Ruiz, E.B., Cooper, M., Fastner, J., Szewzyk, U., 2020b. Manganese-oxidizing bacteria isolated from natural and technical systems remove cylindrospermopsin. Chemosphere 238. https://doi.org/10.1016/j.chemosphere.2019.124625

Martínez-Ruiz, E.B., Cooper, M., Fastner, J., Szewzyk, U., 2020c. Manganese-oxidizing bacteria isolated from natural and technical systems remove cylindrospermopsin. Chemosphere 238. https://doi.org/10.1016/j.chemosphere.2019.124625

May, V., McBarron, E.J., 1973. Occurrence of the blue-green alga, *Anabaena circinalis* Rabenh., in new South Wales and toxicity to mice and honey bees. J. Aust. Inst. Agric. Sci.

McGowan, S., 2016. Algal blooms, in: Shroder, J.F., Sivanpillai, R. (Eds.), Biological and Environmental Hazards, Risks, and Disasters. Elsevier Inc., pp. 5–43. https://doi.org/10.1016/B978-0-12-394847-2.00002-4

Mcnair, K., Zhou, C., Dinsdale, E.A., Souza, B., Edwards, R.A., Hancock, J., 2019.

PHANOTATE: A novel approach to gene identification in phage genomes. Bioinformatics 35, 4537–4542. https://doi.org/10.1093/bioinformatics/btz265

Meerburg, F., Hennebel, T., Vanhaecke, L., Verstraete, W., Boon, N., 2012. Diclofenac and 2-anilinophenylacetate degradation by combined activity of biogenic manganese oxides and silver. Microb. Biotechnol. 5, 388–395. https://doi.org/10.1111/j.1751-7915.2011.00323.x

Meier-Kolthoff, J.P., Auch, A.F., Klenk, H.P., Göker, M., 2013. Genome sequence-based species delimitation with confidence intervals and improved distance functions. BMC Bioinformatics 14. https://doi.org/10.1186/1471-2105-14-60

Meier-Kolthoff, J.P., Göker, M., 2019. TYGS is an automated high-throughput platform for state-of-the-art genome-based taxonomy. Nat. Commun. 10. https://doi.org/10.1038/s41467-019-10210-3

Merel, S., Clément, M., Mourot, A., Fessard, V., Thomas, O., 2010. Characterization of cylindrospermopsin chlorination. Sci. Total Environ. 408, 3433–3442. https://doi.org/10.1016/j.scitotenv.2010.04.033

Merel, S., Walker, D., Chicana, R., Snyder, S., Baurès, E., Thomas, O., 2013. State of knowledge and concerns on cyanobacterial blooms and cyanotoxins. Environ. Int. 59, 303–327. https://doi.org/10.1016/j.envint.2013.06.013

Messineo, V., Bogialli, S., Melchiorre, S., Sechi, N., Lugliè, A., Casiddu, P., Mariani, M.A., Padedda, B.M., Corcia, A. Di, Mazza, R., Carloni, E., Bruno, M., 2009. Cyanobacterial toxins in Italian freshwaters. Limnologica 39, 95–106. https://doi.org/10.1016/j.limno.2008.09.001

Metcalf, J.S., Codd, G.A., 2020. Co-occurrence of cyanobacteria and cyanotoxins with other environmental health hazards: Impacts and implications. Toxin Rev. 12. https://doi.org/doi:10.3390/toxins12100629

Miele, V., Penel, S., Duret, L., 2011. Ultra-fast sequence clustering from similarity networks with SiLiX. BMC Bioinformatics 12. https://doi.org/10.1186/1471-2105-12-116

Miller, M.A., Kudela, R.M., Mekebri, A., Crane, D., Oates, S.C., Tinker, M.T., Staedler, M., Miller, W.A., Toy-Choutka, S., Dominik, C., Hardin, D., Langlois, G., Murray, M., Ward, K., Jessup, D.A., 2010. Evidence for a novel marine harmful algal bloom: Cyanotoxin (microcystin) transfer from land to sea otters. PLoS One 5, 1–11. https://doi.org/10.1371/journal.pone.0012576

Mitchell, A.L., Attwood, T.K., Babbitt, P.C., Blum, M., Bork, P., Bridge, A., Brown, S.D., Chang, H.Y., El-Gebali, S., Fraser, M.I., Gough, J., Haft, D.R., Huang, H., Letunic, I., Lopez, R., Luciani, A., Madeira, F., Marchler-Bauer, A., Mi, H., Natale, D.A., Necci, M., Nuka, G., Orengo, C., Pandurangan, A.P., Paysan-Lafosse, T., Pesseat, S., Potter, S.C., Qureshi, M.A., Rawlings, N.D., Redaschi, N., Richardson, L.J., Rivoire, C., Salazar, G.A.,

Sangrador-Vegas, A., Sigrist, C.J.A., Sillitoe, I., Sutton, G.G., Thanki, N., Thomas, P.D., Tosatto, S.C.E., Yong, S.Y., Finn, R.D., 2019. InterPro in 2019: Improving coverage, classification and access to protein sequence annotations. Nucleic Acids Res. 47, D351–D360. https://doi.org/10.1093/nar/gky1100

Mohamed, Z.A., Alamri, S.A., 2012. Biodegradation of cylindrospermopsin toxin by microcystin-degrading bacteria isolated from cyanobacterial blooms. Toxicon 60, 1390–1395. https://doi.org/10.1016/j.toxicon.2012.10.004

Mohan, S.B., Cole, J.A., 2007. The dissimilatory reduction of nitrate to ammonia by anaerobic bacteria, in: Bothe, H., Ferguson, S.J., Newton, W.E. (Eds.), Biology of the Nitrogen Cycle. Elsevier B.V., pp. 93–106. https://doi.org/10.1016/B978-044452857-5.50008-4

Moraes, A.C.N., Magalhães, V.F., 2018. Renal tubular damage caused by cylindrospermopsin (cyanotoxin) in mice. Toxicol. Lett. 286, 89–95. https://doi.org/10.1016/j.toxlet.2017.12.028

Mouchet, P., 1992. From conventional to biological removal of iron and manganese in France. J. / Am. Water Work. Assoc. 84, 158–167. https://doi.org/10.1002/j.1551-8833.1992.tb07342.x

Mulvenna, V., Dale, K., Priestly, B., Mueller, U., Humpage, A., Shaw, G., Allinson, G., Falconer, I., 2012. Health risk assessment for cyanobacterial toxins in seafood. Int. J. Environ. Res. Public Health 9, 807–820. https://doi.org/10.3390/ijerph9030807

Nagashima, S., Kamimura, A., Shimizu, T., Nakamura-Isaki, S., Aono, E., Sakamoto, K., Ichikawa, N., Nakazawa, H., Sekine, M., Yamazaki, S., Fujita, N., Shimada, K., Hanad, S., Nagashima, K.V.P., 2012. Complete genome sequence of phototrophic betaproteobacterium *Rubrivivax gelatinosus* IL144. J. Bacteriol. 194, 3541–3542. https://doi.org/10.1128/JB.00511-12

Nega, M., 2020. Effects of micropollutants on the Panke River microbial communities and degradation of selected pharmaceuticals by manganese-oxidizing bacteria. Technische Universität Berlin.

Negri, A.P., Jones, G.J., Hindmarsh, M., 1995. Sheep mortality associated with paralytic shellfish poisons from the cyanobacterium *Anabaena circinalis*. Toxicon 33, 1321–1329. https://doi.org/10.1016/0041-0101(95)00068-W

Neumann, C., Bain, P., Shaw, G., 2007. Studies of the comparative *in vitro* toxicology of the cyanobacterial metabolite deoxycylindrospermopsin. J. Toxicol. Environ. Heal. - Part A Curr. Issues 70, 1679–1686. https://doi.org/10.1080/15287390701434869

Neuwirth, E., 2014. RColorBrewer: ColorBrewer palettes. R Packag. version 1.1-2.

Nishimura, Y., Yoshida, T., Kuronishi, M., Uehara, H., Ogata, H., Goto, S., 2017. ViPTree: The viral proteomic tree server. Bioinformatics 33, 2379–2380. https://doi.org/10.1093/bioinformatics/btx157

Nogales, J., García, J.L., Díaz, E., 2017. Degradation of aromatic compounds in *Pseudomonas*: a systems biology view, in: Rojo, F. (Ed.), Aerobic Utilization of Hydrocarbons, Oils and Lipids. Handbook of Hydrocarbon and Lipid Microbiology. Springer International Publishing AG. https://doi.org/10.1007/978-3-319-39782-5_32-1

Norris, R.L., Eaglesham, G.K., Pierens, G., Shaw, G.R., Smith, M.J., Chiswell, R.K., Seawright, A.A., Moore, M.R., 1999. Deoxycylindrospermopsin, an analog of cylindrospermopsin from *Cylindrospermopsis raciborskii*. Environ. Toxicol. 14, 163–165. https://doi.org/10.1002/(SICI)1522-7278(199902)14:1<163::AID-TOX21>3.0.CO;2-V

Norris, R.L.G., Seawright, A.A., Shaw, G.R., Smith, M.J., Chiswell, R.K., Moore, M.R., 2001. Distribution of 14C cylindrospermopsin in vivo in the mouse. Environ. Toxicol. 16, 498–505. https://doi.org/10.1002/tox.10008

Nybom, S.M.K., Salminen, S.J., Meriluoto, J.A.O., 2008. Specific strains of probiotic bacteria are efficient in removal of several different cyanobacterial toxins from solution. Toxicon 52, 214–220. https://doi.org/10.1016/j.toxicon.2008.04.169

O'Neal, S., Zheng, W., 2015. Manganese toxicity upon overexposure: a decade in review. Curr. Environ. Heal. Reports 2, 315–328. https://doi.org/doi:10.1007/s40572-015-0056-x

Oberholster, P.J., Botha, A.-M., Cloete, T.E., 2006. An overview of toxic freshwater cyanobacteria in South Africa with special reference to risk, impact and detection by molecular marker tools. Biokemistri 17, 57–71. https://doi.org/10.4314/biokem.v17i2.32590

Ohtani, I., Moore, R.E., Runnegar, M.T.C., 1992. Cylindrospermopsin: A potent hepatotoxin from the blue-green alga *Cylindrospermopsis raciborskii*. J. Am. Chem. Soc. https://doi.org/https://doi.org/10.1021/ja00046a067

Oliveira, V.R., Carvalho, G.M.C., Avila, M.B., Soares, R.M., Azevedo, S.M.F.O., Ferreira, T.S., Valença, S.S., Faffe, D.S., Zin, W.A., 2012. Time-dependence of lung injury in mice acutely exposed to cylindrospermopsin. Toxicon 60, 764–772. https://doi.org/10.1016/j.toxicon.2012.06.009

Ondov, B.D., Treangen, T.J., Melsted, P., Mallonee, A.B., Bergman, N.H., Koren, S., Phillippy, A.M., 2016. Mash: Fast genome and metagenome distance estimation using MinHash. Genome Biol. 17, 1–14. https://doi.org/10.1186/s13059-016-0997-x

Onstad, G.D., Strauch, S., Meriluoto, J., Codd, G.A., Von Gunten, U., 2007. Selective oxidation of key functional groups in cyanotoxins during drinking water ozonation. Environ. Sci. Technol. 41, 4397–4404. https://doi.org/10.1021/es0625327

Pacini, V.A., Ingallinella, A.M., Sanguinetti, G., 2005. Removal of iron and manganese using biological roughing up flow filtration technology. Water Res. 39, 4463–4475. https://doi.org/10.1016/j.watres.2005.08.027

Paerl, H.W., 2017. Controlling cyanobacterial harmful blooms in freshwater ecosystems.

Microb. Biotechnol. 10, 1106–1110. https://doi.org/10.1111/1751-7915.12725

Pahel, G., Rothstein, D.M., Magasanik, B., 1982. Complex *glnA-glnL-glnG* operon of *Escherichia coli*. J. Bacteriol. 150, 202–213. https://doi.org/10.1128/jb.150.1.202-213.1982

Pal, P., 2017. Industry-Specific water treatment: case studies, in: Pal, P. (Ed.), Industrial Water Treatment Process Technology. Elsevier Inc., pp. 243–511. https://doi.org/http://dx.doi.org/10.1016/B978-0-12-810391-3.00006-0

Palermo, C., Dittrich, M., 2016. Evidence for the biogenic origin of manganese-enriched layers in Lake Superior sediments. Environ. Microbiol. Rep. 8, 179–186. https://doi.org/10.1111/1758-2229.12364

Papadimitriou, T., Katsiapi, M., Vlachopoulos, K., Christopoulos, A., Laspidou, C., Moustaka-Gouni, M., Kormas, K., 2018. Cyanotoxins as the “common suspects” for the Dalmatian pelican (Pelecanus crispus) deaths in a Mediterranean reconstructed reservoir. Environ. Pollut. 234, 779–787. https://doi.org/10.1016/j.envpol.2017.12.022

Parks, D.H., Chuvochina, M., Waite, D.W., Rinke, C., Skarshewski, A., Chaumeil, P.A., Hugenholtz, P., 2018. A standardized bacterial taxonomy based on genome phylogeny substantially revises the tree of life. Nat. Biotechnol. 36, 996. https://doi.org/10.1038/nbt.4229

Parks, D.H., Imelfort, M., Skennerton, C.T., Hugenholtz, P., Tyson, G.W., 2015. CheckM: Assessing the quality of microbial genomes recovered from isolates, single cells, and metagenomes. Genome Res. 25, 1043–1055. https://doi.org/10.1101/gr.186072.114

Parra, F., Britton, P., Castle, C., Jones-Mortimer, M.C., Kornberg, H.L., 1983. Two separate genes involved in sulphate transport in *Escherichia coli* K12. J. Gen. Microbiol. 129, 357–358. https://doi.org/10.1099/00221287-129-2-357

Paulsen, I.T., Press, C.M., Ravel, J., Kobayashi, D.Y., Myers, G.S.A., Mavrodi, D. V., DeBoy, R.T., Seshadri, R., Ren, Q., Madupu, R., Dodson, R.J., Durkin, A.S., Brinkac, L.M., Daugherty, S.C., Sullivan, S.A., Rosovitz, M.J., Gwinn, M.L., Zhou, L., Schneider, D.J., Cartinhour, S.W., Nelson, W.C., Weidman, J., Watkins, K., Tran, K., Khouri, H., Pierson, E.A., Pierson, L.S., Thomashow, L.S., Loper, J.E., 2005. Complete genome sequence of the plant commensal *Pseudomonas fluorescens* Pf-5. Nat. Biotechnol. 23, 873–878. https://doi.org/10.1038/nbt1110

Pearson, L., Mihali, T., Moffitt, M., Kellmann, R., Neilan, B., 2010. On the chemistry, toxicology and genetics of the cyanobacterial toxins, microcystin, nodularin, saxitoxin and cylindrospermopsin, Marine Drugs. https://doi.org/10.3390/md8051650

Peñuelas, J., Sardans, J., Rivas-ubach, A., Janssens, I.A., 2012. The human-induced imbalance between C, N and P in Earth’s life system. Glob. Chang. Biol. 18, 3–6. https://doi.org/10.1111/j.1365-2486.2011.02568.x

Pichardo, S., Cameán, A.M., Jos, A., 2017. *In vitro* toxicological assessment of cylindrospermopsin: A review. Toxins (Basel). 9, 402. https://doi.org/10.3390/toxins9120402

Pizzino, G., Irrera, N., Cucinotta, M., Pallio, G., Mannino, F., Arcoraci, V., Squadrito, F., Altavilla, D., Bitto, A., 2017. Oxidative stress: Harms and benefits for human health. Oxid. Med. Cell. Longev. 2017. https://doi.org/10.1155/2017/8416763

Pluskal, T., Castillo, S., Villar-Briones, A., Orešič, M., 2010. MZmine 2: Modular framework for processing, visualizing, and analyzing mass spectrometry-based molecular profile data. BMC Bioinformatics 11, 395. https://doi.org/10.1186/1471-2105-11-395

Poirier-Larabie, S., Hudon, C., Poirier Richard, H.P., Gagnon, C., 2020. Cyanotoxin release from the benthic, mat-forming cyanobacterium *Microseira* (*Lyngbya*) *wollei* in the St. Lawrence River, Canada. Environ. Sci. Pollut. Res. https://doi.org/10.1007/s11356-020-09290-2

Poniedziałek, B., Rzymski, P., Kokociński, M., 2012. Cylindrospermopsin: Water-linked potential threat to human health in Europe. Environ. Toxicol. Pharmacol. 34, 651–660. https://doi.org/10.1016/j.etap.2012.08.005

Poudel, S., Colman, D.R., Fixen, K.R., Ledbetter, R.N., Zheng, Y., Pence, N., Seefeldt, L.C., Peters, J.W., Harwood, C.S., Boyd, E.S., 2018. Electron transfer to nitrogenase in different genomic and metabolic backgrounds. J. Bacteriol. 200, 1–19. https://doi.org/10.1128/JB.00757-17

Pourcel, C., Touchon, M., Villeriot, N., Vernadet, J.P., Couvin, D., Toffano-Nioche, C., Vergnaud, G., 2020. CRISPRCasdb a successor of CRISPRdb containing CRISPR arrays and *cas* genes from complete genome sequences, and tools to download and query lists of repeats and spacers. Nucleic Acids Res. 48, D535–D544. https://doi.org/10.1093/nar/gkz915

Preisig, O., Zufferey, R., Hennecke, H., 1996. The *Bradyrhizobium japonicum fixGHIS* genes are required for the formation of the high-affinity cbb_3-type cytochrome oxidase. Arch. Microbiol. 165, 297–305. https://doi.org/10.1007/s002030050330

Preußel, K., Wessel, G., Fastner, J., Chorus, I., 2009. Response of cylindrospermopsin production and release in *Aphanizomenon flos-aquae* (Cyanobacteria) to varying light and temperature conditions. Harmful Algae 8, 645–650. https://doi.org/10.1016/j.hal.2008.10.009

Prieto, A.I., Guzmán-Guillén, R., Valderrama-Fernández, R., Jos, Á., Cameán, A.M., 2017. Influence of cooking (microwaving and broiling) on cylindrospermopsin concentration in muscle of nile tilapia (*Oreochromis niloticus*) and characterization of decomposition products. Toxins (Basel). 9, 177. https://doi.org/10.3390/toxins9060177

R Core Team, 2020. R: A language and environment for statistical computing.

https://doi.org/https://www.r-project.org/

R Core Team, 2016. RStudio: Integrated development for R. v1.0.153.

Ramana, C. V., Sasikala, C., Arunasri, K., Anil Kumar, P., Srinivas, T.N.R., Shivaji, S., Gupta, P., Süling, J., Imhoff, J.F., 2006. *Rubrivivax benzoatilyticus* sp. nov., an aromatic hydrocarbon-degradiing purple betaproteobacterium. Int. J. Syst. Evol. Microbiol. 56, 2157–2164. https://doi.org/10.1099/ijs.0.64209-0

Ramos, F., Blanco, G., Gutiérrez, J.C., Luque, F., Tortolero, M., 1993. Identification of an operon involved in the assimilatory nitrate-reducing system of *Azotobacter vinelandii*. Mol. Microbiol. 8, 1145–1153. https://doi.org/10.1111/j.1365-2958.1993.tb01659.x

Reuters Staff, 2020. What are the micro-organisms causing elephant deaths in Botswana? [WWW Document]. Sept. 21. URL https://www.reuters.com/article/us-botswana-elephants-facts-factbox-idUSKCN26C2BC (accessed 11.27.20).

Reva, O.N., Bezuidt, O., 2012. Distribution of horizontally transferred heavy metal resistance operons in recent outbreak bacteria. Mob. Genet. Elements 2, 96–100. https://doi.org/10.4161/mge.19963

Richardson, J., Feuchtmayr, H., Miller, C., Hunter, P.D., Maberly, S.C., Carvalho, L., 2019. Response of cyanobacteria and phytoplankton abundance to warming, extreme rainfall events and nutrient enrichment. Glob. Chang. Biol. 1–16. https://doi.org/10.1111/gcb.14701

Richardson, L.L., Aguilar, C., Nealson, K.H., 1988. Manganese oxidation in pH and O_2 microenvironments produced by phytoplankton. Limnol. Oceanogr. 33, 352–363. https://doi.org/10.4319/lo.1988.33.3.0352

Richardson, L.L., Nealson, K.H., 1989. Distributions of manganese, iron, and manganese-oxidizing bacteria in Lake Superior sediments of different organic carbon content. J. Great Lakes Res. 15, 123–132. https://doi.org/10.1016/S0380-1330(89)71466-0

Richter, M., Rosselló-Móra, R., 2009. Shifting the genomic gold standard for the prokaryotic species definition. Proc. Natl. Acad. Sci. U. S. A. 106, 19126–19131. https://doi.org/10.1073/pnas.0906412106

Richter, M., Rosselló-Móra, R., Oliver Glöckner, F., Peplies, J., 2016. JSpeciesWS: A web server for prokaryotic species circumscription based on pairwise genome comparison. Bioinformatics 32, 929–931. https://doi.org/10.1093/bioinformatics/btv681

Ridge, J.P., Lin, M., Larsen, E.I., Fegan, M., Mcewan, A.G., Sly, L.I., 2007. A multicopper oxidase is essential for manganese oxidation and laccase-like activity in *Pedomicrobium* sp. ACM 3067. Environ. Microbiol. 9, 944–953. https://doi.org/10.1111/j.1462-2920.2006.01216.x

Ronquist, F., Huelsenbeck, J.P., 2003. MrBayes 3: Bayesian phylogenetic inference under mixed models. Bioinformatics 19, 1572–1574.

https://doi.org/10.1093/bioinformatics/btg180

Roy-Lachapelle, A., Solliec, M., Bouchard, M.F., Sauvé, S., 2017. Detection of cyanotoxins in algae dietary supplements. Toxins (Basel). 9, 1–17. https://doi.org/10.3390/toxins9030076

Rücker, J., Stüken, A., Nixdorf, B., Fastner, J., Chorus, I., Wiedner, C., 2007. Concentrations of particulate and dissolved cylindrospermopsin in 21 *Aphanizomenon*-dominated temperate lakes. Toxicon 50, 800–809. https://doi.org/10.1016/j.toxicon.2007.06.019

Rückert, C., Koch, D.J., Rey, D.A., Albersmeier, A., Mormann, S., Pühler, A., Kalinowski, J., 2005. Functional genomics and expression analysis of the *Corynebacterium glutamicum fpr2-cysIXHDNYZ* gene cluster involved in assimilatory sulphate reduction. BMC Genomics 6, 1–18. https://doi.org/10.1186/1471-2164-6-121

Runnegar, M.T., Xie, C., Snider, B.B., Wallace, G.A., Weinreb, S.M., Kuhlenkamp, J., 2002. In vitro hepatotoxicity of the cyanobacterial alkaloid cyclindrospermopsin and related synthetic analogues. Toxicol. Sci. 67, 81–87. https://doi.org/10.1093/toxsci/67.1.81

Rzymski, P., Poniedziałek, B., 2014. In search of environmental role of cylindrospermopsin: A review on global distribution and ecology of its producers. Water Res. 66, 320–337. https://doi.org/10.1016/j.watres.2014.08.029

Sabirova, J.S., Cloetens, L.F.F., Vanhaecke, L., Forrez, I., Verstraete, W., Boon, N., 2008. Manganese-oxidizing bacteria mediate the degradation of 17α-ethinylestradiol. Microb. Biotechnol. 1, 507–512. https://doi.org/10.1111/j.1751-7915.2008.00051.x

Sadler, R., 2015. Towards a more complete understanding of the occurrence and toxicities of the cylindrospermopsins. AIMS Environ. Sci. 2, 827–851. https://doi.org/10.3934/environsci.2015.3.827

Saker, M.L., Eaglesham, G.K., 1999. The accumulation of cylindrospermopsin from the cyanobacterium *Cylindrospermopsis raciborskii* in tissues of the Redclaw crayfish *Cherax quadricarinatus*. Toxicon 37, 1065–1077. https://doi.org/10.1016/S0041-0101(98)00240-2

Sakurai, T., Kataoka, K., 2007. Basic and applied features of multicopper oxidases, CueO, bilirubin oxidase, and laccase. Chem. Rec. 7, 220–229. https://doi.org/10.1002/tcr.20125

Sant'Anna, F.H., Trentini, D.B., De Souto Weber, S., Cecagno, R., Da Silva, S.C., Schrank, I.S., 2009. The PII superfamily revised: A novel group and evolutionary insights. J. Mol. Evol. 68, 322–336. https://doi.org/10.1007/s00239-009-9209-6

Santelli, C.M., Chaput, D.L., Hansel, C.M., 2014. Microbial communities promoting Mn(II) oxidation in Ashumet Pond, a historically polluted freshwater pond undergoing remediation. Geomicrobiol. J. 31, 605–616. https://doi.org/10.1080/01490451.2013.875605

Santoro, A.L., Bastviken, D., Gudasz, C., Tranvik, L., Enrich-Prast, A., 2013. Dark carbon

fixation: An important process in lake sediments. PLoS One 8, 1–7. https://doi.org/10.1371/journal.pone.0065813

Scheer, M., 2010. Charakterisierung der Diversität von Mikroorganismen im Nationalpark “Unteres Odertal.” Technische Universität Dresden.

Schmidt, B., 2018. Neutrophile Eisenbakterien - Untersuchungen von natürlichen Gemeinschaften in Feuerland und Reinkulturen. Technische Universität Berlin.

Schmidt, B., Sánchez, L.A., Fretschner, T., Kreps, G., Ferrero, M.A., Siñeriz, F., Szewzyk, U., 2014. Isolation of *Sphaerotilus-Leptothrix* strains from iron bacteria communities in Tierra del Fuego wetlands. FEMS Microbiol. Ecol. 90, 454–466. https://doi.org/10.1111/1574-6941.12406

Schreier, H.J., Sonenshein, A.L., 1986. Altered regulation of the *glnA* gene in glutamine synthetase mutants of *Bacillus subtilis*. J. Bacteriol. 167, 35–43. https://doi.org/10.1128/jb.167.1.35-43.1986

Schulz, R., 2001. Comparison of spray drift- and runoff-related input of azinphos-methyl and endosulfan from fruit orchards into the Lourens River, South Africa. Chemosphere 45, 543–551. https://doi.org/10.1016/S0045-6535(00)00601-9

Seawright, A.A., Nolan, C.C., Shaw, G.R., Chiswell, R.K., Norris, R.L., Moore, M.R., Smith, M.J., 1999. The oral toxicity for mice of the tropical cyanobacterium *Cylindrospermopsis raciborskii* (Woloszynska). Environ. Toxicol. 14, 135–142. https://doi.org/10.1002/(SICI)1522-7278(199902)14:1<135::AID-TOX17>3.0.CO;2-L

Seguritan, V., Alves, N., Arnoult, M., Raymond, A., Lorimer, D., Burgin, A.B., Salamon, P., Segall, A.M., 2012. Artificial neural networks trained to detect viral and phage structural proteins. PLoS Comput. Biol. 8, e1002657. https://doi.org/10.1371/journal.pcbi.1002657

Senogles-Derham, P.J., Seawright, A., Shaw, G., Wickramisingh, W., Shahin, M., 2003. Toxicological aspects of treatment to remove cyanobacterial toxins from drinking water determined using the heterozygous P53 transgenic mouse model. Toxicon 41, 979–988. https://doi.org/10.1016/S0041-0101(03)00070-9

Sharma, N.K., Rai, A.K., Stal, L.J., 2014. Cyanobacteria: an economic perspective, First edit. ed. John Wiley & Sons, Ltd.

Shaw, G.R., Seawright, A.A., Moore, M.R., Lam, P.K.S., 2000. Cylindrospermopsin, a cyanobacterial alkaloid: Evaluation of its toxicologic activity. Ther. Drug Monit. https://doi.org/10.1097/00007691-200002000-00019

Shaw, G.R., Sukenik, A., Livne, A., Chiswell, R.K., Smith, M.J., Seawright, A.A., Norris, R.L., Eaglesham, G.K., Moore, M.R., 1999. Blooms of the cylindrospermopsin containing cyanobacterium, *Aphanizomenon ovalisporum* (Forti), in newly constructed lakes, Queensland, Australia. Environ. Toxicol. 14, 167–177. https://doi.org/doi.org/10.1002/(SICI)1522-7278(199902)14:1<167::AID-

TOX22>3.0.CO;2-O

Sheu, S.Y., Li, Z.H., Young, C.C., Chen, W.M., 2020. *Rubrivivax albus* sp. nov., isolated from a freshwater pond. Int. J. Syst. Evol. Microbiol. 70, 805–813. https://doi.org/10.1099/ijsem.0.003829

Sies, H., 1997. Oxidative stress: oxidants and antioxidants. Exp. Physiol. 82, 291–295. https://doi.org/10.1113/expphysiol.1997.sp004024

Sirko, A., Zatyka, M., Sadowy, E., Hulanicka, D., 1995. Sulfate and thiosulfate transport in *Escherichia coli* K-12: Evidence for a functional overlapping of sulfate- and thiosulfate-binding proteins. J. Bacteriol. 177, 4134–4136. https://doi.org/10.1128/jb.177.14.4134-4136.1995

Smith, M.J., Shaw, G.R., Eaglesham, G.K., Ho, L., Brookes, J.D., 2008. Elucidating the factors influencing the biodegradation of cylindrospermopsin in drinking water sources. Environ. Toxicol. 23, 413–421. https://doi.org/10.1002/tox.20356

Smith, V.H., Tilman, G.D., Nekola, J.C., 1999. Eutrophication: impacts of excess nutrient inputs on freshwater, marine, and terrestrial ecosystems. Environ. Pollut. 179–196. https://doi.org/https://doi.org/10.1016/S0269-7491(99)00091-3

Sochacki, A., Felis, E., Bajkacz, S., Kalka, J., Michalska, J.K., 2018. Removal and transformation of benzotriazole in manganese-oxide biofilters with Mn(II) feeding. Chemosphere 212, 143–151. https://doi.org/10.1016/j.chemosphere.2018.08.092

Soldatova, A. V., Tao, L., Romano, C.A., Stich, T.A., Casey, W.H., Britt, R.D., Tebo, B.M., Spiro, T.G., 2017. Mn(II) oxidation by the multicopper oxidase complex Mnx: A binuclear activation mechanism. J. Am. Chem. Soc. 139, 11369–11380. https://doi.org/10.1021/jacs.7b02771

Solovyev, V., Salamov, A., 2011. Automatic annotation of microbial genomes and metagenomic sequences, in: Li, R.W. (Ed.), Metagenomics and Its Applications in Agriculture, Biomedicine and Environmental Studies. Nova Science Publishers, pp. 61–78.

Sommers, M.G., Dollhopf, M.E., Douglas, S., 2002. Freshwater ferromanganese stromatolites from lake vermilion, Minnesota: Microbial culturing and environmental scanning electron microscopy investigations. Geomicrobiol. J. 19, 407–427. https://doi.org/10.1080/01490450290098513

Song, W., Yan, S., Cooper, W.J., Dionysiou, D.D., Oshea, K.E., 2012. Hydroxyl radical oxidation of cylindrospermopsin (cyanobacterial toxin) and its role in the photochemical transformation. Environ. Sci. Technol. 46, 12608–12615. https://doi.org/10.1021/es302458h

Spiro, T.G., Bargar, J.R., Sposito, G., Tebo, B.M., 2008. Bacteriogenic manganese oxides. Acc. Chem. Res. 43, 2–9.

Stein, L.Y., La Duc, M.T., Grund, T.J., Nealson, K.H., 2001. Bacterial and archaeal populations associated with freshwater ferromanganous micronodules and sediments. Environ. Microbiol. 3, 10–18. https://doi.org/10.1046/j.1462-2920.2001.00154.x

Sternbeck, J., 1995. Manganese cycling in a eutrophic lake — Rates and pathways. Aquat. Geochemistry 1, 399–426. https://doi.org/10.1007/BF00702741

Stincone, A., Prigione, A., Cramer, T., Wmelink, M.M., Campbell, K., Cheung, E., Olin-Sandoval, V., Grüning, N.-M., Krüger, A., Alam, M.T., Keller, M.A., Breitenbach, M., Brindle, K.M., Rabinowitz, J.D., Ralser, M., 2015. The return of metabolism: biochemistry and physiology of the pentose phosphate pathway. Biol. Rev. Camb. Philos. Soc. 90, 927–963. https://doi.org/10.1111/brv.12140.

Strakhovenko, V.D., Shkol'nik, S.I., Danilenko, I. V., 2018. Ferromanganese nodules of freshwater reservoirs of Ol'khon Island (Baikal) and the Kulunda Plain (West Siberia). Russ. Geol. Geophys. 59, 123–134. https://doi.org/10.1016/j.rgg.2018.01.010

Štraser, A., Filipič, M., Žegura, B., 2013. Cylindrospermopsin induced transcriptional responses in human hepatoma HepG2 cells. Toxicol. Vitr. 27, 1809–1819. https://doi.org/10.1016/j.tiv.2013.05.012

Štraser, A., Filipič, M., Žegura, B., 2011. Genotoxic effects of the cyanobacterial hepatotoxin cylindrospermopsin in the HepG2 cell line. Arch. Toxicol. 85, 1617–1626. https://doi.org/10.1007/s00204-011-0716-z

Sukumaran, J., Holder, M.T., 2010. DendroPy: A Python library for phylogenetic computing. Bioinformatics 26, 1569–1571. https://doi.org/10.1093/bioinformatics/btq228

Sunda, W.G., Kieber, D.J., 1994. Oxidation of humic substances by manganese oxides yields low-molecular-weight organic substrates. Nature 367, 62–64. https://doi.org/10.1038/367062a0

Svirčev, Z., Drobac, D., Tokodi, N., Mijović, B., Codd, G.A., Meriluoto, J., 2017. Toxicology of microcystins with reference to cases of human intoxications and epidemiological investigations of exposures to cyanobacteria and cyanotoxins. Arch. Toxicol. 91, 621–650. https://doi.org/10.1007/s00204-016-1921-6

Svirčev, Z., Lalić, D., Bojadžija Savić, G., Tokodi, N., Drobac Backović, D., Chen, L., Meriluoto, J., Codd, G.A., 2019. Global geographical and historical overview of cyanotoxin distribution and cyanobacterial poisonings. Arch. Toxicol. 93, 2429–2481. https://doi.org/10.1007/s00204-019-02524-4

Szewzyk, U., Szewzyk, R., Schmidt, B., Braun, B., 2011. Neutrophilic iron-depositing microorganisms, in: Flemming, H.-C., Wingender, J., Szewzyk, U. (Eds.), Biofilm Highlights. Springer Berlin Heidelberg, pp. 63–79. https://doi.org/10.1007/978-3-642-19940-0

Tang, W., Liu, Y., Gong, J., Chen, S., Zeng, X., 2019. Analysis of manganese oxidase and its

encoding gene in *Lysinibacillus* strain MK-1. Process Saf. Environ. Prot. 127, 299–305. https://doi.org/10.1016/j.psep.2019.04.002

Tatusov, R.L., 2000. The COG database: a tool for genome-scale analysis of protein functions and evolution. Nucleic Acids Res. 28, 33–36. https://doi.org/10.1093/nar/28.1.33

Tebo, B.M., Bargar, J.R., Clement, B.G., Dick, G.J., Murray, K.J., Parker, D., Verity, R., Webb, S.M., 2004. Biogenic manganese oxides: Properties and mechanisms of formation. Annu. Rev. Earth Planet. Sci. 32, 287–328. https://doi.org/10.1146/annurev.earth.32.101802.120213

Tebo, B.M., Johnson, H.A., McCarthy, J.K., Templeton, A.S., 2005. Geomicrobiology of manganese(II) oxidation. Trends Microbiol. 13, 421–428. https://doi.org/10.1016/j.tim.2005.07.009

Teeling, H., Meyerdierks, A., Bauer, M., Amann, R., Glöckner, F.O., 2004. Application of tetranucleotide frequencies for the assignment of genomic fragments. Environ. Microbiol. 6, 938–947. https://doi.org/10.1111/j.1462-2920.2004.00624.x

Tennant, R.W., Spalding, J., French, J.E., 1996. Evaluation of transgenic mouse bioassays for identifying carcinogens and noncarcinogens. Mutat. Res. - Rev. Genet. Toxicol. 365, 119–127. https://doi.org/10.1016/S0165-1110(96)90016-0

Terao, K., Ohmori, S., Igarashi, K., Ohtani, I., Watanabe, M.F., Harada, K.I., Ito, E., Watanabe, M., 1994. Electron microscopic studies on experimental poisoning in mice induced by cylindrospermopsin isolated from blue-green alga *Umezakia natans*. Toxicon 32, 833–843. https://doi.org/10.1016/0041-0101(94)90008-6

Timofeeva, Y.O., 2008. Accumulation and fractionation of trace elements in soil ferromanganese nodules of different size. Geochemistry Int. 46, 260–267. https://doi.org/10.1134/s0016702908030038

Tobiason, J.E., Bazilio, A., Goodwill, J., Mai, X., Nguyen, C., 2016. Manganese removal from drinking water sources. Curr. Pollut. Reports 2, 168–177. https://doi.org/10.1007/s40726-016-0036-2

Tran, T.N., Kim, D.G., Ko, S.O., 2018. Synergistic effects of biogenic manganese oxide and Mn(II)-oxidizing bacterium *Pseudomonas putida* strain MnB1 on the degradation of 17 α-ethinylestradiol. J. Hazard. Mater. 344, 350–359. https://doi.org/10.1016/j.jhazmat.2017.10.045

Tu, J., Yang, Z., Hu, C., Qu, J., 2014. Characterization and reactivity of biogenic manganese oxides for ciprofloxacin oxidation. J. Environ. Sci. (China) 26, 1154–1161. https://doi.org/10.1016/S1001-0742(13)60505-7

U.S. EPA, n.d. Secondary drinking water standards: Guidance for nuisance chemicals [WWW Document]. URL www.epa.gov/sdwa/secondary-drinking-water-standards-guidance-nuisance-chemicals (accessed 11.27.20).

Vallenet, D., Belda, E., Calteau, A., Cruveiller, S., Engelen, S., Lajus, A., Le Fèvre, F., Longin, C., Mornico, D., Roche, D., Rouy, Z., Salvignol, G., Scarpelli, C., Smith, A.A.T., Weiman, M., Médigue, C., 2013. MicroScope - An integrated microbial resource for the curation and comparative analysis of genomic and metabolic data. Nucleic Acids Res. 41. https://doi.org/10.1093/nar/gks1194

Vallenet, D., Calteau, A., Cruveiller, S., Gachet, M., Lajus, A., Josso, A., Mercier, J., Renaux, A., Rollin, J., Rouy, Z., Roche, D., Scarpelli, C., Medigue, C., 2017. MicroScope in 2017: An expanding and evolving integrated resource for community expertise of microbial genomes. Nucleic Acids Res. 45, D517–D528. https://doi.org/10.1093/nar/gkw1101

Vallenet, D., Calteau, A., Dubois, M., Amours, P., Bazin, A., Beuvin, M., Burlot, L., Bussell, X., Fouteau, S., Gautreau, G., Lajus, A., Langlois, J., Planel, R., Roche, D., Rollin, J., Rouy, Z., Sabatet, V., Médigue, C., 2020. MicroScope: an integrated platform for the annotation and exploration of microbial gene functions through genomic, pangenomic and metabolic comparative analysis. Nucleic Acids Res. 48, D579–D589. https://doi.org/10.1093/nar/gkz926

Van De Kamp, M., Pizzinini, E., Vos, A., Van Der Lende, T.R., Schuurs, T.A., Newbert, R.W., Turner, G., Konings, W.N., Driessen, A.J.M., 1999. Sulfate transport in *Penicillium chrysogenum*: Cloning and characterization of the *sutA* and *sutB* genes. J. Bacteriol. 181, 7228–7234. https://doi.org/10.1128/jb.181.23.7228-7234.1999

Vesper, D.J., 2012. Contamination of cave waters by heavy metals, in: White, W.B., Culver, D.C. (Eds.), Encyclopedia of Caves. Elsevier Inc., pp. 161–166. https://doi.org/10.1016/b978-0-12-383832-2.00024-4

Waack, S., Keller, O., Asper, R., Brodag, T., Damm, C., Fricke, W.F., Surovcik, K., Meinicke, P., Merkl, R., 2006. Score-based prediction of genomic islands in prokaryotic genomes using hidden Markov models. BMC Bioinformatics 7, 1–12. https://doi.org/10.1186/1471-2105-7-142

Walls, J.T., Wyatt, K.H., Doll, J.C., Rubenstein, E.M., Rober, A.R., 2018. Hot and toxic: Temperature regulates microcystin release from cyanobacteria. Sci. Total Environ. 610–611, 786–795. https://doi.org/10.1016/j.scitotenv.2017.08.149

Wang, G., Liu, Y., Wu, M., Zong, W., Yi, X., Zhan, J., Liu, L., Zhou, H., 2019. Coupling the phenolic oxidation capacities of a bacterial consortium and in situ-generated manganese oxides in a moving bed biofilm reactor (MBBR). Water Res. 166, 115047. https://doi.org/10.1016/j.watres.2019.115047

Wang, H., Lv, Z., Song, Y., Wang, Y. nan, Zhang, D., Sun, Y., Tsang, Y.F., Pan, X., 2019. Adsorptive removal of Sb(III) from wastewater by environmentally-friendly biogenic manganese oxide (BMO) materials: Efficiency and mechanisms. Process Saf. Environ. Prot. 124, 223–230. https://doi.org/10.1016/j.psep.2019.02.022

Wang, L., Wang, Q., Xiao, G., Chen, G., Han, L., Hu, T., 2020. Adverse effect of cylindrospermopsin on embryonic development in zebrafish (Danio rerio). Chemosphere 241, 125060. https://doi.org/10.1016/j.chemosphere.2019.125060

Wang, R., Wang, S., Tai, Y., Tao, R., Dai, Y., Guo, J., Yang, Y., Duan, S., 2017. Biogenic manganese oxides generated by green algae *Desmodesmus* sp. WR1 to improve bisphenol A removal. J. Hazard. Mater. 339, 310–319. https://doi.org/10.1016/j.jhazmat.2017.06.026

Wang, S., Pi, Y., Song, Y., Jiang, Y., Zhou, L., Liu, W., Zhu, G., 2020. Hotspot of dissimilatory nitrate reduction to ammonium (DNRA) process in freshwater sediments of riparian zones. Water Res. 173, 115539. https://doi.org/10.1016/j.watres.2020.115539

Wang, X., Yu, M., Wang, L., Lin, H., Li, B., Xue, C.X., Sun, H., Zhang, X.H., 2020. Comparative genomic and metabolic analysis of manganese-oxidizing mechanisms in *Celeribacter manganoxidans* DY25T: Its adaptation to the environment of polymetallic nodules. Genomics 112, 2080–2091. https://doi.org/10.1016/j.ygeno.2019.12.002

Watanabe, J., Tani, Y., Chang, J., Miyata, N., Naitou, H., Seyama, H., 2013. As(III) oxidation kinetics of biogenic manganese oxides formed by *Acremonium strictum* strain KR21-2. Chem. Geol. 347, 227–232. https://doi.org/10.1016/j.chemgeo.2013.03.012

Watson, S.B., Whitton, B.A., Higgins, S.N., Paerl, H.W., Brooks, B.W., Wehr, J.D., 2015. Harmful algal blooms, in: Wehr, J.D., Sheath, R.G., Kociolek, J.P. (Eds.), Freshwater Algae of North America. Ecology and Classification. Elsevier Inc., pp. 873–920. https://doi.org/10.1016/B978-0-12-385876-4.00020-7

Whitton, B.A., 2012. Ecology of cyanobacteria II: their diversity in space and time. Springer Science+Business Media. https://doi.org/10.1007/978-94-007-3855-3

Whitton, B.A., Pentecost, A., 2012. Subaerial cyanobacteria, in: Whitton, B.A. (Ed.), Ecology of Cyanobacteria II: Their Diversity in Space and Time. Springer Science+Business Media, pp. 291–316. https://doi.org/10.1007/978-94-007-3855-3

Wickham, H., 2016. ggplot2: Elegant graphics for data analysis. Springer-Verlag New York.

Wickham, H., Francois, R., Henry, L., Müller, K., 2019. dplyr: A Grammar of data manipulation. R package version 0.8.0.1. https://doi.org/https://CRAN.R-project.org/package=dplyr

Wiedner, C., Rücker, J., Fastner, J., Chorus, I., Nixdorf, B., 2008. Seasonal dynamics of cylindrospermopsin and cyanobacteria in two German lakes. Toxicon 52, 677–686. https://doi.org/10.1016/j.toxicon.2008.07.017

Wilkins, D., 2019. gggenes: Draw gene arrow maps in “ggplot2.” R Packag. version 0.4.0.

Williams, C.D., Burns, J., Chapman, A., Pawlowicz, M., Carmichael, W., 2006. Assessment of cyanotoxins in Florida’s surface waters and associated drinking water resources.

Wimmer, K.M., Strangman, W.K., Wright, J.L.C., 2014. 7-Deoxy-desulfo-cylindrospermopsin and 7-deoxy-desulfo-12-acetylcylindrospermopsin: Two new cylindrospermopsin analogs

isolated from a Thai strain of *Cylindrospermopsis raciborskii*. Harmful Algae 37, 203–206. https://doi.org/10.1016/j.hal.2014.06.006

Winston, G.W., Di Giulio, R.T., 1991. Prooxidant and antioxidant mechanisms in aquatic organisms. Aquat. Toxicol. 19, 137–161. https://doi.org/10.1016/0166-445X(91)90033-6

Withers, P.J.A., Neal, C., Jarvie, H.P., Doody, D.G., 2014. Agriculture and eutrophication: Where do we go from here? Sustainability 6, 5853–5875. https://doi.org/10.3390/su6095853

Wood, R., 2016. Acute animal and human poisonings from cyanotoxin exposure - A review of the literature. Environ. Int. 91, 276–282. https://doi.org/10.1016/j.envint.2016.02.026

World Health Organization, W., 2011. Manganese in drinking-water.

Wormer, L., Cirés, S., Carrasco, D., Quesada, A., 2008. Cylindrospermopsin is not degraded by co-occurring natural bacterial communities during a 40-day study. Harmful Algae 7, 206–213. https://doi.org/10.1016/j.hal.2007.07.004

Wörmer, L., Huerta-Fontela, M., Cirés, S., Carrasco, D., Quesada, A., 2010. Natural photodegradation of the cyanobacterial toxins microcystin and cylindrospermopsin. Environ. Sci. Technol. 44, 3002–3007.

Wu, Y., Shukal, S., Mukherjee, M., Cao, B., 2015. Involvement in denitrification is beneficial to the biofilm lifestyle of *Comamonas testosteroni*: A mechanistic study and its environmental implications. Environ. Sci. Technol. 49, 11551–11559. https://doi.org/10.1021/acs.est.5b03381

Wurtsbaugh, W.A., Paerl, H.W., Dodds, W.K., 2019. Nutrients, eutrophication and harmful algal blooms along the freshwater to marine continuum. Wiley Interdiscip. Rev. Water 6, 1–27. https://doi.org/10.1002/wat2.1373

Yakunin, A.F., Gennaro, G., Hallenbeck, P.C., 1993. Purification and properties of a *nif*-specific flavodoxin from the photosynthetic bacterium *Rhodobacter capsulatus*. J. Bacteriol. 175, 6775–6780. https://doi.org/10.1128/jb.175.21.6775-6780.1993

Yan, S., Jia, A., Merel, S., Snyder, S.A., O'Shea, K.E., Dionysiou, D.D., Song, W., 2016. Ozonation of cylindrospermopsin (cyanotoxin): Degradation mechanisms and cytotoxicity assessments. Environ. Sci. Technol. 50, 1437–1446. https://doi.org/10.1021/acs.est.5b04540

Yang, G., Han, L., Wen, J., Zhou, S., 2013. *Pseudomonas guangdongensis* sp. nov., isolated from an electroactive biofilm, and emended description of the genus *Pseudomonas* Migula 1894. Int. J. Syst. Evol. Microbiol. 63, 4599–4605. https://doi.org/10.1099/ijs.0.054676-0

Yang, W., Zhang, Zhen, Zhang, Zhongming, Chen, H., Liu, J., Ali, M., Liu, F., Li, L., 2013. Population structure of manganese-oxidizing bacteria in stratified soils and properties of manganese oxide aggregates under manganese-complex medium enrichment. PLoS

One 8, e73778. https://doi.org/10.1371/journal.pone.0073778

Yang, X.E., Wu, X., Hao, H.L., He, Z.L., 2008. Mechanisms and assessment of water eutrophication. J. Zhejiang Univ. Sci. B 9, 197–209. https://doi.org/10.1631/jzus.B0710626

Yaroshevsky, A.A., 2006. Abundances of chemical elements in the Earth's crust. Geochemistry Int. 44, 48–55. https://doi.org/10.1134/S001670290601006X

Yokoyama, Y., Sasaki, Y., Terasaki, N., Kawataki, T., Takekawa, K., Iwase, Y., Shimizu, T., Sanoh, S., Ohta, S., 2018. Comparison of drug metabolism and its related hepatotoxic effects in HepaRG, cryopreserved human hepatocytes, and HepG2 cell cultures. Biol. Pharm. Bull. 41, 722–732. https://doi.org/10.1248/bpb.b17-00913

Yu, H., Leadbetter, J.R., 2020. Bacterial chemolithoautotrophy via manganese oxidation. Nature 583, 453–458. https://doi.org/10.1038/s41586-020-2468-5

Yu, Z., Chang, M., Wu, M., Yang, G., Zhou, S., Zhuang, L., 2013. *Pseudomonas oryzae* sp. nov. isolated from a paddy soil in South China. Arch. Microbiol. 195, 815–822. https://doi.org/10.1007/s00203-013-0930-6

Yukioka, Y., Tanahashi, T., Shida, K., Oguchi, H., Ogawa, S., Saito, C., Yajima, S., Ito, S., Ohsawa, K., Shoun, H., Sasaki, Y., 2017. A role of nitrite reductase (NirBD) for NO homeostatic regulation in *Streptomyces coelicolor* A3(2). FEMS Microbiol. Lett. 364, 1–6. https://doi.org/10.1093/femsle/fnw241

Yurgel, S.N., Rice, J., Mulder, M., Kahn, M.L., 2010. GlnB/GlnK PII proteins and regulation of the *Sinorhizobium meliloti* Rm1021 nitrogen stress response and symbiotic function. J. Bacteriol. 192, 2473–2481. https://doi.org/10.1128/JB.01657-09

Zakharova, Y.R., Parfenova, V. V., Granina, L.Z., Kravchenko, O.S., Zemskaya, T.I., 2012. Distribution of iron- and manganese-oxidizing bacteria in the bottom sediments of Lake Baikal. Inl. Water Biol. 3, 313–321. https://doi.org/10.1134/s1995082910040036

Zámocký, M., Hofbauer, S., Schaffner, I., Gasselhuber, B., Nicolussi, A., Soudi, M., Pirker, K.F., Furtmüller, P.G., Obinger, C., 2015. Independent evolution of four heme peroxidase superfamilies. Arch. Biochem. Biophys. 574, 108–119. https://doi.org/10.1016/j.abb.2014.12.025

Zanchett, G., Oliveira-Filho, E.C., 2013. Cyanobacteria and cyanotoxins: From impacts on aquatic ecosystems and human health to anticarcinogenic effects. Toxins (Basel). 5, 1896–1917. https://doi.org/10.3390/toxins5101896

Zerfaß, C., Christie-Oleza, J.A., Soyer, O.S., 2019. Manganese oxide biomineralization provides protection against nitrite toxicity in a cell-density-dependent manner. Appl. Environ. Microbiol. 85, 5–8. https://doi.org/10.1128/AEM.02129-18

Zhang, G., Wurtzler, E.M., He, X., Nadagouda, M.N., O'Shea, K., El-Sheikh, S.M., Ismail, A.A., Wendell, D., Dionysiou, D.D., 2015. Identification of TiO_2 photocatalytic destruction

byproducts and reaction pathway of cylindrospermopsin. Appl. Catal. B Environ. 163, 591–598. https://doi.org/10.1016/j.apcatb.2014.08.034

Zhang, Y., Zhu, H., Szewzyk, U., Geissen, S.U., 2015. Removal of pharmaceuticals in aerated biofilters with manganese feeding. Water Res. 72, 218–226. https://doi.org/10.1016/j.watres.2015.01.009

Zhou, H., Fu, C., 2020. Manganese-oxidizing microbes and biogenic manganese oxides: characterization, Mn(II) oxidation mechanism and environmental relevance. Rev. Environ. Sci. Bio/Technology 1. https://doi.org/10.1007/s11157-020-09541-1

Zhu, B., Zhang, X., Zhao, C., Chen, S., Yang, S., 2018. Comparative genome analysis of marine purple sulfur bacterium *Marichromatium gracile* YL28 reveals the diverse nitrogen cycle mechanisms and habitat-specific traits. Sci. Rep. 8, 1–11. https://doi.org/10.1038/s41598-018-36160-2

8 Appendix

Table A1. PCR reaction mixture for the amplification of the 16S rDNA sequences.

Reagent*	Final concentration
Buffer	1X
Taq	1.25 U
$MgCl_2$	1.5 mM
dNTPs	0.2 mM
Primer 63F#	0.6 µM
Primer 1387R#	0.6 µM

*EURx, Gdańsk, Poland
#Marchesi et al., 1998

Table A2. PCR cycling conditions for the amplification of the 16S rDNA sequences.

Step	Temperature	Time	Cycles
Initial denaturation	95°C	2 min	1
Denaturation	95°C	20 s	
Annealing	58°C	30 s	30
Extension	72°C	2 min	
Terminale extension	72°C	20 min	1

Expected product ~1300 bp.

Table A3. Composition of growth media and trace elements and vitamins solutions.

LSM2	**Ammonium Iron(II) Sulfate Hexahydrate solution (Fe^{2+} solution)**	**Trace elements solution**	**Vitamin solution**
Yeast extract 1 g L^{-1}	$Fe(NH_4)_2(SO_4)_2 \cdot 6H_2O$ 4 g diluted in a solution of 3 g of trisodium citrate dehydrate dissolved in 20 mL	$N(CH_2CO_2H)_3$ 12.8 g L^{-1}	4-Aminobenzoic Acid 10 mg L^{-1}
NH_4Cl 0.3 g L^{-1}		$FeCl_2 \cdot 4\ H_2O$ 2 g L^{-1}	D(+)-Biotin 2 g L^{-1}
$MnCO_3 \cdot H_2O$ 2 g L^{-1}		$ZnCl_2$ 70 mg L^{-1}	Cyanocobalamin 20 mg L^{-1}
Trace elements solution 2 mL L^{-1}		$MnCl_2 \cdot 2\ H_2O$ 80 mg L^{-1}	Nicotinic acid 20 mg L^{-1}
Vitamin solution 2 mL L^{-1}		H_3BO_3 6 mg L^{-1}	D-Calcium pantothenat 5 mg L^{-1}
Fe^{2+} solution 500 µL L^{-1} (added directly to each flask when it was requiered)		$CoCl_2 \cdot 6\ H_2O$ 190 mg L^{-1}	Pyridoxamine dihydrochloride monohydrate 50 mg L^{-1}
pH 7.2 (before autoclaving)		$CuCl_2 \cdot 2\ H_2O$ 2 mg L^{-1}	Thiamine hydrochloride 10 mg L^{-1}
		$NiCl_2 \cdot 6\ H_2O$ 24 mg L^{-1}	
		$Na_2MoO_4 \cdot 2\ H_2O$ 36 mg L^{-1}	
		pH 6 (before autoclaving)	

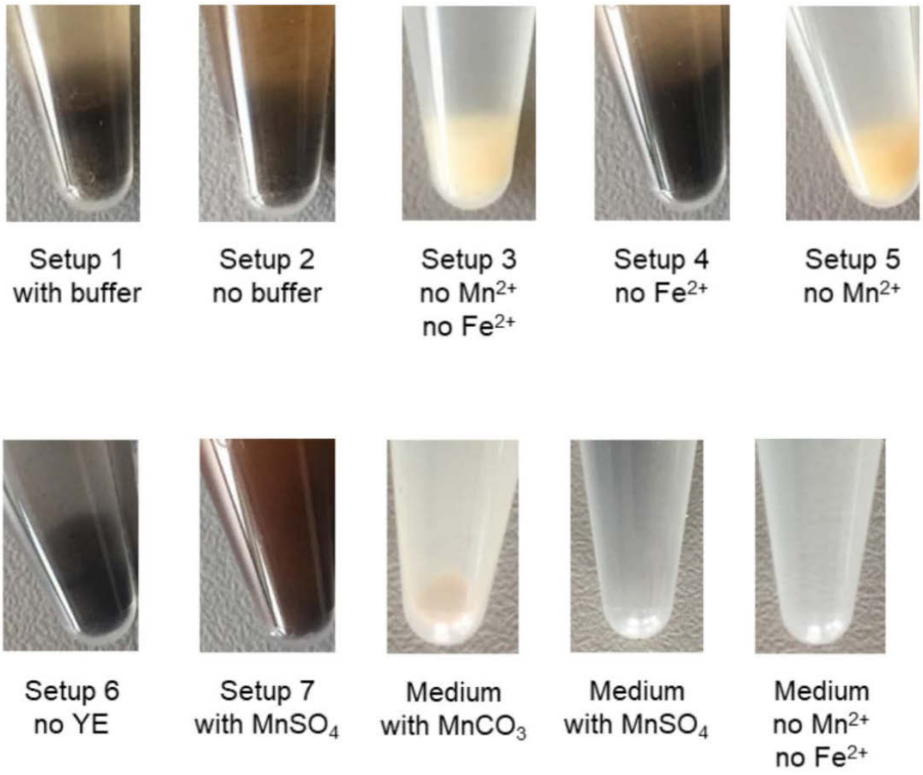

Fig. A1. Example of the brown dark aggregates formed by *Ideonella* sp. A288 under different conditions. On the image of setup 3 and 4, the pellet corresponds to bacteria biomass, while for the other images aggregates and bacteria are mixed. Strains OF001, A210 and A226 formed aggregates with a similar colour as those formed by A288. In medium without bacteria aggregates are not observed. In the medium with $MnCO_3$ the insoluble $MnCO_3$ is observed.

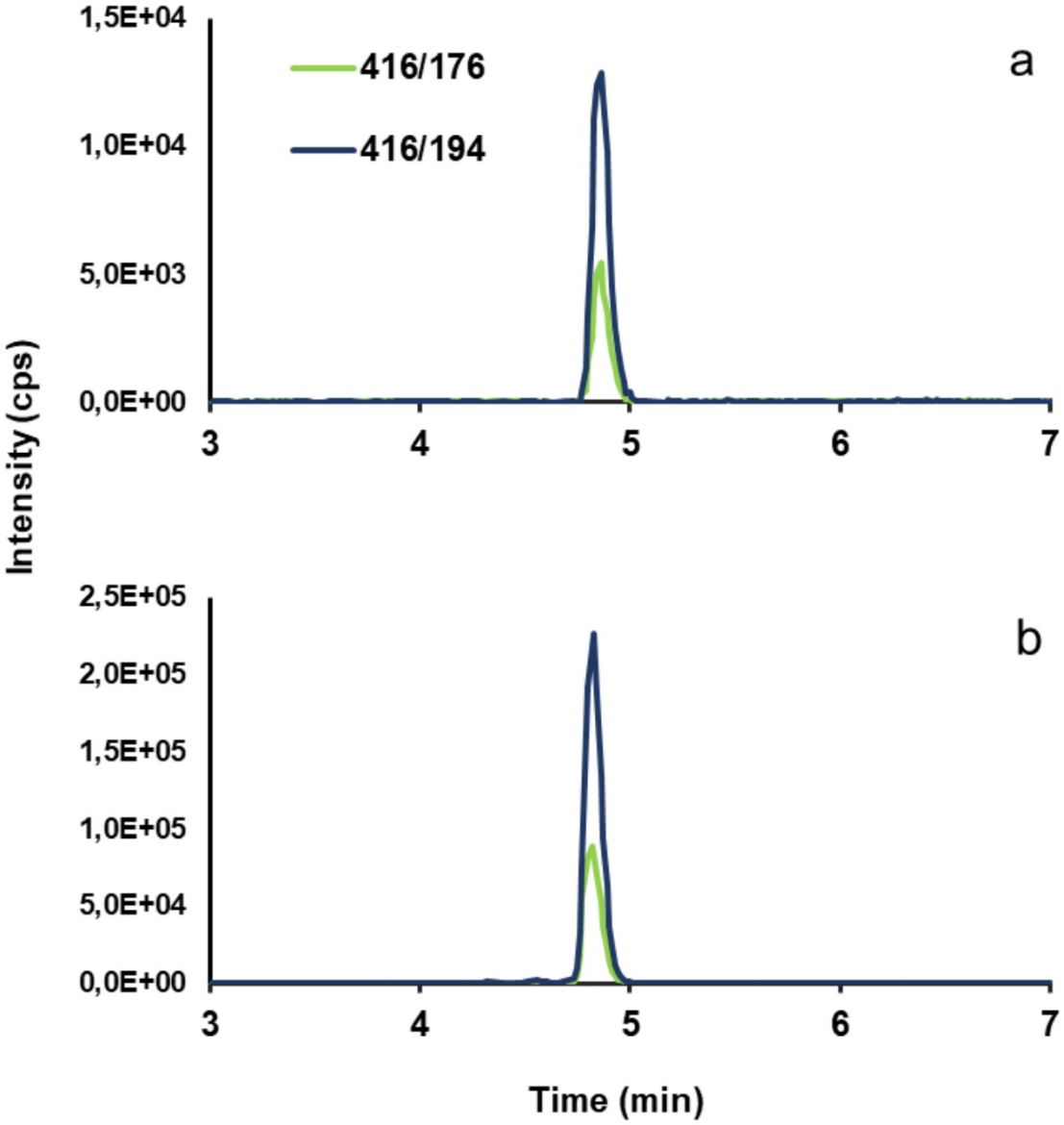

Fig. A2. Reconstructed LC-MS/MS chromatograms of CYN. a) Certified reference standards; b) sample of the control group. Lines show the transitions indicative for CYN

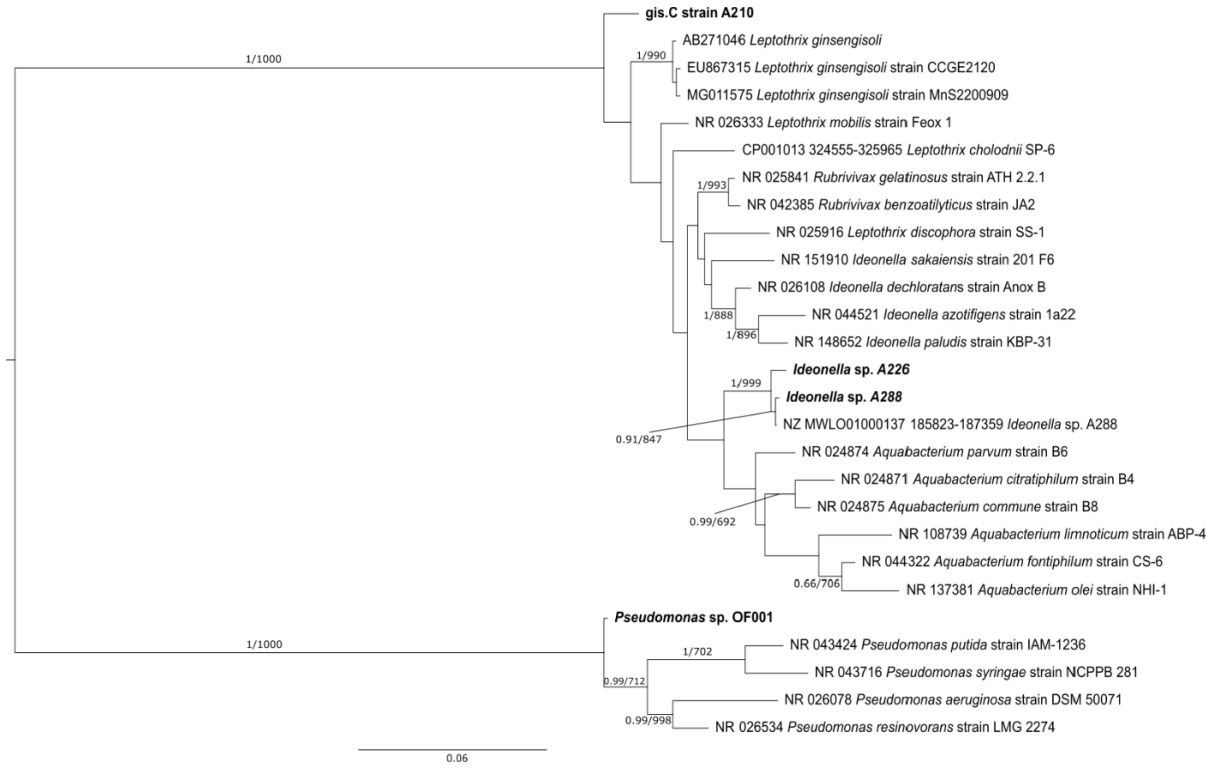

Fig. A3. Consensus phylogenetic tree based on 16S rDNA sequences. Numbers in the branches represent Bayesian posterior probability and bootstrap value from those branches which were present in both, Maximum Likelihood and Bayesian Inference trees. Bold text represent the sequences generated in the present work. Scale bar represent sequence divergence. gis.C: *genera incertae sedis Comamonadaceae*.

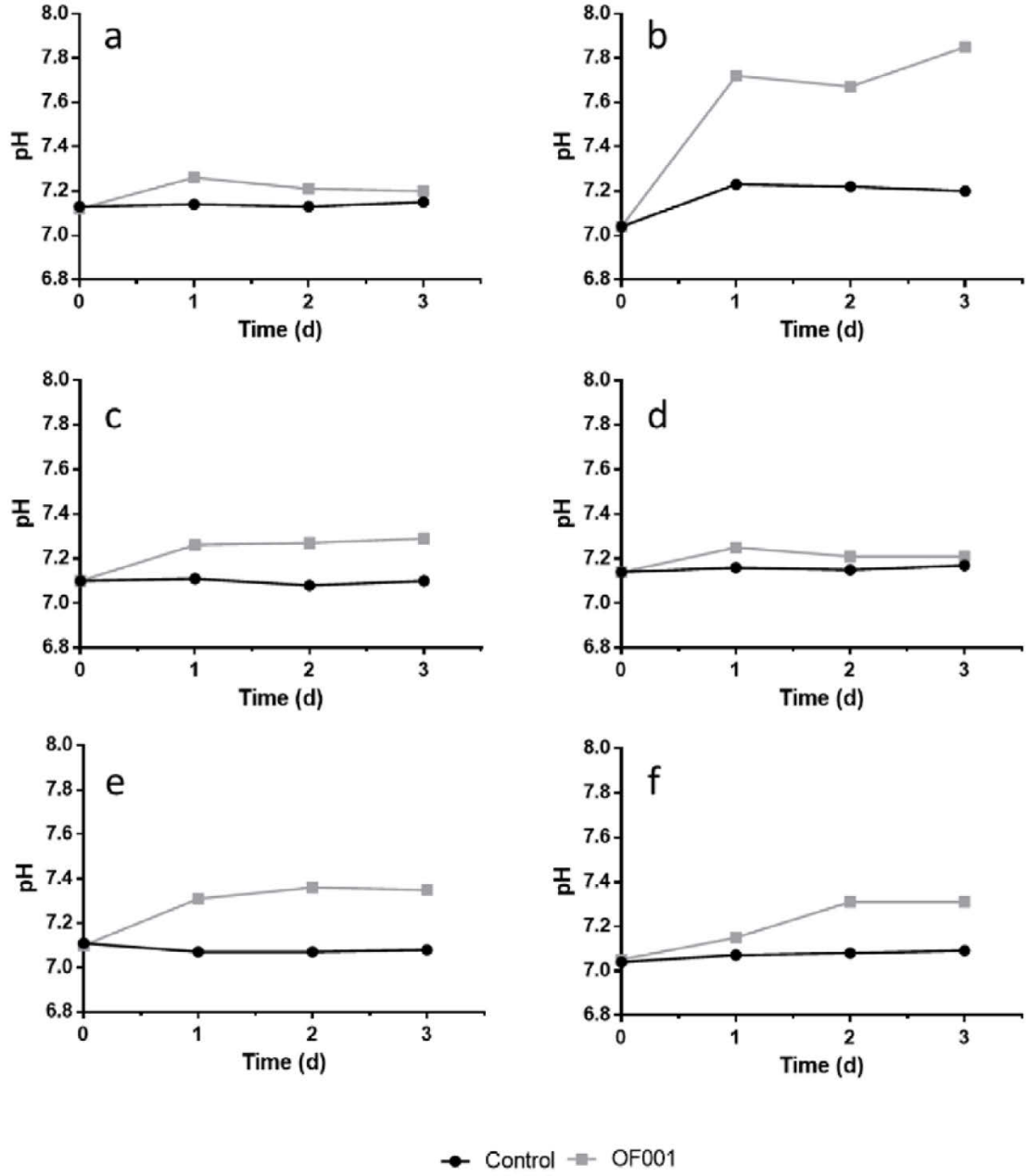

Fig. A4. pH changes throughout the assay time of *Pseudomonas* sp. OF001. a) setup 1 with buffer, b) setup 2 no buffer, c) setup 3 no Mn^{2+} no Fe^{2+}, d) setup 4 no Fe^{2+}; e) setup 5 no Mn^{2+} f) setup 7 with $MnSO_4$. YE: yeast extract.

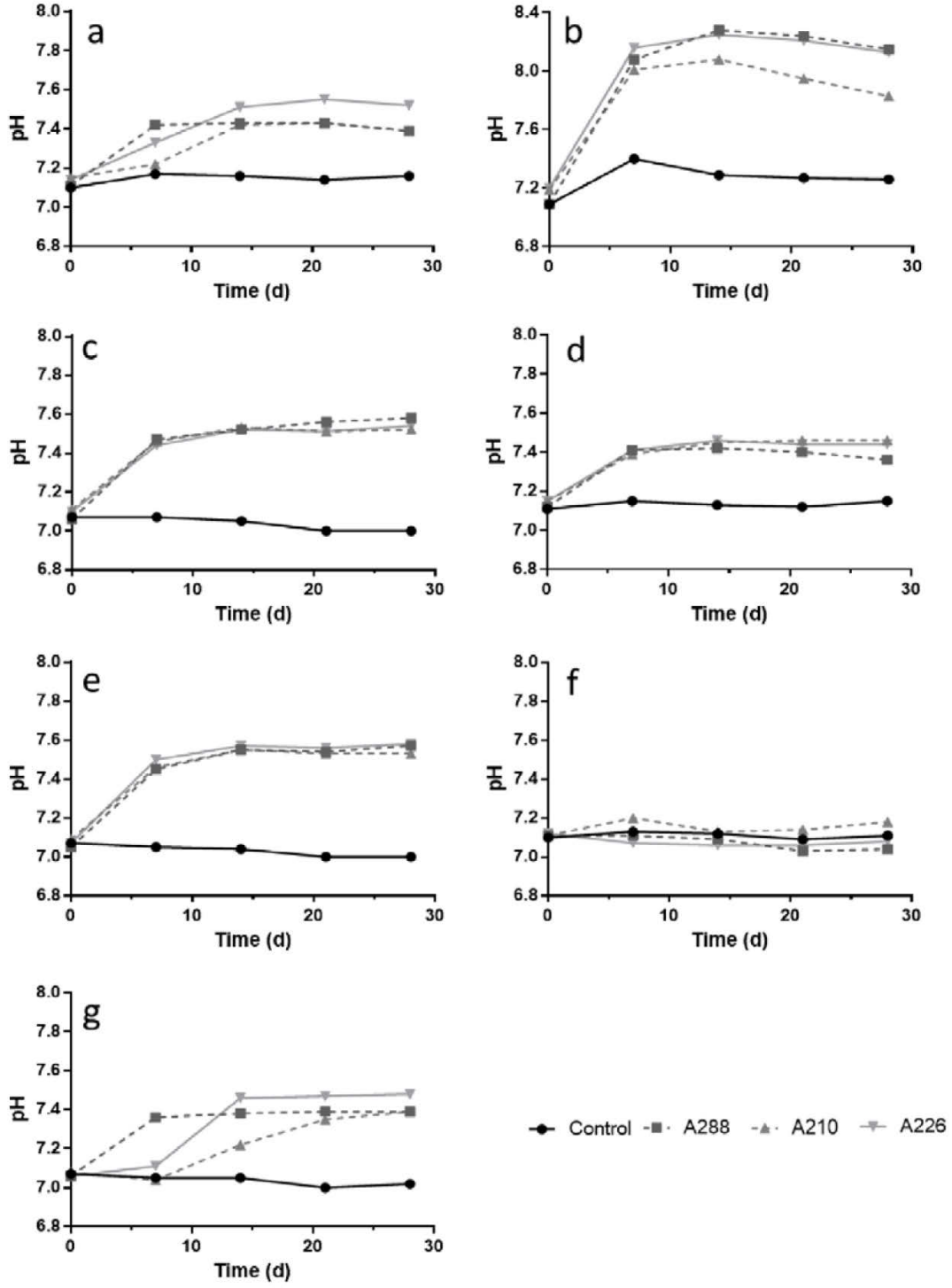

Fig. A5. pH changes throughout the assay time of *Ideonella* sp. A288, *Comamonadaceae* bacterium A210 and *Ideonella* sp. A226. a) setup 1 with buffer, b) setup 2 no buffer, c) setup 3 no Mn^{2+} no Fe^{2+}, d) setup 4 no Fe^{2+}; e) setup 5 no Mn^{2+} f) setup 6 no YE, g) setup 7 with $MnSO_4$. YE: yeast extract.

a

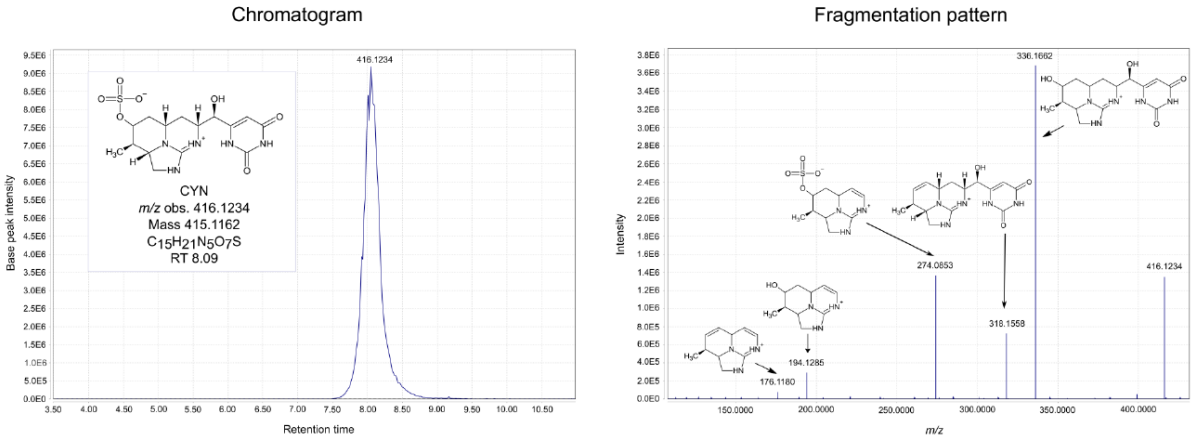
Chromatogram
Fragmentation pattern
CYN
m/z obs. 416.1234
Mass 415.1162
C15H21N5O7S
RT 8.09
416.1234
336.1662
274.0853
318.1558
194.1285
176.1180
Base peak intensity
Intensity
Retention time
m/z

b

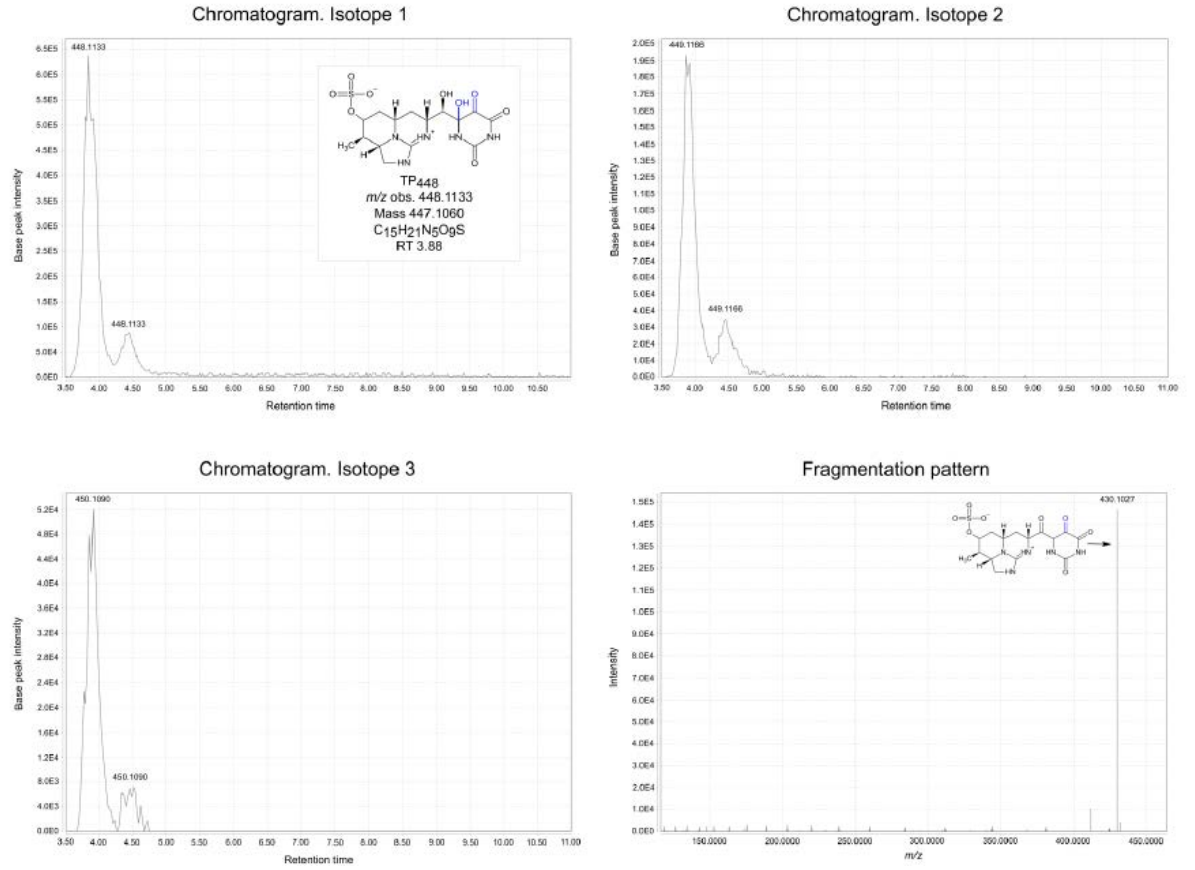
Chromatogram. Isotope 1
Chromatogram. Isotope 2
Chromatogram. Isotope 3
Fragmentation pattern
TP448
m/z obs. 448.1133
Mass 447.1060
C15H21N5O9S
RT 3.88
448.1133
449.1166
450.1090
430.1027
Base peak intensity
Intensity
Retention time
m/z

c

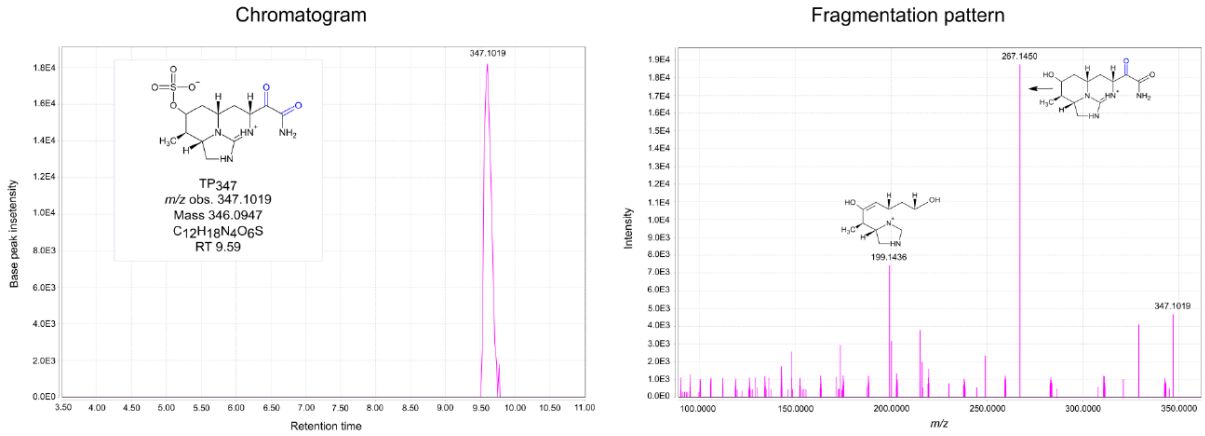
Chromatogram
Fragmentation pattern
TP347
m/z obs. 347.1019
Mass 346.0947
C12H18N4O6S
RT 9.59
347.1019
267.1450
199.1436
Base peak intensity
Intensity
Retention time
m/z

d

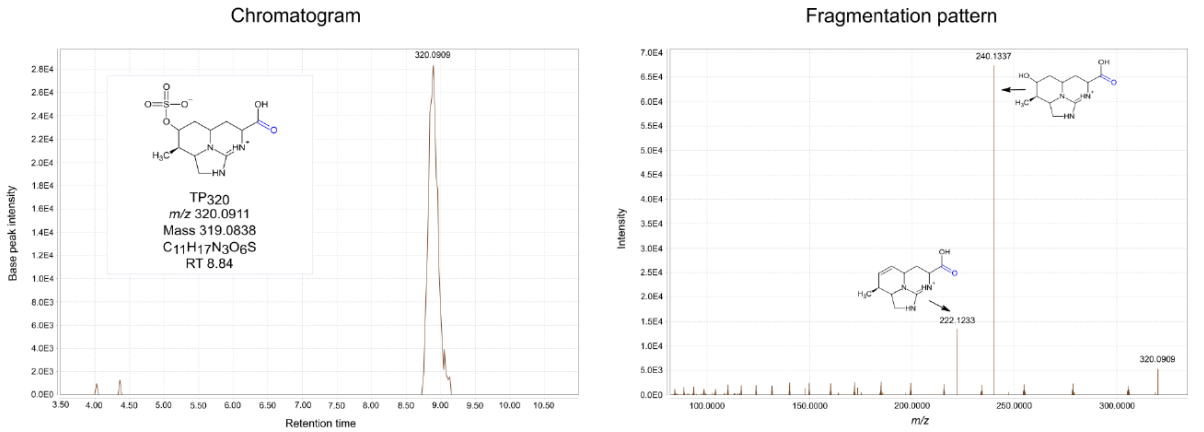
Chromatogram
Fragmentation pattern
TP320
m/z 320.0911
Mass 319.0838
C11H17N3O6S
RT 8.84
320.0909
240.1337
222.1233
Base peak intensity
Intensity
Retention time
m/z

e

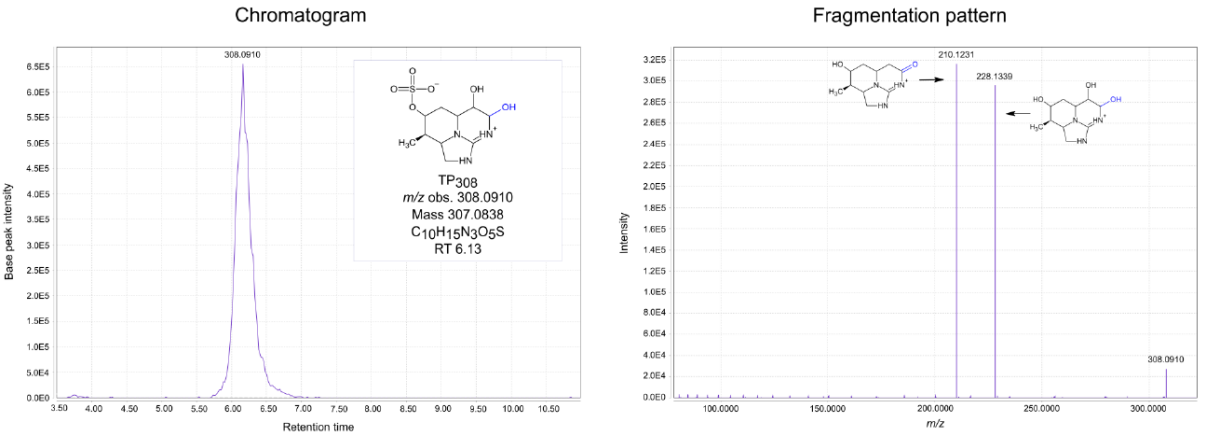
Chromatogram
Fragmentation pattern
TP308
m/z obs. 308.0910
Mass 307.0838
C10H15N3O5S
RT 6.13
308.0910
210.1231
228.1339
Base peak intensity
Intensity
Retention time
m/z

f

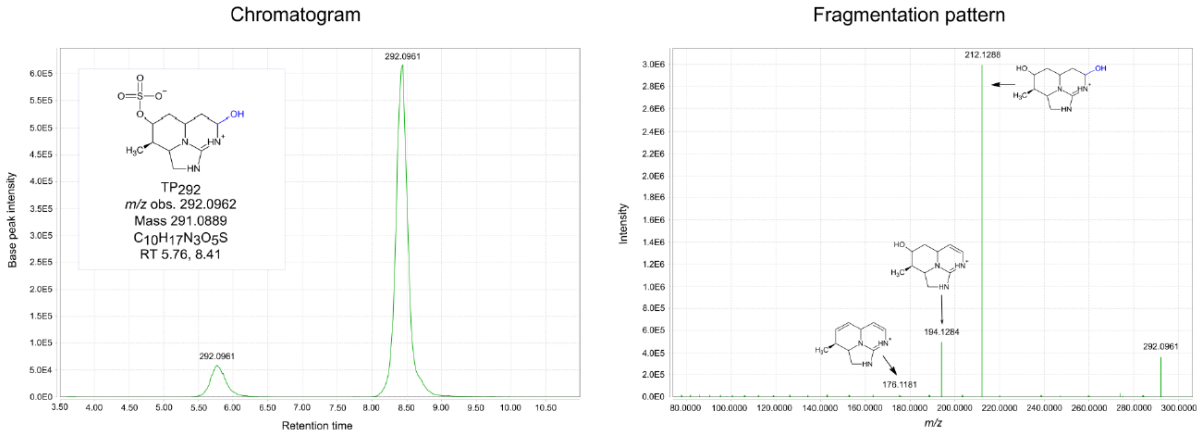

g

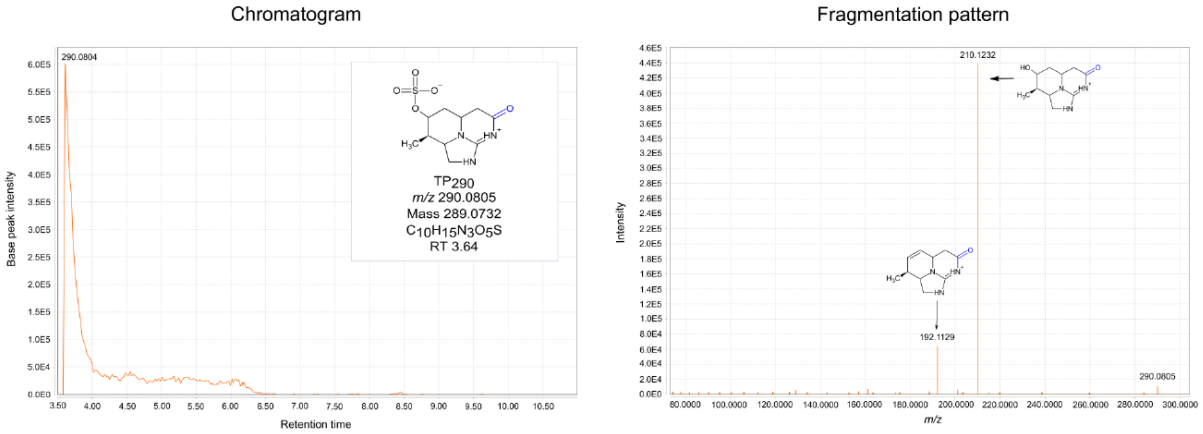

Fig. A6. Chromatograms and MS^2 fragmentation pattern spectra of CYN and CYN transformation products. a) CYN, b) chromatogram of TP_{448} and main isotopes, and fragmentation pattern, and c-g) CYN transformation products. TP represent the transformation product with the observed *m/z* indicated as subscript number. Observed *m/z* values for singly charged ions ($[M+H]^+$). Observed *m/z* and RT is the average value of CYN or transformation products in all the samples. Peaks under 4.0 x 10^4 were considered unspecific peaks. obs.: observed; RT: retention time.

a

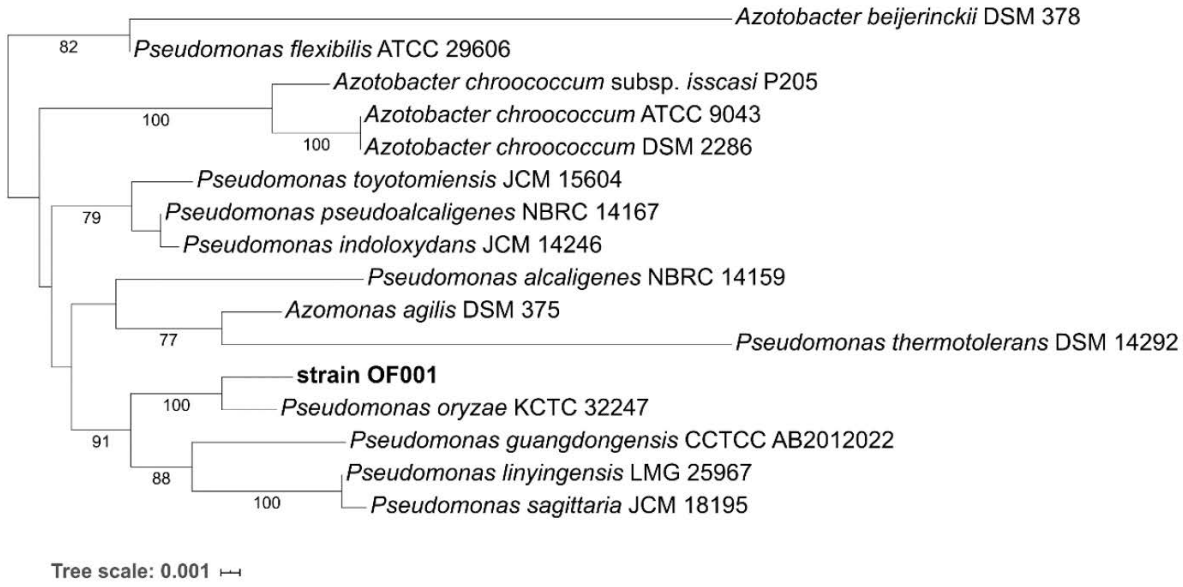

b

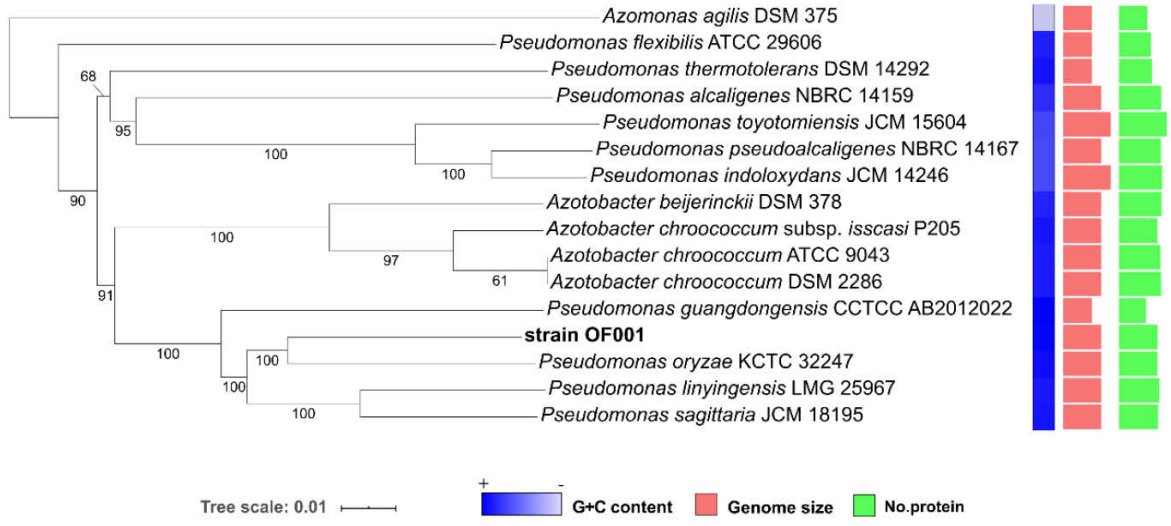

Fig. A7. Phylogenetic tree based on 16S rDNA sequences and whole genome sequences including strain OF001 sequence. Tree inferred with FastME 2.1.6.1 (Lefort et al., 2015) from GBDP distances calculated from a) 16S rDNA gene sequences and b) genome sequences. The branch lengths are scaled in terms of GBDP distance formula d_5. The numbers above branches are GBDP pseudo-bootstrap support values > 60% from 100 replications, with an average branch support of a) 68.8% and b) 92.5%. Tree was rooted at the midpoint (Farris, 1972). Bold text represent the sequences generated in the present work. Scale bar represent sequence divergence.

a

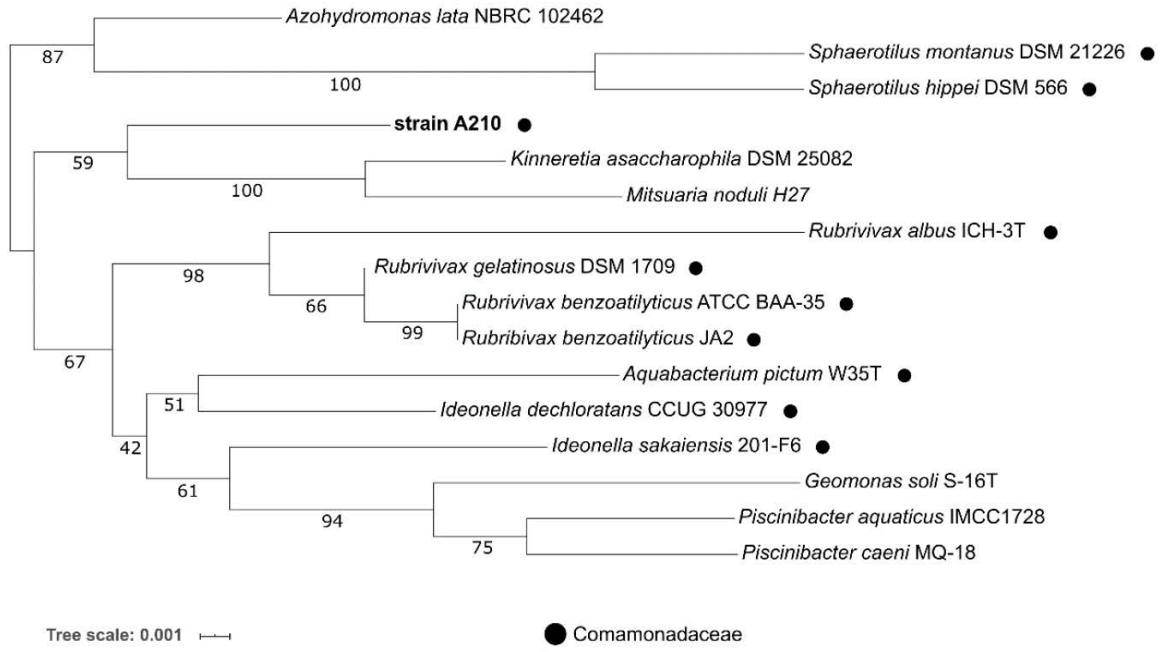

b

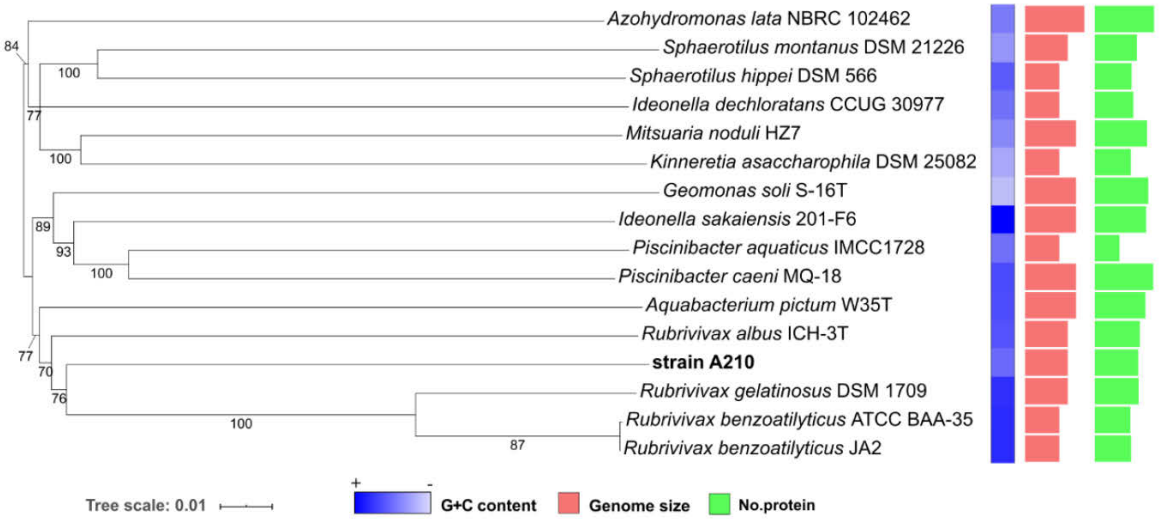

Fig. A8. Phylogenetic tree based on 16S rDNA sequences and whole genome sequences including strain A210 sequence. Tree inferred with FastME 2.1.6.1 (Lefort et al., 2015) from GBDP distances calculated from a) 16S rDNA gene sequences and b) genome sequences. The branch lengths are scaled in terms of GBDP distance formula d_5. The numbers above branches are GBDP pseudo-bootstrap support values > 60% from 100 replications, with an average branch support of a) 76.8% and b) 83.4%. Tree was rooted at the midpoint (Farris, 1972). Bold text represent the sequences generated in the present work. Scale bar represent sequence divergence.

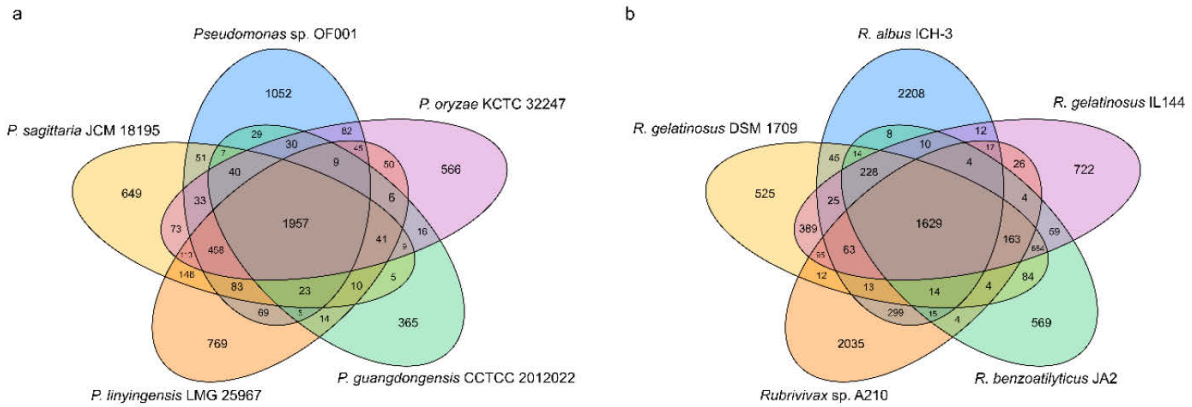

Fig. A9. Pan- and core genome overview. Venn diagram shows the number of shared and specific Microscope gene families (MICFAM) a) among *Pseudomonas* sp. OF001 and the members of the *Pseudomonas*_K group, and b) among *Rubrivivax* sp. A210 and the members of the *Rubrivivax* genus. MICFAM grouping was based on 50% amino acid identity cut-off and at least 80% amino-acid alignment coverage.

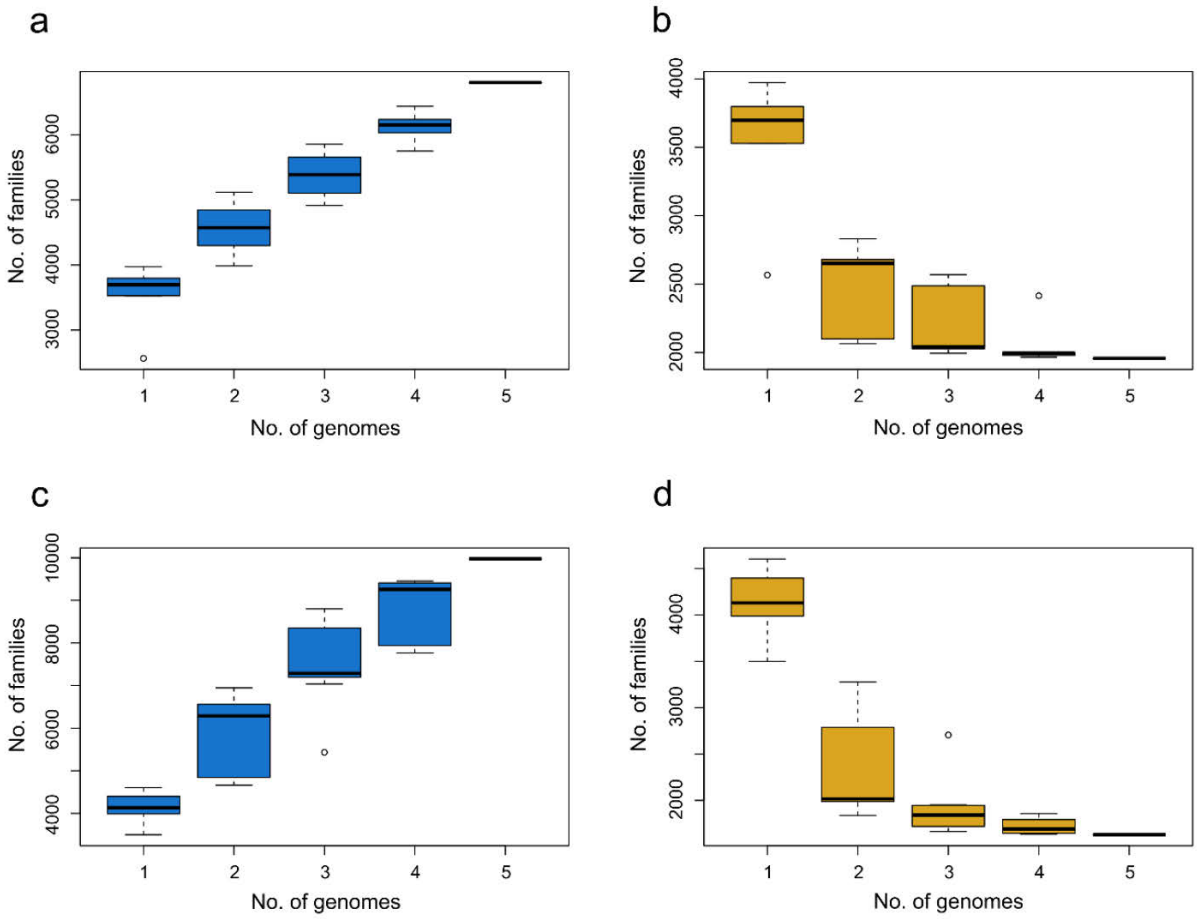

Fig. A10. Pan- and core- genome sizes estimated evolution. a, c) Number of MICFAM families in the pan-genome size by the number of genomes, and b, d) number of MICFAM families in the core-genome by the number of genomes. a, b) Including *Pseudomonas* sp OF001, and c, d) including *Rubrivivax* sp. A210.

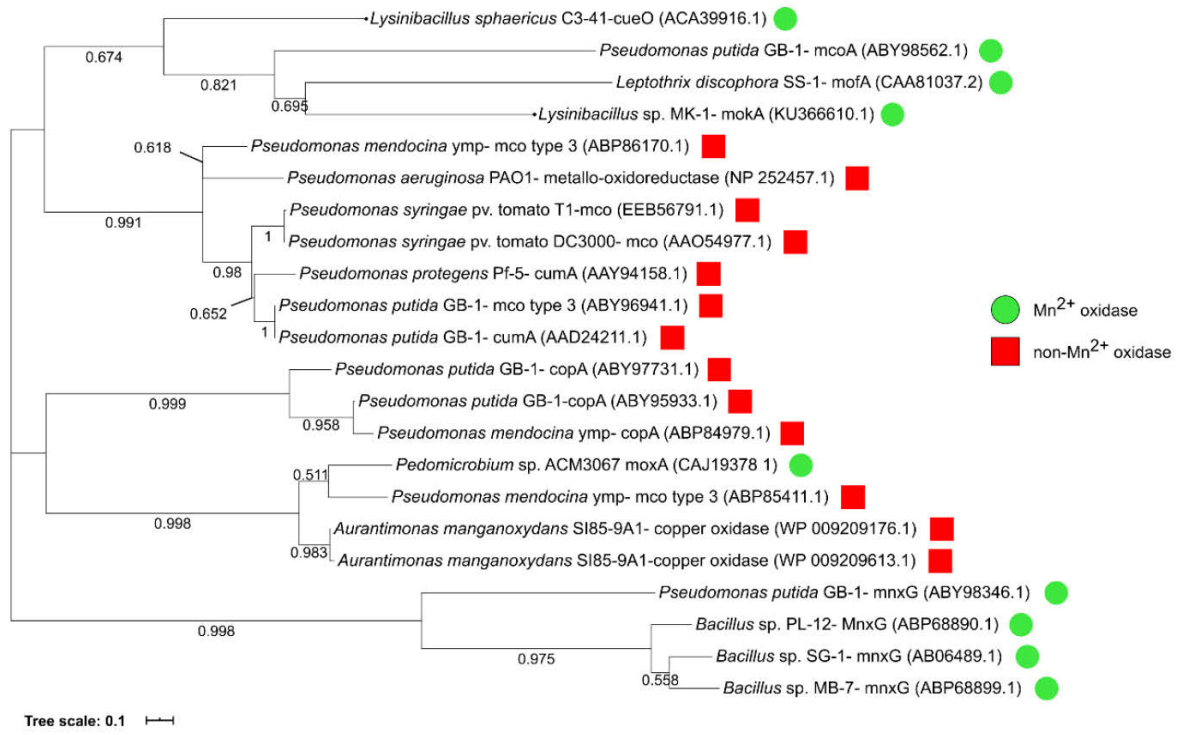

Fig. A11. Maximum Likelihood phylogenetic tree based on multicopper oxidases sequences with and without reported Mn^{2+} oxidation activity. Sequences of the studied strains in the present study are not included. Numbers in the branches represent bootstrap value. Scale bar represent sequence divergence.

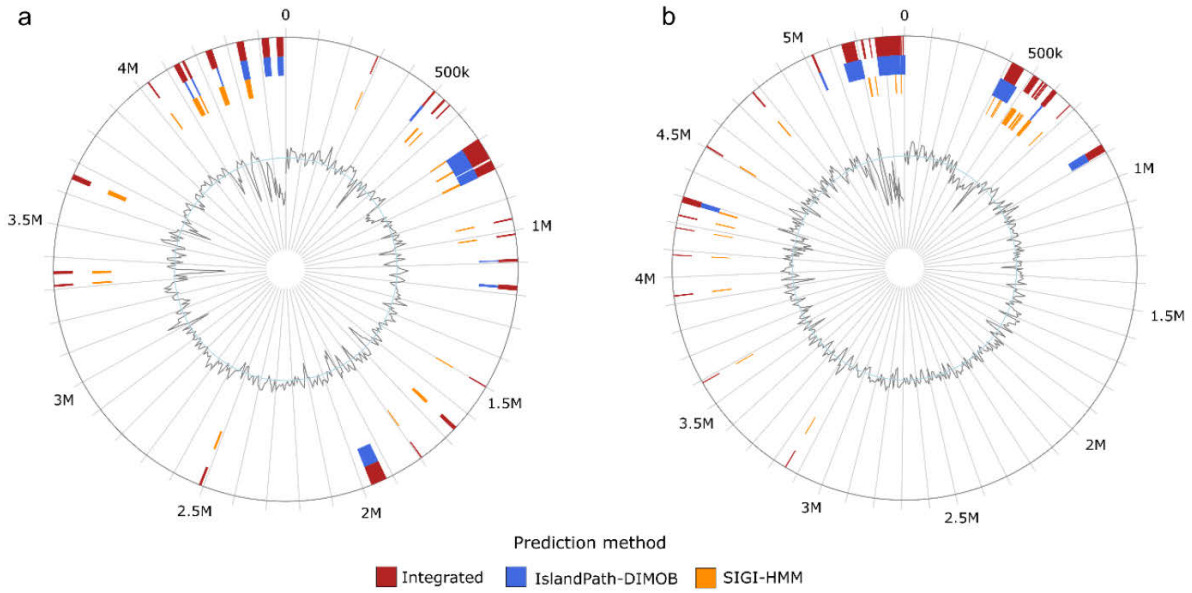

Fig. A12. Putative genomic islands harbored by the studied MOB. a) *Pseudomonas* sp. OF001, and b) *Rubrivivax* sp. A210. Outer circle represents the genome size in Mbps. Genomic islands obtained by different prediction methods are highlighted in color. Integrated represent those islands detected by at least one method.

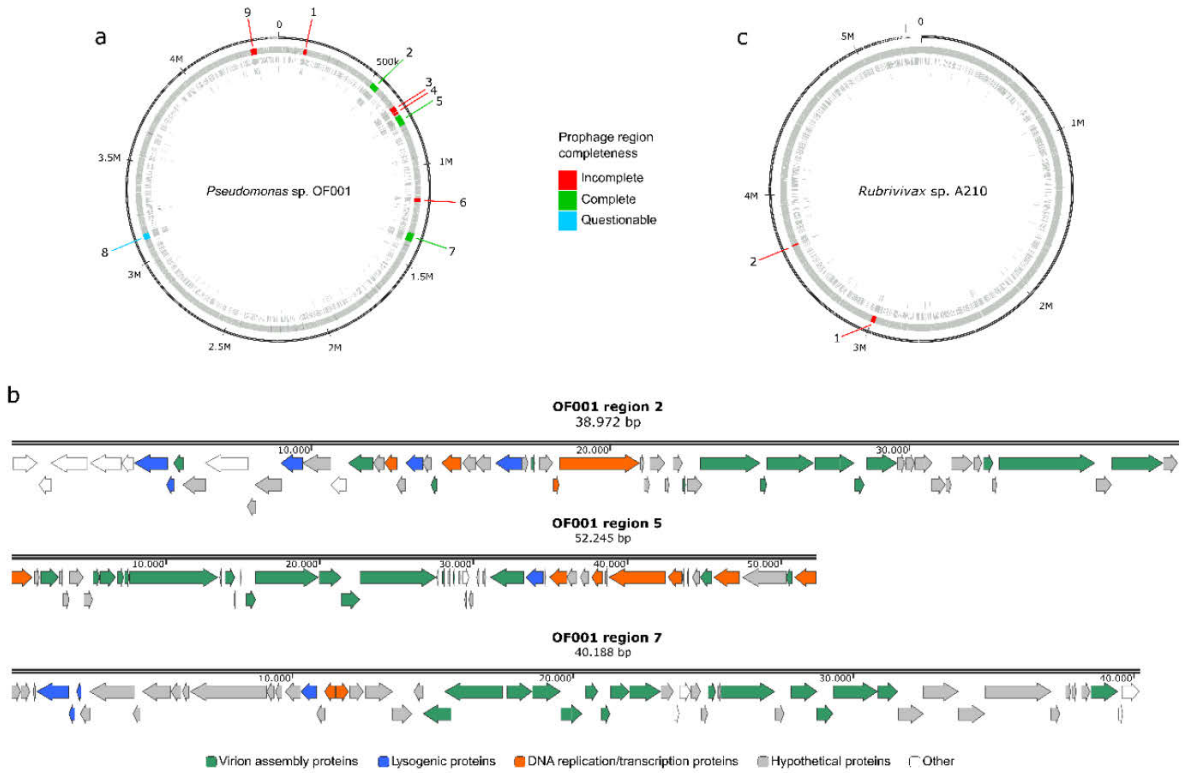

Fig. A13. Distribution and genetic features of prophages detected in *Pseudomonas* sp. OF001 and *Rubrivivax* sp. A210. a) Circular genome map of strain OF001, b) genetic features of the complete prophages in strain OF001, and b) circular genome map of strain A210. In the genome maps location of prophages are highlighted in colors depending on the completeness of the prophages (Table S9). Number assigned to each prophage region is based on the genome location retrieved by PHASTER (Arndt et al., 2016).

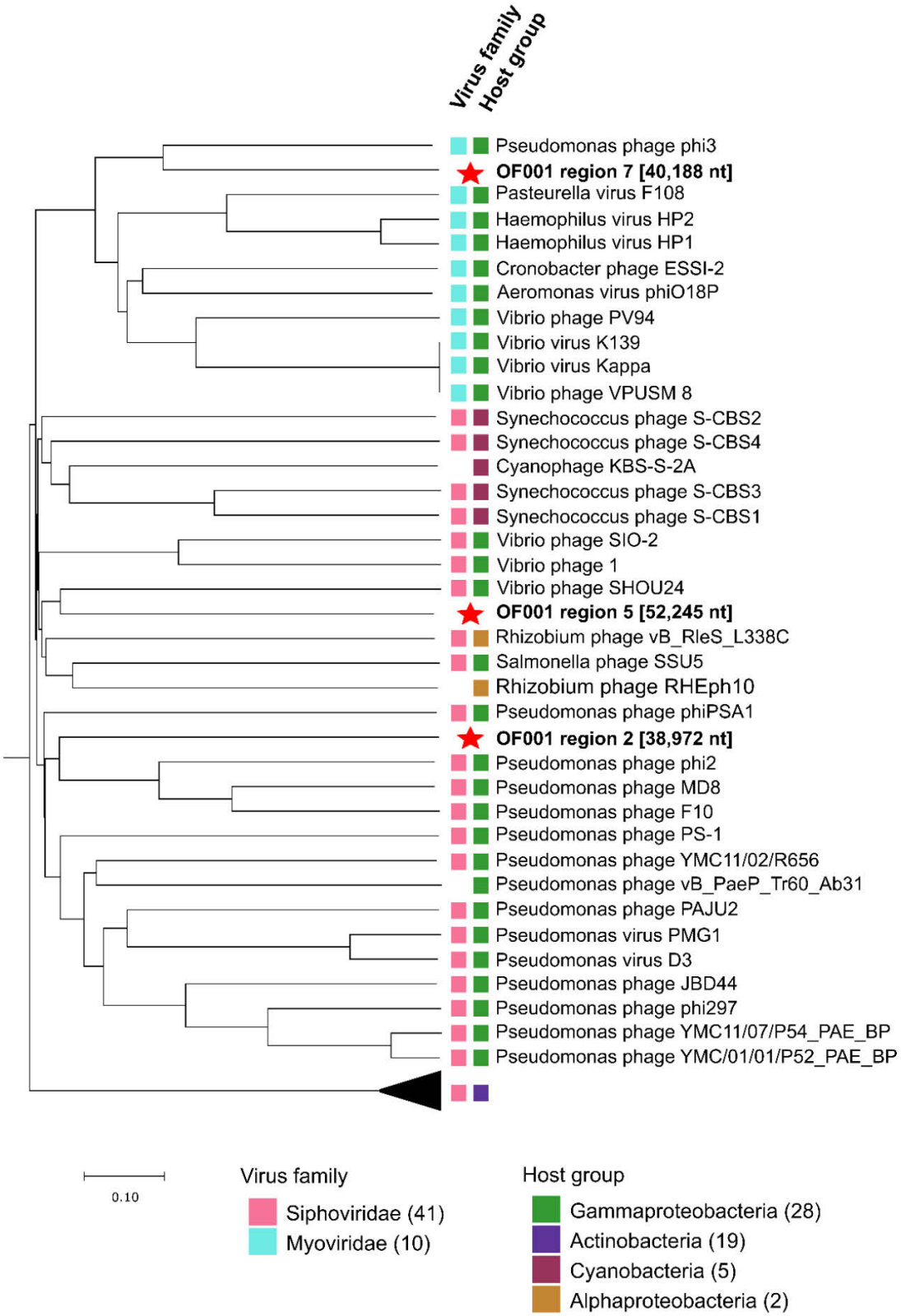

Fig. A14. Whole proteomic tree of *Pseudomonas* sp. OF001 prophages based on genome-wide similarities computed by tBLASTx. The tree was constructed using the VIPTree web server v.1.9 (Nishimura et al., 2017). Numbers in brackets in the figure legend represent the number of virus genomes. Red stars represent the three complete prophages of strain OF001. Scale bar represent sequence divergence.

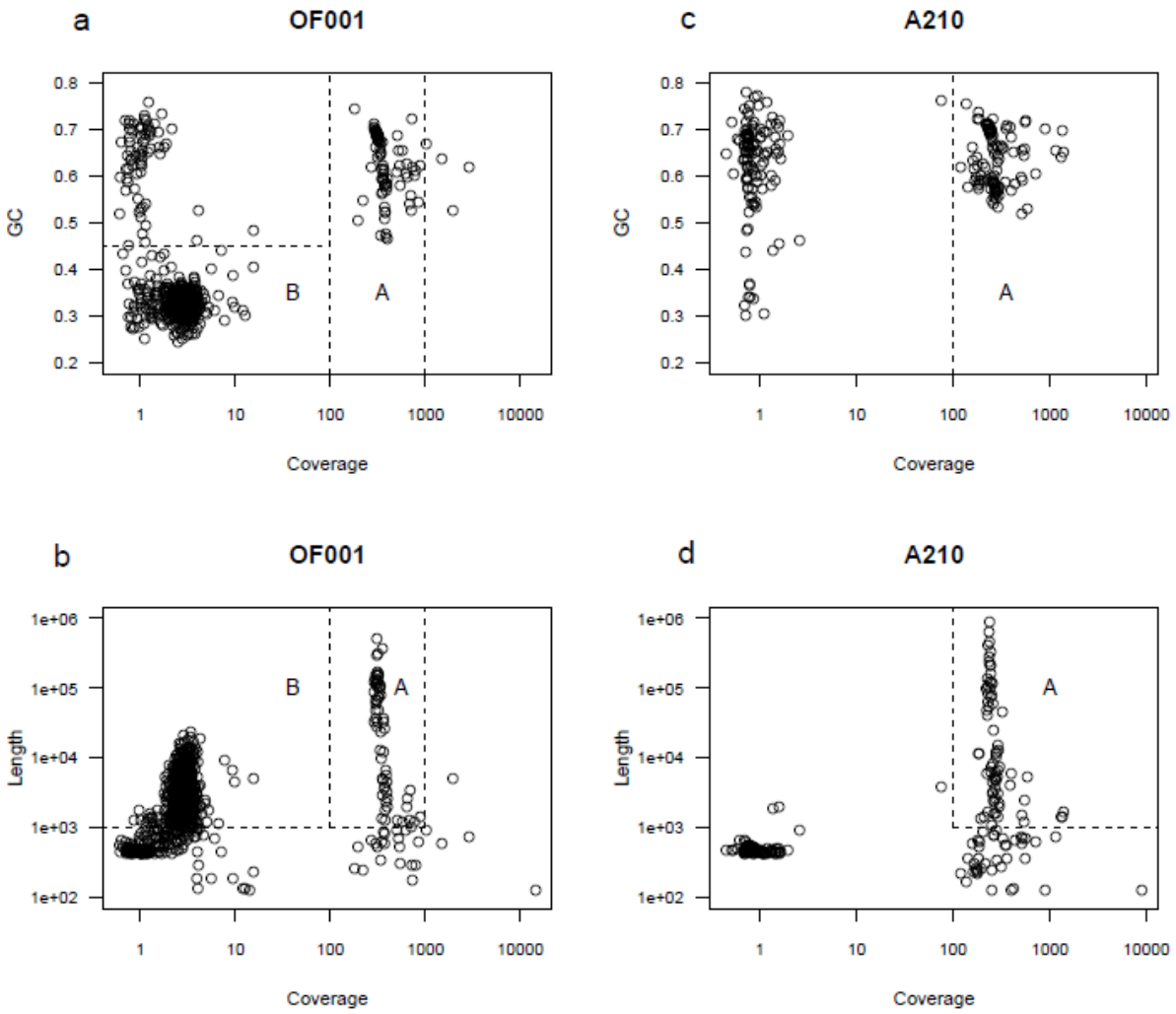

Fig. A15. Coverage-GC plots of contig properties for strain OF001 and A210. a, c) Coverage vs GC content, and b, d) coverage vs length. Both samples has a primary, high abundance cluster of contigs, with GC centered around 0.6 with arise form the primary culture populations. For strain OF001 a second contig cluster with GC centered around 0.35 at a much lower abundance was detected, which might represent a slight DNA contamination.

Table A4. List of genes in strains OF001 and A210 with homology to putative Mn^{2+} oxidases from other MOB.

Gene	Organism	Locus tag (OF001_)	Predicted function	% similarity	E value	Locus tag (RA210_)	Predicted function	% similarity	E value
mcoA (ABY98562.1)	*P. putida* GB-1	u20185	Glycoprotein gp2	80	0	u420004	Glycoprotein gp2	49	3E-11
mnxG (ABY98346.1)	*P. putida* GB-1	u60094	unknown function	83	0	u10102	Unknown function	58	0
						u110082	unknown function	58	0
mofA (CAA81037.2)	*L. discophora* SS-1	n.d.	-	-	-	u30250	Fibronectin type III domain protein	59	0
mnxG (AAB06489.1)	*Bacillus* sp. SG-1	u60094	Unknown function	36	7E-51	u110082	Unknown function	35	7E-51
mnxG (ABP68890.1)	*Bacillus* sp. PL-12	u60094	Unknown function	38	2E-39	u110082	Unknown function	36	3E-32
mnxG (ABP68899.1)	*Bacillus* sp. MB-7	u60094	Unknown function	34	6E-49	u10102	Unknown function	40	5E-24
moxA (CAJ19378.1)	*Pedomicrobium* sp. ACM 3067	u90046	Multicopper oxidase	51	6E-29	u100111	Multicopper oxidase	53	5E-29
cueO precursor (ACA39916.1)	*L. sphaericus* C3-41	u90046	Multicopper oxidase	43	6E-28	u100111	Multicopper oxidase	45	6E-39
mokA gene (KU366610.1)	*Lysinibacillus* sp. MK-1	u20185	Glycoprotein gp2	41	3E-15	u30250	Fibronectin type III domain protein	36	1E-19
putative hemolysin-type calcium-binding peroxidase (EAS51309.1)	*A. manganoxydans* SI85-9A1	u100035	Haem peroxidase	39	1E-85	u10091	Protein of unknown function	48	7E-23
mopA (WP_006833885.1)	*Erythrobacter* sp. SD-21	u220048	Unknown function	38	1E-104	u140033	Protein of unknown function	36	3E-43
mopA (ABY99245.1)	*P. putida* GB-1	u100035	Haem peroxidase	42	2E-166	u10091	Protein of unknown function	54	2E-34

Table A5. List of sequences of MO-mco and non- Mn^{2+} oxidases.

Mn^{2+} oxidases		non-Mn^{2+} oxidases	
Organism	Gene	Organism	Gene/product
P. putida GB-1	*mcoA* (ABY98562.1)	*P. putida* GB-1	*copA* (ABY95933.1)
P. putida GB-1	*mnxG* (ABY98346.1)	*P. putida* GB-1	mco (ABY96941.1)
L. discophora SS-1	*mofA* (CAA81037.2)	*P. putida* GB-1	*copA* (ABY97731.1)
Bacillus sp. SG-1	*mnxG* (AAB06489.1)	*P. putida* GB-1	*cumA* (AAD24211.1)
Bacillus sp. PL-12	*mnxG* (ABP68890.1)	*A. manganoxydans* SI85-9A1	copper oxidase (WP_009209176.1)
Bacillus sp. MB-7	*mnxG* (ABP68899.1)	*A. manganoxydans* SI85-9A1	copper oxidase (WP_009209613.1)
Pedomicrobium sp. ACM 3067	*moxA* (CAJ19378.1)	*P. mendocina* ymp	*copA* (ABP84979.1)
L. sphaericus C3-41	*cueO* precursor (ACA39916.1)	*P. mendocina* ymp	mco type 3 (ABP85411.1)
Lysinibacillus sp. MK-1	*mokA* (KU366610.1)	*P. mendocina* ymp	mco type 3 (ABP86170.1)
		P. aeruginosa PAO1	metallo-oxidoreductase (NP_252457.1)
		P. syringae pv. tomato T1	mco (EEB56791.1)
		P. syringae pv. tomato str. DC3000	mco (AAO54977.1)
		P. protegens Pf-5	*cumA* (AAY94158.1)

Mco: multicopper oxidase, Information about Mn^{2+} oxidation activity is reported in Anderson et al. (2009) and Geszvain et al. (2013).

Table A6. Characteristics of prophage regions identified in *Pseudomonas* sp. OF001 and *Rubrivivax* sp. A210 genome.

	Region	Length (Kb)	Completeness	Score	No. of proteins	Position in genome	Most Common Phage
OF001	1	17.3	incomplete	50	17	128930-146325	Synechococcus phage ACG-2014f (NC_026927)
	2	38.9	complete	140	57	518625-557596	Pseudomonas phage F10 (NC_007805)
	3	28.2	incomplete	30	21	675847-704073	Acinetobacter phage Presley (NC_023581)
	4	11.8	incomplete	10	28	706525-718353	Pseudomonas virus H66 (NC_042342)
	5	52.2	complete	130	48	728248-780492	Vibrio phage SHOU24 (NC_023569)
	6	18.1	incomplete	20	24	1165602-1183706	Pseudomonas phage MD8 (NC_031091)
	7	40.1	complete	100	57	1347817-1388004	Pseudomonas phage phi3 (NC_030940)
	8	32	questionable	70	55	3103053-3135127	Pseudomonas phage phi2 (NC_030931)
	9	30.5	incomplete	30	23	4343162-4373729	Pseudomonas phage phi2 (NC_030931)
A210	1	28.8	incomplete	20	9	2977501-3006322	Agrobacterium phage Atu_ph07 (NC_042013)
	2	9.9	incomplete	20	10	3674006-3684003	Synechococcus phage ACG-2014f (NC_026927)

Number assigned to each prophage region is based on the genome location (Fig. A13). Regions with a score below 70 are classified as incomplete, between 70 to 90 questionable, and greater than 90 as complete (Arndt et al., 2016).

Table A7. CRISPR-Cas systems detected within *Pseudomonas* sp. OF001 and *Rubrivivax* sp. A210 genome.

Strain	CRISPR									Cas		
	Start	End	Length (bp)	Potential orientation	Direction	Repeat length	No. of spacers	Evidence level	Nb. Cas	Cas type	Start	End
OF001	3308018	3310047	2029	Reverse	Unknown	32	30	4	1	General-Class 1	3310229	3317876
A210	3139744	3140141	397	Forward	Unknown	35	5	2	n.d.	-	-	-
	3140249	3141359	1110	Forward	Unknown	35	15	4	1	General-Class 1	3142416	3147642

n.d.: not detected, -: no values correspond to this cell.

Table A 8. Characteristics of the *cas* genes detected within *Pseudomonas* sp. OF001 and *Rubrivivax* sp. A210 genome.

Strain	Cas-type/subtype	Gene status	System	Type	Start	End	Strand
OF001	Cas2_0_I-II-III-V	accessory	General-Class1	CDS	3310229	3310516	-
	Cas1_0_IC	accessory	General-Class1	CDS	3310527	3311567	-
	Cas4_0_I-II	accessory	General-Class1	CDS	3311571	3312197	-
	Cas7_0_IC	accessory	General-Class1	CDS	3312214	3313098	-
	Cas8c_0_IC	accessory	General-Class1	CDS	3313095	3314948	-
	Cas5_0_IC	accessory	General-Class1	CDS	3314945	3315619	-
	Cas3_0_I	accessory	General-Class1	CDS	3315654	3317876	-
A210	Cas3_0_IU	accessory	General-Class1	CDS	3142416	3145061	-
	Csb2_0_IU	accessory	General-Class1	CDS	3145058	3146437	-
	Csb1_0_IU	accessory	General-Class1	CDS	3146449	3147642	-

Table A 9. Comparison of repeats in the CRISPR of confidence level 4 found in strain OF001 to CRISPRCasdb.

Repeat	Matched nucleotides	BLAST score bits	BLAST e-value	Organism	Accesion number
GTTTCAATCCGCGCAGCCGCGTGGGGCGCGAC	30/32	48.1	3E-8	*Chromobacterium violaceum*	AE016825.1_1
	30/32	48.1	3E-8	*Halomonas* sp. Soap Lake #6	CP020469.1_6
	30/32	48.1	3E-8	*Halomonas* sp. Soap Lake #7	CP019915.1_6
GTTTCAATCCACGCGCCCGCGTGAGGCGCGAC	31/32	61.9	2E-12	*Selenomonas sputigena*	CP002637.1_5
	31/32	56	1E-10	*Pelodictyon luteolum*	CP000096.1_1
	31/32	56	1E-10	*Dickeya chrysanthemi*	CM001974.1_4
	31/32	56	1E-10	*Dickeya dianthicola*	CP031560.1_1
	31/32	56	1E-10	*Dickeya dianthicola*	CM001838.1_4
	31/32	56	1E-10	*Dickeya dianthicola*	CM001838.1_5
	31/32	56	1E-10	*Dickeya dianthicola*	AOOM01000229.1_1
	31/32	56	1E-10	*Dickeya dianthicola*	CM002023.1_2
	31/32	56	1E-10	*Dickeya dianthicola*	CM002023.1_1
	31/32	56	1E-10	*Dickeya dianthicola*	CM001840.1_1
	31/32	56	1E-10	*Dickeya dianthicola*	AOOB01000047.1_1
	31/32	56	1E-10	*Dickeya dianthicola*	CM001841.1_2
	31/32	56	1E-10	*Dickeya dianthicola*	CM001841.1_1
	31/32	56	1E-10	*Dickeya dianthicola*	CP017638.1_1
	31/32	56	1E-10	*Halomonas* sp. Soap Lake #6	CP020469.1_6
	31/32	56	1E-10	*Halomonas* sp. Soap Lake #7	CP019915.1_6
	31/32	56	1E-10	*Methylomonas methanica*	CP002738.1_5
	31/32	56	1E-10	*Methylomonas methanica*	CP002738.1_3
	31/32	56	1E-10	*Methylomonas methanica*	CP002738.1_4
	31/32	56	1E-10	*Pseudomonas stutzeri*	LR134319.1_1
	31/32	56	1E-10	*Pseudomonas stutzeri*	CP000304.1_3
	31/32	56	1E-10	*Ramlibacter tataouinensis*	CP000245.1_1
GTTTCAATCCACGCGCCCGCATGAGGCGCGAC	31/32	56	1E-10	*Halomonas* sp. Soap Lake #6	CP020469.1_6
	31/32	56	1E-10	*Halomonas* sp. Soap Lake #7	CP019915.1_6

n.m.: no matches

Table A10. Comparison of spacers in the CRISPR of confidence level 4 found in strain OF001 to CRISPRCasdb.

Spacers	Matched nucleotides	BLAST score bits	BLAST e-value	Organism	Accesion number
ACGGTGCAGCCGCTGCCGCATTGGCCGTCAATC	28/32	50.1	9E-8	*Pseudomonas* sp. phDV1	CP031606.1_2
CAGGCAGGGGCCTGCTAGTGGAATTGGGCGCTCCA	15/32	30.2	0.084	*Corynebacterium* sp. 2184	CP026948.1_3
GGCTGGTTCTCGGCCTGACCCTCGGCGTGCTGGCC	15/36	30.2	0.084	*Haliangium ochraceum*	CP001804.1_12
CTCCATGCCGATGCCCTCGAGCAGCGGGCCGAGGTC	15/35	30.2	0.087	*Nostoc* sp. PCC 7524	CP003552.1_7
GGGCGGCCTTGAGCAGCTCGCGCAGATCCTGGTG	16/37	32.2	0.02	*Blastochloris* sp. GI	AP018907.1_5
GCTGGGAGCGCGACCTGGCCGGCAAGATCCAGGC	16/32	32.2	0.02	*P. aeruginosa*	CP029660.1_3
TGTTGTACCTCCTCGAGACGACGGGGCAGATGCAA	18/36	30.2	0.084	*Halobacterium hubeiense*	LN831303.1_5
GAAACGCATTCCACGCCGTCCTGACCCCAGGCGCG	n.m.				
GCTGCGCCGCCCTCGCCCACTCTGGAGCCAACCAT	n.m.				
TTTGCGTGCGAACCAGAGTGCGAACCTTCTGCGTGC	n.m.				
CTCCGGCCTGCAGGAGCAGACGCAGGTGGAGCAGAG	28/32	50.1	9E-8	*Pseudomonas* sp. phDV1	CP031606.1_2
GGTTGTTGGGCAATTGAAATTTGGTACGATCCGAA	n.m.				
AGGTGGTTCTGTTGTGTTCAAACTCACAGAGGGC	n.m.				
GATCCCAGCCGCCCAGGTACAGCCGGAAGGACTGCA	n.m.				
GTCCACAGCGTCGCATAGCCCTGGGCGATGATCA	n.m.				
TCGGGTTTGTGACGCCATCCAGCGTCATGCTAACC	n.m.				
TGGCCTGTGGGGCAACACCCTCATCATCAAGATGCC	15/37	30.2	0.087	*Sulfolobus solfataricus*	LT549890.1_7
GGATGGTCTGATTGATCGTCGGCGCGTACTCGGT	n.m.				
ACCATTGGGGCCGGCAGCAAAGGAGAAACGACCAT	n.m.				
CGCCTTCGGCAGCCAGGCGGCGCTCGATGGTGTT	n.m.				
ATCACGCACATCCCGACCCCTTCATGGTTGAAGC	n.m.				
TATCGCCGGGCTGCGGGTCGAGGATGACCGCATTG	n.m.				
TTGCCGCCGACGATGCCGGTGCCGACTCCGCCGGC	15/32	30.2	0.084	*Corynebacterium* sp. 2184	CP026948.1_3
ACAGGTCCGGTGGCATCACCCTTGAGGATTACCA	n.m.				
ATGCACTGATGAGCTTCGACCGCATGGCCATCTG	n.m.				
GGACACGGCGCCGAGGGTGCTCAGTTGTTCGTT	n.m.				
CGGCGCCGATGATCTTGCGACCGAGCCCCGCGAT	n.m.				
GTCGGTGGTGGACTTGTGGTTGGTGAAGGCATC	n.m.				

ATTTCGTGGTGCGTTGCACCTACTACGCCAGGGAG	n.m.
CTTCGACTTGAGTGGCCATAGATCACCGCTGGCG	n.m.

n.m.: no matches

Table A 11. Comparison of repeats in the CRISPR of confidence level 4 found in strain A210 to CRISPRCasdb.

Repeat	Matched nucleotides	BLAST score bits	BLAST e-value	Organism	Accesion number
ACTTCAACGATGCCGCGCCCAAAGGGTGCGGTGAG	n.m.				
GCTTCAACGATGCCGCGCCCCAAGGGCGCGGGGAA	n.m.				
GCTTCAACGATGCCGCACCCCATGGGCGCGGTGAG	19/36	32.2	0.002	*Verrucomicrobium spinosum*	ABIZ01000001.1_7
ACTTCAACGATGCCGCGCTTCAAAGGCGCGGTGAG	n.m.				
ACTTCAACGATGCCGCGTCCCAGGGGCGCGGTGAG	n.m.				
GCTTCAACGATGCCACGCCGCATGGGCGTGGTGAG	20/36	34.2	0.0005	*Opitutaceae* bacterium TAV5	CP007053.1_2
GCTTCAACGATGCCGCGCCACAAAGGCGCGGTGAG	n.m.				
GCTTCAATGATGCCGCGCCTCAAAAGCGCAGTGAG	n.m.				
GCTTCAACGATGCCGCGCCACAAAGGCACGGTGAG	n.m.				
GCTTCAACGATGCCGCGCCTCAAAGGCACGGTGAG	n.m.				

n.m.: no matches

Table A12. Comparison of spacers in the CRISPR of confidence level 4 found in strain A210 to CRISPRCasdb.

Spacers	Matched nucleotides	BLAST score bits	BLAST e-value	Organism	Accesion number
GCATGTCGTCCTCGTTCAAGTCGTAGGTCTTGTCCGT	15/46	30.2	0.087	*Raphidiopsis curvata*	AP018317.1_2
CCATCGTGTCGATGACCCGCTTGTGGTGCGTCGTGTT	n.m.				
GCGGGGCATGTTCGAGGTCGCACTCAACCCCTACGC	n.m.				
CCCCGTTCATCGTGCAGGCGACGTGCGTGGTGCCGTT	n.m.				
GCACCACCGTGCCGCGGTCAATCAGCATCTTCGCCGT	n.m.				
GCCGCGATACTCTTCCCAGATCACGCCGCCGAACTC	15/32	30.2	0.087	*Pectobacterium carotovorum*	CP003776.1_2
GCGCATCGTTCAAGACGACGGCGGTGGAGTACATCTT	n.m.				
CCCGTGGGCGCAGCGGTTGCCCTCCACGATGTTGCC	n.m.				
CCTTCTTCAGCGCCTTCATGATCGGGTCTTTGACCGC	n.m.				
CCGGAAGTCGGGCCGGTCCAGCCCGTCGGGCGTGCA	n.m.				
TCGCGATGTCACCAAGACGATGCTGCGGGTCTTCCA	n.m.				
CCGCGGTGCCGGTTCAGGGCCGTGGTGCAGGCGTCGTA	n.m.				
CCCGGCAAGTGGGTGCAGATCGACCCCCGCGCGTGGAA	n.m.				
CCCGGGCCTGATGGGCCAGAAGCTGTACGAGTCGAT	15/46	30.2	0.087	*Raphidiopsis curvata*	AP018317.1_2
CCGTGATCGGCCATAGCGACTGAGAGGGGTTGCAGAC	n.m.				

n.m.: no matches